Modeling and numerical simulation of the deformation and the rupture of the plaque of atherosclerosis in the arteries.

Fatima Abbas

Thèse de Doctorat

Pour obtenir le grade de Docteur de

Université Libanaise
Et Université Le Havre Normandie

Mathematique Appliquées

Présentée et soutenue par

Fatima ABBAS

Le 18 Avril 2019

Modélisation et Simulation Numérique de la Déformation et la Rupture de la Plaque d'Athérosclérose dans Les Artères

---

Directeurs de Thèse:
Pr. Ayman MOURAD et Pr. Adnan YASSINE

Jury:

Directeurs:	Pr. Ayman MOURAD	Université Libanaise, Liban
	Pr. Adnan YASSINE	Université Le Havre Normandie, France
Rapporteurs:	Pr. Toni SAYAH	Université Saint-Joseph, Liban
	Pr. Adélia SEQUEIRA	Université de Lisbonne, Portugal
Examinateurs:	Dr. Hyam ABBOUD	Université libanaise, Liban
	Dr. Nader EL KHATIB	Lebanese American University, Liban
	Dr. Sophie MICHEL	Université Le Havre Normandie, France
	Pr. Nabil NASSIF	American University of Beirut, Liban

To my father, my mother
and my brothers ...

Acknowledgments

Writing this part is not easy as it seems! A search in the thesaurus for at least a single word that can be fair when expressing my gratitude would end up with "no results found". None of the languages or the alphabets can!

Foremost I would like to express my deepest gratitude to Professor Ayman Mourad for his generous guidance throughout the whole PhD journey and for giving me the honor of working with him. In fact, without his kind advices, continuous support, motivation and immense knowledge my work would not have been perfect as it is. I consider myself extremely lucky to have Professor Ayman Mourad as my director.

Besides, my sincere thanks goes to my co-director Professor Adnan Yassine, who provided me with the opportunity to do this research. I am thankful for his precious support and encouragement that flourished my scientific culture. I appreciate his confidence in my research work, without it, this work would not have came to this delightful end.

I would like to thank Professor Adélia Sequeira and Professor Toni Sayah for accepting to be reviewers of this thesis. I thank them for the time, their suggestions and attentive reading of the manuscript. In addition, I would like to thank Doctor Hyam Abboud, Doctor Nader El-Khatib and Doctor Sophie Michel who honored me by being members of the jury. I am greatly indebted to each member in my defense jury for the privilege.

My special thanks are due to Professor Nabil Nassif who accepted to be the president of the jury.

I also take the chance to thank all the members of the KALMA - Université Libanaise, EDST - Université Libanaise and LMAH - Université le Havre Normandie for the knowledge we shared and the lovely moments we spent together.

I would like to thank all my friends and colleagues for their support throughout the whole years of study. For my special friends, those who are close or are aboard thank you for sharing with me this blissful achievement and for being a part of my life journey.

Finally, I am greatly indebted to my beloved parents for their efforts, fatigue and patience. I appreciate their encouragement, support, confidence and trust in my abilities that were the keys in my success. I will be selfish if I say that I have achieved my dream! It is my parents dream as it is mine!

I am grateful to my mother for her strength, for her glittering eyes that stayed up many nights looking after me and for every single moment she spent teaching me. I am greatly indebted to her for all the morals she taught me. I know I end up speechless to thank this great woman for raising me to the person I am.

I am greatly thankful to Professor Hassane Abbas, my father, my role model. I am thankful for his guidance, for every tired muscle of his body and for his faithfulness to his career. I have kept wondering how could anyone be faithful to his career as much as he is. It is the passion of mathematics!

My deepest gratitude is to my brothers for being the support and protecting my back. I know I can always rely on them. I am extremely lucky for having them as my brothers.

Finally, I thank all my friends who attended or helped organize my defense. Having shared this moment with them made it a more cheerfully one.

Abstract

This thesis is devoted to the mathematical modeling of the blood flow in stenosed arteries due to atherosclerosis. Atherosclerosis is a complex vascular disease characterized by the build up of a plaque leading to the narrowing of the artery. It is responsible for heart attacks and strokes. Regardless of the many risk factors that have been identified- cholesterol and lipids, pressure, unhealthy diet and obesity- only mechanical and hemodynamic factors can give a precise cause of this disease.

In the first part of the thesis, we introduce the three dimensional mathematical model describing the blood-wall setting. The model consists of coupling the dynamics of the blood flow given by the Navier-Stokes equations formulated in the Arbitrary Lagrangian Eulerian (ALE) framework with the elastodynamic equations describing the motion of the arterial wall considered as a hyperelastic material modeled by the non-linear Saint Venant-Kirchhoff model as a fluid-structure interaction (FSI) system. Theoretically, we prove local in time existence and uniqueness of solution for this system when the fluid is assumed to be an incompressible Newtonian homogeneous fluid and the structure is described by the quasi-incompressible non-linear Saint Venant-Kirchhoff model. Results are established relying on the key tool; the fixed point theorem.

The second part is devoted for the numerical analysis of the FSI model. The blood is considered to be a non-Newtonian fluid whose behavior and rheological properties are described by Carreau model, while the arterial wall is a homogeneous incompressible material whose motion is described by the quasi-static elastodynamic equations. Simulations are performed in the two dimensional space $\mathbb{R}^2$ using the finite element method (FEM) software FreeFem++. We focus on investigating the pattern of the viscosity, the speed and the maximum shear stress. Further, we aim to locate the recirculation zones which are formed as a consequence of the existence of the stenosis. Based on these results we proceed to detect the solidification zone where the blood transits from liquid state to a jelly-like material. Next, we specify the solidified blood to be a linear elastic material that obeys Hooke's law and which is subjected to an external surface force representing the stress exerted by the blood on the solidification zone. Numerical results concerning the solidified blood are obtained by solving the linear elasticity equations using FreeFem++. Mainly, we analyze the deformation of this zone as well as the wall shear stress. These analyzed results will allow us to give our hypothesis to derive a rupture model.

KEY WORDS

Atherosclerosis, fluid-structure interaction, Navier-Stokes equations, Newtonian, non-Newtonian, homogeneous, elastodynamic equations, variational formulation, elasticity, hyperelasticity, incompressible, quasi-incompressible, quasi-static, non-linear, modeling, simulation, blood, plaque, stenosis, artery, bifurcation, Arbitrary Lagrangian Eulerian, rheology, constitutive law, Saint Venant-Kirchhoff, Cauchy stress tensor, shear stress, viscosity, existence and uniqueness of the solution, fixed point theorem, recirculation zone, solidification zone, Carreau model, rupture.

Résumé

Cette thèse est consacrée à la modélisation mathématique du flux sanguin dans les artères en présence de la sténose à cause de l'athérosclérose. L'athérosclérose est une maladie vasculaire complexe caractérisée par la formation d'une plaque menant au rétrécissement de l'artère. Elle est responsable des crises cardiaques et des accidents vasculaires cérébraux. Quels que soient les nombreux facteurs de risque identifiés - cholestérol et lipides, pression, régime alimentaire malsain et obésité - seuls des facteurs mécaniques et hémodynamiques peuvent donner une cause précise de cette maladie.

Dans la première partie de la thèse, nous introduisons le modèle mathématique tridimensionnel décrivant l'introduction entre le sang et la paroi artérielle. Le modèle consiste à coupler la dynamique du flux sanguin donnée par les équations de Navier-Stokes formulées dans le cadre Arbitrary Lagrangian Eulerian (ALE) avec les équations élastodynamiques décrivant le mouvement de la paroi artérielle considérée comme un matériau hyperélastique modélisé par la loi de comportement non-linéaire de Saint Venant-Kirchhoff en tant que système d'interaction fluide-structure. Théoriquement, nous prouvons l'existence et l'unicité locale dans le temps de la solution pour ce système lorsque le fluide est supposé être un fluide homogène Newtonien incompressible et que la structure est décrite par la loi de comportement non-linéaire quasi-incompressible de Saint-Venant-Kirchhoff. Les résultats sont établis en utilisant l'outil clé; le théorème du point fixe.

La deuxième partie est consacrée à l'analyse numérique de ce modèle. Le sang est considéré comme un fluide non-Newtonien dont le comportement et les propriétés rhéologiques sont décrits par le modèle de Carreau, tandis que la paroi artérielle est un matériau homogène incompressible dont le mouvement est décrit par les équations élastodynamiques quasi-statiques. Les simulations sont effectuées dans l'espace à deux dimensions $\mathbb{R}^2$ à l'aide du logiciel FreeFem ++ en utilisant la méthode des éléments finis. Nous nous concentrons sur l'étude de la viscosité, de la vitesse et des contraintes de cisaillement maximale. En outre, nous visons à localiser les zones de recirculation qui sont formées à la suite de l'existence de la sténose. En se basant sur de ces résultats, nous procédons à la détection de la zone de solidification où le sang passe de l'état liquide à un matériau de type gelée. Ensuite, nous spécifions que le sang solidifié est un matériau élastique linéaire qui obéit à la loi de Hooke et qui subit à une force de surface externe représentant la contrainte exercée par le sang sur la zone de solidification. Les résultats numériques concernant le sang solidifié sont obtenus en résolvant les équations d'élasticité linéaires à l'aide de FreeFem ++. Nous analysons principalement la déformation de cette zone ainsi que les contraintes de cisaillement la paroi. Les résultats obtenus vont nous permettre de porposer une hypothèse pour la formulation d'un modèle de rupture.

Mots-Clés

Athérosclérose, interaction fluide-structure, équations de Navier-Stokes, Newtonien, non-Newtonien, homogène, équations élastodynamiques, formulation variationnelle, élasticité, hyperélasticité, incompressible, quasi-incompressible, quasi-statique, non-linéaire, modélisation, simulation,le sang, plaque, sténose, artère, bifurcation, arbitraire Lagrange-Euler, rhéologie, loi de comportement, Saint Venant-Kirchhoff, tenseur des contraintes de Cauchy, contraintes de cisaillement, viscosité, existence et unicité de la solution, théorème de point fixe, zone de recirculation, zone de solidification, modèle de Carreau, rupture.

Contents

List of Figures

List of Tables

Chapter 1

Introduction

The human's heart- only the size of a fist- is the strongest muscle in the body. It pumps a complex, time-varying output of blood through the blood vessels constituting the circulatory system responsible for providing the body organs with nutrients, oxygen and other supplies needed to function normally. Further, it provides the body with a pulsating pressure waves that propagates throughout the whole cardiovascular system. This muscle starts to beat in the uterus long time before birth, in general 3-4 weeks after conception. The circulatory system has been studied a long time ago. By the action of mummification the Egyptians acquired knowledge about the human's body and its inside. They got introduced to the main blood vessels and the heart's role, though they believed that the variety of the body fluids flow through the heart. The earliest known writings and medical papers are: the Edwin Smith Papyrus (seventeeth century BC), the Ebers Papyrus (sixteeth century BC) and the Kahun Gynecological (nineteenth century BC). In particular, the Ebers Papyrus described the relation between the blood and the arteries, declaring that after a person breathes air into the lungs, the air enters the heart and then flows into the arteries without indicating any role for the red blood cells (RBCs). Egyptians have believed that the heart is the source of emotions and wisdom. With this study, arose the curiosity to observe the heart and the blood. For about 1500 years, an incorrect model was built. In the second century the Greek physician and philosopher Galen of Pergamon came up with a believable model for the circulatory system. Accurately, he acknowledged that the system consists of venous blood (dark red) and arterial blood (bright red) which are of different functions. Though, he proposed that the circulatory system consists of two one-way systems of blood distribution rather than a single way, and that the liver is responsible of producing venous blood that the body consumes. He also thought that the heart was a sucking organ, rather than a pumping one.

Galen's theory and other wrong views reigned in Western medicine until the 1628, when the English physician William Harvey correctly described blood circulation. Then with time, modeling of blood rapidly progressed, and yet it is. Models are proposed to study the blood flow in the blood vessels, the characteristics of the blood cells and plasma and of the heart [TBA11, TBE+11, BKS09]. Further, models describing the coagulation of blood have been subject of intensive research [Bou17, GHZ09, Zhu07]. History and advances in the study of blood can be found in [Col15].

Related to the heart and the blood vessels, are the cardiovascular diseases. Various types of cardiovascular problems exist, for instance, coronary heart disease (CHD), heart attack also known as myocardial infarction, arrhythmia, heart failure, congenital and rheumatic heart diseases, peripheral artery disease, cardiomyopathy and much more. Some cardiovascular problems are related to heart defects that are present at birth. Others can be due to some life habits such as smoking, drinking too much alcohol, physical inactivity or lack of sleep. Stress, anxiety, hypertension, diabetes, cholesterol, etc. are also major factors associated with cardiovascular diseases. Neverthless, cardiovascular diseases are mostly related to *atherosclerosis*. For a rich knowledge on the cardiovascular diseases from physiological and pathological perspectives and some of the associated treatments and remedies the reader can refer to [MMM+05] and the cites therein. Recent statistical surveys done by the Institute for Health Metrics and Evaluation (IHME)[1], showed that 17.65 million people around the world have died due to cardiovascular diseases that is about 32.26% of the total death, revealing that it is the major cause of death worldwide.

1.1 Atherosclerosis and Blood Coagulation

1.1.1 Atherosclerosis

Atherosclerosis is an inflammatory disease characterized by narrowing of the artery due to the build up of a stenosis or plaque on the artery wall resulting from the occupation of the white blood cells. The interior of the arteries is lined up with a smooth layer of cells that keeps them smooth and facilitates the passage of blood. This layer is called *endothelium*. When this layer is damaged it allows the build up of the cholesterol, lipids, macrophages and other substances from the blood causing atherosclerosis. Over time, the plaque can build up with the platelets

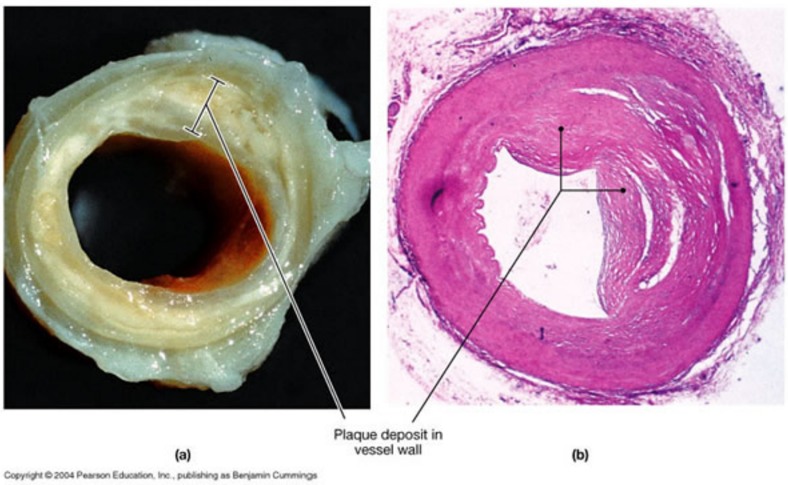

Figure 1.1: Formation of atherosclerosis (Benjamin Cummings).

forming a clot which causes the interruption of the blood flow into the body organs. Blood clots can block the artery or with time and due to the effect of the shear stresses exerted by the blood

[1]It is a research institute that was launched in June 2007 that works in the area of global health statistics and impact evaluation at the University of Washington in Seattle

flow on the stenosis and the clot, the clot will be released into the flow resulting a heart attack or a stroke. Many experiments have shown the steps of the formation of the plaque, which in some cases eventually will end up with a rupture. It is a complex process that mainly involves LDL[2], monocytes, cytokines, macrophage, etc. which ends up with the formation of the fibrous plaques that can rupture and a clot forms as the platelets try to fix the rupture.

It is worth to distinguish between arteriosclerosis and atherosclerosis. Atherosclerosis is a specific type of arteriosclerosis, which is the stiffening or hardening of the artery walls. All people with atherosclerosis have arteriosclerosis, but those with arteriosclerosis might not necessarily have atherosclerosis. However, the two terms are frequently used with the same meaning.

To deal with atherosclerosis and discover preventive therapies and remedies in order to heal patients, mathematicians handle these situations from their mathematical perspectives by employing mathematical models and performing numerical simulations. A first step is modeling the blood flow in blood vessels. In 1775, Euler developed his equations aiming to describe the blood flow [Eul89]. In this context, the first two dimensional model to study the blood flow in heart was developed in the Ph.D. thesis [Pes72] using immersed method to a dog model. Successfully, the work was extended to a three dimensional model to a heart model [Pes02, PM89]. Based on the complexity of the formation of atherosclerosis, mathematical modeling of this process can involve non-linear partial differential equations (PDEs) describing the blood flow and the elasticity of the arterial wall taking into consideration the complexity of the layers of this wall. Moreover, it can also lead to interaction systems, chemical reactions, coagulation and growth processes. Hence, many mathematical models have been studied by considering some conditions of this complex process [BD12, LT10, CEMR09, CHM+10, KGKV09, KGV07, KGKV11]. The work [KGKV09, KGV07] presented one and two dimensional models that describe the formation of atherosclerosis as an auto-amplification inflammatory phenomenon based on the reaction-diffusion equations where the concentration of the oxidized LDL is the significant parameter. No focus on the interaction of the blood and the plaque has been considered. Based on this model, a new model has been built in [CEMR09] by considering the atherosclerosis to be an inflammatory process that starts at the stage of intima when the LDL penetrate and get oxidized. A coupled system has been set up from the reaction-diffusion equation describing the inflammatory phenomenon and the Navier-Stokes equations describing the dynamics of the blood flow. An improvement of this model is presented in [CHM+10] by coupling the inflammatory process with transport equations, transfer equations and Navier-Stokes equations each describing the LDL in the intima, the endothelial wall and the blood flow dynamics, respectively.

1.1.2 Blood Coagulation

Atherosclerosis provokes blood coagulation [ADK12] which involves the secretation of cytokine and chemokine by the inflamed site and the activation of the platlets and the endothelial cells. Blood coagulation is the process by which the blood changes in state from liquid to- a more viscous material- a jelly-like material, which results a blood clot. Coagulation is an instant process that is activated once the endothelium is damaged. The process of coagulation depends mainly on the platelets and the insoluble fibrin protein. The fibrin proteins are formed by a

[2]Low density Lipoproteins.

process known as the coagulation cascade [DR64] which involves many biochemical reactions where the blood clotting factors are activated [Bou17]. Blood clots are mainly associated to atherosclerosis and are formed whenever the flowing blood comes in contact with a foreign substance in the skin or in the blood vessels wall. In particular, in the situations where plaques formed from fats, lipids, cholesterol or other foreign substances found in the blood are identified, over time, they harden causing the narrowing of the artery leading to a blood clot formation. Two major types of blood clots are: thrombi, which are stationary clots, though they can cause the blockage of a flow; emboli, which are break loose which may detach into the blood flow and can, somewhere in a site far away, block the flow. This type of clots is dangerous and causes infarctions, more precisely, if the blockage occurs in the brain it results a stroke, if it occurs in the heart a heart attack would result, or in the lungs it would cause pulmonary embolism. Many mathematical models have been developed for the description of the coagulation cascade by representing the biochemical reactions using a system of ordinary differential equations (ODEs) [BZOC+12, MNR08, SV15]. The work [SSB11] has been devoted for the stability results of a mathematical model of the coagulation cascade.

Mathematical models can provide a deep view of the coagulation process. Usually, the dynamics of the blood flow is given by the Navier-Stokes equations whereas advection-diffusion-reactions are employed to describe the concentration of the clotting factors and the fibrin polymers. The interaction of the blood flow and the clot growth is given in spatiotemporal representation inside the blood vessel using the continuous approach. Both models are simulated on the same domain and are solved on the same numerical mesh. Some models have neglected the effect of the fribin polymers on the blood flow dynamics [JC11], while others have assumed the dependence of the blood viscosity on them by employing the generalized Newtonian model for the blood flow [BS08, SB14]. Further, some continuous models have dealt with the clot as a solid [SvdV14] and detected its growth using FSI system. Whereas, other models have considered the fibrin to be a porous medium [LF10, GRRM16]. Hybrid models have also been employed in order to achieve a realistic representation of the clot formation [FG08, XCL+12, YLHK17, TAB+13, TAB+15].

In general, all the mathematical models used to model atherosclerosis are simple which capture only some essential features of atherosclerosis without taking into consideration the complexity of the atherosclerosis and the composition of blood. More suitable models are needed through which the physiological parameters associated to the atherosclerosis must be investigated clinically. In addition, the vessel wall must be considered as a multi-component structure taking into account the effect of the plaque growth and its rupture on their mechanism. Further, a more realistic model must be derived by analyzing the timescales of the biological processes carried out by the LDL, oxidized LDL and macrophages involved in this phenomenon, also, the time for a one pulse corresponding to the blood flow; about few seconds; and the time of the plaque growth which can be months.

In this thesis, the modeling of the blood flow through a stenosed artery will be studied as a fluid-structure interaction (FSI) model. Theoretically, existence and uniqueness of a regular weak solution of this model are proved locally in time. Numerically, by analyzing the pattern of the blood viscosity, the blood flow and the wall shear stress we will introduce our assumption concerning the location of the solidification zone and its characteristics. Furthermore, we will study the effect of the external forces representing the shear stress of the blood on this zone which constitutes a first step forward to propose a rupture model.

1.2 An Overview on the Thesis

1.2.1 Chapter 2: Modeling of the Fluid-Structure Interaction System

In this chapter, we introduce the FSI system that models the interaction between the blood flow and the arterial wall when a stenosis exists. The system consists of two sub-problems; a fluid sub-problem describing the dynamics of the blood flow through the lumen of the artery and a structure sub-problem that describes the motion of the arterial wall. The blood is considered to be a homogeneous incompressible fluid whose dynamics is given by the incompressible Navier-Stokes equations. On the other hand, the arterial wall is considered to be a hyperelastic material . The interaction between the blood and the arterial wall prompts the introduction of the Arbitrary Lagrangian Eulerian (ALE) formulation. In particular, the fluid computational domain $\Omega_f(t)$ must obey the motion of the blood-wall interface $\Gamma_c(t)$, thus it cannot be fixed in time. Consequently we adopt the Navier-Stokes equations in the ALE frame. While, the elastodynamic equations are given in the Lagrangian framework. The two sub-problems are coupled by imposing coupling conditions on the interface $\Gamma_c(t)$.

In the first section we introduce the modeling of the blood flow which is governed by the incompressible Navier-Stokes equations that are written in the Eulerian framework. We distinguish between the case of a two dimensional and a three dimensional domain. Further, we reformulate these equations on any arbitrary reference configuration. The last step in this section is formulating the Navier-Stokes equations in the ALE framework.

The elastodynamic equations describing the motion of the arterial wall are given in Section 2.2. We highlight two cases: the case of a non-linear elastic material; and the case of a linear elastic material. The non-linear elastic material is considered to be a hyperelastic structure . The elastodynamic equations are formulated in the Lagrangian frame on the reference configuration $\tilde{\Omega}_s$. On the other hand, the linear elastic materials obey Hooke's law and their associated elastodynamic equations are given on the actual configuration $\Omega_s(t)$.

Having the two sub-problems; the Navier-Stokes equations in the ALE frame and the elastodynamic equations in the Lagrangian frame, the FSI problem is set up in the third section. Indeed, to have a well built system we impose some coupling conditions on the blood-wall interface $\Gamma_c(t)$. These conditions ensure the global energy balance of the system. In particular, the velocity fields and the stresses must be continuous on the interface. Further, a geometrical condition is imposed which is given as a relation between the displacement $\tilde{\boldsymbol{\xi}}_f$ of the fluid domain $\tilde{\Omega}_f$ and the displacement $\tilde{\boldsymbol{\xi}}_s$ of the structure domain $\tilde{\Omega}_s$. More precisely, the displacement $\tilde{\boldsymbol{\xi}}_f$ is considered to be a reasonable extension of $\tilde{\boldsymbol{\xi}}_s$.

1.2.2 Chapter 3: Analysis of the Interaction Between an Incompressible Fluid and a Quasi-Incompressible Non-Linear Elastic Structure

In this chapter we focus on proving the local in time existence and uniqueness of a regular weak solution of the FSI system corresponding to the lumen-wall model. We consider the fluid to be a homogeneous incompressible Newtonian fluid whose dynamics is given by the Navier-Stokes equations formulated in the Eulerian coordinates on an actual configuration $\Omega_f(t) \subset \mathbb{R}^3$. The arterial wall is a hyperelastic quasi-incompressible structure modeled by the non-linear Saint Venant-Kirchhoff model. Its corresponding elastodynamic equations are given on the actual configuration $\Omega_s(t) \subset \mathbb{R}^3$. These equations are coupled by imposing conditions representing the continuity of velocity fields and stresses on the lumen-wall interface $\Gamma_c(t)$. A rewriting of the Navier-Stokes equations in the Lagrangian reference framework results linear equations and a fixed domain where we can deal easily with these equations. Local existence and uniqueness of solution of the coupled system is established based on the key tool; the fixed point theorem.

In the first section, we introduce the Navier-Stokes equations governing the flow of velocity $\boldsymbol{v}$ and pressure $\boldsymbol{p}_f$, and the elastodynamic equations satisfied by the structure displacement $\boldsymbol{\xi}_s$, each with their associated boundary conditions. A compatible FSI is obtained by imposing some coupling conditions representing the continuity of velocities and stresses on the lumen-wall interface $\Gamma_c(t)$. We make use of the deformation maps $\boldsymbol{\mathcal{A}}$ and $\boldsymbol{\varphi}_s$ of the fluid and the structure domains $\Omega_f(0)$ and $\Omega_s(0)$, respectively, in order to rewrite the coupled system in the Lagrangian framework, in particular, in the reference configuration corresponding to the time $t = 0$. Explicit rewritings of the Saint Venant-Kirchhoff model and the quasi-incompressibility condition in the spirit of [Gaw02] are introduced which enable us to deal with them easily when applying the fixed point theorem.

A step forward in the second section is to partially linearize the FSI system by considering the deformation maps $\boldsymbol{\mathcal{A}}$ and $\boldsymbol{\varphi}$ to be given for a chosen fluid velocity $\breve{\boldsymbol{v}}$ and a structure displacement $\breve{\boldsymbol{\xi}}_s$ in a fixed point space. Estimates on the given deformation maps $\breve{\boldsymbol{\mathcal{A}}}$ and $\breve{\boldsymbol{\varphi}}$ as well as on the Saint Venant-Kirchhoff model are derived based on Grönwall's inequality (B.1) and the generalized Poincaré inequality [BF13, Proposition III.2.38].

Based on the partially linear system, in Section 3.3, we formulate an auxiliary problem by a slight change on the coupling conditions attributed to the elastodynamic equations. Considering a transformation of a divergence-free setting we formulate the variational formulation associated to the auxiliary problem in which the pressure term disappears. Proceeding with Faedo-Galerkin approach we define the Galerkin approximations of the solutions and derive a priori estimates on them. Passing to the limit, using compactness results [Bre10, Chapter 9] and Aubin-Lions-Simon theorem [BF13, Theorem II.5.16] yield the existence and uniqueness of the solution of the auxiliary problem.

Concerning the partially linear system, we derive a priori estimates on its solution. Then based on the results concerning the auxiliary problem and using the fixed point theorem we prove the existence and uniqueness of the solution of the linear system in Section 3.4.

Regularity of the solution and some a priori estimates are presented in Section 3.5.

In Section 3.6, using the preceding results of the linear system and using the fixed point theorem we prove the existence and uniqueness of a weak solution of the non-linear FSI system.

At last, verifying the inf-sup condition [Bre74] we establish the existence of an L^2 fluid pressure. Then, based on the regularity of the solution $(\boldsymbol{v}, \boldsymbol{\xi})$ we get a more regular fluid pressure.

1.2.3 Chapter 4: Discretization and Numerical Simulations

The mathematical modeling and the numerical analysis of the blood flow in a stenosed artery is the subject of the study in this chapter. In particular, the blood-wall is modeled as a FSI model obtained by coupling the fluid model representing the blood flow in the lumen $\Omega_f(t)$ with the structure model describing the motion of the arterial wall $\Omega_s(t)$ by imposing some coupling conditions on the lumen-artery interface $\Gamma_c(t)$. The dynamics of the blood flow is governed by the incompressible Navier-Stokes equations, while the motion of the arterial wall is described by the quasi-static elastodynamic equations. We assume that the arterial wall is a hyperelastic incompressible material. The variational formulation associated to the FSI system is formulated by deriving the variational formulation corresponding to each sub-problem using appropriate test functions. The system is then discretized using the partitioned approach. The discretized system is solved using FreeFem++ software by considering reliable physiological data and assuming that the blood viscosity obeys Carreau model. Numerical simulations have shown a deep insight of processes occurring in stenosed arteries. Indeed, the blood flow, the deformation of the stenosis, the maximum shear stress and the recirculation zones are configured in the case of a pipe-shaped stenosed artery and in the case of a bifurcated stenosed artery. Results have shown that the peak of the stenosis is characterized by a high displacement and its neighborhood possesses a high shear stress. These results help us in configuring three major regions; the neighborhood of the peak, the recirculation zone and the solidification zone. The pattern of the blood speed, the maximum shear stress and the blood viscosity are investigated in these three regions. In addition, comparison between a Newtonian blood and a non-Newtonian blood is demonstrated by analyzing the blood speed, the viscosity and the maximum shear stress.

In the first section we introduce the three dimensional FSI system corresponding to the blood-wall setting that we deal with by adopting the ALE approach. The variational formulation associated to each sub-problem is derived using appropriate test functions that take into account the boundary conditions. Space discretization are applied on the Navier-Stokes equations and the elastodynamic equations by employing the finite element method (FEM). Then, the Navier-Stokes equations are semi-discretized in time by considering the convective term and the fluid viscosity at the instant t_n while other terms are considered at the instant t_{n+1}. On the other hand, the quasi-static elastodynamic equation is solved using Newton-Raphson method by linearizing it with respect to the deformation $\boldsymbol{\varphi}_s$ and the hydrostatic pressure p_{hs} associated to the structure domain $\tilde{\Omega}_s$. After solving the Navier-Stokes equations, we solve the elastodynamic equations to get the displacement $\tilde{\boldsymbol{\xi}}_s$ of the structure domain. The ALE map $\boldsymbol{\mathcal{A}}$ representing the evolution of the fluid domain $\Omega_f(t)$ is constructed assuming that the displacement $\tilde{\boldsymbol{\xi}}_f$ of the fluid domain is the harmonic extension of the displacement $\tilde{\boldsymbol{\xi}}_s$ of the interface $\Gamma_c(t)$.

The second section is devoted for the numerical results obtained upon performing numerical simulations using the FreeFem++ software in a two dimensional space. The blood flow is analyzed during a time duration of 3 seconds when a pulsatile periodic inlet velocity $\boldsymbol{v}_{\text{in}}$ is enforced on the inlet of the lumen. The figures showed a high blood flow in the neighborhood of the peak of the stenosis, which undergoes a significant deformation. Maximum shear stress is investigated and its highest value is detected in the neighborhood of the peak of the stenosis. Further, a conspicuous recirculation zone is identified after the stenosis. This zone is characterized by a negligible speed at its center, which increases as the diameter of the circular region increases. The case of a bifurcated artery where one and two stenosis exist is also investigated. Analyzing the behavior of the flow, the viscosity, the maximum shear stress and detecting the recirculation zones came to an agreement to the case of pipe-shaped artery. Based on the analyzed variables, three major regions are studied (Figure 4.12). A region "A" representing the neighborhood of the peak, a region "C" corresponding to the recirculation zone and an intermediate region "B" spotted at the edge of the stenosis. Region "A" is characterized by the highest speed among others, whereas Region "B" is of the highest viscosity value, while Region "C" possesses the highest shear stress. These results will constitute an essential key for the detection of the solidification zone and its characteristics. Moreover, a comparison between a Newtonian blood and a non-Newtonian blood is drawn is Subsection 4.2.3. A Newtonian blood is characterized by a higher speed and a lower viscosity and wall shear stress than a non-Newtonian blood. Indeed, the non-Newtonian blood is more viscous so that, its viscous behavior forms a resistance factor and acts as an obstacle against the flow leading to a smaller speed.

1.2.4 Chapter 5: Solidification of Blood and a First Step Towards a Rupture Model

Regardless of the progress encountered on the modeling of the cardiovascular system in the last few decades, it is still a challenging problem that has gain the attention of mathematicians and engineers. The complexity of the cardiovascular system and the composition of blood motivate us to derive an appropriate model that best describes the behavior of blood flow and the mechanism of the artery wall, in particular, in the case of a plaque formation. To our knowledge, non of the derived models have captured the physiological properties of blood and arterial wall, hence we are still away from attaining a reliable model.

The aim of this chapter is to propose a rupture model based on the rheological properties of the non-Newtonian blood. In the first section, a brief overview on the viscous behavior of blood is presented. We introduce the widely used constitutive models to capture this property in Subsection 5.1.1.

The second section is devoted for the detection of the solidification zone in order to propose the rupture model. Based on the results obtained in Section 4.2, in particular, the observation of three regions where the pattern of flow and viscosity are remarkable, we give our hypothesis for the characteristics of the solidification zone $\mathcal{R}_{\mathfrak{s}}(t)$. In fact, we consider this zone to be of a negligible blood speed and of a high viscosity, so that blood in this region can be considered a jelly-like material. After a precise location of this zone at the edge of the stenosis , we assume that it is a linear elastic material of displacement $\boldsymbol{u}$ that satisfies the elastodynamic equations with the Cauchy stress tensor $\boldsymbol{\sigma}_{\mathfrak{s}}(\boldsymbol{u})$ obeying Hooke's law. Boundary conditions are set such that, we ensure continuity of the displacements on the stenosis-zone interface $\Gamma_2(t)$, while on the blood-zone interface $\Gamma_1(t)$ an external surface force $\boldsymbol{f}_{\mathfrak{s}}$ is applied representing the stress exerted by the blood. After deriving its weak formulation and discrete formulation, we solve the equations numerically using the FreeFem++ software. Results show a high shear stress exerted by the blood on the interface $\Gamma_1(t)$ opposed by the zone deformation resulting from the stenosis deformation. The pattern of the maximum shear stress and the external surface force $\boldsymbol{f}_{\mathfrak{s}}$ are analyzed. Based on these observations, we give our assumption for a first step in a rupture model, by assuming that the effect of the wall shear stress acting as a resistance factor against the zone motion will scrape and dig the crust of the solidification zone leading to the fragmentation of some solidified pieces and their release into the flow which can cause the blockage of the artery in some faraway sites resulting an infarction.

Chapter 2

Modeling of the Fluid-Structure Interaction System

Contents

Introduction

Cardiovascular diseases, mainly due to atherosclerosis, form the highest rate of death in the world. Curiosity of finding cures for these diseases lead scientists, in particular mathematicians, to study this issue from their mathematical viewpoint. The blood-wall setting can be modeled as a fluid-structure interaction (FSI) system. This system is a multiphysics coupling between equations describing the fluid dynamics and the structural mechanics. The interaction takes place between a deformable structure- arterial wall- and an internal fluid flow. In general, fluid flows are governed by the Navier-Stokes equations or Stokes equations. Whereas, the structure mechanics are described by the elastodynamic equations. The coupling of these equations is set up by imposing some conditions on the common boundary. Both Navier-Stokes equations and elastodynamic equations are derived using the principal physical conservation laws [BF13, FQV09, Ric17, Mal]. Navier-Stokes equations are adopted in the Eulerian framework. The Eulerian approach describes the flow with its control volume through which the fluid flows. Indeed, the physical quantities such as velocities and pressure are considered to behave as fields in the volume, rather than considering the property of each particle. In other words, they are defined to be functions of time and space. In fact, in the Eulerian description, one is not concerned about the location or velocity of any particular particle, but rather about the velocity, acceleration, etc. of whatever particle happens to be at a particular location of interest at a particular time t.

On the other hand, elastodynamic equations are given in the Lagrangian framework. This approach tracks as a function of time each particle by its position, velocity, acceleration, etc.. In complex fields, positions of each solo particle is difficult to be tracked, therefore this approach is rarely used in describing fluid dynamics.

As for the physical laws, such as the conservation of mass and energy or Newton's laws, they are easily applied in Lagrangian description by applying them to each individual particle. Whereas, in Eulerian description some reformulations of these laws are required [Ric17, Chapter 2].

In many FSI systems of particular interest for instance for blood flowing in arteries the computational fluid domain cannot be fixed in time since it is affected by the deformation of the structure domain, consequently it ought to follow the motion of the common interface. If we consider employing the Lagrangian approach, this means we must follow the evolution of the blood particles throughout the whole domain, which we certainly do not want! To get over these obstacles, we consider a domain $\Omega_f(t)$ which is neither fixed, nor a material. Indeed, this is due to the fact that its evolution does not agree with the fluid motion, rather, obeys the displacement of its boundary $\partial\Omega_f(t)$ which is linked to the displacement of the structure. The introduction of this intermediate frame is known as the Arbitrary Lagrangian Eulerian (ALE) approach.

In this chapter we introduce the FSI system that models a blood-wall setting. In the first section we introduce the Navier-Stokes equations governing the blood flow in the actual configuration, reference configuration and in the ALE frame. The second section is concerned about the elastodynamic equations describing the structural mechanics. Using these two equations and imposing some coupling conditions on the interface, in the third section, we present the coupled system associated to the blood-wall model in the ALE framework.

2.1 Blood Flow Modeling with the Navier-Stokes Equations

Consider at time $t = 0$ a domain Ω_0^f. At time $t > 0$, let $\Omega_f(t)$ be the volume occupied by the fluid particles which have occupied Ω_0^f. The total forces exerted on the fluid in $\Omega_f(t)$ are the volumetric force $\boldsymbol{f}_f$ and the surface force represented by the Cauchy stress tensor $\boldsymbol{\sigma}_f$ given by

$$\boldsymbol{\sigma}_f(\boldsymbol{v}, p_f) = 2\mu\boldsymbol{D}(\boldsymbol{v}) + \lambda(\nabla\cdot\boldsymbol{v})\mathbf{Id} - p_f\ \mathbf{Id}, \tag{2.1}$$

where $\boldsymbol{v}$ is the fluid velocity, $\boldsymbol{D}(\boldsymbol{v}) = \dfrac{1}{2}\big(\boldsymbol{\nabla v} + (\boldsymbol{\nabla v})^t\big)$ is the rate of deformation tensor and p_f is the pressure of the fluid whose density is ρ_f. The terms λ and μ depend on the invariants of tensors I_1, I_2 and I_3 of the matrix $\boldsymbol{D}(\boldsymbol{v})$ [Mal, Ric17]. The invariants of the tensor $\boldsymbol{D}(\boldsymbol{v})$ are given by

$$I_1\big(\boldsymbol{D}(\boldsymbol{v})\big) = \mathrm{tr}\big(\boldsymbol{D}(\boldsymbol{v})\big),\ I_2\big(\boldsymbol{D}(\boldsymbol{v})\big) = \frac{1}{2}\Big[\mathrm{tr}^2\big(\boldsymbol{D}(\boldsymbol{v})\big) - \mathrm{tr}\big(\boldsymbol{D}(\boldsymbol{v})\big)^2\Big] \text{ and } I_3\big(\boldsymbol{D}(\boldsymbol{v})\big) = \det\big(\boldsymbol{D}(\boldsymbol{v})\big).$$

In particular, the quantity μ stands for the dynamic viscosity of the fluid. In general μ is a function of $\boldsymbol{\nabla v}$ or other related quantities. In this case the fluid is said to be *non-Newtonian*. However, if μ is constant then the fluid is called *Newtonian*. The term $2\mu\boldsymbol{D}(\boldsymbol{v}) + \lambda(\nabla \cdot \boldsymbol{v})\mathbf{Id}$ is denoted by $\boldsymbol{\tau}_d$ and is called the *Deviatoric stress tensor*.

The derivation of (2.1) is based on some assumptions about the deviatoric stress tensor (linear, isotropic, symmetric). These assumptions are essential to give a specific representation of it that depends on the invariants I_1, I_2 and I_3 of the matrix $\boldsymbol{D}(\boldsymbol{v})$. Moreover, some results from Spectral theory are used. For the full derivation, the reader can refer to [Mal, Section 14]. In case of a non-Newtonain fluid, the Navier-Stokes equations are given by

$$\boxed{\rho_f \frac{\partial \boldsymbol{v}}{\partial t} + \rho_f(\boldsymbol{v}\nabla\cdot)\boldsymbol{v} - \boldsymbol{\nabla}\cdot\boldsymbol{\sigma}_f(\boldsymbol{v}, p_f) = \rho_f \boldsymbol{f}_f. \qquad (2.2)}$$

In the case of a Newtonian fluid the Cauchy stress tensor $\boldsymbol{\sigma}_f$ can be simplified. Indeed, as μ is constant, simple calculations give

$$\boldsymbol{\nabla}\cdot\boldsymbol{\tau}_d = (\lambda+\mu)\boldsymbol{\nabla}(\nabla\cdot\boldsymbol{v}) + \mu\boldsymbol{\nabla}^2\boldsymbol{v}. \tag{2.3}$$

Recall that, the divergence of a second-order tensor $\boldsymbol{T}$ is

$$\boldsymbol{\nabla}_{\boldsymbol{x}}\cdot\boldsymbol{T} = \sum_{k,i=1}^{3} \frac{\partial T_{ki}}{\partial x_i}\boldsymbol{e}_k$$

where $\boldsymbol{e}_k, k = 1, 2, 3$ are the canonical basis of $\mathbb{R}^3$. In particular, for a scalar function p and the tensor $\mathbf{Id}$, we have

$$\boldsymbol{\nabla}_{\boldsymbol{x}}\cdot(p\ \mathbf{Id}) = \sum_{k,i=1}^{3}\frac{\partial(p\ \mathbf{Id})_{ki}}{\partial x_i}\boldsymbol{e}_k = \sum_{k=1}^{3}\frac{\partial(p\ \mathbf{Id})_{kk}}{\partial x_k}\boldsymbol{e}_k = \sum_{k=1}^{3}\frac{\partial p}{\partial x_k}\boldsymbol{e}_k = \boldsymbol{\nabla}_{\boldsymbol{x}}p. \tag{2.4}$$

Using the Cauchy equation of motion (A.3) with (2.3) and (2.4) yield

$$\boxed{\rho_f \frac{\partial \boldsymbol{v}}{\partial t} + \rho_f(\boldsymbol{v}\nabla\cdot)\boldsymbol{v} = -\boldsymbol{\nabla}p_f + (\lambda+\mu)\boldsymbol{\nabla}(\nabla\cdot\boldsymbol{v}) + \mu\boldsymbol{\Delta v} + \rho_f\boldsymbol{f}_f \qquad (2.5)}$$

where $\boldsymbol{\Delta} = \boldsymbol{\nabla}^2$ is the Laplacian operator.

In case of compressible fluid flows we have an additional equation known as the equation of state, which is commonly used in the form of a relationship between the pressure p_f and the density ρ_f.

However, we are interested in the incompressible homogeneous flows. In order to give the equations corresponding to them, we first need to introduce some concepts.

Definition 2.1.1 (Incompressible Flow) *Let $\Omega_f(t)$ be the volume occupied by the fluid at instant $t > 0$. The fluid (flow) is said to be incompressible, if for any subregion V_0 of $\Omega_f(t)$, the volume of V_0 is constant in time.*

Corollary 2.1.1 *The following statements are equivalent*

1. *A fluid is incompressible;*
2. $\det(\mathbf{Id} + \boldsymbol{\nabla} \boldsymbol{v}) = 1$*;*
3. *The velocity field* $\boldsymbol{v}(\boldsymbol{x}, t)$ *is divergence free, that is to say* $\nabla \cdot \boldsymbol{v} = 0$*;*

Proof. *The proof is based on Equation* (A.1). *See* [Mal, Section 6]. ∎

Definition 2.1.2 (Homogeneous Fluid) *A fluid is said to be homogeneous if its mass density* ρ_f *is constant in space.*

2.1.1 Incompressible Navier-Stokes Equations

These equations are derived using the incompressibiltiy condition $\nabla \cdot \boldsymbol{v} = 0$. Therefore, the incompressible Navier-Stokes equations for a non-Newtonian fluid are

$$\begin{cases} \rho_f \left(\dfrac{\partial \boldsymbol{v}}{\partial t} + (\boldsymbol{v} \cdot \nabla) \boldsymbol{v} \right) - \boldsymbol{\nabla} \cdot \boldsymbol{\sigma}_f(\boldsymbol{v}, p_f) = \rho_f \boldsymbol{f}_f & \text{on } \Omega_f(t) \times (0, T), \\ \nabla \cdot \boldsymbol{v} = 0 & \text{on } \Omega_f(t) \times (0, T). \end{cases} \tag{2.6}$$

where $\boldsymbol{\sigma}_f(\boldsymbol{v}, p_f)$ is the Cauchy stress tensor given by the expression

$$\boldsymbol{\sigma}_f(\boldsymbol{v}, p_f) = 2\mu \boldsymbol{D}(\boldsymbol{v}) - p_f \, \mathbf{Id}. \tag{2.7}$$

For a Newtonian fluid, we get the associated equation by substituting the incompressibilty condition into (2.5).

As for the imposed boundary conditions, they mainly depend on the nature of the problem we are modeling. It is worth to distinguish between the cases of two dimensional and three dimensional models.

A Two Dimensional Model

In this case, the domain boundary $\partial\Omega_f(t)$ is considered to be composed of four parts as shown in Figure 2.1.

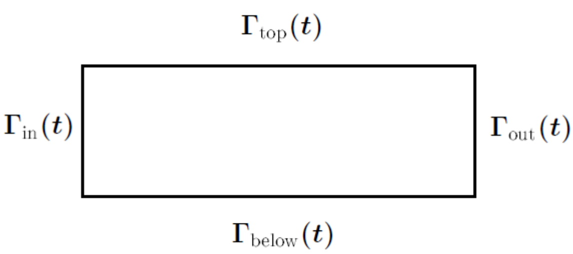

Figure 2.1: A two dimensional fluid domain.

If we consider a structure coupled to both boundaries $\Gamma_{\text{top}}(t)$ and $\Gamma_{\text{below}}(t)$, then a Neumann boundary condition is imposed, representing external loads $\boldsymbol{g}_1^f$ and $\boldsymbol{g}_2^f$ respectively, affecting these boundaries. On the other hand, on the inlet $\Gamma_{\text{in}}(t)$ we impose a given profile velocity $\boldsymbol{v}_{\text{in}}$. Whereas, a free-exit boundary condition is enforced on the outlet $\Gamma_{\text{out}}(t)$. This condition is expressed as

$$\boldsymbol{\sigma}_f(\boldsymbol{v}, p_f)\ \boldsymbol{n}_f = 0 \qquad \text{on } \Gamma_{\text{out}}(t) \times (0, T). \tag{2.8}$$

Hence, the boundary conditions are given by

$$\begin{cases} \boldsymbol{v} = \boldsymbol{v}_{\text{in}} & \text{on } \Gamma_{\text{in}}(t) \times (0, T), \\ \boldsymbol{\sigma}_f(\boldsymbol{v}, p_f)\ \boldsymbol{n}_f = 0 & \text{on } \Gamma_{\text{out}}(t) \times (0, T), \\ \boldsymbol{\sigma}_f(\boldsymbol{v}, p_f)\ \boldsymbol{n}_f = \boldsymbol{g}_1^f & \text{on } \Gamma_{\text{top}}(t) \times (0, T), \\ \boldsymbol{\sigma}_f(\boldsymbol{v}, p_f)\ \boldsymbol{n}_f = \boldsymbol{g}_2^f & \text{on } \Gamma_{\text{below}}(t) \times (0, T), \end{cases} \tag{2.9}$$

where $\boldsymbol{n}_f$ is the outward normal vector associated to each boundary.

On the contrary, if a structure is coupled to both $\Gamma_{\text{below}}(t)$ and $\Gamma_{\text{top}}(t)$, with the assumption that one of them is fixed, or if it is coupled to either one of them; say $\Gamma_{\text{below}}(t)$; then a load $\boldsymbol{g}_f$ is imposed on $\Gamma_{\text{below}}(t)$. In addition, on $\Gamma_{\text{top}}(t)$ we impose a very commonly used boundary condition

$$\boldsymbol{v} = 0 \quad \text{on } \Gamma_{\text{top}}(t) \times (0, T), \tag{2.10}$$

which is known as the *no slip* boundary condition. Physically, this condition means that there is no tangential flow on this boundary. Therefore, in this case the boundary conditions are

$$\begin{cases} \boldsymbol{v} = \boldsymbol{v}_{\text{in}} & \text{on } \Gamma_{\text{in}}(t) \times (0, T), \\ \boldsymbol{\sigma}_f(\boldsymbol{v}, p_f)\ \boldsymbol{n}_f = 0 & \text{on } \Gamma_{\text{out}}(t) \times (0, T), \\ \boldsymbol{v} = 0 & \text{on } \Gamma_{\text{top}}(t) \times (0, T), \\ \boldsymbol{\sigma}_f(\boldsymbol{v}, p_f)\ \boldsymbol{n}_f = \boldsymbol{g}_f & \text{on } \Gamma_{\text{below}}(t) \times (0, T). \end{cases} \tag{2.11}$$

We are concerned of this case when performing numerical simulations in Chapter 4.

In a two dimensional space, the incompressible Navier-Stokes equations on the actual domain $\Omega_f(t)$ are

$$\begin{cases} \rho_f\Big(\dfrac{\partial \boldsymbol{v}}{\partial t} + (\boldsymbol{v}\cdot\nabla)\boldsymbol{v}\Big) - \boldsymbol{\nabla}\cdot\boldsymbol{\sigma}_f(\boldsymbol{v}, p_f) = \rho_f \boldsymbol{f}_f & \text{on } \Omega_f(t) \times (0, T), \\ \nabla\cdot\boldsymbol{v} = 0 & \text{on } \Omega_f(t) \times (0, T), \\ (2.9) \quad \text{or} \quad (2.11). \end{cases} \tag{2.12}$$

A Three Dimensional Model

The boundary $\Omega_f(t)$ is composed of three parts. An inlet $\Gamma_{\text{in}}(t)$, an outlet $\Gamma_{\text{out}}(t)$ and the surrounding boundary $\Gamma_f(t)$. See Figure 2.2.

An inlet velocity $\boldsymbol{v}_{\text{in}}$ is enforced on the inlet of the domain. At the outlet, the fluid is left to flow, by imposing the free-exit boundary condition (2.8). Further, an external load $\boldsymbol{g}_f$ is imposed on the surrounding boundary $\Gamma_f(t)$.

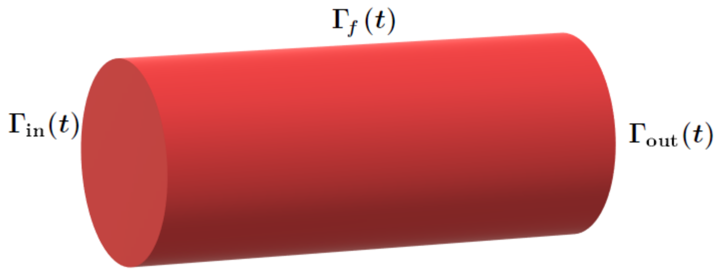

Figure 2.2: A three dimensional fluid domain.

Whence, on a three dimensional domain $\Omega_f(t)$, the incompressible Navier-Stokes equations are

$$\begin{cases} \rho_f\Big(\dfrac{\partial \boldsymbol{v}}{\partial t} + (\boldsymbol{v}\cdot\nabla)\boldsymbol{v}\Big) - \boldsymbol{\nabla}\cdot\boldsymbol{\sigma}_f(\boldsymbol{v},p_f) = \rho_f \boldsymbol{f}_f & \text{on } \Omega_f(t)\times(0,T), \\ \nabla\cdot\boldsymbol{v} = 0 & \text{on } \Omega_f(t)\times(0,T), \\ \boldsymbol{v} = \boldsymbol{v}_{\text{in}} & \text{on } \Gamma_{\text{in}}(t)\times(0,T), \\ \boldsymbol{\sigma}_f(\boldsymbol{v},p_f)\,\boldsymbol{n}_f = 0 & \text{on } \Gamma_{\text{out}}(t)\times(0,T), \\ \boldsymbol{\sigma}_f(\boldsymbol{v},p_f)\,\boldsymbol{n}_f = \boldsymbol{g}_f & \text{on } \Gamma_f(t)\times(0,T). \end{cases} \tag{2.13}$$

In what follows, the work is concerned about a three dimensional domain $\Omega_f(t)$, hence, we are concerned of the System (2.13).

2.1.2 The Navier-Stokes Equations in the Reference Configuration

In some situations, where the Navier-Stokes equations are coupled with a structure, a rewriting of the Navier-Stokes equations on an arbitrary reference domain is needed. We consider the evolution of the reference configuration $\tilde{\Omega}_f$ into the current configuration $\Omega_f(t)$ by a smooth map $\boldsymbol{\varphi}_f$ defined by

$$\begin{aligned} \boldsymbol{\varphi}_f(.,t) : \tilde{\Omega}_f &\longrightarrow \Omega_f(t) \\ \tilde{\boldsymbol{x}} &\longrightarrow \boldsymbol{\varphi}_f(\tilde{\boldsymbol{x}},t) = \boldsymbol{x} \quad \text{for } t\in(0,T). \end{aligned} \tag{2.14}$$

In what follows elements in the reference configuration are characterized by the symbol "$\tilde{}$". In particular, the velocity and the pressure are given in the reference configuration $\tilde{\Omega}_f$ as

$$\tilde{\boldsymbol{v}}(\tilde{\boldsymbol{x}},t) = \boldsymbol{v}(\boldsymbol{\varphi}_f(\tilde{\boldsymbol{x}},t),t) \quad \text{and} \quad \tilde{p}_f(\tilde{\boldsymbol{x}},t) = p_f(\boldsymbol{\varphi}_f(\tilde{\boldsymbol{x}},t),t), \qquad \forall\, \tilde{\boldsymbol{x}}\in\tilde{\Omega}_f.$$

The variable $\partial_t\boldsymbol{\varphi}_f$ which appears in the formulation of the Navier-Stokes equations on the reference configuration corresponds to the velocity of the domain.
Using formulas of transformation between reference and actual configuration [Ric17, Section 2.1] we have

$$\begin{aligned} \partial_t\boldsymbol{v} &= \partial_t\tilde{\boldsymbol{v}} - (\boldsymbol{F}_f^{-1}\partial_t\boldsymbol{\varphi}_f\cdot\nabla_{\tilde{\boldsymbol{x}}})\tilde{\boldsymbol{v}}, \\ (\boldsymbol{v}\cdot\nabla_{\boldsymbol{x}})\boldsymbol{v} &= \boldsymbol{\nabla}_{\boldsymbol{x}}\boldsymbol{v}\boldsymbol{v} = \boldsymbol{\nabla}_{\tilde{\boldsymbol{x}}}\tilde{\boldsymbol{v}}\boldsymbol{F}_f^{-1}\tilde{\boldsymbol{v}} = (\boldsymbol{F}_f^{-1}\tilde{\boldsymbol{v}}\cdot\nabla_{\tilde{\boldsymbol{x}}})\tilde{\boldsymbol{v}}, \end{aligned}$$

which yields

$$\partial_t \boldsymbol{v} + (\boldsymbol{v}\cdot\nabla_{\boldsymbol{x}})\boldsymbol{v} = \partial_t \tilde{\boldsymbol{v}} + \big(\boldsymbol{F}_f^{-1}(\tilde{\boldsymbol{v}} - \partial_t \boldsymbol{\varphi}_f)\cdot\nabla_{\tilde{\boldsymbol{x}}}\big)\tilde{\boldsymbol{v}}, \qquad \text{on} \quad \tilde{\Omega}_f, \tag{2.15}$$

where $\boldsymbol{F}_f = \boldsymbol{\nabla}_{\tilde{\boldsymbol{x}}}\boldsymbol{\varphi}_f$ and $J_f = \det(\boldsymbol{F}_f)$.
For the stress tensor we have

$$\boldsymbol{\nabla}_x \cdot \boldsymbol{\sigma}_f(\boldsymbol{v}, p_f) = \widetilde{\operatorname{div}}\big(J_f \tilde{\boldsymbol{\sigma}}(\tilde{\boldsymbol{v}}, \tilde{p}_f)\boldsymbol{F}_f^{-t}\big),$$

with

$$\tilde{\boldsymbol{\sigma}}_f(\tilde{\boldsymbol{v}}, \tilde{p}_f) = \mu\Big(\boldsymbol{\nabla}_{\tilde{\boldsymbol{x}}}\tilde{\boldsymbol{v}}\ \boldsymbol{F}_f^{-1} + \boldsymbol{F}_f^{-t}\ (\boldsymbol{\nabla}_{\tilde{\boldsymbol{x}}}\tilde{\boldsymbol{v}})^t\Big) - \tilde{p}_f\ \mathbf{Id}.$$

Hence, the Navier-Stokes equations are written on the reference configuration $\tilde{\Omega}_f$ as follows

$$\begin{cases} \rho_f J_f\big[\partial_t \tilde{\boldsymbol{v}} + \big(\boldsymbol{F}_f^{-1}(\tilde{\boldsymbol{v}} - \partial_t\boldsymbol{\varphi}_f)\cdot\nabla_{\tilde{\boldsymbol{x}}}\big)\tilde{\boldsymbol{v}}\big] - \widetilde{\operatorname{div}}\Big(J_f\tilde{\boldsymbol{\sigma}}_f(\tilde{\boldsymbol{v}}, \tilde{p}_f)\boldsymbol{F}_f^{-t}\Big) = J_f\rho_f\tilde{\boldsymbol{f}}_f & \text{in} \quad \tilde{\Omega}_f \times (0,T), \\ \widetilde{\operatorname{div}}(J_f\boldsymbol{F}_f^{-1}\tilde{\boldsymbol{v}}) = 0 & \text{on} \quad \tilde{\Omega}_f \times (0,T), \\ \tilde{\boldsymbol{v}} = \boldsymbol{v}_{\text{in}} \circ \boldsymbol{\varphi}_f & \text{on} \quad \tilde{\Gamma}_{\text{in}} \times (0,T), \\ J_f\tilde{\boldsymbol{\sigma}}_f(\tilde{\boldsymbol{v}}, \tilde{p}_f)\boldsymbol{F}_f^{-t}\ \tilde{\boldsymbol{n}}_f = 0 & \text{on} \quad \tilde{\Gamma}_{\text{out}} \times (0,T), \\ J_f\tilde{\boldsymbol{\sigma}}_f(\tilde{\boldsymbol{v}}, \tilde{p}_f)\boldsymbol{F}_f^{-t}\ \tilde{\boldsymbol{n}}_f = J_f\tilde{\boldsymbol{g}}_f & \text{on} \quad \tilde{\Gamma}_f \times (0,T), \end{cases} \tag{2.16}$$

where $\tilde{\boldsymbol{f}}_f = \boldsymbol{f}_f \circ \boldsymbol{\varphi}_f$ and $\tilde{\boldsymbol{g}}_f = \boldsymbol{g}_f \circ \boldsymbol{\varphi}_f$.

Remark 2.1.1 *If the domain $\tilde{\Omega}_f$ is considered to be the Lagrangian reference configuration, then $\partial_t\boldsymbol{\varphi}_f = \tilde{\boldsymbol{v}}$. Hence, $(2.16)_1$ reduces to*

$$\rho_f J_f \partial_t \tilde{\boldsymbol{v}} - \widetilde{\operatorname{div}}\Big(J_f\tilde{\boldsymbol{\sigma}}_f(\tilde{\boldsymbol{v}}, \tilde{p}_f)\boldsymbol{F}_f^{-t}\Big) = J_f\rho_f\tilde{\boldsymbol{f}}_f \qquad \text{on} \quad \tilde{\Omega}_f \times (0,T). \tag{2.17}$$

2.1.3 The Navier-Stokes Equations in the ALE Frame

In some cases, as in the case of blood flowing in the arteries, the computational domain of the fluid cannot be considered to be fixed in time. In fact, its motion has to obey the motion of the common boundary. This issue leads to the introduction of the Arbitrary Lagrangian Eulerian (ALE) frame. Thus, we consider a computational domain $\Omega_f(t)$ which is neither fixed nor material. The ALE formulation of the fluid motion is based on the parametrization of the motion of $\Omega_f(t)$ by a smooth map

$$\begin{aligned} \boldsymbol{\mathcal{A}}(.,t) : \tilde{\Omega}_f &\longrightarrow \Omega_f(t) \\ \tilde{\boldsymbol{x}} &\longrightarrow \boldsymbol{\mathcal{A}}(\tilde{\boldsymbol{x}}, t) = \boldsymbol{x} \quad \text{for } t \in (0,T), \end{aligned} \tag{2.18}$$

that is, $\Omega_f(t) = \boldsymbol{\mathcal{A}}(\tilde{\Omega}_f, t)$.

As $\boldsymbol{\mathcal{A}}(.,t)$ is fixed for any t, we can also denote this map by $\boldsymbol{\mathcal{A}}_t(.)$. The map $\boldsymbol{\mathcal{A}}$ is called the *ALE map*. The initial fixed configuration $\tilde{\Omega}_f$ corresponds to the reference configuration, which does not necessarily correspond to the initial position at $t = 0$. In the ALE formulation, we distinguish between two motions; the motion of the medium in $\Omega_f(t)$ which is governed by the physical laws, and the motion of the computational domain, which is arbitrary, taking into consideration that the given law for the domain boundary movement is respected.

The ALE map gives data on the deformation of the domain at any time $t \geq 0$. For any function $\tilde{f} \in \tilde{\Omega}_f \times [0,T] \longrightarrow \mathbb{R}$, we define its Eulerian counterpart by

$$f(\boldsymbol{x},t) = \tilde{f}(\boldsymbol{\mathcal{A}}_t^{-1}(\boldsymbol{x}),t), \qquad \forall\, \boldsymbol{x} \in \Omega_f(t),\ t \geq 0, \tag{2.19}$$

which can also be written as $f(.,t) = \tilde{f} \circ \boldsymbol{\mathcal{A}}_t^{-1}(.)$. Based on the fact that the velocity is a kinematic quantity, defined as the time derivative of the displacement $\boldsymbol{x} = \boldsymbol{\mathcal{A}}_t(\tilde{\boldsymbol{x}}) - \tilde{\boldsymbol{x}}$, then we can define the ALE velocity, as

$$\tilde{\boldsymbol{w}} = \frac{\partial \boldsymbol{\mathcal{A}}}{\partial t}(\tilde{\boldsymbol{x}},t), \qquad \forall\, \tilde{\boldsymbol{x}} \in \tilde{\Omega}_f, \tag{2.20}$$

which can be given in the Eulerian frame using (2.19) as $\boldsymbol{w}(\boldsymbol{x},t) = \tilde{\boldsymbol{w}} \circ \boldsymbol{\mathcal{A}}^{-1}(\boldsymbol{x},t)$, for any $\boldsymbol{x} \in \Omega_f(t)$. In short hand notation, $\boldsymbol{w} = \partial_t \boldsymbol{\mathcal{A}}_t \circ \boldsymbol{\mathcal{A}}_t^{-1}$.

The ALE time derivative of any function f defined in the Eulerian frame, is given by

$$\partial_t f|_{\boldsymbol{\mathcal{A}}} = \partial_t f + \boldsymbol{w} \cdot \boldsymbol{\nabla}_{\boldsymbol{x}} f. \tag{2.21}$$

which can be expressed in terms of its counter part $\tilde{f}$ defined in the ALE frame by the relation

$$\partial_t f|_{\boldsymbol{\mathcal{A}}}(\boldsymbol{x},t) = \partial_t \tilde{f} \circ \boldsymbol{\mathcal{A}}^{-1}(\boldsymbol{x},t), \qquad \forall\, (\boldsymbol{x},t) \in \Omega_f(t) \times (0,T).$$

Applying (2.21) on $\boldsymbol{v}$ then combining it with (2.2) we get the non-conservative form of the incompressible Navier-Stokes equations in the ALE frame

$$\rho_f \Big(\partial_t \boldsymbol{v}|_{\boldsymbol{\mathcal{A}}} + (\boldsymbol{v} - \boldsymbol{w})^t \boldsymbol{\nabla} \boldsymbol{v} \Big) - \boldsymbol{\nabla} \cdot \boldsymbol{\sigma}_f(\boldsymbol{v}, p_f) = \rho_f \boldsymbol{f}_f \qquad \text{on } \Omega_f(t) \times (0,T). \tag{2.22}$$

The equation (2.22) must be completed with compatible boundary conditions. We impose the following boundary conditions

$$\begin{cases} \boldsymbol{v} = \boldsymbol{v}_{\text{in}} & \text{on} \quad \Gamma_{\text{in}}(t) \times (0,T), \\ \boldsymbol{\sigma}_f(\boldsymbol{v}, p_f)\ \boldsymbol{n}_f = 0 & \text{on} \quad \Gamma_{\text{out}}(t) \times (0,T), \\ \boldsymbol{\sigma}_f(\boldsymbol{v}, p_f)\ \boldsymbol{n}_f = \boldsymbol{g}_f & \text{on} \quad \Gamma_f(t) \times (0,T). \end{cases} \tag{2.23}$$

By these conditions we impose a given velocity $\boldsymbol{v}_{\text{in}}$ on the inlet of the fluid domain, and a given surface density load $\boldsymbol{g}_f$ on the surrounding boundary $\Gamma_f(t)$. Moreover, a free-exit condition is enforced on the outlet $\Gamma_{\text{out}}(t)$.

The time derivative in the ALE frame constitutes the main tool when performing simulations for fluids in moving domains. In fact, if we consider working with Eulerian derivatives in moving domains, then discretization cannot be performed. Indeed, a point $\boldsymbol{x}$ of the domain at the time step t_{n-1} would not necessarily be on it at the time step t_n, and vice versa. Then to overcome this obstacle we must track the points of the domain that accompany its evolution.

In order to solve these equations, the map $\boldsymbol{\mathcal{A}}$ should be known. In general no information is provided on this map nor on the time derivative of the velocity in the ALE frame or any other related quantities. Only the boundary displacement $\boldsymbol{\xi}$ is known. Then using an appropriate extension operator [Ric17, Section 5.3, pp. 247], the ALE map is given by the following expression

$$\boldsymbol{\mathcal{A}}_t(\tilde{\boldsymbol{x}}) = \tilde{\boldsymbol{x}} + \mathcal{E}xt(\boldsymbol{\xi}(\tilde{\boldsymbol{x}}, t)\big|_{\partial\Omega_f}).$$

The notation $\mathcal{E}xt$ stands for an appropriate extension of the boundary displacement $\boldsymbol{\xi}$.

Remark 2.1.2 *In general $\boldsymbol{w}(\boldsymbol{x}, t) \neq \boldsymbol{v}(\boldsymbol{x}, t)$. But we should note out two cases:*

1. $\boldsymbol{w} = 0$ *: The domain is fixed, and we consider working with the initial configuration $\tilde{\Omega}_f$. In other words, the Eulerian formulation is recovered.*

2. $\boldsymbol{w} = \boldsymbol{u}$ *: The domain $\tilde{\Omega}_f$ is material and we track its displacement. That is, the Lagrangian formulation is recovered.*

2.2 Arterial Wall Modeling by the Elastodynamic Equations

Even though the arterial wall looks thin, it is composed of numerous number of layers as shown in Figure 2.3.

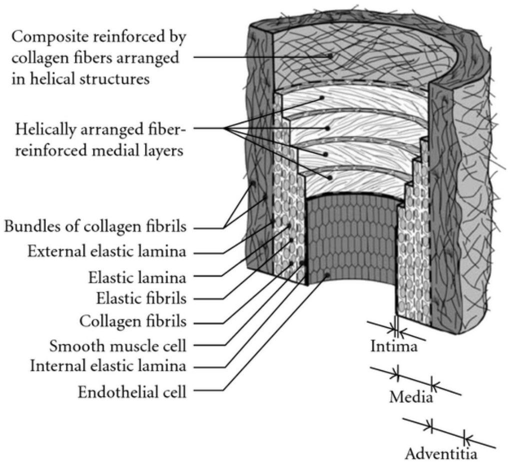

Figure 2.3: The layers of the arterial wall [HGO00].

Elasticity of the arterial wall depends on the number of collagen and elastin filaments in the tunica media, which gives it the ability to stretch in response to each pulse. Moreover, it helps to maintain a relatively constant pressure in the arteries despite the pulsating nature of the blood flow. By elasticity we mean the ability of a body to resist a distorting influence or an external stress and to recover its original size and shape when the stresses or exerted forces are removed. Solid objects deform when forces are applied on them. If the material is elastic, the object will return to its initial shape and size upon removing these forces.

Some arteries show viscoelastic properties, however, they are usually of small magnitude so that the arterial wall can be modeled as a hyperelastic incompressible material. Elastic arteries include the largest arteries in the body, those closest to the heart. The artery wall being considered as a structure is modeled by the elastodynamic equations. The derivation of these equations is achieved using the conservation principles [FQV09, Section 3.3], [Ric17, Chapter 2].

The elasticity of the artery wall will be the subject of our study in this section. We highlight the case of non-linear and linear elastic structures.

Let $\tilde{\Omega}_s$ be a region that represents the reference configuration of the structure domain at a given instant $t_0 \geq 0$, and $\Omega_s(t)$ be the domain corresponding to the deformed structure at time $t > t_0$, generated by the deformation map $\boldsymbol{\varphi}_s$. The actual configuration $\Omega_s(t)$ of density ρ_s, is under the effect of an external volumetric force $\boldsymbol{f}_s$ and the stress is represented by the Cauchy stress tensor $\boldsymbol{\sigma}_s$. The structure is adopted using the Lagrangian approach, that is, unlike Navier-Stokes equations no convective term appears. The elasticity equation aims to find the displacement field $\tilde{\boldsymbol{\xi}}_s : \tilde{\Omega}_s \times \mathbb{R}^+ \longrightarrow \mathbb{R}^3$ of the structure. At any time t, the displacement $\tilde{\boldsymbol{\xi}}_s$ is expressed as a function of the deformation $\boldsymbol{\varphi}_s$ as

$$\tilde{\boldsymbol{\xi}}_s(\tilde{\boldsymbol{x}}, t) = \boldsymbol{\varphi}_s(\tilde{\boldsymbol{x}}, t) - \tilde{\boldsymbol{x}}, \qquad \forall\, \tilde{\boldsymbol{x}} \in \tilde{\Omega}_s.$$

The deformation map $\boldsymbol{\varphi}_s : \tilde{\Omega}_s \times \mathbb{R}^+ \longrightarrow \mathbb{R}^3$, is a smooth application of class $\mathcal{C}^1$ at least, such that $J_s = \det(\boldsymbol{\nabla}_{\tilde{\boldsymbol{x}}} \boldsymbol{\varphi}_s) > 0$. Hence, it is invertible and we consider its inverse $\boldsymbol{\varphi}_s^{-1}$ to be of class $\mathcal{C}^1$ as well. Indeed, we can assume that $\boldsymbol{\varphi}_s$ is as smooth as needed so that all mathematical operations performed are justified (for instance, differentiation of integral depending on parameter, integration by parts, etc.). In what follows we set

$$\boldsymbol{F}_s = \boldsymbol{\nabla}_{\tilde{\boldsymbol{x}}} \boldsymbol{\varphi}_s, \quad \tilde{\boldsymbol{f}}_s = \boldsymbol{f}_s \circ \boldsymbol{\varphi}_s, \quad \text{and} \quad \tilde{\rho}_s = \rho_s \circ \boldsymbol{\varphi}_s.$$

In the Lagrangian frame, the momentum equation is

$$\frac{d}{dt} \int_{\tilde{\Omega}_s} J_s \tilde{\rho}_s \partial_t \tilde{\boldsymbol{\xi}}_s \, d\tilde{\boldsymbol{x}} = \int_{\tilde{\Omega}_s} J_s \tilde{\rho}_s \tilde{\boldsymbol{f}}_s \, d\tilde{\boldsymbol{x}} - \int_{\tilde{\Omega}_s} J_s [\boldsymbol{\nabla}_{\boldsymbol{x}} \cdot \boldsymbol{\sigma}_s(\boldsymbol{x})] \circ \boldsymbol{\varphi}_s \, d\tilde{\boldsymbol{x}}.$$

Combining this equation with the continuity equation (A.2) we get the elastodynamic equation given on the reference configuration as

$$J_s \tilde{\rho}_s \partial_t^2 \tilde{\boldsymbol{\xi}}_s - J_s [\boldsymbol{\nabla}_{\boldsymbol{x}} \cdot \boldsymbol{\sigma}_s(\boldsymbol{x})] \circ \boldsymbol{\varphi}_s = J_s \tilde{\rho}_s \tilde{\boldsymbol{f}}_s, \qquad \text{on } \tilde{\Omega}_s \times (0, T). \tag{2.24}$$

Note that the divergence of $\boldsymbol{\sigma}_s$ is defined on $\Omega_s(t)$. We make use of (A.8) and (A.9) to reformulate it in terms of the divergence of the first Piola-Kirchhoff stress tensor $\boldsymbol{P}$ on $\tilde{\Omega}_s$. In other words, we get the term [Ric17, Lemma 2.12, p. 31]

$$\boldsymbol{\nabla}_{\tilde{\boldsymbol{x}}} \cdot \boldsymbol{P}(\tilde{\boldsymbol{x}}).$$

Therefore, the elastodynamic equation is

$$\boxed{J_s \tilde{\rho}_s \partial_t^2 \tilde{\boldsymbol{\xi}}_s - \boldsymbol{\nabla}_{\tilde{\boldsymbol{x}}} \cdot \boldsymbol{P} = J_s \tilde{\rho}_s \tilde{\boldsymbol{f}}_s. \qquad (2.25)}$$

Since we are dealing with a non-linear structure, then the map $\boldsymbol{\varphi}_s$ is unknown, consequently the actual deformed configuration $\Omega_s(t)$ is unknown. This explains the efficiency of writing the elastodynamic equations on the given reference configuration $\tilde{\Omega}_s$.

We assume that the structure is a homogeneous incompressible hyperelastic material governed by the equation (2.25). Hence, its density is constant, i.e, $\tilde{\rho}_s = \rho_s$. The incompressibility condition is represented by

$$J_s = 1.$$

Definition 2.2.1 (Hyperelasticity) [Ric17, Section 2.2] *A structure is said to be hyperlastic if there exists a function W called the strain-energy density function $W = W(\boldsymbol{F}_s)$ or $W = W(\boldsymbol{E})$ such that*

$$\boldsymbol{P} = \frac{\partial W(\boldsymbol{F}_s)}{\partial \boldsymbol{F}_s}, \quad \text{or} \quad \boldsymbol{S} = \frac{\partial W(\boldsymbol{E})}{\partial \boldsymbol{E}}.$$

This function relates the first Piola-Kirchhoff stress tensor $\boldsymbol{P}$ to the deformation gradient $\boldsymbol{F}_s$, or the second Piola-Kirchhoff stress tensor $\boldsymbol{S}$ to the Green-Lagrange strain tensor $\boldsymbol{E}$ given by the expression [Ric17, Section 2.1.3]

$$\boldsymbol{E}(\boldsymbol{F}_s) = \frac{1}{2}(\boldsymbol{F}_s^t \boldsymbol{F}_s - \mathbf{Id}). \tag{2.26}$$

In the case of an incompressible material, the strain-energy density functions are of the following form

$$W_{\text{inc}} = W(\boldsymbol{F}_s) + p_{hs}(\det(\boldsymbol{F}_s) - 1) \tag{2.27}$$

where p_{hs} plays the role of the Lagrange multiplier associated to the incompressibility condition $\det(\boldsymbol{F}_s) = 1$. The variable p_{hs} is known as the *hydrostatic pressure*. On the other hand, if the structure is a quasi-incompressible material then the strain-energy density functions are of the form

$$W_{\text{Qinc}} = W(\boldsymbol{F}_s) + \frac{\mathsf{C}}{2}(\det(\boldsymbol{F}_s) - 1)^2 \tag{2.28}$$

where C is a sufficiently large constant.

The boundary $\partial\tilde{\Omega}_s$ is composed of two parts (see Figure 2.4) the outer part with the left and right edges are denoted by $\tilde{\Gamma}_1$, and the inner part is $\tilde{\Gamma}_2$. We assume that the structure is fixed at $\tilde{\Gamma}_2$, that is,

$$\tilde{\boldsymbol{\xi}}_s(\tilde{\boldsymbol{x}}, t) = 0 \qquad \text{on} \quad \tilde{\Gamma}_2 \times (0, T). \tag{2.29}$$

On the contrary, its inner wall is subjected to a normal force, this condition reads

$$\boldsymbol{P}_{\text{inc}} \tilde{\boldsymbol{n}}_s = \tilde{\boldsymbol{g}}_s \qquad \text{on} \quad \tilde{\Gamma}_1 \times (0, T), \tag{2.30}$$

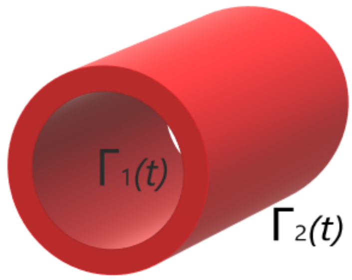

Figure 2.4: A three dimensional arterial wall.

where $\tilde{\boldsymbol{n}}_s$ is the outward normal vector to the boundary $\tilde{\Gamma}_1$.
To sum up, the elastodynamic equations on the reference configuration $\tilde{\Omega}_s$ are

$$\begin{cases} J_s\rho_s\partial_t^2\tilde{\boldsymbol{\xi}}_s - \boldsymbol{\nabla}_{\tilde{\boldsymbol{x}}}\cdot\boldsymbol{P}_{\text{inc}} = J_s\rho_s\tilde{\boldsymbol{f}}_s & \text{on } \tilde{\Omega}_s\times(0,T), \\ J_s = 1 & \text{on } \tilde{\Omega}_s\times(0,T), \\ \boldsymbol{P}_{\text{inc}}\tilde{\boldsymbol{n}}_s = \tilde{\boldsymbol{g}}_s & \text{on } \tilde{\Gamma}_1\times(0,T), \\ \tilde{\boldsymbol{\xi}}_s(\tilde{\boldsymbol{x}},t) = 0 & \text{on } \tilde{\Gamma}_2\times(0,T), \end{cases} \tag{2.31}$$

where $\boldsymbol{P}_{\text{inc}} = \boldsymbol{P} + p_{hs}\text{cof}(\boldsymbol{F}_s)$.

The resultant system is of insufficient number of partial differential equations of -in general- ten unknowns: density (respectively pressure) ρ_s (respectively p_s), the velocity $\partial_t\tilde{\boldsymbol{\xi}}_s$ and the six components of the Cauchy stress tensor $\boldsymbol{\sigma}_s$ (or the first Piola-Kirchhoff stress tensor $\boldsymbol{P}$). This will lead to undetermined system! For this purpose, additional equations are essential. The purpose of these equations is to build a link between two physical quantities especially a non-linear relation between kinetic and kinematic. In both fluid mechanics and structural analysis these equations relate applied stresses or forces to the velocity or the density or the deformation. We assume that the stress tensors depend on the strain, strain rate or the deformation gradient $\boldsymbol{F}_s$. We will adopt the Saint-Venant Kirchhoff model whose strain-energy density function W is given by

$$W(\boldsymbol{E}) = \frac{\lambda_s}{2}\Big(\text{tr}(\boldsymbol{E})\Big)^2 + \mu_s\text{tr}(\boldsymbol{E}^2), \tag{2.32}$$

where λ_s and μ_s are the Lamé constants. The second Piola-Kirchhoff stress tensor $\boldsymbol{S}$ associated to the Saint-Venant Kirchhoff model is

$$\boldsymbol{S}(\boldsymbol{E}) = 2\mu_s\boldsymbol{E} + \lambda_s\text{tr}(\boldsymbol{E})\mathbf{Id}. \tag{2.33}$$

Using the relation $\boldsymbol{P} = \boldsymbol{F}_s\boldsymbol{S}$ between the first and the second Piola-Kirchhoff stress tensors we get

$$\boldsymbol{P}(\boldsymbol{F}_s) = \boldsymbol{F}_s\Big(2\mu_s\boldsymbol{E} + \lambda_s\text{tr}(\boldsymbol{E})\mathbf{Id}\Big).$$

Linear Elastic Equation

A simple case is the case of a linear elastic material. These materials are characterized by a linear relation between the strain $\boldsymbol{\varepsilon}$ and the stress $\boldsymbol{\sigma}_s$, given by Hooke's law. If a linear elastic material is under the effect of an external force, when removed, it returns to the original shape. In addition, if an elastic material undergoes a small deformation, so that, the deformation map can be approximated by the identity mapping Id_{Ω_s}, then the associated constitutive law is linearized and can be considered as a linear elastic model. Indeed, in this case the Green-Lagrange strain tensor $\boldsymbol{E}$ can be approximated by the linearized strain tensor $\boldsymbol{\varepsilon}$ given by the formula

$$\boldsymbol{\varepsilon}(\boldsymbol{\xi}_s) = \frac{1}{2}(\boldsymbol{\nabla}\boldsymbol{\xi}_s + \boldsymbol{\nabla}^t\boldsymbol{\xi}_s).$$

The well-known Hooke's law associated to the linear elastic materials has the following Cauchy stress tensor

$$\boldsymbol{\sigma}_s(\boldsymbol{\xi}_s) = 2\mu_s\boldsymbol{\varepsilon}(\boldsymbol{\xi}_s) + \lambda_s \mathrm{tr}(\boldsymbol{\varepsilon}(\boldsymbol{\xi}_s))\mathbf{Id}. \tag{2.34}$$

As $\mathrm{tr}(\boldsymbol{\varepsilon}(\boldsymbol{\xi}_s)) = \nabla \cdot \boldsymbol{\xi}_s$, then Hooke's Law can be rewritten as

$$\boldsymbol{\sigma}_s(\boldsymbol{\xi}_s) = 2\mu_s\boldsymbol{\varepsilon}(\boldsymbol{\xi}_s) + \lambda_s(\nabla \cdot \boldsymbol{\xi}_s)\mathbf{Id}. \tag{2.35}$$

The parameters λ_s and μ_s are the Lamé constants given in terms of the Young's modulus E and the Poisson's ratio ν by the following relations

$$\lambda_s = \frac{\nu E}{(1-2\nu)(1+\nu)} \quad \text{and} \quad \mu_s = \frac{E}{2(1+\nu)}.$$

Now we proceed to give the equation that models the linear elastic isotropic incompressible materials. Since the deformation mapping is the identity mapping, then $\boldsymbol{F}_s$ is the identity matrix $\mathbf{Id}_{\mathbb{M}_3}$, consequently $J_s = 1$. Thus, Equation (2.31) is

$$\begin{cases} \rho_s\partial_t^2\boldsymbol{\xi}_s - \boldsymbol{\nabla}\cdot\boldsymbol{\sigma}_s(\boldsymbol{\xi}_s) = \rho_s\boldsymbol{f}_s & \text{in } \Omega_s(t)\times(0,T). \\ \nabla\cdot\boldsymbol{\xi}_s = 0 & \text{in } \Omega_s(t)\times(0,T), \\ \boldsymbol{\sigma}_s(\boldsymbol{\xi}_s)\ \boldsymbol{n}_s = \boldsymbol{g}_s & \text{on } \Gamma_1(t)\times(0,T), \\ \boldsymbol{\xi}_s = 0 & \text{on } \Gamma_2(t)\times(0,T), \end{cases} \tag{2.36}$$

For more details about the linearization, the interested reader can consult [FQV09, Chapter 3, p.103].

2.3 The Fluid Structure Interaction Problem

The fluid-structure interaction problem describing the blood-wall model is set up using the Navier-Stokes equations and the elastodynamic equations introduced in Sections 2.1 and 2.2, respectively. In this case, the computational fluid domain cannot be fixed in time since it is affected by the deformation of the artery wall, consequently it must follow the motion of the common interface. Thus, we consider a domain $\Omega_f(t)$ which is neither fixed, nor a material.

Indeed, this is due to the fact that its evolution does not agree with the fluid motion, rather, obeys the displacement of its boundary $\partial\Omega_f(t)$ which, due to the coupling, is linked to the displacement of the artery wall $\tilde{\xi}_s$. With the same notion as above, elements in the reference configurations are characterized by the symbol "˜".

To couple the sub-problems, we must ensure a global energy balance of the system. For this aim, three interface coupling conditions must be imposed.

Geometry Condition

The aim is to construct the ALE map $\boldsymbol{\mathcal{A}}$ using the deformation $\boldsymbol{\varphi}_s$ of the structure. Indeed, we impose that the moving domain $\Omega_f(t)$ follows the motion of the interface $\tilde{\Gamma}_c = \partial\tilde{\Omega}_f \cap \partial\tilde{\Omega}_s = \tilde{\Gamma}_1 \equiv \tilde{\Gamma}_f$. This is to say

$$\boldsymbol{\mathcal{A}}_t = \boldsymbol{\varphi}_s \qquad \text{on} \quad \tilde{\Gamma}_c \tag{2.37}$$

This condition can be rewritten as a relation between the displacement of the volume $\tilde{\Omega}_f$ and the displacement $\tilde{\boldsymbol{\xi}}_s$ of the structure domain $\tilde{\Omega}_s$. Using the definition of the ALE map, the displacement $\tilde{\boldsymbol{\xi}}_f : \tilde{\Omega}_f \times \mathbb{R}^+ \to \mathbb{R}^3$ of the fluid domain $\tilde{\Omega}_f$ is defined by

$$\tilde{\boldsymbol{\xi}}_f(\tilde{\boldsymbol{x}}, t) = \boldsymbol{\mathcal{A}}_t(\tilde{\boldsymbol{x}}) - \tilde{\boldsymbol{x}}, \qquad \forall\, \tilde{\boldsymbol{x}} \in \tilde{\Omega}_f$$

Hence, (2.37) reduces to

$$\tilde{\boldsymbol{\xi}}_f = \tilde{\boldsymbol{\xi}}_s \qquad \text{on} \quad \tilde{\Gamma}_c. \tag{2.38}$$

The term $\tilde{\boldsymbol{\xi}}_f$ is the displacement of the domain $\tilde{\Omega}_f$, thus, differentiating it in time gives the velocity of the domain denoted by $\tilde{\boldsymbol{w}}$. Whence, differentiating (2.38) in time yields

$$\tilde{\boldsymbol{w}} = \partial_t \tilde{\boldsymbol{\xi}}_s \qquad \text{on} \quad \tilde{\Gamma}_c \tag{2.39}$$

By (2.13) we have that the boundaries $\tilde{\Gamma}_{\text{in}}$, $\tilde{\Gamma}_{\text{out}}$ are fixed, consequently the displacement $\tilde{\boldsymbol{\xi}}_f$ is null on these boundaries. On the contrary, no information on $\tilde{\boldsymbol{\xi}}_f$ is provided inside $\tilde{\Omega}_f$, therefore it can be considered as any arbitrary extension of the artery wall displacement $\tilde{\boldsymbol{\xi}}_s$. This is described as

$$\tilde{\boldsymbol{\xi}}_f(\tilde{\boldsymbol{x}}, t) = \mathcal{E}xt(\tilde{\boldsymbol{\xi}}_s(\tilde{\boldsymbol{x}}, t)|_{\tilde{\Gamma}_c}) \qquad \text{in} \quad \tilde{\Omega}_f \times (0, T). \tag{2.40}$$

Types of possible extensions can be found in [Ric17, Section 5.3, pp. 247], [Cha13, Chapter 2].

Velocity and Stress Conditions

Due to the viscosity of the fluid, it becomes in contact with the interface and may stick to it. For this reason, the velocity fields must be continuous on the interface. Therefore, we set

$$\boldsymbol{v} = \partial_t \tilde{\boldsymbol{\xi}}_s \circ \boldsymbol{\varphi}_s^{-1} \qquad \text{on} \quad \Gamma_c(t).$$

To simplify the notation we use (2.37) and (2.39) to get

$$\boldsymbol{v} = \tilde{\boldsymbol{w}} \circ \boldsymbol{\mathcal{A}}^{-1} = \boldsymbol{w} \qquad \text{on} \quad \Gamma_c(t). \tag{2.41}$$

Finally, Newton's third law (action-reaction principle) states :"*For every action, there is an equal and opposite reaction*". Hence, due to the interaction between the fluid and the structure, the force exerted by the fluid on the structure is equal and opposite to the force exerted by the structure on the fluid. On the interface $\tilde{\Gamma}_c$, the existing surface forces are characterized by the stresses. Thus, the following condition

$$J_f \tilde{\boldsymbol{\sigma}}_f(\tilde{\boldsymbol{v}}, \tilde{p}_f) \boldsymbol{F}_f^{-t} \, \tilde{\boldsymbol{n}}_f = -\boldsymbol{P}_{\text{inc}} \tilde{\boldsymbol{n}}_s \qquad \text{on} \quad \tilde{\Gamma}_c \times (0, T) \tag{2.42}$$

must hold. The condition (2.41) is a kinematic condition, whereas (2.42) is a dynamic one.

The Coupled Fluid-Structure Problem

Using the sub-problems (2.22) and (2.31) with the boundary conditions (2.23),(2.29) and (2.30) together with the coupling conditions (2.40)-(2.42), the coupled problem reads:

Find

$$\tilde{\boldsymbol{v}} : \tilde{\Omega}_f \times \mathbb{R}^+ \longrightarrow \mathbb{R}^3,$$
$$\tilde{p}_f : \tilde{\Omega}_f \times \mathbb{R}^+ \longrightarrow \mathbb{R},$$
$$\tilde{\boldsymbol{\xi}}_{\boldsymbol{f}} : \tilde{\Omega}_f \times \mathbb{R}^+ \longrightarrow \mathbb{R}^3,$$
$$\tilde{\boldsymbol{\xi}}_s : \tilde{\Omega}_s \times \mathbb{R}^+ \longrightarrow \mathbb{R}^3,$$
$$\tilde{p}_{hs} : \tilde{\Omega}_s \times \mathbb{R} \longrightarrow \mathbb{R},$$

such that,

- **Fluid sub-problem**

$$\begin{cases} \rho_f \partial_t \boldsymbol{v}|_{\boldsymbol{\mathcal{A}}} + \rho_f (\boldsymbol{v} - \boldsymbol{w})^t \boldsymbol{\nabla}_{\boldsymbol{x}} \boldsymbol{v} - \boldsymbol{\nabla}_{\boldsymbol{x}} \cdot \boldsymbol{\sigma}_f(\boldsymbol{v}, p_f) = \rho_f \boldsymbol{f}_f & \text{on} \quad \Omega_f(t) \times (0, T), \\ \nabla_{\boldsymbol{x}} \cdot \boldsymbol{v} = 0 & \text{on} \quad \Omega_f(t) \times (0, T), \\ \boldsymbol{v} = \boldsymbol{v}_{\text{in}} & \text{on} \quad \Gamma_{\text{in}}(t) \times (0, T), \\ \boldsymbol{\sigma}_f(\boldsymbol{v}, p_f) \; \boldsymbol{n}_f = 0 & \text{on} \quad \Gamma_{\text{out}}(t) \times (0, T), \\ \boldsymbol{\sigma}_f(\boldsymbol{v}, p_f) \; \boldsymbol{n}_f = \boldsymbol{g}_f & \text{on} \quad \Gamma_f(t) \times (0, T), \end{cases} \tag{2.43}$$

- **Structure sub-problem**

$$\begin{cases} J_s \tilde{\rho}_s \partial_t^2 \tilde{\boldsymbol{\xi}}_s - \boldsymbol{\nabla}_{\tilde{\boldsymbol{x}}} \cdot \boldsymbol{P}_{\text{inc}} = J_s \tilde{\rho}_s \tilde{\boldsymbol{f}}_s & \text{on} \quad \tilde{\Omega}_s \times (0, T), \\ J_s = 1 & \text{on} \quad \tilde{\Omega}_s \times (0, T), \\ \boldsymbol{P}_{\text{inc}} \; \tilde{\boldsymbol{n}}_s = \tilde{\boldsymbol{g}}_s & \text{on} \quad \tilde{\Gamma}_1 \times (0, T), \\ \tilde{\boldsymbol{\xi}}_s = 0 & \text{on} \quad \tilde{\Gamma}_2 \times (0, T), \end{cases} \tag{2.44}$$

- **Coupling Conditions**

$$\begin{cases} \tilde{\boldsymbol{\xi}}_f = \mathcal{E}xt(\tilde{\boldsymbol{\xi}}_s|_{\tilde{\Gamma}_c}), & \text{in} \quad \tilde{\Omega}_f \times (0,T), \\ \Omega_f(t) = \boldsymbol{\mathcal{A}}_t(\tilde{\Omega}_f), & \\ \tilde{\boldsymbol{w}} = \partial_t \tilde{\boldsymbol{\xi}}_f & \text{in} \quad \tilde{\Omega}_f \times (0,T), \\ \boldsymbol{v} = \boldsymbol{w} & \text{on} \quad \Gamma_c(t) \times (0,T), \\ \boldsymbol{P}_{\text{inc}}\ \tilde{\boldsymbol{n}}_s + J_f \tilde{\boldsymbol{\sigma}}_f(\tilde{\boldsymbol{v}}, \tilde{p}_f) \boldsymbol{F}_f^{-t}\ \tilde{\boldsymbol{n}}_f = 0 & \text{on} \quad \tilde{\Gamma}_c \times (0,T), \end{cases} \tag{2.45}$$

where $\boldsymbol{v} = \tilde{\boldsymbol{v}} \circ \boldsymbol{\mathcal{A}}^{-1}$, $p_f = \tilde{p}_f \circ \boldsymbol{\mathcal{A}}^{-1}$ and

$$\tilde{\boldsymbol{\sigma}}_f(\tilde{\boldsymbol{v}}, \tilde{p}_f) = \Big(\boldsymbol{\nabla} \tilde{\boldsymbol{v}} (\boldsymbol{\nabla} \boldsymbol{\mathcal{A}})^{-1} + (\boldsymbol{\nabla} \boldsymbol{\mathcal{A}})^{-t} (\boldsymbol{\nabla} \tilde{\boldsymbol{v}})^t \Big) - \tilde{p}_f\ \mathbf{Id}.$$

In the next chapter, theoretical results concerning this system are obtained by transforming it to the reference domain in the Lagrangian formulation. Then, in Chapter 4 we solve this system numerically and present some numerical results revealing what is happening in the artery.

Chapter 3

Analysis of the Interaction Between an Incompressible Fluid and a Quasi-Incompressible Non-Linear Elastic Structure

Contents

Introduction

Fluid-structure interaction (FSI) problem is a wide spread subject, which has gain a lot of concern and interest among mathematicians. This is due to the fact that many real-world problems consider the analysis of FSI problems as an essential tool to avoid failure. For example, they are considered in the design of many engineering systems such as aircrafts, engines and bridges, where the fluid-structure interaction oscillations are studied. Also, in biological field, FSI problems play an important role in the analysis of aneurysms and blood flow in stenosed arteries. Various kinds of FSI problems have been studied by modeling the fluid by either Stokes or Navier-Stokes equations coupled with an equation modeling the structure. Some deal with incompressible fluids [Bou06,CS04,GM00], others with compressible fluids [BG17,BG10]. Structures modeled with plate equations or shell equations were treated in [FO99]. The Stokes equations coupled with beam equation were analyzed in [Gra98]. The case of a free boundary FSI where the flow is incompressible and coupled with a linear Kirchhoff elastic material has been treated in [CS04], where the existence and uniqueness locally in time of such motion has been proved. In [GM00] the existence locally in time of a weak solution for an incompressible fluid with a rigid structure has been proved. Similar model has been studied in [DE99] considering a variable density where the global existence of the solution has been proved, that is, the existence of the solution until collisions occur between either the structure and boundaries or between two structures. For the coupling of an incompressible fluid with elastic structure, the existence of global weak solutions has been proved in [Bou06] when adding a regularizing term to the structure motion. In 3D, the work in [Gra02] has proved the existence of steady solutions of the incompressible Navier-Stokes equations when coupled with the non-linear Saint Venant-Kirchhoff model. Whereas, the existence and uniqueness of a regular solution has been proved in the case of compressible Navier-Stokes equations coupled with the non-linear Saint Venant-Kirchhoff model in [BG17], and with linear elastic model in [BG10].

In this chapter we establish local in time existence and uniqueness of a weak solution of the FSI problem that describes the interaction between an incompressible homogeneous Newtonian fluid modeled by the Navier-Stokes equations, and a hyperelastic quasi-incompressible structure modeled by the non-linear Saint Venant-Kirchhoff model.

In the first section we introduce the homogeneous incompressible Navier-Stokes equations and the elastodynamic equations. We couple them on one domain, by considering a common boundary and imposing some conditions on it. First, we introduce the coupled system at time t, which consists of the incompressible homogeneous Navier-Stokes equations with the elastodynamic equations modeled by the non-linear Saint Venant-Kirchhoff model. From mathematical point of view, Navier-Stokes equations are studied in the Eulerian (spatial) framework, whereas elastic structures are studied in the Lagrangian (material) framework. In order to be able to study the coupled system we use the deformation maps of both the fluid and the structure domains to rewrite the coupled system in the Lagrangian framework, in particular, in the reference configuration corresponding to the time $t = 0$. Indeed, since we are working with a problem involving a free moving boundary, the Lagrangian frame allows us to consider working on a fixed domain. As for the Saint Venant-Kirchhoff model we rewrite it in an explicit form which enables us to easily deal with it when applying the fixed point theorem as well as to find some bounds on it.

In the second section we partially linearize our system by considering the deformation maps to be given for given fluid velocity $\breve{\boldsymbol{v}}$ and structure displacement $\breve{\boldsymbol{\xi}}$, such that the pair $(\breve{\boldsymbol{v}}, \breve{\boldsymbol{\xi}})$ is in some fixed point space. In the third section we formulate an auxiliary problem, which comes from the classical system by changing slightly the coupling conditions related to the elastodynamic equations associated to the structure. The weak formulation is derived by considering a transformation of a divergence-free setting, so that the fluid pressure term disappears. Using Faedo-Galerkin approach we define Galerkin approximations of the solutions and derive a priori estimates for the Galerkin sequence. By passing to the limit, and using compactness results with Aubin-Lions-Simon theorem we prove the existence and uniqueness of a solution for the auxiliary problem. Based on the results concerning the auxiliary problem, and using the fixed point theorem we prove the existence and uniqueness of the solution of the partially linearized problem In Section 3.4. After that, in Section 3.5 we prove the regularity of the solution and derive some a priori estimates on it. Coming back to the non-linear problem, in Section 3.6 we use the fixed point theorem approach to prove the existence of a solution for the non-linear FSI problem. Finally, in Section 3.7, we establish the existence and uniquness of an L^2 fluid pressure by verifying the inf-sup condition, then based on the regularity result on $(\tilde{\boldsymbol{v}}, \tilde{\boldsymbol{\xi}})$ we get a more regular fluid pressure.

3.1 Fluid-Structure Interaction Problem

In this chapter we deal with the FSI problems from theoretical point of view. The fluid is governed by the homogeneous incompressible Navier-Stokes equations and the structure is a hyperelastic quasi-incompressible material such that its constitutive law is assumed to be the non-linear Saint Venant-Kirchhoff model. Let $T > 0$ be given. At time t, let $\Omega_f(t) \subset \mathbb{R}^3$ denotes a regular (enough) bounded connected domain representing the lumen of the artery. Recall that, the incompressible Navier-Stokes equations formulated in the Eulerain coordinates are

$$\begin{cases} \rho_f\Big(\partial_t \boldsymbol{v} + (\boldsymbol{v}\cdot\nabla)\boldsymbol{v}\Big) - \boldsymbol{\nabla}\cdot\boldsymbol{\sigma}_f(\boldsymbol{v}, p_f) = 0 & \text{in } \Omega_f(t)\times(0,T), \quad (3.1a)\\ \nabla\cdot\boldsymbol{v} = 0 & \text{in } \Omega_f(t)\times(0,T), \quad (3.1b)\\ \boldsymbol{\sigma}_f(\boldsymbol{v}, p_f)\ \boldsymbol{n}_f = \boldsymbol{g}_f & \text{on } \Gamma_f(t)\times(0,T), \quad (3.1c)\\ \boldsymbol{v} = \boldsymbol{v}_{\text{in}} & \text{on } \Gamma_{\text{in}}(t)\times(0,T), \quad (3.1d)\\ \boldsymbol{\sigma}_f(\boldsymbol{v}, p_f)\ \boldsymbol{n}_f = 0 & \text{on } \Gamma_{\text{out}}(t)\times(0,T), \quad (3.1e)\\ \boldsymbol{v} = \boldsymbol{v}_0 & \text{in } \Omega_f(t) \text{ at } t=0, \quad (3.1f)\end{cases}$$

where $\boldsymbol{v} = (v_1, v_2, v_3)^t$ is the fluid velocity, p_f is its pressure and $\rho_f > 0$ is its density. The term $\boldsymbol{\sigma}_f(\boldsymbol{v}, p_f)$ is the shear stress of the fluid of expression

$$\boldsymbol{\sigma}_f(\boldsymbol{v}, p_f) = 2\mu \boldsymbol{D}(\boldsymbol{v}) - p_f\ \mathbf{Id},$$

with μ is its dynamic viscosity and $\boldsymbol{D}(\boldsymbol{v})$ is the symmetric gradient given by $\boldsymbol{D}(\boldsymbol{v}) = \dfrac{\boldsymbol{\nabla v} + (\boldsymbol{\nabla v})^t}{2}$.

- Equation(3.1b) represents the incompressibility condition.
- Equation(3.1c) represents an external load on $\Gamma_f(t)$.
- Equation(3.1e) is the free exit condition.

On the other hand, the structure is considered to be a quasi-incompressible homogeneous hyperelastic material. We denote by $\Omega_s(t) \subset \mathbb{R}^3$ a regular enough domain that represents the structure at any time $t > 0$ and by $\partial\Omega_s(t)$ its smooth boundary such that $\partial\Omega_s(t) = \Gamma_1(t) \cup \Gamma_2(t)$. The structure displacement $\boldsymbol{\xi}_s$ satisfies the following equations

$$\begin{cases} \rho_s \partial_t^2 \boldsymbol{\xi}_s - \boldsymbol{\nabla} \cdot \boldsymbol{\sigma}^s_{\mathrm{Qinc}}(\boldsymbol{\xi}_s) = 0 & \text{in } \Omega_s(t) \times (0,T), \\ \boldsymbol{\sigma}^s_{\mathrm{Qinc}}(\boldsymbol{\xi}_s)\ \tilde{\boldsymbol{n}}_s = \boldsymbol{g}_s & \text{on } \Gamma_1(t) \times (0,T), \\ \boldsymbol{\xi}_s = 0 & \text{on } \Gamma_2(t) \times (0,T), \end{cases} \tag{3.2}$$

where $\boldsymbol{\sigma}^s_{\mathrm{Qinc}}$ is the Cauchy stress tensor characterizing the quasi-incompressible property of the structure. Its associated strain-energy density function W_{Qinc} is of the form (2.28). A surface external force $\boldsymbol{g}_s$ is applied on $\Gamma_1(t)$. Note that, the elastodynamic equations are formulated in the Lagrangian coordinates.

In order to get the FSI system, the domains $\Omega_f(t)$ and $\Omega_s(t)$ are coupled by considering $\Gamma_1(t) \equiv \Gamma_f(t)$. Here and after the common boundary will be denoted by $\Gamma_c(t)$. To ensure the compatibility of this system, some coupling conditions representing the continuity of the velocities and stresses must be imposed on the boundary $\Gamma_c(t)$. These coupling conditions are given as

$$\begin{cases} \boldsymbol{v} = \partial_t \boldsymbol{\xi}_s, & \text{on} \quad \Gamma_c(t) \times (0,T), \\ \boldsymbol{\sigma}_f(\boldsymbol{v}, p_f)\ \boldsymbol{n} = \boldsymbol{\sigma}^s_{\mathrm{Qinc}}(\boldsymbol{\xi}_s)\boldsymbol{n} & \text{on} \quad \Gamma_c(t) \times (0,T), \end{cases} \tag{3.3}$$

where $\boldsymbol{n}$ is the outward normal from $\Omega_f(t)$ to $\Gamma_c(t)$.
Finally, we introduce the initial conditions

- $\boldsymbol{v}(.,0) = \boldsymbol{v}_0 \quad \text{in} \quad \Omega_f(0)$,
- $\boldsymbol{\xi}_s(.,0) = \boldsymbol{\xi}_0 \quad \text{in} \quad \Omega_s(0)$,
- $\partial_t \boldsymbol{\xi}_s(.,0) = \boldsymbol{\xi}_1 \quad \text{in} \quad \Omega_s(0)$,
- $p_f(.,0) = p_{f_0} \quad \text{in} \quad \Omega_f(0)$,

which satisfy

$$\boldsymbol{v}_0 \in H^6(\Omega_f(0)),\ \boldsymbol{\xi}_0 \in H^4(\Omega_s(0)),\ \boldsymbol{\xi}_1 \in H^3(\Omega_s(0)) \text{ and } \ p_{f_0} \in H^3(\Omega_f(0)). \tag{3.4}$$

Let $\Omega(t) = \left[\overline{\Omega_f(t)} \cup \overline{\Omega_s(t)}\right]^\circ$ and $\partial\Omega(t) = [\partial\Omega_f(t) \cup \partial\Omega_s(t)] \setminus [\partial\Omega_f(t) \cap \partial\Omega_s(t)]$.
At time $t > 0$, the coupled system is given by

$$\begin{cases} \rho_f\Big(\partial_t \boldsymbol{v} + (\boldsymbol{v}\cdot\nabla)\boldsymbol{v}\Big) - \boldsymbol{\nabla}\cdot\boldsymbol{\sigma}_f(\boldsymbol{v}, p_f) = 0 & \text{in } \Omega_f(t)\times(0,T), & (3.5a)\\ \nabla\cdot\boldsymbol{v} = 0 & \text{in } \Omega_f(t)\times(0,T), & (3.5b)\\ \boldsymbol{v} = \boldsymbol{v}_{\text{in}} & \text{on } \Gamma_{\text{in}}(t)\times(0,T), & (3.5c)\\ \boldsymbol{\sigma}_f(\boldsymbol{v}, p_f)\ \boldsymbol{n} = 0 & \text{on } \Gamma_{\text{out}}(t)\times(0,T), & (3.5d)\\ \rho_s\partial_t^2\boldsymbol{\xi}_s - \boldsymbol{\nabla}\cdot\boldsymbol{\sigma}^s_{\text{Qinc}}(\boldsymbol{\xi}_s) = 0 & \text{in } \Omega_s(t)\times(0,T), & (3.5e)\\ \boldsymbol{\xi}_s = 0 & \text{on } \Gamma_2(t)\times(0,T), & (3.5f)\\ \boldsymbol{v} = \partial_t\boldsymbol{\xi}_s & \text{on } \Gamma_c(t)\times(0,T), & (3.5g)\\ \boldsymbol{\sigma}_f(\boldsymbol{v}, p_f)\ \boldsymbol{n} = \boldsymbol{\sigma}^s_{\text{Qinc}}(\boldsymbol{\xi}_s)\ \boldsymbol{n} & \text{on } \Gamma_c(t)\times(0,T), & (3.5h)\\ \boldsymbol{v}(.,0) = \boldsymbol{v}_0 \text{ and } p_f(.,0) = p_{f_0} & \text{in } \Omega_f(0), & (3.5i)\\ \boldsymbol{\xi}_s(.,0) = \boldsymbol{\xi}_0 \text{ and } \partial_t\boldsymbol{\xi}_s(.,0) = \boldsymbol{\xi}_1 & \text{in } \Omega_s(0). & (3.5j) \end{cases}$$

The Navier-Stokes equations are defined on the domain $\Omega_f(t)$ which evolves over time from the initial configuration $\Omega_f(0)$ according to a position function

$$\begin{aligned} \boldsymbol{\mathcal{A}}(.,t) : \Omega_f(0) &\longrightarrow \Omega_f(t)\\ \tilde{\boldsymbol{x}} &\longrightarrow \boldsymbol{\mathcal{A}}(\tilde{\boldsymbol{x}}, t) = \boldsymbol{x} \end{aligned}$$

that associates to the Lagrangian coordinate of a fluid particle its Eulerian coordinate. For all $\tilde{\boldsymbol{x}} \in \Omega_f(0)$ the function $\boldsymbol{\mathcal{A}}(\tilde{\boldsymbol{x}}, .)$ satisfies

$$\begin{cases} \partial_t\boldsymbol{\mathcal{A}}(\tilde{\boldsymbol{x}}, t) = \boldsymbol{v}(\boldsymbol{\mathcal{A}}(\tilde{\boldsymbol{x}}, t), t) & \text{for } t \in (0,T),\\ \boldsymbol{\mathcal{A}}(\tilde{\boldsymbol{x}}, 0) = \tilde{\boldsymbol{x}}. \end{cases}$$

The function $\boldsymbol{\mathcal{A}}$ is called the Arbitrary Lagrangian-Eulerian (ALE) map.

Similarly, the elastodynamic equations in the displacement $\boldsymbol{\xi}_s$ are defined on the domain $\Omega_s(t)$ which evolves over time from the initial configuration $\Omega_s(0)$ according to a position function

$$\begin{aligned} \boldsymbol{\varphi}_s(.,t) : \Omega_s(0) &\longrightarrow \Omega_s(t)\\ \tilde{\boldsymbol{y}} &\longrightarrow \boldsymbol{\varphi}_s(\tilde{\boldsymbol{y}}, t) = \boldsymbol{y} \end{aligned}$$

and we have

$$\boldsymbol{\varphi}_s(\tilde{\boldsymbol{y}}, t) = \tilde{\boldsymbol{y}} + \boldsymbol{\xi}_s(\boldsymbol{\varphi}_s(\tilde{\boldsymbol{y}}, t), t). \tag{3.6}$$

Notice that, using (3.6) we have

$$\boldsymbol{\varphi}_s(\tilde{\boldsymbol{y}}, 0) = \tilde{\boldsymbol{y}} + \boldsymbol{\xi}_s(\tilde{\boldsymbol{y}}, 0), \text{ that is } \tilde{\boldsymbol{y}} = \tilde{\boldsymbol{y}} + \boldsymbol{\xi}_0$$

which yields $\boldsymbol{\xi}_0 = \mathbf{0}$.
In the sequel, we omit the subscript s of the structure displacement and deformation, that is, we write $\boldsymbol{\xi}_s \equiv \boldsymbol{\xi}$ and $\boldsymbol{\varphi}_s \equiv \boldsymbol{\varphi}$. Further, we refer to the space elements in Ω_0^f and Ω_0^s by $\tilde{\boldsymbol{x}}$.

The definition of these two mappings enables us to write System (3.5a)-(3.5j) on the domain $\Omega(0)$. To do so, we consider the following change of variables in terms of the deformation mappings $\boldsymbol{\mathcal{A}}$ and $\boldsymbol{\varphi}$. For all $\tilde{\boldsymbol{x}}$ in $\Omega_f(0)$ and $\Omega_s(0)$ and t in $(0,T)$ set

$$\tilde{\boldsymbol{v}}(\tilde{\boldsymbol{x}},t) = \boldsymbol{v}(\boldsymbol{\mathcal{A}}(\tilde{\boldsymbol{x}},t),t),\ \tilde{\boldsymbol{\xi}}(\tilde{\boldsymbol{x}},t) = \boldsymbol{\xi}(\boldsymbol{\varphi}(\tilde{\boldsymbol{x}},t),t) \text{ and } \tilde{p}_f(\tilde{\boldsymbol{x}},t) = p_f(\boldsymbol{\mathcal{A}}(\tilde{\boldsymbol{x}},t),t). \tag{3.7}$$

On the reference domain $\Omega_f(0)$, the fluid stress tensor is given by [Ric17, Section 2.1.7]

$$\begin{aligned}\tilde{\boldsymbol{\sigma}}^0_f(\tilde{\boldsymbol{v}},\tilde{p}_f) &= \det(\boldsymbol{\nabla}\boldsymbol{\mathcal{A}})\Big(\boldsymbol{\sigma}_f(\tilde{\boldsymbol{v}}\circ\boldsymbol{\mathcal{A}}^{-1},\tilde{p}_f\circ\boldsymbol{\mathcal{A}}^{-1})\Big)(\boldsymbol{\nabla}\boldsymbol{\mathcal{A}})^{-t}\\ &= \Big(\mu\big(\boldsymbol{\nabla}\tilde{\boldsymbol{v}}(\boldsymbol{\nabla}\boldsymbol{\mathcal{A}})^{-1} + (\boldsymbol{\nabla}\boldsymbol{\mathcal{A}})^{-t}(\boldsymbol{\nabla}\tilde{\boldsymbol{v}})^t\big) - \tilde{p}_f\mathbf{Id}\Big)\mathrm{cof}(\boldsymbol{\nabla}\boldsymbol{\mathcal{A}})\\ &= \tilde{\boldsymbol{\sigma}}^0_f(\tilde{\boldsymbol{v}}) - \tilde{p}_f\mathrm{cof}(\boldsymbol{\nabla}\boldsymbol{\mathcal{A}}).\end{aligned} \tag{3.8}$$

As for the quasi-incompressible structure, the Cauchy stress tensor is given in terms of the first Piola-Kirchhoff stress tensor $\boldsymbol{P}$ as [Ric17, Lemma 2.12]

$$\begin{aligned}\boldsymbol{P}_{\mathrm{Qinc}} &= \det(\boldsymbol{\nabla}\boldsymbol{\varphi})\big(\boldsymbol{\sigma}^s_{\mathrm{Qinc}}(\boldsymbol{\xi})\circ\boldsymbol{\varphi}\big)(\boldsymbol{\nabla}\boldsymbol{\varphi})^{-t}\\ &= \boldsymbol{P} + \mathsf{C}(\det(\boldsymbol{\nabla}\boldsymbol{\varphi})-1)\mathrm{cof}(\boldsymbol{\nabla}\boldsymbol{\varphi})\end{aligned} \tag{3.9}$$

with $\mathsf{C} > 0$ a sufficiently large constant and

$$\boldsymbol{P} = \boldsymbol{\nabla}\boldsymbol{\varphi}\boldsymbol{S}(\boldsymbol{\nabla}\boldsymbol{\varphi}) \tag{3.10}$$

where

$$\boldsymbol{S}(\boldsymbol{\nabla}\boldsymbol{\varphi}) = 2\mu_s\boldsymbol{E}(\boldsymbol{\nabla}\boldsymbol{\varphi}) + \lambda_s\mathrm{tr}(\mathbf{E}(\boldsymbol{\nabla}\boldsymbol{\varphi}))\mathbf{Id}$$

is the second Piola-Kirchhoff stress tensor and

$$\boldsymbol{E}(\boldsymbol{\nabla}\boldsymbol{\varphi}) = \frac{1}{2}((\boldsymbol{\nabla}\boldsymbol{\varphi})^t\boldsymbol{\nabla}\boldsymbol{\varphi} - \mathbf{Id})$$

is the Green-Lagrange strain tensor and $(\mu_s,\lambda_s)\in\mathbb{R}^*_+\times\mathbb{R}_+$ are the Lamé coefficients.
In particular, when considering the Saint Venant-Kirchhoff stress tensor, Expression (3.10) can be rewritten in terms of the displacement $\boldsymbol{\xi}$ as

$$\boldsymbol{P} = (\mathbf{Id} + \boldsymbol{\nabla}\tilde{\boldsymbol{\xi}})\Big(\mu_s\Big(\boldsymbol{\nabla}\tilde{\boldsymbol{\xi}} + (\boldsymbol{\nabla}\tilde{\boldsymbol{\xi}})^t + (\boldsymbol{\nabla}\tilde{\boldsymbol{\xi}})^t\boldsymbol{\nabla}\tilde{\boldsymbol{\xi}}\Big) + \frac{\lambda_s}{2}\Big(2\nabla\cdot\tilde{\boldsymbol{\xi}} + |\boldsymbol{\nabla}\tilde{\boldsymbol{\xi}}|^2\Big)\mathbf{Id}\Big). \tag{3.11}$$

Using relations (3.7)-(3.9) we reformulate the Navier-Stokes equations and the elastodynamic equations in the Lagrangian coordinates. Hence, we can rewrite the coupled System (3.5a)-(3.5j) on $\Omega_f(0)$ and $\Omega_s(0)$ as

$$\begin{cases}\rho_f\det(\boldsymbol{\nabla}\boldsymbol{\mathcal{A}})\partial_t\tilde{\boldsymbol{v}} - \boldsymbol{\nabla}\cdot\tilde{\boldsymbol{\sigma}}^0_f(\tilde{\boldsymbol{v}},\tilde{p}_f) = 0 & \text{in } \Omega_f(0)\times(0,T),\\ \nabla\cdot\Big(\det(\boldsymbol{\nabla}\boldsymbol{\mathcal{A}})(\boldsymbol{\nabla}\boldsymbol{\mathcal{A}})^{-1}\tilde{\boldsymbol{v}}\Big) = 0 & \text{in } \Omega_f(0)\times(0,T),\\ \tilde{\boldsymbol{v}} = \boldsymbol{v}_{\mathrm{in}}\circ\boldsymbol{\mathcal{A}} & \text{on } \Gamma_{\mathrm{in}}(0)\times(0,T),\\ \tilde{\boldsymbol{\sigma}}^0_f(\tilde{\boldsymbol{v}},\tilde{p}_f)\ \tilde{\boldsymbol{n}} = 0 & \text{on } \Gamma_{\mathrm{out}}(0)\times(0,T),\\ \rho_s\det(\boldsymbol{\nabla}\boldsymbol{\varphi})\partial^2_t\tilde{\boldsymbol{\xi}} - \boldsymbol{\nabla}\cdot\boldsymbol{P} - \boldsymbol{\nabla}\cdot\Big[\mathsf{C}(\det(\boldsymbol{\nabla}\boldsymbol{\varphi})-1)\mathrm{cof}(\boldsymbol{\nabla}\boldsymbol{\varphi})\Big] = 0 & \text{in } \Omega_s(0)\times(0,T),\\ \tilde{\boldsymbol{\xi}} = 0 & \text{on } \Gamma_2(0)\times(0,T),\\ \tilde{\boldsymbol{v}} = \partial_t\tilde{\boldsymbol{\xi}} & \text{on } \Gamma_c(0)\times(0,T),\\ \tilde{\boldsymbol{\sigma}}^0_f(\tilde{\boldsymbol{v}},\tilde{p}_f)\tilde{\boldsymbol{n}} = [\boldsymbol{P} + \mathsf{C}(\det(\boldsymbol{\nabla}\boldsymbol{\varphi})-1)\mathrm{cof}(\boldsymbol{\nabla}\boldsymbol{\varphi})]\,\tilde{\boldsymbol{n}} & \text{on } \Gamma_c(0)\times(0,T),\\ \tilde{\boldsymbol{v}}(.,0) = \boldsymbol{v}_0 \quad \text{and} \quad \tilde{p}_f(.,0) = p_{f_0} & \text{in } \Omega_f(0),\\ \tilde{\boldsymbol{\xi}}(.,0) = \boldsymbol{\xi}_0 = 0 \quad \text{and} \quad \partial_t\tilde{\boldsymbol{\xi}}(.,0) = \boldsymbol{\xi}_1 & \text{in } \Omega_s(0),\end{cases} \tag{3.12}$$

where $\boldsymbol{\nabla\varphi} = \mathbf{Id} + \boldsymbol{\nabla}\tilde{\boldsymbol{\xi}}$ is the gradient of the deformation and $\tilde{\boldsymbol{n}}$ is the outward normal of $\Omega_f(0)$ on $\Gamma_c(0)$.

In order to deal with the structure model, we write the elasticity model in the spirit of [Gaw02], that is, we define

$$c_{i\alpha j\beta} = \frac{\partial \boldsymbol{P}_{i\alpha}}{\partial(\partial_\beta \tilde{\boldsymbol{\xi}}_j)}. \tag{3.13}$$

Let us set

$$c_{i\alpha j\beta}(\boldsymbol{\nabla}\tilde{\boldsymbol{\xi}}) = \mu_s(\delta_{\beta i}\delta_{\alpha j} + \delta_{\alpha\beta}\delta_{ij}) + \lambda_s(\delta_{i\alpha}\delta_{j\beta}) + c^l_{i\alpha j\beta}(\boldsymbol{\nabla}\tilde{\boldsymbol{\xi}}) + c^q_{i\alpha j\beta}(\boldsymbol{\nabla}\tilde{\boldsymbol{\xi}}), \tag{3.14}$$

where $c^l_{i\alpha j\beta}(\boldsymbol{\nabla}\tilde{\boldsymbol{\xi}})$ is the linear part given by

$$\begin{aligned} c^l_{i\alpha j\beta}(\boldsymbol{\nabla}\tilde{\boldsymbol{\xi}}) = \mu_s\big(&\delta_{ij}\partial_\beta\tilde{\xi}_\alpha + \delta_{\alpha j}\partial_\beta\tilde{\xi}_i + \delta_{ij}\partial_\alpha\tilde{\xi}_\beta + \delta_{\alpha\beta}\partial_j\tilde{\xi}_i + \delta_{i\beta}\partial_\alpha\tilde{\xi}_j + \delta_{\alpha\beta}\partial_i\tilde{\xi}_j\big) \\ &+ \lambda_s\big(\delta_{i\alpha}\partial_\beta\tilde{\xi}_j + \delta_{\alpha\beta}\delta_{ij}(\nabla\cdot\tilde{\boldsymbol{\xi}}) + \delta_{j\beta}\partial_\alpha\tilde{\xi}_i\big) \end{aligned} \tag{3.15}$$

and $c^q_{i\alpha j\beta}$ is the quadratic part written as

$$c^q_{i\alpha j\beta}(\boldsymbol{\nabla}\tilde{\boldsymbol{\xi}}) = \mu_s\left(\delta_{ij}(\partial_\beta\xi\cdot\partial_\alpha\tilde{\xi}) + \partial_\beta\xi_i\partial_\alpha\tilde{\xi}_j + \delta_{\alpha\beta}(\boldsymbol{\nabla}\tilde{\boldsymbol{\xi}}_j\cdot\boldsymbol{\nabla}\tilde{\boldsymbol{\xi}}_i)\right) + \lambda_s\left(\frac{1}{2}\delta_{ij}\delta_{\alpha\beta}|\boldsymbol{\nabla}\tilde{\boldsymbol{\xi}}|^2 + \partial_\alpha\tilde{\xi}_i\partial_\beta\tilde{\xi}_j\right). \tag{3.16}$$

Hence, $c_{i\alpha j\beta}$ can be rewritten as

$$c_{i\alpha j\beta}(\boldsymbol{\nabla}\tilde{\boldsymbol{\xi}}) = Cst + L(\boldsymbol{\nabla}\tilde{\boldsymbol{\xi}}) + Q(\boldsymbol{\nabla}\tilde{\boldsymbol{\xi}}), \tag{3.17}$$

where Cst is a constant, L is a linear function in $\boldsymbol{\nabla}\tilde{\boldsymbol{\xi}}$ and Q is a quadratic function in $\boldsymbol{\nabla}\tilde{\boldsymbol{\xi}}$. Remark that the coefficients $c_{i\alpha j\beta}$ are symmetric, that is,

$$c_{i\alpha j\beta} = c_{j\beta i\alpha} \qquad \forall\ i, \alpha, j, \beta \in \{1, 2, 3\}. \tag{3.18}$$

Lemma 3.1.1 *For $k = i, \alpha, j, \beta \in \{1, 2, 3\}$, we denote by ∂_k the partial derivative in space and by ∂_t and ∂_s the partial derivatives with respect to time. Some consequences of the relation (3.18) are the following*

1- The partial derivatives of $\boldsymbol{P}$ with respect to time and space are respectively

$$\partial_s\boldsymbol{P}_{i\alpha} = \sum_{j,\beta=1}^{3} c_{i\alpha j\beta}(\boldsymbol{\nabla}\tilde{\boldsymbol{\xi}})\partial^2_{s\beta}\tilde{\xi}_j \quad \textit{and} \quad \partial_k\boldsymbol{P}_{i\alpha} = \sum_{j,\beta=1}^{3} c_{i\alpha j\beta}(\boldsymbol{\nabla}\tilde{\boldsymbol{\xi}})\partial^2_{k\beta}\tilde{\xi}_j \qquad \forall\ i, \alpha = 1, 2, 3.$$

2- The $i-th$ component of the divergence of $\boldsymbol{P}$ is given by

$$(\boldsymbol{\nabla}\cdot\boldsymbol{P})_i = \sum_{\alpha,j,\beta=1}^{3} c_{i\alpha j\beta}(\boldsymbol{\nabla}\tilde{\boldsymbol{\xi}})\partial^2_{\alpha\beta}\tilde{\xi}_j \quad \forall\ i = 1, 2, 3. \tag{3.19}$$

3- *Assuming that* $\boldsymbol{P}(\tilde{\boldsymbol{\xi}}(.,0)) = 0$ *on* $\Gamma_1(0)$*, the normal component of the stress tensor* $\boldsymbol{P}$ *on the boundary* $\Gamma_1(0)$ *is*

$$\sum_{\alpha=1}^{3} \boldsymbol{P}_{i\alpha}\tilde{n}_\alpha = \sum_{\alpha,j,\beta=1}^{3} \left(\int_0^t c_{i\alpha j\beta}(\boldsymbol{\nabla}\tilde{\boldsymbol{\xi}}) \partial^2_{s\beta}\tilde{\xi}_j \; ds \right) \tilde{n}_\alpha \quad \forall\, i = 1, 2, 3. \tag{3.20}$$

4- *The* $i\alpha$*-th component of* $\boldsymbol{P}$ *is given by*

$$\boldsymbol{P}_{i\alpha} = \sum_{\alpha,j,\beta=1}^{3} \left(\int_0^t c_{i\alpha j\beta}(\boldsymbol{\nabla}\tilde{\boldsymbol{\xi}}) \partial^2_{s\beta}\tilde{\xi}_j \; ds \right) \quad \forall\, i = 1, 2, 3.$$

Proof.

1- Let r be the index that represents either the time derivative or the space derivative. For the $i\alpha$-th component of $\boldsymbol{P}(\tilde{\boldsymbol{\xi}})$ we have

$$\partial_r(\boldsymbol{P}(\tilde{\boldsymbol{\xi}}))_{i\alpha} = \sum_{j,\beta=1}^{3} \frac{\partial(\boldsymbol{P}(\tilde{\boldsymbol{\xi}}))_{i\alpha}}{\partial(\partial_\beta\tilde{\xi}_j)} \frac{\partial(\partial_\beta\tilde{\xi}_j)}{\partial_r} = \sum_{j,\beta=1}^{3} c_{i\alpha j\beta}(\boldsymbol{\nabla}\tilde{\boldsymbol{\xi}}) \partial^2_{r\beta}\tilde{\xi}_j.$$

2- Considering $r = \alpha$ in the first part yields

$$\partial_\alpha(\boldsymbol{P}(\tilde{\boldsymbol{\xi}}))_{i\alpha} = \sum_{j,\beta=1}^{3} c_{i\alpha j\beta}(\boldsymbol{\nabla}\tilde{\boldsymbol{\xi}}) \partial^2_{\alpha\beta}\tilde{\xi}_j.$$

But for $i = 1, 2, 3$ we have

$$(\boldsymbol{\nabla} \cdot \boldsymbol{P}(\tilde{\boldsymbol{\xi}}))_i = \sum_{\alpha=1}^{3} \partial_\alpha(\boldsymbol{P}(\tilde{\boldsymbol{\xi}}))_{i\alpha} = \sum_{\alpha,j,\beta=1}^{3} c_{i\alpha j\beta}(\boldsymbol{\nabla}\tilde{\boldsymbol{\xi}}) \partial^2_{\alpha\beta}\tilde{\xi}_j.$$

3- For any $\tilde{\boldsymbol{\xi}}$ in $\Omega_s(0)$ we have

$$\boldsymbol{P}_{i\alpha}(\tilde{\boldsymbol{\xi}}(.,t)) - \boldsymbol{P}_{i\alpha}(\tilde{\boldsymbol{\xi}}(.,0)) = \int_0^t \partial_s \boldsymbol{P}_{i\alpha}(\tilde{\boldsymbol{\xi}}(.,s)) \; ds \quad \forall\, i, \alpha = 1, 2, 3.$$

Substituting $\partial_s \boldsymbol{P}(\tilde{\boldsymbol{\xi}}(.,s))$ by its expression from the first part gives

$$\boldsymbol{P}_{i\alpha}(\tilde{\boldsymbol{\xi}}(.,t)) - \boldsymbol{P}_{i\alpha}(\tilde{\boldsymbol{\xi}}(.,0)) = \sum_{j,\beta=1}^{3} \int_0^t c_{i\alpha j\beta}(\boldsymbol{\nabla}\tilde{\boldsymbol{\xi}}) \partial^2_{s\beta}\tilde{\xi}_j \; ds \quad \forall\, i, \alpha = 1, 2, 3.$$

In particular, on $\Gamma_1(0)$ we have $\boldsymbol{P}(\tilde{\boldsymbol{\xi}}(.,0)) = 0$. Consequently, taking the summation over α yields

$$\sum_{\alpha=1}^{3} \boldsymbol{P}_{i\alpha}(\tilde{\boldsymbol{\xi}}(.,t))\tilde{n}_\alpha = \sum_{\alpha,j,\beta=1}^{3} \int_0^t \big(c_{i\alpha j\beta}(\boldsymbol{\nabla}\tilde{\boldsymbol{\xi}}) \partial^2_{s\beta}\tilde{\xi}_j \; ds \big) \tilde{n}_\alpha \quad \forall\, i = 1, 2, 3.$$

$\blacksquare$

The Quasi-Incompressibility Condition

We write the condition of quasi-incompressibility in a way similar to that of the first Piola-Kirchhoff stress tensor (3.14). In order to do so, we use the notation introduced in [Cia88, p. 5]. Indeed, in three dimensions we define the third-order orientation tensor $(\boldsymbol{\varepsilon_{ijk}})$ whose components are the Levi-Civita symbol $\{\varepsilon_{ijk}\}_{ijk}$ defined by

$$\varepsilon_{ijk} = \begin{cases} 1 & \text{if } \{i,j,k\} \text{ is an even permutation of } \{1,2,3\}, \\ -1 & \text{if } \{i,j,k\} \text{ is an odd permutation of } \{1,2,3\}, \\ 0 & \text{if at least two of the indices are equal.} \end{cases}$$

Using Levi-Civita symbol and Einstein summation convention, we can define the ij-th element of the matrix $\mathrm{cof}(\boldsymbol{\nabla\varphi})$ to be

$$(\mathrm{cof}(\boldsymbol{\nabla\varphi}))_{ij} = \frac{1}{2}\varepsilon_{mni}\varepsilon_{pqj}\partial_p\varphi_m\partial_q\varphi_n.$$

Further, the determinant of the 3-by3-matrix $\boldsymbol{\nabla\varphi}$ is given in terms of the Levi-Civita symbol using Einstein summation convention, as

$$\det(\boldsymbol{\nabla\varphi}) = \frac{1}{6}\varepsilon_{ijk}\varepsilon_{pqr}\partial_p\varphi_i\partial_q\varphi_j\partial_r\varphi_k. \tag{3.21}$$

We define

$$d_{i\alpha j\beta}(\boldsymbol{\nabla}\tilde{\boldsymbol{\xi}}) = \frac{\partial}{\partial(\partial_\beta\tilde{\xi}_j)}\Big[\big(\det(\boldsymbol{\nabla\varphi})-1\big)\ \mathrm{cof}(\boldsymbol{\nabla\varphi})\Big]_{i\alpha} \tag{3.22}$$

which can be written explicitly as

$$\begin{aligned} d_{i\alpha j\beta}(\boldsymbol{\nabla}\tilde{\boldsymbol{\xi}}) = & \frac{1}{12}\varepsilon_{i_1j_1k_1}\varepsilon_{p_1q_1r_1}\varepsilon_{mni}\varepsilon_{pq\alpha}\big(\partial_p\tilde{\xi}_m+\delta_{pm}\big)\big(\partial_q\tilde{\xi}_n+\delta_{qn}\big)\big[\delta_{\beta i_1}\delta_{jp_1}\big(\partial_{j_1}\tilde{\xi}_{q_1}\delta_{\beta i_1}\big)\big(\partial_{k_1}\tilde{\xi}_{r_1}\delta_{k_1r_1}\big) \\ & +\delta_{j_1\beta}\delta_{jq_1}\big(\partial_{i_1}\tilde{\xi}_{p_1}\delta_{i_1p_1}\big)\big(\partial_{k_1}\tilde{\xi}_{r_1}\delta_{k_1r_1}\big)+\delta_{k_1\beta}\delta_{r_1j}\big(\partial_{i_1}\tilde{\xi}_{p_1}\delta_{i_1p_1}\big)\big(\partial_{j_1}\tilde{\xi}_{q_1}\delta_{j_1q_1}\big)\big] \\ & +\frac{1}{12}\varepsilon_{i_1j_1k_1}\varepsilon_{p_1q_1r_1}\varepsilon_{mni}\varepsilon_{pq\alpha}\big[\delta_{p\beta}\delta_{mj}\big(\partial_q\tilde{\xi}_n+\delta_{qn}\big)+\delta_{q\beta}\delta_{nj}\big(\partial_p\tilde{\xi}_m+\delta_{pm}\big)\big] \\ & \big[\big(\partial_{i_1}\tilde{\xi}_{p_1}+\delta_{i_1p_1}\big)\big(\partial_{j_1}\tilde{\xi}_{q_1}+\delta_{j_1q_1}\big)\big(\partial_{k_1}\tilde{\xi}_{r_1}+\delta_{k_1r_1}\big)-1\big]. \end{aligned} \tag{3.23}$$

Clearly, $d_{i\alpha j\beta}(\boldsymbol{\nabla}\tilde{\boldsymbol{\xi}})$ is a polynomial in $\boldsymbol{\nabla}\tilde{\boldsymbol{\xi}}$ of degree at most 4. Moreover, for $i=\alpha$ and $j=\beta$ we get the constant terms of this polynomial. Then we can write

$$d_{i\alpha j\beta}(\boldsymbol{\nabla}\tilde{\boldsymbol{\xi}}) = Cst + d^L_{i\alpha j\beta}(\boldsymbol{\nabla}\tilde{\boldsymbol{\xi}}) + d^Q_{i\alpha j\beta}(\boldsymbol{\nabla}\tilde{\boldsymbol{\xi}}) + d^T_{i\alpha j\beta}(\boldsymbol{\nabla}\tilde{\boldsymbol{\xi}}) + d^F_{i\alpha j\beta}(\boldsymbol{\nabla}\tilde{\boldsymbol{\xi}}) \tag{3.24}$$

where $d^L_{i\alpha j\beta}, d^Q_{i\alpha j\beta}, d^T_{i\alpha j\beta}$ and $d^F_{i\alpha j\beta}$ stand for polynomials in $\boldsymbol{\nabla}\tilde{\boldsymbol{\xi}}$ with respective degree 1,2,3 and 4. This writing enables us to give the $i-th$ component of $\boldsymbol{\nabla}\cdot[\mathsf{C}(\det(\boldsymbol{\nabla\varphi})-1)\mathrm{cof}(\boldsymbol{\nabla\varphi})]$. In fact,

$$\Big[\boldsymbol{\nabla}\cdot\Big(\mathsf{C}(\det(\boldsymbol{\nabla\varphi})-1)\mathrm{cof}(\boldsymbol{\nabla\varphi})\Big)\Big]_i = \mathsf{C}\sum_{\alpha,j,\beta=1}^{3} d_{i\alpha j\beta}(\boldsymbol{\nabla}\tilde{\boldsymbol{\xi}})\partial^2_{\alpha\beta}\tilde{\xi}_j \quad \text{for} \quad i=1,2,3. \tag{3.25}$$

In a way similar to (3.20), the normal component of the quasi-incompressible condition on the boundary $\Gamma_1(0)$ is

$$\sum_{\alpha=1}^{3}\left[(\det(\boldsymbol{\nabla\varphi})-1)\mathrm{cof}(\boldsymbol{\nabla\varphi})\right]_{i\alpha}\tilde{n}_\alpha=\sum_{\alpha,j,\beta=1}^{3}\left(\int_0^t d_{i\alpha j\beta}(\boldsymbol{\nabla}\tilde{\boldsymbol{\xi}})\partial^2_{s\beta}\tilde{\xi}_j ds\right)\tilde{n}_\alpha,\quad\forall\, i=1,2,3,\tag{3.26}$$

provided that $\big(\det(\boldsymbol{\nabla\varphi})-1)\mathrm{cof}(\boldsymbol{\nabla\varphi})\big)(.,0)=0$ on $\Gamma_1(0)$.
In what follows, for simplicity we set

$$b_{i\alpha j\beta}=c_{i\alpha j\beta}+\mathsf{C}d_{i\alpha j\beta}.\tag{3.27}$$

Using Relations (3.19), (3.20), (3.25) and (3.26), System (3.12) can be rewritten as

$$\begin{cases}\rho_f\det(\boldsymbol{\nabla\mathcal{A}})\partial_t\tilde{\boldsymbol{v}}-\boldsymbol{\nabla}\cdot\tilde{\boldsymbol{\sigma}}^0_f(\tilde{\boldsymbol{v}},\tilde{p}_f)=0 & \text{in } \Omega_f(0)\times(0,T),\\ \nabla\cdot(\det(\boldsymbol{\nabla\mathcal{A}})(\boldsymbol{\nabla\mathcal{A}})^{-1}\tilde{\boldsymbol{v}})=0 & \text{in } \Omega_f(0)\times(0,T),\\ \tilde{\boldsymbol{v}}=\boldsymbol{v}_{\text{in}}\circ\boldsymbol{\mathcal{A}} & \text{on } \Gamma_{\text{in}}(0)\times(0,T),\\ \tilde{\boldsymbol{\sigma}}^0_f(\tilde{\boldsymbol{v}},\tilde{p}_f)\ \tilde{\boldsymbol{n}}=0 & \text{on } \Gamma_{\text{out}}(0)\times(0,T),\\ \rho_s\det(\boldsymbol{\nabla}\tilde{\boldsymbol{\xi}}+\mathbf{Id})\partial^2_t\tilde{\xi}_i-\displaystyle\sum_{\alpha,j,\beta=1}^{3}b_{i\alpha j\beta}(\boldsymbol{\nabla}\tilde{\boldsymbol{\xi}})\partial^2_{\alpha\beta}\tilde{\xi}_j=0,\quad i=1,2,3 & \text{in } \Omega_s(0)\times(0,T),\\ \tilde{\boldsymbol{\xi}}=\mathbf{0} & \text{on } \Gamma_2(0)\times(0,T),\\ \tilde{\boldsymbol{v}}=\partial_t\tilde{\boldsymbol{\xi}} & \text{on } \Gamma_c(0)\times(0,T),\\ \left[\tilde{\boldsymbol{\sigma}}^0_f(\tilde{\boldsymbol{v}},\tilde{p}_f)\tilde{\boldsymbol{n}}\right]_i=\displaystyle\sum_{\alpha,j,\beta=1}^{3}\left(\int_0^t b_{i\alpha j\beta}(\boldsymbol{\nabla}\tilde{\boldsymbol{\xi}})\partial^2_{s\beta}\tilde{\xi}_j ds\right)\tilde{n}_\alpha,\quad i=1,2,3 & \text{on } \Gamma_c(0)\times(0,T),\\ \tilde{\boldsymbol{v}}(.,0)=\boldsymbol{v}_0\quad\text{and}\quad\tilde{p}_f(.,0)=p_{f_0} & \text{in } \Omega_f(0),\\ \tilde{\boldsymbol{\xi}}(.,0)=\mathbf{0}\quad\text{and}\quad\partial_t\tilde{\boldsymbol{\xi}}(.,0)=\boldsymbol{\xi}_1 & \text{in } \Omega_s(0).\end{cases}\tag{3.28}$$

Notice that, unlike System (3.12), in this system the boundary condition related to the elastodynamic equation is incompatible with it. Indeed, for Equations $(3.28)_6$ and $(3.28)_9$ to combine we must have

$$[\tilde{\boldsymbol{\sigma}}^0_f(\boldsymbol{v},\tilde{p}_f)\boldsymbol{n}]_i=\sum_{\alpha,j,\beta=1}^{3}\left(b_{i\alpha j\beta}(\boldsymbol{\nabla}\tilde{\boldsymbol{\xi}})\partial_\beta\tilde{\xi}_j\right)\tilde{n}_\alpha,\quad i=1,2,3,\ \text{on}\quad\Gamma_c(0)\times(0,T).\tag{3.29}$$

This rewriting $(3.28)_5$ of the elasticity equation is efficient when performing the fixed point theorem on the system. In fact, it helps to get over the difficulties emerging from the non-linearity of the Saint Venant-Kirchhoff model and the hyperbolic type of the equation. Due to this disagreement issue between Equations $(3.28)_6$ and $(3.28)_9$, the first step of the work is to consider an *auxiliary problem* including the natural boundary condition (3.29).

By considering the boundary and initial conditions we assume that the following compatibility conditions hold on the initial values

$$\begin{cases} \boldsymbol{v}_0 = \boldsymbol{\xi}_1 & \text{on} \quad \Gamma_c(0), \\ \boldsymbol{\sigma}_f(\boldsymbol{v}_0, p_{f_0})\boldsymbol{n} = \boldsymbol{0} & \text{on} \quad \Gamma_c(0), \\ p_{f_0} = 2\mu \boldsymbol{D}(\boldsymbol{v}_0) & \text{in} \quad \Omega_f(0), \\ \nabla p_{f_0} = \mu \Delta \boldsymbol{v}_0 & \text{in} \quad \Omega_f(0), \\ \boldsymbol{\nabla} \cdot \boldsymbol{\sigma}_f(\boldsymbol{v}_0, p_{f_0}) = 0 & \text{on} \quad \Gamma_c(0), \\ \partial_t p_f|_{t=0}\boldsymbol{n} = S_1\boldsymbol{n} + E_1\boldsymbol{n} & \text{on} \quad \Gamma_c(0), \\ \boldsymbol{\nabla} \cdot \rho_s \Big[S_1 + \partial_t p_f|_{t=0}\mathbf{Id}\Big] = \rho_f \boldsymbol{\nabla} \cdot E_1 & \text{on} \quad \Gamma_c(0), \\ \rho_f\Big(2(\nabla \cdot \boldsymbol{v}_0)\boldsymbol{\nabla} \cdot E_1 + \boldsymbol{\nabla} \cdot E_2\Big) = \boldsymbol{\nabla} \cdot S_2 & \text{on} \quad \Gamma_c(0), \\ \Big(E_2 - 2\big((\nabla \cdot \boldsymbol{v}_0)S_3 + S_4\big)\Big)\boldsymbol{n} = \rho_s S_2 \boldsymbol{n} & \text{on} \quad \Gamma_c(0). \end{cases} \tag{3.30}$$

where

- $S_1 = -\mu\Big((\boldsymbol{D}(\boldsymbol{v}_0))^2 - 2(\boldsymbol{\nabla}\boldsymbol{v}_0)^t\boldsymbol{\nabla}\boldsymbol{v}_0\Big) + \boldsymbol{\sigma}_f(\boldsymbol{v}_0, p_{f_0})S_3.$
- $E_1 = 2\mu_s\boldsymbol{\epsilon}(\boldsymbol{\xi}_1) + \lambda_s(\nabla \cdot \boldsymbol{\xi}_1)\mathbf{Id} + \nabla \cdot \boldsymbol{v}_0\mathbf{Id}.$
- $S_2 = \partial_t^2 p_f|_{t=0}\mathbf{Id} + 2\partial_t p_f|_{t=0}S_3 + p_{f_0}S_4 + 2\mu\boldsymbol{\epsilon}(\boldsymbol{\nabla} \cdot E_1)$
  $\quad - 2\Big((\boldsymbol{D}(\boldsymbol{v}_0))^2 - 2(\boldsymbol{\nabla}\boldsymbol{v}_0)^t\boldsymbol{\nabla}\boldsymbol{v}_0\Big)S_3 + 2\boldsymbol{D}(\boldsymbol{v}_0)S_4.$
- $E_2 = 2\boldsymbol{\nabla}\boldsymbol{\xi}_1\ E_1 + 2\mu_s\big((\boldsymbol{\nabla}\boldsymbol{\xi}_1)^t\boldsymbol{\nabla}\boldsymbol{\xi}_1 + \lambda_s\boldsymbol{\nabla}\boldsymbol{\xi}_1 + 2\big((\nabla \cdot \boldsymbol{v}_0)S_3 + S_4\big).$
- $S_3 = (\nabla \cdot \boldsymbol{v}_0)\mathbf{Id} - (\boldsymbol{\nabla}\boldsymbol{v}_0)^t.$
- $S_4 = \dfrac{1}{\rho_f}\boldsymbol{\nabla} \cdot \big(\boldsymbol{\nabla} \cdot \boldsymbol{\sigma}_f(\boldsymbol{v}_0, p_{f_0})\big)\mathbf{Id} - \dfrac{1}{\rho_f}\boldsymbol{\nabla}\big(\boldsymbol{\nabla} \cdot \boldsymbol{\sigma}_f(\boldsymbol{v}_0, p_{f_0})\big) + 2\mathrm{cof}(\boldsymbol{\nabla}\boldsymbol{v}_0).$

These conditions are obtained from (3.12) by considering $t = 0$, differentiating in time once and twice $(3.12)_1$, $(3.12)_5$, $(3.12)_7$ and $(3.12)_8$ then considering $t = 0$ and taking into consideration the following identities

$$\partial_t\big((\boldsymbol{\nabla}\boldsymbol{\mathcal{A}})^{-1}\big)(.,0) = -\boldsymbol{\nabla}\boldsymbol{v}_0 \quad \text{and} \quad \partial_t\big(\det(\boldsymbol{\nabla}\boldsymbol{\mathcal{A}})\big)(.,0) = \nabla \cdot \boldsymbol{v}_0 \qquad \text{in} \quad \Omega_f(0).$$

Definition 3.1.1 *Let us define the following spaces*

$$S_m^T = L^\infty\big(0,T; H^m(\Omega_s(0))\big) \cap W^{m,\infty}\big(0,T; L^2(\Omega_s(0))\big) \qquad 0 \le m \le 4,$$

$$F_1^T = L^\infty\big(0,T; L^2(\Omega_f(0))\big) \cap L^2\big(0,T; H^1(\Omega_f(0))\big),$$

$$F_2^T = L^\infty\big(0,T; H^2(\Omega_f(0))\big) \cap H^1\big(0,T; H^1(\Omega_f(0))\big) \cap W^{1,\infty}\big(0,T; L^2(\Omega_f(0))\big),$$

$$F_4^T = L^\infty\big(0,T; H^4(\Omega_f(0))\big) \cap H^3\big(0,T; H^1(\Omega_f(0))\big) \cap W^{2,\infty}\big(0,T; H^2(\Omega_f(0))\big) \cap W^{3,\infty}\big(0,T; L^2(\Omega_f(0))\big),$$

$$\mathcal{P}_3^T = L^\infty\big(0,T;H^3(\Omega_f(0))\big)\cap H^3\big(0,T;L^2(\Omega_f(0))\big)\cap W^{1,\infty}\big(0,T;H^2(\Omega_f(0))\big)\cap W^{2,\infty}\big(0,T;H^1(\Omega_f(0))\big),$$

$$H_l^1\big(0,T;L^2(\Gamma_c(0))\big) := \{\psi \in H^1\big(0,T;(\Gamma_c(0))\big);\psi(0)=0\}.$$

Then, for $M>1$ and $T>0$ we define the following fixed point space

$$\begin{aligned} A_M^T &= \Big\{(\breve{\boldsymbol{v}},\breve{\boldsymbol{\xi}}) \in F_4^T \times S_4^T,\ \breve{\boldsymbol{\xi}}(.,0)=\mathbf{0},\ \partial_t\breve{\boldsymbol{\xi}}(.,0)=\boldsymbol{\xi}_1 \text{ in } \Omega_s(0) \text{ and } \|\breve{\boldsymbol{v}}\|_{F_4^T}\le M,\ \|\breve{\boldsymbol{\xi}}\|_{S_4^T}\le M\Big\} \\ &:= A_{M_1}^T \times A_{M_2}^T \end{aligned}$$

After introducing the spaces needed, we are ready to state the main result of the work.

Theorem 3.1.1 (Main Theorem) *Let $(\boldsymbol{v}_0,\boldsymbol{\xi}_1,p_{f_0})$ satisfy (3.4) and (3.30). Then, there exists $\overline{T}>0$ such that System (3.28) admits a unique solution defined on $(0,\overline{T})$ satisfying*

$$(\boldsymbol{v}\circ\boldsymbol{\mathcal{A}},\boldsymbol{\xi}\circ\boldsymbol{\varphi},p_f\circ\boldsymbol{\mathcal{A}}) \in F_4^{\overline{T}} \times S_4^{\overline{T}} \times \mathcal{P}_3^{\overline{T}} \tag{3.31}$$

$$\boldsymbol{\mathcal{A}} \in W^{1,\infty}\big(0,\overline{T};H^2(\Omega_f(0))\big) \times W^{2,\infty}\big(0,\overline{T};L^2(\Omega_f(0))\big) \tag{3.32}$$

and

$$\boldsymbol{\varphi} \in S_2^{\overline{T}}. \tag{3.33}$$

For simplicity, for all $m,r\geqslant 0$ and $p,q\in[1,+\infty]$, we denote the spaces $W^{m,p}\big(0,T;W^{r,q}(\Omega_f(0))\big)$ and $W^{m,p}\big(0,T;W^{r,q}(\Omega_s(0))\big)$ by $W^{m,p}\big(W^{r,q}(\Omega_f(0))\big)$ and $W^{m,p}\big(W^{r,q}(\Omega_s(0))\big)$, respectively. Also the domain's notation is simplified by writing $\Omega_f(0)=\Omega_0^f$, $\Omega_s(0)=\Omega_0^s$ and $\Omega(0)=\Omega_0$. Further, for all $t>0$, define

$$\Sigma_t = \Gamma_c(0)\times(0,t).$$

3.2 A Partially Linear System

Let $(\boldsymbol{v}_0,\boldsymbol{\xi}_1,p_{f_0})$ satisfy (3.4) and (3.30). Let $0<T<1$ and consider $(\breve{\boldsymbol{v}},\breve{\boldsymbol{\xi}})\in A_M^T$ to be given. For these given functions we define the associated fluid flow $\breve{\boldsymbol{\mathcal{A}}}$ and structure deformation $\breve{\boldsymbol{\varphi}}$ by

$$\breve{\boldsymbol{\mathcal{A}}}(\tilde{\boldsymbol{x}},t) = \tilde{\boldsymbol{x}} + \int_0^t \breve{\boldsymbol{v}}(\tilde{\boldsymbol{x}},s)\,ds \qquad \forall\ \tilde{\boldsymbol{x}}\in\Omega_0^f, \tag{3.34}$$

and

$$\breve{\boldsymbol{\varphi}}(\tilde{\boldsymbol{x}},t) = \tilde{\boldsymbol{x}} + \breve{\boldsymbol{\xi}}(\tilde{\boldsymbol{x}},t) \qquad \forall\ \tilde{\boldsymbol{x}}\in\Omega_0^s. \tag{3.35}$$

We use the given $(\breve{\boldsymbol{v}},\breve{\boldsymbol{\xi}})$ to partially linearize the non-linear system. Indeed, we consider the non-linear terms to be given in terms of $(\breve{\boldsymbol{v}},\breve{\boldsymbol{\xi}})$. We will give the statement of a corollary of Sobolev embeddings which is useful in finding some estimates.

Corollary 3.2.1 [Bre10, Corollary 9.13] *For any integer $m \in \mathbb{N}^*$ and $1 \leq p \leq \infty$.,*

$$\text{if } \frac{1}{p} - \frac{m}{N} < 0 \text{ then } W^{m,p}(\mathbb{R}^N) \subset L^\infty(\mathbb{R}^N),$$

and it is a continuous injection. In particular the inclusion holds true for any subset Ω of $\mathbb{R}^N$.

Lemma 3.2.1 *For any subset Ω of $\mathbb{R}^3$, we have the following embedding*

$$H^2(\Omega) \subset L^\infty(\Omega).$$

This yields the existence of a constant C(depending only on N=3 and p=2) such that

$$||\boldsymbol{u}||_{L^\infty(\Omega)} \leq C||\boldsymbol{u}||_{H^2(\Omega)} \quad \forall\ \boldsymbol{u} \in H^2(\Omega).$$

Let $T \leq 1/M^4$ and $M > 1$. We shall repeatedly use the following two lemmas which provide bounds on various norms of the deformation maps $\breve{\boldsymbol{\mathcal{A}}}$ and $\breve{\boldsymbol{\varphi}}$.

Lemma 3.2.2 *For the fluid flow $\breve{\boldsymbol{\mathcal{A}}}$ given by (3.34) for a given $\breve{\boldsymbol{v}} \in A^T_{M_1}$, there exists a constant $C = C(\Omega^f_0) > 0$ and a constant $\kappa > 0$ such that*

1- $||\breve{\boldsymbol{\mathcal{A}}}||_{W^{1,\infty}(H^4)\cap W^{3,\infty}(H^2)\cap W^{4,\infty}(L^2)\cap H^4(H^1)} \leq C(1+M)$.

2- $||\boldsymbol{\nabla}\breve{\boldsymbol{\mathcal{A}}} - \mathbf{Id}||_{W^{1,\infty}(H^3)\cap W^{3,\infty}(H^1)\cap H^4(L^2)} \leq CM$.

3- $||\boldsymbol{\nabla}\breve{\boldsymbol{\mathcal{A}}}||_{L^\infty(H^3)} \leq C$.

4- $||\mathrm{cof}(\boldsymbol{\nabla}\breve{\boldsymbol{\mathcal{A}}})||_{L^\infty(H^3)} \leq C$.

5- $||\partial_t \mathrm{cof}(\boldsymbol{\nabla}\breve{\boldsymbol{\mathcal{A}}})(t)||_{L^2(H^3)} \leq CT^{1/2}M$.

6- $||(\boldsymbol{\nabla}\breve{\boldsymbol{\mathcal{A}}})^{-1}(t)||_{L^\infty} \leq C||\boldsymbol{\nabla}\breve{\boldsymbol{\mathcal{A}}}(t)||^2_{L^\infty} \qquad$ *for $t \in [0,T]$.*

7- $||\mathrm{cof}(\boldsymbol{\nabla}\breve{\boldsymbol{\mathcal{A}}}) - \mathbf{Id}||_{L^\infty(H^3)} + ||(\boldsymbol{\nabla}\breve{\boldsymbol{\mathcal{A}}})^{-1} - \mathbf{Id}||_{L^\infty(H^3)} \leq CT^\kappa M$.

8- $||\partial_t(\boldsymbol{\nabla}\breve{\boldsymbol{\mathcal{A}}})^{-1}(t)||_{L^r} \leq C||\boldsymbol{\nabla}\breve{\boldsymbol{v}}(t)||_{L^r}$, *for $r \in [1,+\infty]$ and $t \in [0,T]$.*

9- $||\det(\boldsymbol{\nabla}\breve{\boldsymbol{\mathcal{A}}})||_{L^\infty(H^3)} \leq CM \quad$ and $\quad ||\partial_t \det(\boldsymbol{\nabla}\breve{\boldsymbol{\mathcal{A}}})||_{L^\infty(H^2)} \leq CM$.

10- $||\det(\boldsymbol{\nabla}\breve{\boldsymbol{\mathcal{A}}}) - 1||_{L^\infty(H^3)} \leq CT^\kappa M$.

Proof.

1- Let $G = W^{1,\infty}(H^4) \cap W^{3,\infty}(H^2) \cap W^{4,\infty}(L^2) \cap H^4(H^1)$.
For all $\tilde{\boldsymbol{x}} \in \Omega^f_0$ we have $\breve{\boldsymbol{\mathcal{A}}}(\tilde{\boldsymbol{x}},t) = \tilde{\boldsymbol{x}} + \displaystyle\int_0^t \breve{\boldsymbol{v}}(\tilde{\boldsymbol{x}},s)\ ds$, then

$$||\breve{\boldsymbol{\mathcal{A}}}(\tilde{\boldsymbol{x}},t)||_G \leq ||\tilde{\boldsymbol{x}}||_G + \Big|\Big| \int_0^t \breve{\boldsymbol{v}}(\tilde{\boldsymbol{x}},s)\ ds \Big|\Big|_G.$$

Notice that as $\int_0^t \breve{\boldsymbol{v}}(s)ds|_{t=0} = 0$ then applying the generalized Poincaré inequality [BF13, Proposition III.2.38] there exists a constant C such that

$$\Big|\Big| \int_0^t \breve{\boldsymbol{v}}(\tilde{\boldsymbol{x}}, s)\ ds \Big|\Big|_G \leq C||\breve{\boldsymbol{v}}||_{F_4^T}.$$

Whence,

$$||\breve{\boldsymbol{\mathcal{A}}}(\tilde{\boldsymbol{x}}, t)||_G \leq C + C||\breve{\boldsymbol{v}}||_{F_4^T} \leq C(1+M).$$

2- We have $\boldsymbol{\nabla}\breve{\boldsymbol{\mathcal{A}}}(\tilde{\boldsymbol{x}}, t) = \mathbf{Id}_{\Omega_0^f} + \displaystyle\int_0^t \boldsymbol{\nabla}\breve{\boldsymbol{v}}(\tilde{\boldsymbol{x}}, s)\ ds$, so $\boldsymbol{\nabla}\breve{\boldsymbol{\mathcal{A}}}(\tilde{\boldsymbol{x}}, t) - \mathbf{Id}_{\Omega_0^f} = \displaystyle\int_0^t \boldsymbol{\nabla}\breve{\boldsymbol{v}}(\tilde{\boldsymbol{x}}, s)ds$. Hence, using the generalized Poincaré inequality there exists a constant C_T in $(0, T)$ such that we have

$$\begin{aligned}
||\boldsymbol{\nabla}\breve{\boldsymbol{\mathcal{A}}}(\tilde{\boldsymbol{x}}, t) - \mathbf{Id}_{\Omega_0^f}||_{W^{1,\infty}(H^3)\cap W^{3,\infty}(H^1)\cap H^4(L^2)} &\leq \Big|\Big| \int_0^t \boldsymbol{\nabla}\breve{\boldsymbol{v}}(\tilde{\boldsymbol{x}}, s)ds \Big|\Big|_{W^{1,\infty}(H^3)\cap W^{3,\infty}(H^1)\cap H^4(L^2)} \\
&\leq C_T||\boldsymbol{\nabla}\breve{\boldsymbol{v}}||_{L^\infty(H^3)\cap W^{2,\infty}(H^1)\cap H^3(L^2)} \\
&\leq C_T||\breve{\boldsymbol{v}}||_{F_4^T} \leq CM.
\end{aligned}$$

3- For $\tilde{\boldsymbol{x}} \in \Omega_0^f$ we have that $\boldsymbol{\nabla}\breve{\boldsymbol{\mathcal{A}}}(\tilde{\boldsymbol{x}}, t) = \mathbf{Id}_{\Omega_0^f} + \displaystyle\int_0^t \boldsymbol{\nabla}\breve{\boldsymbol{v}}(\tilde{\boldsymbol{x}}, s)ds$. Whence

$$\begin{aligned}
||\boldsymbol{\nabla}\breve{\boldsymbol{\mathcal{A}}}||_{L^\infty(H^3)} &= ||\mathbf{Id}_{\Omega_0^f}||_{L^\infty(H^3)} + \Big|\Big| \int_0^t \boldsymbol{\nabla}\breve{\boldsymbol{v}}(\tilde{\boldsymbol{x}}, s)ds \Big|\Big|_{L^\infty(H^3)} \\
&\leq C + CT||\breve{\boldsymbol{v}}||_{F_4^T} \\
&\leq C + CTM = C.
\end{aligned}$$

4- For $\boldsymbol{\nabla}\breve{\boldsymbol{\mathcal{A}}}$, its cofactor matrix $\operatorname{cof}(\boldsymbol{\nabla}\breve{\boldsymbol{\mathcal{A}}})$ is a 3-by-3 matrix whose components are $\dfrac{\partial \breve{\mathcal{A}}_i}{\partial \tilde{x}_j}\dfrac{\partial \breve{\mathcal{A}}_k}{\partial \tilde{x}_l}$, $i, j, k, l = 1, 2, 3$. Hence, as $H^3(\Omega_0^f) \subset L^\infty(\Omega_0^f)$ by Lemma 3.2.1 then each component of the matrix can be bounded by the norm $||\boldsymbol{\nabla}\breve{\boldsymbol{\mathcal{A}}}||^2_{L^\infty(H^3)}$. In addition, using the previous part gives

$$||\operatorname{cof}(\boldsymbol{\nabla}\breve{\boldsymbol{\mathcal{A}}})||_{L^\infty(H^3)} \leq C||\boldsymbol{\nabla}\breve{\boldsymbol{\mathcal{A}}}||^2_{L^\infty(L^\infty)} \leq C||\boldsymbol{\nabla}\breve{\boldsymbol{\mathcal{A}}}||^2_{L^\infty(H^3)} \leq C.$$

5- Using previous part we deduce that the components of $\partial_t\operatorname{cof}(\boldsymbol{\nabla}\breve{\boldsymbol{\mathcal{A}}})$ are $\dfrac{\partial \breve{\mathcal{A}}_i}{\partial \tilde{x}_j}\dfrac{\partial \partial_t \breve{\mathcal{A}}_k}{\partial \tilde{x}_l}$. From the definition (3.34) we have $\boldsymbol{\nabla}\breve{\boldsymbol{\mathcal{A}}} = \mathbf{Id}_{\Omega_0^f} + \int_0^t \boldsymbol{\nabla}\breve{\boldsymbol{v}}(s)ds$, which after differentiating in time gives $\partial_t(\boldsymbol{\nabla}\breve{\boldsymbol{\mathcal{A}}}) = \boldsymbol{\nabla}\tilde{\boldsymbol{v}}$. Hence, the components of $\partial_t\operatorname{cof}(\boldsymbol{\nabla}\breve{\boldsymbol{\mathcal{A}}})$ are $\dfrac{\partial \breve{\mathcal{A}}_i}{\partial \tilde{x}_j}\dfrac{\partial \breve{v}_k}{\partial \tilde{x}_l}$.

Therefore,

$$\begin{aligned}||\partial_t \mathrm{cof}(\nabla \breve{\mathcal{A}})||_{L^\infty(H^3)} &\le C||\nabla \breve{\boldsymbol{v}}||_{L^\infty(H^3)}||\nabla \breve{\mathcal{A}}||_{L^\infty(H^3)} \\ &\le CM.\end{aligned}$$

As $||\partial_t \mathrm{cof}(\nabla \breve{\mathcal{A}})||_{L^2(H^3)}\le T^{1/2}||\partial_t \mathrm{cof}(\nabla \breve{\mathcal{A}})||_{L^\infty(H^3)}$, it yields

$$||\partial_t \mathrm{cof}(\nabla \breve{\mathcal{A}})||_{L^2(L^\infty)}\le CT^{1/2}M.$$

6- From the second part of this lemma, as $||\nabla \breve{\mathcal{A}} - \mathbf{Id}||_{L^\infty(H^3)}\le TM < 1$, then $\nabla \breve{\mathcal{A}}$ is invertible. For $t < T$ we have,

$$\begin{aligned}||(\nabla \breve{\mathcal{A}})^{-1}(t)||_{L^\infty}\le C\left|\left|\frac{1}{\det((\nabla \breve{\mathcal{A}})(t))}\right|\right|_{L^\infty}\Big|\Big|\mathrm{cof}(\nabla \breve{\mathcal{A}}(t))\Big|\Big|_{L^\infty} &\le C\Big|\Big|\mathrm{cof}(\nabla \breve{\mathcal{A}}(t))\Big|\Big|_{L^\infty} \\ &\le C||\nabla \breve{\mathcal{A}}||^2_{L^\infty},\end{aligned}$$

where we used part 4 of this lemma to get the last inequality.

7- For the matrix $(\nabla \breve{\mathcal{A}})^{-1}$ we have $\nabla \breve{\mathcal{A}}(\nabla \breve{\mathcal{A}})^{-1} = \mathbf{Id}_{\Omega_0^f}$. Differentiating this relation in time gives

$$\partial_t(\nabla \breve{\mathcal{A}})^{-1}\nabla \breve{\mathcal{A}} + (\nabla \breve{\mathcal{A}})^{-1}\partial_t(\nabla \breve{\mathcal{A}}) = 0,$$

which is equivalent to

$$\partial_t(\nabla \breve{\mathcal{A}})^{-1} = (\nabla \breve{\mathcal{A}})^{-1}\partial_t(\nabla \breve{\mathcal{A}})(\nabla \breve{\mathcal{A}})^{-1}.$$

Using the fact that $\partial_t((\nabla \breve{\mathcal{A}})^{-1} - \mathbf{Id}) = \partial_t((\nabla \breve{\mathcal{A}})^{-1})$ yeilds

$$\begin{aligned}\partial_t((\nabla \breve{\mathcal{A}})^{-1} - \mathbf{Id}) &= -(\nabla \breve{\mathcal{A}})^{-1}\cdot \nabla \breve{\boldsymbol{v}} \cdot (\nabla \breve{\mathcal{A}})^{-1} \\ &= -\big((\nabla \breve{\mathcal{A}})^{-1} - \mathbf{Id}\big)\cdot \nabla \breve{\boldsymbol{v}} \cdot \big((\nabla \breve{\mathcal{A}})^{-1} - \mathbf{Id}\big) - \nabla \breve{\boldsymbol{v}} \cdot \big((\nabla \breve{\mathcal{A}})^{-1} - \mathbf{Id}\big) \\ &- \big((\nabla \breve{\mathcal{A}})^{-1} - \mathbf{Id}\big)\cdot \nabla \breve{\boldsymbol{v}} - \nabla \breve{\boldsymbol{v}}.\end{aligned}$$

Using the inequality [KP88]

$$||abc||_{H^p}\le C\Big(||a||_{H^p}||b||_{L^\infty}||c||_{L^\infty}+||a||_{L^\infty}||b||_{H^p}||c||_{L^\infty}+||a||_{L^\infty}||b||_{L^\infty}||c||_{H^p}\Big), \tag{3.36}$$

we thus obtain

$$\begin{aligned}||((\nabla \breve{\mathcal{A}})^{-1} - \mathbf{Id})(t)||_{H^3} &\le \int_0^t ||\partial_t\big((\nabla \breve{\mathcal{A}})^{-1} - \mathbf{Id}\big)(s)||_{H^3}\, ds \\ &\le\ C\int_0^t ||(\nabla \breve{\mathcal{A}})^{-1} - \mathbf{Id}||_{H^3}||(\nabla \breve{\mathcal{A}})^{-1} - \mathbf{Id}||_{L^\infty}||\nabla \breve{\boldsymbol{v}}||_{L^\infty}\, ds \\ &+ C\int_0^t ||(\nabla \breve{\mathcal{A}})^{-1} - \mathbf{Id}||^2_{L^\infty}||\nabla \breve{\boldsymbol{v}}||_{H^3}\, ds \\ &+ C\int_0^t ||(\nabla \breve{\mathcal{A}})^{-1} - \mathbf{Id}||_{H^1}||\nabla \breve{\boldsymbol{v}}||_{H^3}\, ds + C\int_0^t ||\nabla \breve{\boldsymbol{v}}||_{H^3}\, ds.\end{aligned}$$

Hence we get

$$\begin{aligned}||((\nabla\breve{\mathcal{A}})^{-1}-\mathbf{Id})(t)||_{H^3} &\leq C\int_0^t ||(\nabla\breve{\mathcal{A}})^{-1}(s)-\mathbf{Id}||_{H^3}||\nabla\breve{\boldsymbol{v}}(s)||_{H^3}\ ds + C\int_0^t ||\nabla\breve{\boldsymbol{v}}(s)||_{H^3}\ ds\\ &\leq C||\nabla\breve{\boldsymbol{v}}||_{L^\infty(H^4)}\int_0^t ||(\nabla\breve{\mathcal{A}})^{-1}(s)-\mathbf{Id}||_{H^3}\ ds + CT||\nabla\breve{\boldsymbol{v}}||_{L^\infty(H^4)}\\ &\leq CM\int_0^t ||(\nabla\breve{\mathcal{A}})^{-1}(s)-\mathbf{Id}||_{H^3}\ ds + CTM.\end{aligned}$$

Using Grönwall's inequality (B.1) we the existence of a $\kappa > 0$ such that

$$||(\nabla\breve{\mathcal{A}})^{-1}-\mathbf{Id}||_{L^\infty(H^3)}\leq T\ e^{(CTM)} \leq CT^\kappa M,$$

for T sufficiently small with respect to M.
As for $||\mathrm{cof}(\nabla\breve{\mathcal{A}})-\mathbf{Id}||_{L^\infty(H^3)}$ we use the mean value theorem. First, let us define the spaces

$$F_3^T = H^3\big(0,T;L^2(\Omega_0^f))\big)\cap L^\infty\big(0,T;H^3(\Omega_0^f)\big)\cap W^{2,\infty}\big(0,T;H^1(\Omega_0^f)\big)$$

and

$$C_{M_1}^T = \{\boldsymbol{F}\in F_3^T, \boldsymbol{F}=\nabla\tilde{\boldsymbol{v}};\ \text{for some } \tilde{\boldsymbol{v}}\in A_{M_1}^T, ||\boldsymbol{F}||_{F_3^T}\leq M\}.$$

Further, define the function

$$h : \boldsymbol{A}(\tilde{\boldsymbol{x}},t)\in H^3(\Omega_0^f)\longrightarrow \mathrm{cof}(\boldsymbol{A})\in H^3(\Omega_0^f).$$

Now we proceed to find the Fréchet Derivative of h. For any matrix $\boldsymbol{A}\in H^3(\Omega_0^f)$ we have

$$h(\boldsymbol{A}) = \det(\boldsymbol{A})\boldsymbol{A}^{-t}.$$

Whence, for any $\boldsymbol{H}\in H^3(\Omega_0^f)$,

$$\begin{aligned}Dh(\boldsymbol{A})\boldsymbol{H} &= \mathrm{cof}(\boldsymbol{A}) : \boldsymbol{H}\boldsymbol{A}^{-t} + \det(\boldsymbol{A})[-\boldsymbol{A}^{-t}\boldsymbol{H}^t\boldsymbol{A}^{-t}]\\ &= \mathrm{cof}(\boldsymbol{A})\boldsymbol{H}\boldsymbol{A}^{-t} - \mathrm{cof}(\boldsymbol{A})\boldsymbol{H}^t\boldsymbol{A}^{-t}\\ &= -\mathrm{cof}(\boldsymbol{A})[\boldsymbol{H}-\boldsymbol{H}^t]\boldsymbol{A}^{-t}.\end{aligned}$$

Using the embedding $H^3(\Omega_0^f)\subset L^\infty(\Omega_0^f)$ we have $||Dh(\boldsymbol{A})||_{\mathcal{L}(H^3)}\leq 4||\mathrm{cof}(\boldsymbol{A})||_{H^3}||\boldsymbol{A}^{-t}||_{H^3}$.
Applying the mean value theorem to the function h and using parts 2, 4 and 6 of this lemma yields

$$\begin{aligned}||h(\nabla\breve{\mathcal{A}})-h(\mathbf{Id})||_{L^\infty(H^3)} &\leq \sup_{s\in[0,1]}||Dh(\boldsymbol{A}+s(\mathbf{Id}-\boldsymbol{A}))||_{L^\infty(\mathcal{L}(H^3))}||(\nabla\breve{\mathcal{A}})-\mathbf{Id}||_{L^\infty(H^3)}\\ &\leq \sup_{s\in[0,1]}||Dh(\boldsymbol{A}+s(\mathbf{Id}-\boldsymbol{A}))||_{C_{M_1}^T}||(\nabla\breve{\mathcal{A}})-\mathbf{Id}||_{L^\infty(H^3)}\\ &\leq C||\nabla\breve{\mathcal{A}}||_{L^\infty(H^3)}||(\nabla\breve{\mathcal{A}})^{-1}-\mathbf{Id}||_{L^\infty(H^3)}\\ &\leq CT^\kappa M.\end{aligned}$$

Notice that, as $C^T_{M_1}$ is a convex set, then for any $\boldsymbol{A} \in C^T_{M_1}$, $\boldsymbol{A} + s(\mathbf{Id} - \boldsymbol{A}) \in C^T_{M_1}$ for $s \in [0,1]$. Thus,

$$\begin{aligned}
&\sup_{s\in[0,1]} ||Dh(\boldsymbol{A} + s(\mathbf{Id} - \boldsymbol{A}))||_{L^\infty(H^3)} \\
&\qquad \leq C \sup_{s\in[0,1]} ||\mathrm{cof}(\boldsymbol{A} + s(\mathbf{Id} - \boldsymbol{A}))||_{L^\infty(H^3)} ||[\boldsymbol{A} + s(\mathbf{Id} - \boldsymbol{A})]^{-1}||_{L^\infty(H^3)} \\
&\qquad \leq C \sup_{s\in[0,1]} ||\mathrm{cof}(\boldsymbol{A} + s(\mathbf{Id} - \boldsymbol{A}))||_{C^T_{M_1}} ||[\boldsymbol{A} + s(\mathbf{Id} - \boldsymbol{A})]^{-1}||_{L^\infty(H^3)} \\
&\qquad \leq C \sup_{s\in[0,1]} ||\boldsymbol{A} + s(\mathbf{Id} - \boldsymbol{A})||^3_{F^T_3} \leq C \quad \text{(using parts 4 and 6).}
\end{aligned}$$

8- We have that $\partial_t(\boldsymbol{\nabla}\breve{\boldsymbol{\mathcal{A}}}(t))^{-1} = -(\boldsymbol{\nabla}\breve{\boldsymbol{\mathcal{A}}})^{-1} \cdot \boldsymbol{\nabla}\breve{\boldsymbol{v}} \cdot (\boldsymbol{\nabla}\breve{\boldsymbol{\mathcal{A}}})^{-1}$. Then

$$||\partial_t(\boldsymbol{\nabla}\breve{\boldsymbol{\mathcal{A}}}(t))^{-1}||_{L^r} \leq ||(\boldsymbol{\nabla}\breve{\boldsymbol{\mathcal{A}}}(t))^{-1}||^2_{L^\infty} ||\boldsymbol{\nabla}\breve{\boldsymbol{v}}(t)||_{L^r} \leq C||\boldsymbol{\nabla}\breve{\boldsymbol{v}}(t)||_{L^r},$$

where we used previous parts for the last inequality.

In particular, for $r = +\infty$ we have

$$||\partial_t(\boldsymbol{\nabla}\breve{\boldsymbol{\mathcal{A}}}(t))^{-1}||_{L^\infty} \leq ||(\boldsymbol{\nabla}\breve{\boldsymbol{\mathcal{A}}}(t))^{-1}||^2_{L^\infty} ||\boldsymbol{\nabla}\breve{\boldsymbol{v}}(t)||_{L^\infty} \leq C||\boldsymbol{\nabla}\breve{\boldsymbol{v}}(t)||_{L^\infty}.$$

Taking supremum of t in $(0,T)$ we get

$$||\partial_t(\boldsymbol{\nabla}\breve{\boldsymbol{\mathcal{A}}}(t))^{-1}||_{L^\infty(L^\infty)} \leq C||\boldsymbol{\nabla}\breve{\boldsymbol{v}}(t)||_{L^\infty(L^\infty)} \leq CM,$$

which yields

$$||\partial_t(\boldsymbol{\nabla}\breve{\boldsymbol{\mathcal{A}}}(t))^{-1}||_{L^2(L^\infty)} \leq CT^{1/2}||\boldsymbol{\nabla}\breve{\boldsymbol{v}}(t)||_{L^\infty(L^\infty)} \leq CT^{1/2}M.$$

9- We have that $\breve{\boldsymbol{\mathcal{A}}} = (\breve{\mathcal{A}}_1, \breve{\mathcal{A}}_2, \breve{\mathcal{A}}_3)^t$. The Jacobian matrix of $\breve{\boldsymbol{\mathcal{A}}}$ is given by the following matrix

$$\boldsymbol{\nabla}\breve{\boldsymbol{\mathcal{A}}} = \begin{pmatrix} \dfrac{\partial\breve{\mathcal{A}}_1}{\partial\tilde{x}_1} & \dfrac{\partial\breve{\mathcal{A}}_1}{\partial\tilde{x}_2} & \dfrac{\partial\breve{\mathcal{A}}_1}{\partial\tilde{x}_3} \\[2ex] \dfrac{\partial\breve{\mathcal{A}}_2}{\partial\tilde{x}_1} & \dfrac{\partial\breve{\mathcal{A}}_2}{\partial\tilde{x}_2} & \dfrac{\partial\breve{\mathcal{A}}_2}{\partial\tilde{x}_3} \\[2ex] \dfrac{\partial\breve{\mathcal{A}}_3}{\partial\tilde{x}_1} & \dfrac{\partial\breve{\mathcal{A}}_3}{\partial\tilde{x}_2} & \dfrac{\partial\breve{\mathcal{A}}_3}{\partial\tilde{x}_3} \end{pmatrix}.$$

Hence, using (3.21)

$$\det(\boldsymbol{\nabla}\breve{\boldsymbol{\mathcal{A}}}) = \frac{1}{6}\varepsilon_{ijk}\varepsilon_{pqr}\partial_p\breve{\mathcal{A}}_i\partial_q\breve{\mathcal{A}}_j\partial_r\breve{\mathcal{A}}_k \quad \text{with the summation convention.}$$

Then,

$$||\det(\boldsymbol{\nabla}\breve{\boldsymbol{\mathcal{A}}})||_{L^\infty(H^3)}\leq C||\boldsymbol{\nabla}\breve{\boldsymbol{\mathcal{A}}}||^3_{L^\infty(H^3)}\leq C.$$

Moreover, the time derivative of the determinant is

$$\partial_t\det(\boldsymbol{\nabla}\breve{\boldsymbol{\mathcal{A}}}) = \frac{1}{6}\varepsilon_{ijk}\varepsilon_{pqr}\Big[(\partial_t\partial_p\breve{\mathcal{A}}_i)\partial_q\breve{\mathcal{A}}_j\partial_r\breve{\mathcal{A}}_k + \partial_p\breve{\mathcal{A}}_i(\partial_t\partial_q\breve{\mathcal{A}}_j)\partial_r\breve{\mathcal{A}}_k + \partial_p\breve{\mathcal{A}}_i\partial_q\breve{\mathcal{A}}_j(\partial_r\partial_k\breve{\mathcal{A}}_k)\Big]$$

with the summation convention.

Consequently,

$$\begin{aligned}
||\partial_t\det(\boldsymbol{\nabla}\breve{\boldsymbol{\mathcal{A}}})||_{L^\infty(H^2)} &\leq C||\partial_t\boldsymbol{\nabla}\breve{\boldsymbol{\mathcal{A}}}||_{L^\infty(L^\infty)}||\boldsymbol{\nabla}\breve{\boldsymbol{\mathcal{A}}}||^2_{L^\infty(H^2)}\\
&\leq C||\partial_t\boldsymbol{\nabla}\breve{\boldsymbol{\mathcal{A}}}||_{L^\infty(H^2)}||\boldsymbol{\nabla}\breve{\boldsymbol{\mathcal{A}}}||^2_{L^\infty(H^2)}\\
&\leq C||\boldsymbol{\nabla}\breve{\boldsymbol{v}}||_{L^\infty(H^2)}||\boldsymbol{\nabla}\breve{\boldsymbol{\mathcal{A}}}||^2_{L^\infty(H^2)}\\
&\leq CM.
\end{aligned}$$

10- Consider the function $f = \det(\boldsymbol{F})$, for $\boldsymbol{F}(\tilde{\boldsymbol{x}}, t) \in H^3(\Omega_0^f)$. The function f is continuous, and differentiable. Its Fréchet derivative is given by

$$Df(\boldsymbol{F})\boldsymbol{H} = \mathrm{cof}(\boldsymbol{F}) : \boldsymbol{H}, \qquad \forall\ \boldsymbol{H} = \boldsymbol{H}(\tilde{\boldsymbol{x}}, t) \in H^3(\Omega_0^f).$$

Using the embedding of $H^3(\Omega_0^f) \subset L^\infty(\Omega_0^f)$ yields

$$\begin{aligned}
||Df(\boldsymbol{F})\boldsymbol{H}||_{H^3} &\leq ||\mathrm{cof}(\boldsymbol{F})||_{L^\infty}||\boldsymbol{H}||_{H^3}+||\mathrm{cof}(\boldsymbol{F})||_{H^3}||\boldsymbol{H}||_{L^\infty}\\
&\leq C||\mathrm{cof}(\boldsymbol{F})||_{H^3}||\boldsymbol{H}||_{H^3}.
\end{aligned}$$

Therefore, we have $||Df(\boldsymbol{F})||_{\mathcal{L}(H^3)}\leq ||\mathrm{cof}(\boldsymbol{F})||_{H^3}$. Applying the mean value theorem to the function f and using parts 2 and 4 of this lemma yield

$$\begin{aligned}
||\det(\boldsymbol{\nabla}\breve{\boldsymbol{\mathcal{A}}}) - \det(\mathbf{Id})||_{L^\infty(H^3)} &\leq \sup_{s\in[0,1]}||Df(\boldsymbol{F} + s(\mathbf{Id} - \boldsymbol{F}))||_{L^\infty(H^3)}||(\boldsymbol{\nabla}\breve{\boldsymbol{\mathcal{A}}})^{-1} - \mathbf{Id}||_{L^\infty(H^3)}\\
&\leq \sup_{s\in[0,1]}||\mathrm{cof}(\boldsymbol{F} + s(\mathbf{Id} - \boldsymbol{F}))||_{L^\infty(H^3)}||(\boldsymbol{\nabla}\breve{\boldsymbol{\mathcal{A}}})^{-1} - \mathbf{Id}||_{L^\infty(H^3)}\\
&\leq C||(\boldsymbol{\nabla}\breve{\boldsymbol{\mathcal{A}}})^{-1} - \mathbf{Id}||_{L^\infty(H^3)}\\
&\leq CT^\kappa M.
\end{aligned}$$

Indeed, we have used that $L^\infty(H^3) \subset C^T_{M_1}$ and part 4 of this lemma which give

$$\sup_{s\in[0,1]}||\mathrm{cof}(\boldsymbol{F} + s(\mathbf{Id} - \boldsymbol{F}))||_{L^\infty(H^3)}\leq \sup_{s\in[0,1]}||\mathrm{cof}(\boldsymbol{F} + s(\mathbf{Id} - \boldsymbol{F}))||_{C^T_{M_1}}\leq C.$$

■

Remark 3.2.1 *The last part of Lemma 3.2.2 gives*

$$||\det(\boldsymbol{\nabla}\breve{\boldsymbol{\mathcal{A}}}) - 1||_{L^\infty(L^\infty)}\leq CT^\kappa M.$$

That is, for all t in $(0,T)$ and $\tilde{\boldsymbol{x}}$ in Ω_0^f we have

$$-CT^\kappa M \leq \det(\boldsymbol{\nabla}\breve{\boldsymbol{\mathcal{A}}})(\tilde{\boldsymbol{x}},t) - 1 \leq CT^\kappa M.$$

This gives

$$\det(\boldsymbol{\nabla}\breve{\boldsymbol{\mathcal{A}}})(\tilde{\boldsymbol{x}},t) \geq 1 - CT^\kappa M \qquad \forall\ (\tilde{\boldsymbol{x}},t) \in \Omega_0^f \times (0,T).$$

Remark 3.2.2 *For $0 < n \leq 4$, the quantity CTM^n can be approximated by $CT^\kappa M$, with $\kappa > 0$. Indeed, as $TM^4 < 1$, then we can find $\kappa > 0$ such that $TM^4 \leq T^\kappa$.*

Lemma 3.2.3 *Let $M > 1$, $T > 0$ and $\breve{\boldsymbol{\xi}} \in A_{M_2}^T$ be given. There exists $C > 0$ such that for all $i, \alpha, j, \beta \in \{1,2,3\}$, we have:*

1-

$$\left|\left|c^l_{i\alpha j\beta}(\boldsymbol{\nabla}\breve{\boldsymbol{\xi}}) + c^q_{i\alpha j\beta}(\boldsymbol{\nabla}\breve{\boldsymbol{\xi}})\right|\right|_{S_3^T} \leq C(M + M^2) \tag{3.37}$$

where $c^l_{i\alpha j\beta}$ and $c^q_{i\alpha j\beta}$ are defined by the expressions (3.15) and (3.16) respectively.

2- For any matrix $\boldsymbol{A} \in \mathcal{M}_3(\mathbb{R})$, we have

$$\sum_{i,\alpha,j,\beta=1}^{3} c_{i\alpha j\beta}(\boldsymbol{\nabla}\breve{\boldsymbol{\xi}}) A_{j\beta} A_{i\alpha} \geq \frac{\mu_s}{2}|A + A^t|^2 + \lambda_s |\mathrm{tr}(A)|^2 - CT(M + M^2)|A|^2. \tag{3.38}$$

3-

$$\left|\left|d^l_{i\alpha j\beta}(\boldsymbol{\nabla}\breve{\boldsymbol{\xi}}) + d^Q_{i\alpha j\beta}(\boldsymbol{\nabla}\breve{\boldsymbol{\xi}}) + d^T_{i\alpha j\beta}(\boldsymbol{\nabla}\breve{\boldsymbol{\xi}}) + d^F_{i\alpha j\beta}(\boldsymbol{\nabla}\breve{\boldsymbol{\xi}})\right|\right|_{S_3^T} \leq C(M + M^2 + M^3 + M^4). \tag{3.39}$$

4- For any matrix $\boldsymbol{A} \in \mathcal{M}_3(\mathbb{R})$ we have

$$\sum_{i,\alpha,j,\beta=1}^{3} d_{i\alpha j\beta}(\boldsymbol{\nabla}\breve{\boldsymbol{\xi}}) A_{j\beta} A_{i\alpha} \geq \mathsf{C}|\mathrm{tr}(A)|^2 - CT(M + M^2 + M^3 + M^4)|A|^2. \tag{3.40}$$

5-

$$||\boldsymbol{\nabla}\breve{\boldsymbol{\varphi}}||_{L^\infty(H^2(\Omega_0^s))} \leq C. \tag{3.41}$$

6-

$$||\mathrm{cof}(\boldsymbol{\nabla}\breve{\boldsymbol{\varphi}})||_{L^\infty(H^2(\Omega_0^s))} \leq C \quad \textit{and} \quad ||\mathrm{cof}(\boldsymbol{\nabla}\breve{\boldsymbol{\varphi}})||_{L^2(H^2(\Omega_0^s))} \leq CT^{1/2}. \tag{3.42}$$

7- We have

$$||\det(\boldsymbol{\nabla}\breve{\boldsymbol{\varphi}})||_{L^\infty(H^2)} \leq C \quad \textit{and} \quad ||\partial_t \det(\boldsymbol{\nabla}\breve{\boldsymbol{\varphi}})||_{L^\infty(H^2)} \leq CM. \tag{3.43}$$

8-

$$||(\boldsymbol{\nabla}\breve{\boldsymbol{\varphi}})^{-1}||_{L^\infty(H^2(\Omega_0^s))}\leq C. \tag{3.44}$$

9- For $\breve{\boldsymbol{\xi}} \in A^T_{M_2}$ *we have*

$$||\det(\boldsymbol{\nabla}\breve{\boldsymbol{\varphi}}) - 1||_{L^\infty(H^2(\Omega_0^s))}\leq CTM. \tag{3.45}$$

Proof.

1- From the definition (3.15) of the linear part $c^l_{i\alpha j\beta}(\boldsymbol{\nabla}\breve{\boldsymbol{\xi}})$ we have

$$||c^l_{i\alpha j\beta}(\boldsymbol{\nabla}\breve{\boldsymbol{\xi}})||_{L^2}\leq C||\boldsymbol{\nabla}\breve{\boldsymbol{\xi}}||_{L^2}\leq C||\breve{\boldsymbol{\xi}}||_{H^1}. \tag{3.46}$$

While from the definition (3.16) of the quadratic part $c^q_{i\alpha j\beta}(\boldsymbol{\nabla}\breve{\boldsymbol{\xi}})$ we have

$$\begin{aligned}||c^q_{i\alpha j\beta}(\boldsymbol{\nabla}\breve{\boldsymbol{\xi}})||_{H^3}\leq C||\partial_\beta\tilde{\xi}_j\partial_\alpha\tilde{\xi}_i||^2_{H^3} &\leq C||\partial_\beta\tilde{\xi}_j||_{H^3}||\partial_\alpha\tilde{\xi}_i||_{L^\infty}+C||\partial_\beta\tilde{\xi}_j||_{L^\infty}||\partial_\alpha\tilde{\xi}_i||_{H^3}\\ &\leq C||\boldsymbol{\nabla}\breve{\boldsymbol{\xi}}||_{H^3}||\boldsymbol{\nabla}\breve{\boldsymbol{\xi}}||_{H^3}+C||\boldsymbol{\nabla}\breve{\boldsymbol{\xi}}||_{H^3}||\boldsymbol{\nabla}\breve{\boldsymbol{\xi}}||_{H^3}\\ &\leq C||\boldsymbol{\nabla}\breve{\boldsymbol{\xi}}||^2_{H^3}\leq ||\breve{\boldsymbol{\xi}}||^2_{H^4(\Omega_0^s)}.\end{aligned}$$

Here we have used the Sobolev embedding of H^3 into L^∞ obtained by Corollary 3.2.1. Using the above two inequalities we get

$$\begin{aligned}||c^l_{i\alpha j\beta}(\boldsymbol{\nabla}\breve{\boldsymbol{\xi}})+c^q_{i\alpha j\beta}(\boldsymbol{\nabla}\breve{\boldsymbol{\xi}})||_{H^3} &\leq ||c^l_{i\alpha j\beta}(\boldsymbol{\nabla}\breve{\boldsymbol{\xi}})||_{H^3}+||c^q_{i\alpha j\beta}(\boldsymbol{\nabla}\breve{\boldsymbol{\xi}})||_{H^3}\\ &\leq C\Big(||\breve{\boldsymbol{\xi}}||_{H^4}+||\breve{\boldsymbol{\xi}}||^2_{H^4}\Big).\end{aligned}$$

Taking supremum on $(0,T)$ yields

$$||c^l_{i\alpha j\beta}(\boldsymbol{\nabla}\breve{\boldsymbol{\xi}})+c^q_{i\alpha j\beta}(\boldsymbol{\nabla}\breve{\boldsymbol{\xi}})||_{L^\infty(H^3)}\leq C\Big(||\breve{\boldsymbol{\xi}}||_{L^\infty(H^4)}+||\breve{\boldsymbol{\xi}}||^2_{L^\infty(H^4)}\Big)\leq C(M+M^2). \tag{3.47}$$

On the other hand, using the fact that $||\partial_t\boldsymbol{\nabla}\breve{\boldsymbol{\xi}}||_{L^\infty(H^3)}\leq ||\breve{\boldsymbol{\xi}}||_{S_4^T}$ we obtain

$$\begin{aligned}||\partial_t c^l_{i\alpha j\beta}(\boldsymbol{\nabla}\breve{\boldsymbol{\xi}})+\partial_t c^q_{i\alpha j\beta}(\boldsymbol{\nabla}\breve{\boldsymbol{\xi}})||_{L^\infty(L^2)} &\leq ||\partial_t c^l_{i\alpha j\beta}(\boldsymbol{\nabla}\breve{\boldsymbol{\xi}})||_{L^\infty(L^2)}+||\partial_t c^q_{i\alpha j\beta}(\boldsymbol{\nabla}\breve{\boldsymbol{\xi}})||_{L^\infty(L^2)}\\ &\leq C\Big(||\breve{\boldsymbol{\xi}}||_{S_4^T}+||\breve{\boldsymbol{\xi}}||^2_{S_4^T}\Big)\\ &\leq C(M+M^2).\end{aligned} \tag{3.48}$$

Where we used

$$||\partial_t\boldsymbol{\nabla}\breve{\boldsymbol{\xi}}\boldsymbol{\nabla}\breve{\boldsymbol{\xi}}||_{L^2}\leq C(\Omega_0^s)||\partial_t\boldsymbol{\nabla}\breve{\boldsymbol{\xi}}||_{L^2}||\boldsymbol{\nabla}\breve{\boldsymbol{\xi}}||_{L^\infty}\leq C||\breve{\boldsymbol{\xi}}||_{S_4^T}||\breve{\boldsymbol{\xi}}||_{H^2}\leq C||\breve{\boldsymbol{\xi}}||^2_{S_4^T}.$$

Proceeding in a similar way, one can show that

$$||\partial_t^k c^l_{i\alpha j\beta}(\boldsymbol{\nabla}\breve{\boldsymbol{\xi}})+\partial_t^k c^q_{i\alpha j\beta}(\boldsymbol{\nabla}\breve{\boldsymbol{\xi}})||_{L^\infty(L^2)}\leq C(M+M^2)\qquad \text{for } k=2,3. \tag{3.49}$$

Combining (3.47)-(3.49) gives the desired result.

2- We have

$$R_1 = \sum_{i,\alpha,j,\beta=1}^{3} (\delta_{\beta i}\delta_{\alpha j} + \delta_{\alpha\beta}\delta_{ij})A_{j\beta}A_{i\alpha} = \sum_{i,j=1}^{3}[(1+0)A_{ji}A_{ij}] + \sum_{i,\alpha=1}^{3}(1+0)A_{i\alpha}A_{i\alpha}$$
$$= \mathrm{tr}(\boldsymbol{A}^t\boldsymbol{A}) + |A|^2. \tag{3.50}$$

But, using the fact that $(a+b)^2 \leq 2(a^2+b^2)$ gives

$$\mathrm{tr}(\boldsymbol{A}^t\boldsymbol{A}) = |\boldsymbol{A}|^2 = \frac{1}{2}(|\boldsymbol{A}|^2 + |\boldsymbol{A}^t|^2) \geq \frac{1}{4}|\boldsymbol{A} + \boldsymbol{A}^t|^2 \tag{3.51}$$

Hence,

$$\mu_s R_1 \geq \frac{\mu_s}{2}|\boldsymbol{A} + \boldsymbol{A}^t|^2.$$

Also,

$$R_2 = \sum_{i,\alpha,j,\beta=1}^{3} (\delta_{i\alpha}\delta_{j\beta})A_{j\beta}A_{i\alpha} = \sum_{i,j=1}^{3} A_{jj}A_{ii} = \sum_{i=1}^{3} A_{ii}\sum_{j=1}^{3} A_{jj} = |\mathrm{tr}(\boldsymbol{A})|^2. \tag{3.52}$$

As a result we obtain

$$\lambda_s R_2 \geq \lambda_s |\mathrm{tr}(A)|^2.$$

Finally, thanks to (3.37) we have that

$$\begin{aligned} R_3 &= \sum_{i,\alpha,j,\beta=1}^{3} \left(c^l_{i\alpha j\beta}(\boldsymbol{\nabla}\breve{\boldsymbol{\xi}}) + c^q_{i\alpha j\beta}(\boldsymbol{\nabla}\breve{\boldsymbol{\xi}})\right)A_{j\beta}A_{i\alpha} \\ &\geq -\sum_{i,\alpha,j,\beta=1}^{3} \left|c^l_{i\alpha j\beta}(\boldsymbol{\nabla}\breve{\boldsymbol{\xi}}) + c^q_{i\alpha j\beta}(\boldsymbol{\nabla}\breve{\boldsymbol{\xi}})\right||A_{j\beta}A_{i\alpha}| \\ &\geq -T\sum_{i,\alpha,j,\beta=1}^{3} ||c^l_{i\alpha j\beta}(\boldsymbol{\nabla}\breve{\boldsymbol{\xi}}) + c^q_{i\alpha j\beta}(\boldsymbol{\nabla}\breve{\boldsymbol{\xi}})||_{S_1^T}|A_{j\beta}A_{i\alpha}| \\ &\geq -CT(M+M^2)|\boldsymbol{A}|^2. \end{aligned} \tag{3.53}$$

In fact, in order to get the norm $|\boldsymbol{A}|^2$, we use the identity $|ab| \leq C(|a|^2+|b|^2)$. Indeed, we have

$$\sum_{i,\alpha,j,\beta=1}^{3} |A_{j\beta}A_{i\alpha}| \leq \frac{1}{2}\left[|\boldsymbol{A}|^2 + |\boldsymbol{A}^t|^2\right] \leq |\boldsymbol{A}|^2.$$

Therefore, combining the estimates on R_1, R_2 and R_3 we get the desired result.

3- Using the definition (3.24), the inequality (3.36) and the embedding $H^3 \subset L^\infty$, we have

$$\begin{aligned} ||d^F_{i\alpha j\beta}(\boldsymbol{\nabla}\breve{\boldsymbol{\xi}}(t))||_{H^3} &\leq ||\boldsymbol{\nabla}\breve{\boldsymbol{\xi}}(t)||^3_{L^\infty}||\boldsymbol{\nabla}\breve{\boldsymbol{\xi}}(t)\boldsymbol{\nabla}\breve{\boldsymbol{\xi}}(t)\boldsymbol{\nabla}\breve{\boldsymbol{\xi}}(t)||_{H^3} \\ &\leq ||\boldsymbol{\nabla}\breve{\boldsymbol{\xi}}(t)||^4_{H^3} \\ &\leq ||\breve{\boldsymbol{\xi}}(t)||^4_{H^4}. \end{aligned}$$

Taking supremum over $(0,T)$ we get

$$||d^F_{i\alpha j\beta}||_{L^\infty(H^3)} \leq M^4.$$

In a similar manner we show that

$$||d^L_{i\alpha j\beta}||_{L^\infty(H^3)} \leq ||\breve{\boldsymbol{\xi}}||_{S_4^T},\ ||d^Q_{i\alpha j\beta}||_{L^\infty(H^3)} \leq ||\breve{\boldsymbol{\xi}}||^2_{S_4^T} \text{ and } ||d^T_{i\alpha j\beta}||_{L^\infty(H^3)} \leq ||\breve{\boldsymbol{\xi}}||^3_{S_4^T}.$$

4- Using the definition (3.23) of $d_{i\alpha j\beta}$ we can see that for $i=\alpha$ and $j=\beta$ we get the constant terms. Hence for $i=\alpha$ and $\beta=j$

$$\sum_{i,\alpha,j,\beta=1}^{3} d_{i\alpha j\beta}A_{j\beta}A_{i\alpha} = \mathsf{C}\sum_{i,j=1}^{3} A_{ii}A_{jj} = \mathsf{C}|\mathrm{tr}(\boldsymbol{A})|^2.$$

Proceeding in a similar manner as in part 2, we get the desired result.

5- For $t \in [0,T]$, we have that

$$\begin{aligned}\boldsymbol{\nabla}\breve{\boldsymbol{\varphi}}(t) &= \mathbf{Id}_{\Omega_0^s} + \boldsymbol{\nabla}\breve{\boldsymbol{\xi}}(t)\\ &= \mathbf{Id}_{\Omega_0^s} + \int_0^t \partial_s \boldsymbol{\nabla}\breve{\boldsymbol{\xi}}(s)\ ds,\end{aligned}$$

then,

$$\begin{aligned}||\boldsymbol{\nabla}\breve{\boldsymbol{\varphi}}||_{L^\infty(H^2(\Omega_0^s))} &\leq ||\mathbf{Id}_{\Omega_0^s}||_{L^\infty(H^2(\Omega_0^s))} + T||\partial_t\boldsymbol{\nabla}\breve{\boldsymbol{\xi}}||_{L^\infty(H^2((\Omega_0^s))}\\ &\leq C + CT||\breve{\boldsymbol{\xi}}||_{S_4^T} \leq C.\end{aligned}$$

6- Arguing as in part 4 of Lemma 3.2.2. The components of the matrix $\mathrm{cof}(\boldsymbol{\nabla}\breve{\boldsymbol{\varphi}})$ are $\dfrac{\partial\breve{\varphi}_i}{\partial\tilde{x}_j}\dfrac{\partial\breve{\varphi}_k}{\partial\tilde{x}_l}$, where $i,j,k,l=1,2,3$. Hence

$$||\mathrm{cof}(\boldsymbol{\nabla}\breve{\boldsymbol{\varphi}})||_{L^\infty(H^2(\Omega_0^s))} \leq ||\boldsymbol{\nabla}\breve{\boldsymbol{\varphi}}||^2_{L^\infty(H^2(\Omega_0^s))} \leq C. \tag{3.54}$$

We can then deduce that

$$||\mathrm{cof}(\boldsymbol{\nabla}\breve{\boldsymbol{\varphi}})||_{L^2(H^2(\Omega_0^s))} \leq CT.$$

7- We have $\breve{\boldsymbol{\varphi}} = (\breve{\varphi}_1, \breve{\varphi}_2, \breve{\varphi}_3)^t$. The Jacobian matrix of $\breve{\boldsymbol{\varphi}}$ is given by the following matrix

$$\boldsymbol{\nabla}\breve{\boldsymbol{\varphi}} = \begin{pmatrix} \dfrac{\partial\breve{\varphi}_1}{\partial\tilde{x}_1} & \dfrac{\partial\breve{\varphi}_1}{\partial\tilde{x}_2} & \dfrac{\partial\breve{\varphi}_1}{\partial\tilde{x}_3}\\[2ex] \dfrac{\partial\breve{\varphi}_2}{\partial\tilde{x}_1} & \dfrac{\partial\breve{\varphi}_2}{\partial\tilde{x}_2} & \dfrac{\partial\breve{\varphi}_2}{\partial\tilde{x}_3}\\[2ex] \dfrac{\partial\breve{\varphi}_3}{\partial\tilde{x}_1} & \dfrac{\partial\breve{\varphi}_3}{\partial\tilde{x}_2} & \dfrac{\partial\breve{\varphi}_3}{\partial\tilde{x}_3} \end{pmatrix}.$$

Hence,

$$\det(\boldsymbol{\nabla}\breve{\boldsymbol{\varphi}}) = \frac{1}{6}\varepsilon_{ijk}\varepsilon_{pqr}\partial_p\breve{\varphi}_i\partial_q\breve{\varphi}_j\partial_r\breve{\varphi}_k \quad \text{with the summation convention.}$$

This yields

$$||\det(\boldsymbol{\nabla}\breve{\boldsymbol{\varphi}})||_{L^\infty(H^2)} \leq ||\boldsymbol{\nabla}\breve{\boldsymbol{\varphi}}||^3_{L^\infty(H^2)} \leq C.$$

In addition, for the time derivative of the determinant we have

$$\partial_t\det(\boldsymbol{\nabla}\breve{\boldsymbol{\varphi}}) = \frac{1}{6}\varepsilon_{ijk}\varepsilon_{pqr}\Big[(\partial_t\partial_p\breve{\varphi}_i)\partial_q\breve{\varphi}_j\partial_r\breve{\varphi}_k + \partial_p\breve{\varphi}_i(\partial_t\partial_q\breve{\varphi}_j)\partial_r\breve{\varphi}_k + \partial_p\breve{\varphi}_i\partial_q\breve{\varphi}_j(\partial_t\partial_r\breve{\varphi}_k)\Big]$$
$$\text{with the summation convention.}$$

Whence,

$$\begin{aligned}
||\partial_t\det(\boldsymbol{\nabla}\breve{\boldsymbol{\varphi}})||_{L^\infty(H^2)} &\leq C||\boldsymbol{\nabla}\breve{\boldsymbol{\varphi}}||_{L^\infty(L^\infty)}||\partial_t\boldsymbol{\nabla}\breve{\boldsymbol{\varphi}}||^2_{L^\infty(H^2)} \\
&\leq C||\partial_t\boldsymbol{\nabla}\breve{\boldsymbol{\varphi}}||_{L^\infty(H^2)}||\boldsymbol{\nabla}\breve{\boldsymbol{\varphi}}||^2_{L^\infty(H^2)} \\
&\leq C||\partial_t\boldsymbol{\nabla}\breve{\boldsymbol{\xi}}||_{L^\infty(H^2)}||\boldsymbol{\nabla}\breve{\boldsymbol{\varphi}}||^2_{L^\infty(H^2)} \\
&\leq CM.
\end{aligned}$$

8- The inverse of the deformation gradient can be expressed as $(\boldsymbol{\nabla}\breve{\boldsymbol{\varphi}})^{-1} = \dfrac{[\mathrm{cof}(\boldsymbol{\nabla}\breve{\boldsymbol{\varphi}})]^t}{\det(\boldsymbol{\nabla}\breve{\boldsymbol{\varphi}})}$. Then we have

$$\begin{aligned}
||(\boldsymbol{\nabla}\breve{\boldsymbol{\varphi}})^{-1}||_{L^\infty(L^\infty(\Omega_0^s))} &\leq C\left|\left|\frac{1}{\det(\boldsymbol{\nabla}\breve{\boldsymbol{\varphi}})}\right|\right|_{L^\infty(L^\infty)}\left|\left|\mathrm{cof}(\boldsymbol{\nabla}\breve{\boldsymbol{\varphi}})\right|\right|_{L^\infty(L^\infty)} \\
&\leq C\left|\left|\mathrm{cof}(\boldsymbol{\nabla}\breve{\boldsymbol{\varphi}})\right|\right|_{L^\infty(L^\infty)} \leq C.
\end{aligned}$$

9- Similarly as in Lemma 3.2.2, we apply the mean value theorem to the function $f(F) = \det(F)$. We have $Df(F)H = \mathrm{cof}(F)H$. Then $||Df(F)||_{\mathcal{L}(H^3)} \leq ||\mathrm{cof}(F)||_{H^3} \leq C$.
Applying the mean value theorem gives

$$\begin{aligned}
||\det(\boldsymbol{\nabla}\breve{\boldsymbol{\varphi}}) - \det(\mathbf{Id})||_{L^\infty(H^2)} &\leq C||\boldsymbol{\nabla}\breve{\boldsymbol{\varphi}} - \mathbf{Id}||_{L^\infty(H^2)} \\
&\leq C\left|\left|\int_0^t \partial_s\boldsymbol{\nabla}\breve{\boldsymbol{\xi}}(s)\ ds\right|\right|_{L^\infty(H^2)} \\
&\leq CTM.
\end{aligned}$$

In particular, we have $||\det(\boldsymbol{\nabla}\breve{\boldsymbol{\varphi}}) - \det(\mathbf{Id})||_{L^\infty(L^\infty)} \leq CTM$. Proceeding as in Remark 3.2.1, gives

$$\det(\boldsymbol{\nabla}\breve{\boldsymbol{\varphi}}) \geq 1 - CTM \geq 1 - CT^\kappa M. \tag{3.55}$$

■

The main step to establish the local in time existence and uniqueness of solution of the coupled problem is to partially linearize it. This is achieved by considering the non-linear terms to be given, thus the flow map and deformation are given by (3.34) and (3.35) respectively. For the given $\breve{\boldsymbol{\mathcal{A}}}, \breve{\boldsymbol{\varphi}}$ and $(\breve{\boldsymbol{v}}, \breve{\boldsymbol{\xi}}) \in A_M^T$ we denote $b_{i\alpha j\beta}(\boldsymbol{\nabla}\breve{\boldsymbol{\xi}})$ by $\breve{b}_{i\alpha j\beta}$ and the fluid shear stress is denoted by $\breve{\boldsymbol{\sigma}}_f^0(\tilde{\boldsymbol{v}}, \tilde{p}_f)$ when considering $\breve{\boldsymbol{\mathcal{A}}}$ in the expression (3.8). Now we write the system (3.28) in the reference configuration at time $t = 0$. Equation $(3.28)_1$ is replaced by

$$\rho_f \det(\boldsymbol{\nabla}\breve{\boldsymbol{\mathcal{A}}})\partial_t \tilde{\boldsymbol{v}} - \boldsymbol{\nabla} \cdot \breve{\boldsymbol{\sigma}}_f^0(\tilde{\boldsymbol{v}}, \tilde{p}_f) = 0 \quad \text{in } \Omega_0^f \times (0, T)$$

and Equation $(3.28)_5$ is replaced by

$$\rho_s \det(\boldsymbol{\nabla}\breve{\boldsymbol{\varphi}})\partial_t^2 \tilde{\xi}_i - \sum_{\alpha,j,\beta=1}^{3} \breve{b}_{i\alpha j\beta}\partial_{\alpha\beta}^2 \tilde{\xi}_j = 0, \quad i = 1, 2, 3 \quad \text{in } \Omega_0^s \times (0, T).$$

The coupling conditions on Σ_T are given by

$$\begin{cases} \tilde{\boldsymbol{v}} = \partial_t \tilde{\boldsymbol{\xi}}, \\ \left[\breve{\boldsymbol{\sigma}}_f^0(\tilde{\boldsymbol{v}}, \tilde{p}_f)\ \tilde{\boldsymbol{n}}\right]_i = \displaystyle\sum_{\alpha,j,\beta=1}^{3} \left(\int_0^t \breve{b}_{i\alpha j\beta}\partial_{s\beta}^2 \tilde{\xi}_j ds\right) \tilde{n}_\alpha \quad \text{for} \quad i = 1, 2, 3. \end{cases} \tag{3.56}$$

For $(\breve{\boldsymbol{v}}, \breve{\boldsymbol{\xi}})$ being given in A_M^T , we introduce the following mapping

$$\Psi : (\breve{\boldsymbol{v}}, \breve{\boldsymbol{\xi}}) \longrightarrow (\tilde{\boldsymbol{v}}, \tilde{\boldsymbol{\xi}})$$

where $(\tilde{\boldsymbol{v}}, \tilde{\boldsymbol{\xi}})$ together with $\tilde{p}_f$ form the solution of the partially linearized system.

First, we start by defining an auxiliary problem that considers the boundary condition (3.29). Choosing a suitable functional space we write the variational formulation where the pressure term disappears. Uniqueness and existence of a solution of the auxiliary problem are established in the next section.

3.3 An Auxiliary Problem

As we mentioned before, there is a disagreement between the elasticity equation and the stress coupling condition on Σ_T attributed to it. Thus, we set up an auxiliary problem in which the natural boundary condition (3.29) is used. This problem constitutes the first tool in establishing the existence and uniqueness of the strong solution of the FSI problem. We start by introducing the auxiliary problem. Let $\boldsymbol{g} = [g_1, g_2, g_3]^t$ be a function in $H_l^1\big([0, T]; L^2(\Gamma_c(0))\big)$, and consider the following system:

$$\begin{cases} \rho_f \mathrm{det}(\boldsymbol{\nabla}\breve{\boldsymbol{\mathcal{A}}})\partial_t\tilde{\boldsymbol{v}} - \boldsymbol{\nabla}\cdot\breve{\boldsymbol{\sigma}}_f^0(\tilde{\boldsymbol{v}},\tilde{p}_f) = 0 & \text{in } \Omega_0^f\times(0,T),\\ \nabla\cdot\big(\mathrm{det}(\boldsymbol{\nabla}\breve{\boldsymbol{\mathcal{A}}})(\boldsymbol{\nabla}\breve{\boldsymbol{\mathcal{A}}})^{-1}\tilde{\boldsymbol{v}}\big) = 0 & \text{in } \Omega_0^f\times(0,T),\\ \tilde{\boldsymbol{v}} = \boldsymbol{v}_{\mathrm{in}}\circ\breve{\boldsymbol{\mathcal{A}}} & \text{on } \Gamma_{\mathrm{in}}(0)\times(0,T),\\ \breve{\boldsymbol{\sigma}}_f^0(\tilde{\boldsymbol{v}},\tilde{p}_f)\,\tilde{\boldsymbol{n}} = 0 & \text{on } \Gamma_{\mathrm{out}}(0)\times(0,T),\\ \rho_s\mathrm{det}(\boldsymbol{\nabla}\breve{\boldsymbol{\varphi}})\partial_t^2\tilde{\xi}_i - \displaystyle\sum_{\alpha,j,\beta=1}^{3}\breve{b}_{i\alpha j\beta}\partial^2_{\alpha\beta}\tilde{\xi}_j = 0 \quad i=1,2,3, & \text{in } \Omega_0^s\times(0,T),\\ \tilde{\boldsymbol{\xi}} = \boldsymbol{0} & \text{on } \Gamma_2(0)\times(0,T),\\ \tilde{\boldsymbol{v}} = \partial_t\tilde{\boldsymbol{\xi}} & \text{on } \Gamma_c(0)\times(0,T),\\ \big[\breve{\boldsymbol{\sigma}}_f^0(\tilde{\boldsymbol{v}},\tilde{p}_f)\tilde{\boldsymbol{n}}\big]_i = \displaystyle\sum_{\alpha,j,\beta=1}^{3}\Big(\breve{b}_{i\alpha j\beta}\partial_\beta\tilde{\xi}_j\Big)\tilde{n}_\alpha + g_i \quad i=1,2,3, & \text{on } \Gamma_c(0)\times(0,T),\\ \tilde{\boldsymbol{v}}(.,0) = \boldsymbol{v}_0, \quad \text{and} \quad \tilde{p}_f(.,0) = p_{f_0} & \text{in } \Omega_0^f,\\ \tilde{\boldsymbol{\xi}}(.,0) = 0 \quad \text{and} \quad \partial_t\tilde{\boldsymbol{\xi}}(.,0) = \boldsymbol{\xi}_1 & \text{in } \Omega_0^s. \end{cases} \tag{3.57}$$

The following lemma states the existence and uniqueness of solution for the auxiliary problem.

Lemma 3.3.1 *Let $(\breve{\boldsymbol{v}},\breve{\boldsymbol{\xi}})\in A_M^T$, $\boldsymbol{v}_0\in L^2(\Omega_0^f)$, $\boldsymbol{\xi}_1\in L^2(\Omega_0^s)$ and $p_{f_0}\in L^2(\Omega_0^f)$. For T small with respect to M and the initial conditions, there exists a unique weak solution $(\tilde{\boldsymbol{v}},\tilde{\boldsymbol{\xi}})\in F_1^T\times S_1^T$ of (3.57). In addition, this solution satisfies the following a priori estimate*

$$||\tilde{\boldsymbol{v}}||^2_{F_1^T} + ||\tilde{\boldsymbol{\xi}}||^2_{S_1^T} \leq C\Big[\frac{\rho_f}{2}||\boldsymbol{v}_0||^2_{L^2(\Omega_0^f)} + \frac{\rho_s}{2}||\boldsymbol{\xi}_1||^2_{L^2(\Omega_0^s)} + ||\boldsymbol{g}||^2_{H^1(L^2(\Gamma_c(0)))}\Big]. \tag{3.58}$$

Remark 3.3.1 *Taking T small with respect to M and the initial conditions, means that there exists $n_0>0$ and ε positive such that*

$$T \leq \left\{\frac{\varepsilon}{M^{n_0}}, \frac{\varepsilon}{h(||\boldsymbol{v}_0||_{H^6(\Omega_0^f)}, ||\boldsymbol{\xi}_1||_{H^3(\Omega_0^s)}, ||p_{f0}||_{L^2(\Omega_0^f)})}\right\}.$$

From here on, we simplify the notation for all the norms by omitting the indication for the domain as it is always clear from the context. For instance, we write $||\tilde{\boldsymbol{v}}||_{L^2} = ||\tilde{\boldsymbol{v}}||_{L^2(\Omega_0^f)}$ and $||\tilde{\boldsymbol{\xi}}||_{L^2} = ||\tilde{\boldsymbol{\xi}}||_{L^2(\Omega_0^s)}$.

In order to prove Lemma 3.3.1 we proceed as follows. First, we write the variational formulation corresponding to the coupled system using a divergence-free functional space. Then, we use a Faedo-Galerkin approach to find an approximation of the solution, which enables us to find some a priori estimates on the Galerkin sequences. Using the estimates and compactness results we prove the existence and uniqueness of the solution.

3.3.1 Variational Formulation

Consider the following divergence-free functional space

$$\widetilde{\mathcal{W}} = \Big\{\tilde{\boldsymbol{\eta}}\in H^1(\Omega_0)|\ \nabla\cdot(\mathrm{det}(\boldsymbol{\nabla}\breve{\boldsymbol{\mathcal{A}}})(\boldsymbol{\nabla}\breve{\boldsymbol{\mathcal{A}}})^{-1}\tilde{\boldsymbol{\eta}}) = 0 \quad \text{on} \quad \Omega_0^f \quad \text{and} \quad \tilde{\boldsymbol{\eta}} = 0 \quad \text{on} \quad \Omega_0\setminus\tilde{\Gamma}_{\mathrm{out}}(0)\Big\}.$$

Let $[[.,.]]$ denote the weighted L^2 inner product defined by

$$[[\tilde{\boldsymbol{\gamma}},\tilde{\boldsymbol{\eta}}]] = \int_{\Omega_0^f} \rho_f \tilde{\boldsymbol{\gamma}} \cdot \tilde{\boldsymbol{\eta}}\; d\tilde{\boldsymbol{x}} + \int_{\Omega_0^s} \rho_s \tilde{\boldsymbol{\gamma}} \cdot \tilde{\boldsymbol{\eta}}\; d\tilde{\boldsymbol{x}} \qquad \forall\; \tilde{\boldsymbol{\gamma}},\tilde{\boldsymbol{\eta}} \in \widetilde{\mathcal{W}}.$$

This norm is equivalent to the norm $||\;.\;||_{L^2(\Omega_0)}$.

In order to derive the variational formulation of (3.57), we multiply Equations $(3.57)_1$ and $(3.57)_5$ by a test function $\tilde{\boldsymbol{\eta}} \in \widetilde{\mathcal{W}}$ and integrate by parts to get

$$\begin{cases} \rho_f \displaystyle\int_{\Omega_0^f} \det(\boldsymbol{\nabla}\breve{\boldsymbol{\mathcal{A}}})\partial_t \tilde{\boldsymbol{v}} \cdot \tilde{\boldsymbol{\eta}}\; d\tilde{\boldsymbol{x}} + \int_{\Omega_0^f} \breve{\boldsymbol{\sigma}}_f^0(\tilde{\boldsymbol{v}}) : \boldsymbol{\nabla}\tilde{\boldsymbol{\eta}}\; d\tilde{\boldsymbol{x}} - \int_{\Gamma_c(0)} \breve{\boldsymbol{\sigma}}_f^0(\tilde{\boldsymbol{v}},\tilde{p}_f)\tilde{\boldsymbol{n}}_f \cdot \tilde{\boldsymbol{\eta}}\; d\tilde{\Gamma} \\ +\rho_s \displaystyle\int_{\Omega_0^s} \det(\boldsymbol{\nabla}\breve{\boldsymbol{\varphi}})\partial_t^2 \tilde{\boldsymbol{\xi}} \cdot \tilde{\boldsymbol{\eta}}\; d\tilde{\boldsymbol{x}} - \sum_{i,\alpha,j,\beta=1}^{3} \int_{\Omega_0^s} \breve{b}_{i\alpha j\beta}\partial^2_{\alpha\beta}\tilde{\xi}_j\; \tilde{\eta}_i\; d\tilde{\boldsymbol{x}} \end{cases} \tag{3.59}$$

but we have,

$$\partial_\alpha(\breve{b}_{i\alpha j\beta}\partial_\beta\tilde{\xi}_j) = \partial_\alpha\breve{b}_{i\alpha j\beta}\partial_\beta\tilde{\xi}_j + \breve{b}_{i\alpha j\beta}\partial^2_{\alpha\beta}\tilde{\xi}_j.$$

Hence,

$$-\sum_{i,\alpha,j,\beta=1}^{3} \int_{\Omega_0^s} \breve{b}_{i\alpha j\beta}\partial^2_{\alpha\beta}\tilde{\xi}_j\; \tilde{\eta}_i\; d\tilde{\boldsymbol{x}} = \sum_{i,\alpha,j,\beta=1}^{3} \int_{\Omega_0^s} \partial_\alpha\breve{b}_{i\alpha j\beta}\partial_\beta\tilde{\xi}_j\; \tilde{\eta}_i\; d\tilde{\boldsymbol{x}} - \sum_{i,\alpha,j,\beta=1}^{3} \int_{\Omega_0^s} \partial_\alpha(\breve{b}_{i\alpha j\beta}\partial_\beta\tilde{\xi}_j)\; \tilde{\eta}_i\; d\tilde{\boldsymbol{x}}.$$

Applying integration by parts to the last integral gives

$$\sum_{i,\alpha,j,\beta=1}^{3} \int_{\Omega_0^s} \partial_\alpha(\breve{b}_{i\alpha j\beta}\partial_\beta\tilde{\xi}_j)\; \tilde{\eta}_i\; d\tilde{\boldsymbol{x}} = -\sum_{i,\alpha,j,\beta=1}^{3} \int_{\Omega_0^s} \breve{b}_{i\alpha j\beta}\partial_\beta\tilde{\xi}_j\; \partial_\alpha\tilde{\eta}_i\; d\tilde{\boldsymbol{x}} + \sum_{i,\alpha,j,\beta=1}^{3} \int_{\Gamma_c(0)} \breve{b}_{i\alpha j\beta}\partial_\beta\tilde{\xi}_j\; \tilde{n}_\alpha\; \tilde{\eta}_i\; d\tilde{\Gamma}.$$

On the other hand, due to the condition $(3.57)_8$, the integrals across the common boundary $\Gamma_c(0)$ will sum up to give $-\displaystyle\int_{\Gamma_c(0)} \boldsymbol{g} \cdot \tilde{\boldsymbol{\eta}}\; d\tilde{\Gamma}$. Therefore formulation (3.59) is written as

$$\begin{cases} \rho_f \displaystyle\int_{\Omega_0^f} \det(\boldsymbol{\nabla}\breve{\boldsymbol{\mathcal{A}}})\partial_t \tilde{\boldsymbol{v}} \cdot \tilde{\boldsymbol{\eta}}\; d\tilde{\boldsymbol{x}} + \int_{\Omega_0^f} \breve{\boldsymbol{\sigma}}_f^0(\tilde{\boldsymbol{v}}) : \boldsymbol{\nabla}\tilde{\boldsymbol{\eta}}\; d\tilde{\boldsymbol{x}} + \rho_s \int_{\Omega_0^s} \det(\boldsymbol{\nabla}\breve{\boldsymbol{\varphi}})\partial_t^2 \tilde{\boldsymbol{\xi}} \cdot \tilde{\boldsymbol{\eta}}\; d\tilde{\boldsymbol{x}} \\ + \displaystyle\sum_{i,\alpha,j,\beta=1}^{3} \int_{\Omega_0^s} \breve{b}_{i\alpha j\beta}\partial_\beta\tilde{\xi}_j\; \partial_\alpha\tilde{\eta}_i\; d\tilde{\boldsymbol{x}} + \sum_{i,\alpha,j,\beta=1}^{3} \int_{\Omega_0^s} \partial_\alpha\breve{b}_{i\alpha j\beta}\partial_\beta\tilde{\xi}_j\; \tilde{\eta}_i\; d\tilde{\boldsymbol{x}} \\ = \displaystyle\int_{\Gamma_c(0)} \boldsymbol{g} \cdot \tilde{\boldsymbol{\eta}}\; d\tilde{\Gamma} \qquad \forall\; \tilde{\boldsymbol{\eta}} \in \widetilde{\mathcal{W}}. \end{cases} \tag{3.60}$$

Note that, the space $\widetilde{\mathcal{W}}$ is the transformation of the space

$$\mathcal{W} = \Big\{ \boldsymbol{\eta} \in H^1(\Omega(t)) \mid \nabla \cdot \boldsymbol{\eta} = 0 \quad \text{on} \quad \Omega_f(t) \quad \text{and} \quad \boldsymbol{\eta} = 0 \quad \text{on} \quad \partial\Omega(t) \setminus \Gamma_{\text{out}}(t) \Big\}.$$

This explains the disappearance of the pressure term $\tilde{p}_f$ from the weak formulation.

Remark 3.3.2 *":" corresponds to the Hadamard product of matrices defined by*

$$\boldsymbol{A} : \boldsymbol{B} = \sum_{i,j=1}^{n} A_{i,j} B_{i,j}, \ \textit{for } \boldsymbol{A}, \boldsymbol{B} \in \mathbb{M}_n(\mathbb{R}).$$

In order to derive the weak formulation we consider a global test function $\tilde{\boldsymbol{\eta}}$ in $\widetilde{\mathcal{W}}$. This will simplify the work. In fact, rather than looking for two solutions using two independent test functions on each sub-domain, we search for one solution $\tilde{\boldsymbol{\gamma}}$ over the domain Ω_0. By considering a global test function we are able to embed the stress condition into the formulation in such a way that it would cancel out on the entire domain. Further, we will guarantee the existence of a weak solution $\tilde{\boldsymbol{\gamma}}$ in $\widetilde{\mathcal{W}}$. Consequently, $\tilde{\boldsymbol{v}}$ and $\tilde{\boldsymbol{\xi}}$ are considered to be the restriction of $\tilde{\boldsymbol{\gamma}}$ on the sub-domains Ω_0^f and Ω_0^s, respectively. Note that, if we consider the restriction of $\tilde{\boldsymbol{\eta}}$ on the two sub-domains Ω_0^f and Ω_0^s, we cannot guarantee the existence of the weak solutions in the restriction of $\widetilde{\mathcal{W}}$ on each sub-domain. Thus, we introduce the auxiliary function $\tilde{\boldsymbol{\gamma}}$ defined by

$$\tilde{\boldsymbol{\gamma}} = \begin{cases} \tilde{\boldsymbol{v}} & \text{in } \Omega_0^f, \\ \partial_t \tilde{\boldsymbol{\xi}} & \text{in } \Omega_0^s, \end{cases} \qquad \text{and} \qquad \tilde{\boldsymbol{\gamma}}_0 = \begin{cases} \boldsymbol{v}_0 & \text{in } \Omega_0^f, \\ \boldsymbol{\xi}_1 & \text{in } \Omega_0^s, \end{cases} \tag{3.61}$$

which is a continuous function on Ω_0, due to the continuity of velocities across the interface $\Gamma_c(0)$ which is given by the condition $(3.57)_7$. By this definition, we can write $\tilde{\boldsymbol{v}}(t) = \tilde{\boldsymbol{\gamma}}(t)$ on Ω_0^f, and $\tilde{\boldsymbol{\xi}}(t) = \int_0^t \tilde{\boldsymbol{\gamma}}(s)ds$ on Ω_0^s, based on the fact that $\tilde{\boldsymbol{\xi}}(0) = \boldsymbol{\xi}_0 = 0$. Then, for all test functions $\tilde{\boldsymbol{\eta}}$ in $\widetilde{\mathcal{W}}$ the weak formulation (3.60) is equivalent to

$$\begin{cases} \rho_f \displaystyle\int_{\Omega_0^f} \det(\boldsymbol{\nabla}\breve{\boldsymbol{\mathcal{A}}}) \partial_t \tilde{\boldsymbol{\gamma}} \cdot \tilde{\boldsymbol{\eta}} \, d\tilde{\boldsymbol{x}} + \rho_s \displaystyle\int_{\Omega_0^s} \det(\boldsymbol{\nabla}\breve{\boldsymbol{\varphi}}) \partial_t \tilde{\boldsymbol{\gamma}} \cdot \tilde{\boldsymbol{\eta}} \, d\tilde{\boldsymbol{x}} + \displaystyle\int_{\Omega_0^f} \breve{\boldsymbol{\sigma}}_f^0(\tilde{\boldsymbol{\gamma}}) : \boldsymbol{\nabla}\tilde{\boldsymbol{\eta}} \, d\tilde{\boldsymbol{x}} \\ + \displaystyle\sum_{i,\alpha,j,\beta=1}^{3} \int_{\Omega_0^s} \breve{b}_{i\alpha j\beta} \partial_\beta \big(\textstyle\int_0^t \tilde{\gamma}(s)ds\big)_j \; \partial_\alpha \tilde{\eta}_i \, d\tilde{\boldsymbol{x}} + \displaystyle\sum_{i,\alpha,j,\beta=1}^{3} \int_{\Omega_0^s} \partial_\alpha \breve{b}_{i\alpha j\beta} \partial_\beta \big(\textstyle\int_0^t \tilde{\gamma}(s)ds\big)_j \; \tilde{\eta}_i \, d\tilde{\boldsymbol{x}} \\ = \displaystyle\int_{\Gamma_c(0)} \boldsymbol{g} \cdot \tilde{\boldsymbol{\eta}} \, d\tilde{\Gamma}, \\ \tilde{\gamma}(0) = \tilde{\gamma}_0, \\ \displaystyle\int_0^t \left(\tilde{\gamma}(s)|_{\Omega_0^f} \right) \Big|_{\Gamma_c(0)} ds = \int_0^t \left(\tilde{\gamma}(s)|_{\Omega_0^s} \right) \Big|_{\Gamma_c(0)} ds, \qquad \forall \, t \in [0, T]. \end{cases} \tag{3.62}$$

3.3.2 Galerkin Approximation

In order to show that the system admits a unique solution we will use a Faedo-Galerkin approach. Let $\{\boldsymbol{\psi}_l\}_{l=1}^n$ be a basis of $\widetilde{\mathcal{W}}$ in $L^2(\Omega_0)$ which is orthogonal for the H^1-Norm and orthonormal for the L^2-Norm.
Take $\widetilde{\mathcal{W}}_n = \text{span}\{\boldsymbol{\psi}_1, \ldots, \boldsymbol{\psi}_n\}$. We seek to find a Galerkin approximation $\{\tilde{\boldsymbol{\gamma}}_n\}_n \in \mathcal{C}^1(0, T; \widetilde{\mathcal{W}}_n)$ of the form

$$\tilde{\boldsymbol{\gamma}}_n = \sum_{l=1}^{n} f_l^n(t) \boldsymbol{\psi}_l(\tilde{\boldsymbol{x}}) \tag{3.63}$$

satisfying

$$\begin{cases} \rho_f \displaystyle\int_{\Omega_0^f} \det(\nabla \breve{\mathcal{A}}) \partial_t \tilde{\gamma}_n \cdot \tilde{\boldsymbol{\eta}}_n \, d\tilde{\boldsymbol{x}} + \rho_s \int_{\Omega_0^s} \det(\nabla \breve{\boldsymbol{\varphi}}) \partial_t \tilde{\gamma}_n \cdot \tilde{\boldsymbol{\eta}}_n \, d\tilde{\boldsymbol{x}} + \int_{\Omega_0^f} \breve{\boldsymbol{\sigma}}_f^0(\tilde{\gamma}_n) : \nabla \tilde{\boldsymbol{\eta}}_n \, d\tilde{\boldsymbol{x}} \\ + \displaystyle\sum_{i,\alpha,j,\beta=1}^{3} \int_{\Omega_0^s} \breve{b}_{i\alpha j\beta} \partial_\beta (\textstyle\int_0^t \tilde{\gamma}_n(s) ds)_j \; \partial_\alpha \tilde{\eta}_{n,i} \, d\tilde{\boldsymbol{x}} + \displaystyle\sum_{i,\alpha,j,\beta=1}^{3} \int_{\Omega_0^s} \partial_\alpha \breve{b}_{i\alpha j\beta} \partial_\beta (\textstyle\int_0^t \tilde{\gamma}_n(s) ds)_j \; \tilde{\eta}_{n,i} \, d\tilde{\boldsymbol{x}} \\ = \displaystyle\int_{\Gamma_c(0)} \boldsymbol{g} \cdot \tilde{\boldsymbol{\eta}}_n \, d\tilde{\Gamma} \qquad \forall \; \tilde{\boldsymbol{\eta}}_n \in \widetilde{\mathcal{W}}_n, \end{cases} \tag{3.64}$$

and

$$[[\tilde{\gamma}_n(0), \tilde{\boldsymbol{\eta}}_n]] = [[\tilde{\gamma}_0, \tilde{\boldsymbol{\eta}}_n]], \qquad \forall \; \tilde{\boldsymbol{\eta}}_n \in \widetilde{\mathcal{W}}_n. \tag{3.65}$$

Notice that, trivially $\tilde{\gamma}_n$ defined in (3.63) satisfies

$$\int_0^t \left(\tilde{\gamma}_n(s)|_{\Omega_0^f} \right) \Big|_{\Gamma_c(0)} ds = \int_0^t \left(\tilde{\gamma}_n(s)|_{\Omega_0^s} \right) \Big|_{\Gamma_c(0)} ds, \qquad \forall \; t \in [0, T]. \tag{3.66}$$

We can write (3.64)-(3.65) as an equivalent system of first-order, linear ordinary differential equation (ODE) for $\{f_l^n\}_{l=1}^n$.

Set $h_l^n(t) = \int_0^t f_l^n(s) ds$ for $l = 1, \cdots, n$. For $1 \le k \le n$, the problem (3.64)-(3.65) is equivalent to the following ODE initial value problem

$$\begin{cases} \displaystyle\sum_{l=1}^{n} \frac{d}{dt} f_l^n(t) \left[\rho_f \int_{\Omega_0^f} \det(\nabla \breve{\mathcal{A}}) \boldsymbol{\psi}_l \cdot \boldsymbol{\psi}_k \, d\tilde{\boldsymbol{x}} + \rho_s \int_{\Omega_0^s} \det(\nabla \breve{\boldsymbol{\varphi}}) \boldsymbol{\psi}_l \cdot \boldsymbol{\psi}_k \, d\tilde{\boldsymbol{x}} \right] \\ + \displaystyle\sum_{l=1}^{n} f_l^n(t) \int_{\Omega_0^f} \breve{\boldsymbol{\sigma}}_f^0(\boldsymbol{\psi}_l) : \nabla \boldsymbol{\psi}_k \, d\tilde{\boldsymbol{x}} \\ + \displaystyle\sum_{l=1}^{n} h_l^n(t) \underbrace{\left(\sum_{i,\alpha,j,\beta=1}^{3} \int_{\Omega_0^s} \breve{b}_{i\alpha j\beta} \partial_\beta \psi_{l,j} \; \partial_\alpha \psi_{k,i} \, d\tilde{\boldsymbol{x}} + \sum_{i,\alpha,j,\beta=1}^{3} \int_{\Omega_0^s} \partial_\alpha \breve{b}_{i\alpha j\beta} \partial_\beta \psi_{l,j} \; \psi_{k,i} \, d\tilde{\boldsymbol{x}} \right)}_{[D_{i,\alpha,j,\beta}]_k} \\ = \displaystyle\int_{\Gamma_c(0)} \boldsymbol{g} \cdot \boldsymbol{\psi}_k \, d\tilde{\Gamma}, \\ \dfrac{d}{dt} h_l^n(t) = f_l^n(t) \qquad \forall \; 1 \le l \le n, \\ \displaystyle\sum_{l=1}^{n} [[\boldsymbol{\psi}_l, \boldsymbol{\psi}_k]] f_l^n(0) = [[\tilde{\gamma}_0, \boldsymbol{\psi}_k]], \\ h_l^n(0) = 0 \qquad \forall \; 1 \le l \le n. \end{cases} \tag{3.67}$$

System (3.67) can be rewritten in the following matrix form

$$
\underbrace{\left[\begin{array}{c|c} [[\boldsymbol{\psi}_l,\boldsymbol{\psi}_k]]_{l,k=1}^n & \mathbf{0}_n \\ \hline \mathbf{0}_n & \boldsymbol{I}_n \end{array}\right]}_{\boldsymbol{A}} \underbrace{\frac{d}{dt}\left[\begin{array}{c} f_1^n(t) \\ \vdots \\ f_n^n(t) \\ \hline h_1^n(t) \\ \vdots \\ h_n^n(t) \end{array}\right]}_{\frac{d}{dt}\boldsymbol{F}} = \underbrace{\left[\begin{array}{c|c} \boldsymbol{S}_n & [\boldsymbol{D}]_n \\ \hline \boldsymbol{I}_n & \mathbf{0}_n \end{array}\right]}_{\boldsymbol{B}} \underbrace{\left[\begin{array}{c} f_1^n(t) \\ \vdots \\ f_n^n(t) \\ \hline h_1^n(t) \\ \vdots \\ h_n^n(t) \end{array}\right]}_{\boldsymbol{F}} + \underbrace{\left[\begin{array}{c} \left[\int_{\Gamma_c(0)} \boldsymbol{g}\cdot\boldsymbol{\psi}_k \, d\tilde{\Gamma}\right]_{k=1}^n \\ \hline \mathbf{0}_{n\times 1} \end{array}\right]}_{\boldsymbol{C}} \tag{3.68}
$$

with

$$
[[\boldsymbol{\psi}_l,\boldsymbol{\psi}_k]]_{l,k=1}^n = \left[\rho_f \int_{\Omega_0^f} \det(\boldsymbol{\nabla}\breve{\boldsymbol{\mathcal{A}}})\boldsymbol{\psi}_l\cdot\boldsymbol{\psi}_k \, d\tilde{\boldsymbol{x}} + \rho_s \int_{\Omega_0^s} \det(\boldsymbol{\nabla}\breve{\boldsymbol{\varphi}})\boldsymbol{\psi}_l\cdot\boldsymbol{\psi}_k \, d\tilde{\boldsymbol{x}}\right]_{l,k=1}^n,
$$

$$
\boldsymbol{S}_n = \left[\int_{\Omega_0^f} \breve{\boldsymbol{\sigma}}_f^0(\boldsymbol{\psi}_l) : \boldsymbol{\nabla}\boldsymbol{\psi}_k \, d\tilde{\boldsymbol{x}}\right]_{l,k=1}^n \quad \text{and} \quad [\boldsymbol{D}]_n = [D_{i,\alpha,j,\beta}]_{l,k=1}^n.
$$

The matrix $\boldsymbol{A}$ is a positive definite matrix as the function set $\{\boldsymbol{\psi}_i\}_{i=1}^n$ is linearly independent. Moreover, $\boldsymbol{A}$ is bounded on $(0,T)$. Further, matrices $\boldsymbol{B}$ and $\boldsymbol{C}$ are bounded on $(0,T)$. Hence by theory for systems of linear first order ODEs, we get that system (3.67) admits a unique $\mathcal{C}^1$-solution $\{f_1^n,\dots,f_n^n,h_1^n,\dots,h_n^n\}$ which yields the existence of a unique Galerkin approximation $\{\tilde{\boldsymbol{\gamma}}_n\}_n$ of (3.64)-(3.65) such that $\tilde{\boldsymbol{\gamma}}_n \in W^{1,\infty}(0,T;H^1(\Omega_0))$.

Now we proceed to derive *a priori* estimates on $\tilde{\boldsymbol{\gamma}}_n$.

3.3.3 A Priori Estimates

Step 1: Estimates on $\tilde{\boldsymbol{\gamma}}_n$

We aim to find some estimates on $\tilde{\boldsymbol{\gamma}}_n$. In order to do so, we set $\tilde{\boldsymbol{\eta}}_n = \tilde{\boldsymbol{\gamma}}_n$ in (3.64) to get

$$
\begin{cases}
\rho_f \displaystyle\int_{\Omega_0^f} \det(\boldsymbol{\nabla}\breve{\boldsymbol{\mathcal{A}}})\partial_t\tilde{\boldsymbol{\gamma}}_n\cdot\tilde{\boldsymbol{\gamma}}_n \, d\tilde{\boldsymbol{x}} + \int_{\Omega_0^f} \breve{\boldsymbol{\sigma}}_f^0(\tilde{\boldsymbol{\gamma}}_n) : \boldsymbol{\nabla}\tilde{\boldsymbol{\gamma}}_n \, d\tilde{\boldsymbol{x}} + \rho_s \int_{\Omega_0^s} \det(\boldsymbol{\nabla}\breve{\boldsymbol{\varphi}})\partial_t\tilde{\boldsymbol{\gamma}}_n\cdot\tilde{\boldsymbol{\gamma}}_n \, d\tilde{\boldsymbol{x}} \\
+ \displaystyle\sum_{i,\alpha,j,\beta=1}^{3} \int_{\Omega_0^s} \breve{b}_{i\alpha j\beta}\partial_\beta\left(\textstyle\int_0^t \tilde{\gamma}_n(s)ds\right)_j \, \partial_{\alpha t}^2\left(\textstyle\int_0^t \tilde{\gamma}_n(s)ds\right)_i \, d\tilde{\boldsymbol{x}} \\
+ \displaystyle\sum_{i,\alpha,j,\beta=1}^{3} \int_{\Omega_0^s} \partial_\alpha\breve{b}_{i\alpha j\beta}\partial_\beta\left(\textstyle\int_0^t \tilde{\gamma}_n(s)ds\right)_j \, \tilde{\gamma}_{n,i} \, d\tilde{\boldsymbol{x}} = \int_{\Gamma_c(0)} \boldsymbol{g}\cdot\tilde{\boldsymbol{\gamma}}_n \, d\tilde{\Gamma}.
\end{cases} \tag{3.69}
$$

Then, integrating over $(0,t)$ and applying integration by parts yield

$$\begin{cases} \dfrac{\rho_f}{2}\displaystyle\int_{\Omega_0^f}\det(\nabla\breve{\mathcal{A}})(t)|\tilde{\gamma}_n(t)|^2\ d\tilde{\boldsymbol{x}} + \dfrac{\rho_s}{2}\int_{\Omega_0^s}\det(\nabla\breve{\boldsymbol{\varphi}})(t)|\tilde{\gamma}_n(t)|^2\ d\tilde{\boldsymbol{x}} \\ +\displaystyle\int_0^t\int_{\Omega_0^f}\frac{\mu}{2}\det(\nabla\breve{\mathcal{A}})|\nabla\tilde{\gamma}_n(\nabla\breve{\mathcal{A}})^{-1} + (\nabla\breve{\mathcal{A}})^{-t}(\nabla\tilde{\gamma}_n)^t|^2\ d\tilde{\boldsymbol{x}}\ ds \\ +\dfrac{1}{2}\displaystyle\sum_{i,\alpha,j,\beta=1}^{3}\int_{\Omega_0^s}\breve{b}_{i\alpha j\beta}(t)\ \partial_\beta(\textstyle\int_0^t\tilde{\gamma}_n(s)ds)_j\ \partial_\alpha(\int_0^t\tilde{\gamma}_n(s)ds)_i\ d\tilde{\boldsymbol{x}} - \dfrac{\rho_s}{2}\displaystyle\int_0^t\int_{\Omega_0^s}\partial_s\det(\nabla\breve{\boldsymbol{\varphi}})|\tilde{\gamma}_n|^2\ d\tilde{\boldsymbol{x}}\ ds \\ -\dfrac{1}{2}\displaystyle\sum_{i,\alpha,j,\beta=1}^{3}\int_0^t\int_{\Omega_0^s}\partial_s\breve{b}_{i\alpha j\beta}\ \partial_\beta(\textstyle\int_0^s\tilde{\gamma}_n(\tau)d\tau)_j\ \partial_\alpha(\int_0^s\tilde{\gamma}_n(\tau)d\tau)_i\ d\tilde{\boldsymbol{x}}\ ds \\ -\dfrac{\rho_f}{2}\displaystyle\int_0^t\int_{\Omega_0^f}\partial_s\det(\nabla\breve{\mathcal{A}})|\tilde{\gamma}_n|^2\ d\tilde{\boldsymbol{x}}\ ds + \sum_{i,\alpha,j,\beta=1}^{3}\int_0^t\int_{\Omega_0^s}\partial_\alpha\breve{b}_{i\alpha j\beta}\partial_\beta(\textstyle\int_0^s\tilde{\gamma}_n(\tau)d\tau)_j\partial_s(\int_0^s\tilde{\gamma}_n(\tau)d\tau)_i\ d\tilde{\boldsymbol{x}}\ ds \\ = \displaystyle\int_0^t\int_{\Gamma_c(0)}\boldsymbol{g}\cdot\tilde{\gamma}_n\ d\tilde{\Gamma}\ ds + \frac{\rho_f}{2}\int_{\Omega_0^f}|\tilde{\gamma}_n(0)|^2\ d\tilde{\boldsymbol{x}} + \frac{\rho_s}{2}\int_{\Omega_0^s}|\tilde{\gamma}_n(0)|^2\ d\tilde{\boldsymbol{x}}. \end{cases} \tag{3.70}$$

Where we have integrated by parts with respect to time as indicated below

$$\int_0^t\partial_s(\breve{b}_{i\alpha j\beta}\partial_\beta(\textstyle\int_0^s\tilde{\gamma}_n(\tau)d\tau)_j\partial_\alpha(\int_0^s\tilde{\gamma}_n(\tau)d\tau)_i)\ ds = \displaystyle\int_0^t\partial_s\breve{b}_{i\alpha j\beta}\partial_\beta(\textstyle\int_0^s\tilde{\gamma}_n(\tau)d\tau)_j\partial_\alpha(\int_0^s\tilde{\gamma}_n(\tau)d\tau)_i\ ds$$
$$+\underbrace{\int_0^t\breve{b}_{i\alpha j\beta}\ \partial_\beta\tilde{\gamma}_{n,j}(s)\ \partial_\alpha(\textstyle\int_0^s\tilde{\gamma}_n(\tau)d\tau)_i\ ds + \displaystyle\int_0^t\breve{b}_{i\alpha j\beta}\partial_\beta(\textstyle\int_0^s\tilde{\gamma}_n(\tau)d\tau)_j\partial_\alpha\tilde{\gamma}_{n,i}(s)\ ds}_{\text{equal by exchanging indices and using (3.18)}}.$$

Hence,

$$\breve{b}_{i\alpha j\beta}(t)\partial_\beta(\textstyle\int_0^t\tilde{\gamma}_n(s)ds)_j\partial_\alpha(\int_0^t\tilde{\gamma}_n(s)ds)_i - \underbrace{\left[\breve{b}_{i\alpha j\beta}(t)\partial_\beta(\int_0^t\tilde{\gamma}_n(s)ds)_j\partial_\alpha(\int_0^t\tilde{\gamma}_n(s)ds)_i\right]\Big|_{t=0}}_{=0}$$
$$= \int_0^t\partial_s\breve{b}_{i\alpha j\beta}\partial_\beta(\textstyle\int_0^s\tilde{\gamma}_n(\tau)d\tau)_j\partial_\alpha(\int_0^s\tilde{\gamma}_n(\tau)d\tau)_i\ ds + 2\displaystyle\int_0^t\breve{b}_{i\alpha j\beta}\partial_\beta(\textstyle\int_0^s\tilde{\gamma}_n(\tau)d\tau)_j\partial_\alpha\tilde{\gamma}_{n,i}(s)\ ds.$$

We start by deriving estimates on the terms of (3.70).

First of all, as $\det(\boldsymbol{\nabla}\breve{\boldsymbol{\mathcal{A}}})-1\geqslant -CT^\kappa M$, then we have

$$\begin{aligned}
&\frac{\rho_f}{2}\int_{\Omega_0^f}\det(\boldsymbol{\nabla}\breve{\boldsymbol{\mathcal{A}}})|\tilde{\gamma}_n(t)|^2\,d\tilde{\boldsymbol{x}}-\frac{\rho_f}{2}\int_0^t\int_{\Omega_0^f}\partial_s\det(\boldsymbol{\nabla}\breve{\boldsymbol{\mathcal{A}}})|\tilde{\gamma}_n|^2\,d\tilde{\boldsymbol{x}}\,ds\\
&\geq\frac{\rho_f}{2}(1-CT^\kappa M)||\tilde{\gamma}_n||^2_{L^\infty(L^2)}-\frac{\rho_f}{2}||\partial_t\det(\boldsymbol{\nabla}\breve{\boldsymbol{\mathcal{A}}})||_{L^2(H^2)}||\tilde{\gamma}_n||^2_{L^\infty(L^2)}\\
&\geq\frac{\rho_f}{2}(1-CT^\kappa M-CT^\kappa M)||\tilde{\gamma}_n||^2_{L^\infty(L^2(\Omega_0^f))}.
\end{aligned}\tag{3.71}$$

Similarly, using the same relation for the stress term of the fluid we get

$$\begin{aligned}
&\frac{\mu}{2}\det(\boldsymbol{\nabla}\breve{\boldsymbol{\mathcal{A}}})\Big|\boldsymbol{\nabla}\tilde{\gamma}_n(\boldsymbol{\nabla}\breve{\boldsymbol{\mathcal{A}}})^{-1}+(\boldsymbol{\nabla}\breve{\boldsymbol{\mathcal{A}}})^{-t}(\boldsymbol{\nabla}\tilde{\gamma}_n)^t\Big|^2\\
&\quad=\frac{\mu}{2}\Big|\boldsymbol{\nabla}\tilde{\gamma}_n(\boldsymbol{\nabla}\breve{\boldsymbol{\mathcal{A}}})^{-1}+(\boldsymbol{\nabla}\breve{\boldsymbol{\mathcal{A}}})^{-t}(\boldsymbol{\nabla}\tilde{\gamma}_n)^t\Big|^2+\frac{\mu}{2}(\det(\boldsymbol{\nabla}\breve{\boldsymbol{\mathcal{A}}})-1)\Big|\boldsymbol{\nabla}\tilde{\gamma}_n(\boldsymbol{\nabla}\breve{\boldsymbol{\mathcal{A}}})^{-1}+(\boldsymbol{\nabla}\breve{\boldsymbol{\mathcal{A}}})^{-t}(\boldsymbol{\nabla}\tilde{\gamma}_n)^t\Big|^2\\
&\quad=N_1+N_2.
\end{aligned}$$

For N_1 we have

$$\begin{aligned}
N_1&\geq\frac{\mu}{2}\Big|\boldsymbol{\nabla}\tilde{\gamma}_n(\boldsymbol{\nabla}\breve{\boldsymbol{\mathcal{A}}})^{-1}+(\boldsymbol{\nabla}\breve{\boldsymbol{\mathcal{A}}})^{-t}(\boldsymbol{\nabla}\tilde{\gamma}_n)^t\Big|^2\\
&=\frac{\mu}{2}\Big|\boldsymbol{\nabla}\tilde{\gamma}_n\Big((\boldsymbol{\nabla}\breve{\boldsymbol{\mathcal{A}}})^{-1}-\mathbf{Id}+\mathbf{Id}\Big)+\Big((\boldsymbol{\nabla}\breve{\boldsymbol{\mathcal{A}}})^{-t}-\mathbf{Id}+\mathbf{Id}\Big)(\boldsymbol{\nabla}\tilde{\gamma}_n)^t\Big|^2\\
&\geq\frac{\mu}{2}\Big|\boldsymbol{\nabla}\tilde{\gamma}_n+(\boldsymbol{\nabla}\tilde{\gamma}_n)^t+\boldsymbol{\nabla}\tilde{\gamma}_n\Big((\boldsymbol{\nabla}\breve{\boldsymbol{\mathcal{A}}})^{-1}-\mathbf{Id}\Big)+\Big((\boldsymbol{\nabla}\breve{\boldsymbol{\mathcal{A}}})^{-t}-\mathbf{Id}\Big)(\boldsymbol{\nabla}\tilde{\gamma}_n)^t\Big|^2\\
&\geq\frac{\mu}{2}\Big|\boldsymbol{\nabla}\tilde{\gamma}_n+(\boldsymbol{\nabla}\tilde{\gamma}_n)^t\Big|^2-\frac{\mu}{2}\Big|\boldsymbol{\nabla}\tilde{\gamma}_n\Big((\boldsymbol{\nabla}\breve{\boldsymbol{\mathcal{A}}})^{-1}-\mathbf{Id}\Big)\Big|^2-\frac{\mu}{2}\Big|\Big((\boldsymbol{\nabla}\breve{\boldsymbol{\mathcal{A}}})^{-t}-\mathbf{Id}\Big)(\boldsymbol{\nabla}\tilde{\gamma}_n)^t\Big|^2\\
&\geq\mu\Big|\boldsymbol{\epsilon}(\tilde{\gamma}_n)\Big|^2-\mu\Big|\boldsymbol{\nabla}\tilde{\gamma}_n\Big((\boldsymbol{\nabla}\breve{\boldsymbol{\mathcal{A}}})^{-1}-\mathbf{Id}\Big)\Big|^2.
\end{aligned}$$

Thus, using Korn's inequality [GR86, Fic73] and Lemma 3.2.2 yields to

$$\begin{aligned}
&\int_0^t\int_{\Omega_0^f}\frac{\mu}{2}|\boldsymbol{\nabla}\tilde{\gamma}_n(\boldsymbol{\nabla}\breve{\boldsymbol{\mathcal{A}}})^{-1}+(\boldsymbol{\nabla}\breve{\boldsymbol{\mathcal{A}}})^{-t}(\boldsymbol{\nabla}\tilde{\gamma}_n)^t|^2\,d\tilde{\boldsymbol{x}}\,ds\\
&\qquad\geq\int_0^t\int_{\Omega_0^f}\mu\Big|\boldsymbol{\epsilon}(\tilde{\gamma}_n)\Big|^2-\mu\Big|\boldsymbol{\nabla}\tilde{\gamma}_n\Big((\boldsymbol{\nabla}\breve{\boldsymbol{\mathcal{A}}})^{-1}-\mathbf{Id}\Big)\Big|^2d\tilde{\boldsymbol{x}}\,ds\\
&\qquad\geq\mu\int_0^t\Big[||\boldsymbol{\epsilon}(\tilde{\gamma}_n)(s)||^2_{L^2(\Omega_0^f)}-CT^\kappa M||\tilde{\gamma}_n(s)||^2_{H^1(\Omega_0^f)}\Big]\,ds\\
&\qquad\geq\mu(C_k-CT^\kappa M)||\tilde{\gamma}_n||^2_{L^2(H^1(\Omega_0^f))}.
\end{aligned}$$

Whereas for N_2 we have

$$N_2\geq-\frac{\mu}{2}|\det(\boldsymbol{\nabla}\breve{\boldsymbol{\mathcal{A}}})-1|\Big|\boldsymbol{\nabla}\tilde{\gamma}_n(\boldsymbol{\nabla}\breve{\boldsymbol{\mathcal{A}}})^{-1}+(\boldsymbol{\nabla}\breve{\boldsymbol{\mathcal{A}}})^{-t}(\boldsymbol{\nabla}\tilde{\gamma})_n^t\Big|^2.$$

Hence, using Lemma 3.2.2 we have

$$
\begin{aligned}
-\int_0^t \int_{\Omega_0^f} \frac{\mu}{2}(\det(\nabla\breve{\mathcal{A}})-1)\left|\nabla\tilde{\gamma}_n(\nabla\breve{\mathcal{A}})^{-1}+(\nabla\breve{\mathcal{A}})^{-t}(\nabla\tilde{\gamma}_n)^t\right|^2 d\tilde{\boldsymbol{x}}\ ds \\
\geq -\|\det(\nabla\breve{\mathcal{A}})-1\|_{L^\infty(H^3)}\|\tilde{\gamma}_n\|^2_{L^2(H^1)}\|(\nabla\breve{\mathcal{A}})^{-1}\|^2_{L^\infty(H^3)} \\
\geq \mu C T^\kappa M\|\tilde{\gamma}_n\|^2_{L^2(H^1(\Omega_0^f))}.
\end{aligned}
$$

Therefore,

$$
\int_0^t \int_{\Omega_0^f} \frac{\mu}{2}\det(\nabla\breve{\mathcal{A}})\left|\nabla\tilde{\gamma}_n(\nabla\breve{\mathcal{A}})^{-1}+(\nabla\breve{\mathcal{A}})^{-t}(\nabla\tilde{\gamma}_n)^t\right|^2 d\tilde{\boldsymbol{x}}\ ds \geq \mu(C_k - CT^\kappa M)\|\tilde{\gamma}_n\|^2_{L^2(H^1(\Omega_0^f))}. \tag{3.72}
$$

As for the integrals on the domain Ω_0^s, first of all using (3.55) we have

$$
\int_{\Omega_0^s} \det(\nabla\breve{\boldsymbol{\varphi}})|\gamma_n(t)|^2\ d\tilde{\boldsymbol{x}} \geq (1-CT^\kappa M)\|\tilde{\gamma}_n\|^2_{L^\infty(L^2(\Omega_0^s))}. \tag{3.73}
$$

Thanks to (3.43) it holds

$$
\begin{aligned}
\int_0^t \int_{\Omega_0^s} \left|\partial_s \det(\nabla\breve{\boldsymbol{\varphi}})\tilde{\gamma}_n^2(t)\right|\ d\tilde{\boldsymbol{x}}\ ds &\leq T\|\partial_t \det(\nabla\breve{\boldsymbol{\varphi}})\|_{L^\infty(H^2(\Omega_0^s))}\|\tilde{\gamma}_n\|^2_{L^\infty(L^2(\Omega_0^s))} \\
&\leq CTM\|\tilde{\gamma}_n\|^2_{L^\infty(L^2(\Omega_0^s))} \\
&\leq CT^\kappa M\|\tilde{\gamma}_n\|^2_{L^\infty(L^2(\Omega_0^s))}.
\end{aligned} \tag{3.74}
$$

Using (3.38) and (3.40) together with Korn's Inequality, then there exists $C_k > 0$ such that

$$
\begin{aligned}
&\frac{1}{2}\sum_{i,\alpha,j,\beta=1}^{3}\int_{\Omega_0^s} \breve{b}_{i\alpha j\beta}(t)\partial_\beta(\textstyle\int_0^t\tilde{\gamma}_n(s)ds)_j\ \partial_\alpha(\textstyle\int_0^t\tilde{\gamma}_n(s)ds)_i\ d\tilde{\boldsymbol{x}} \\
&\geq \mu_s\|\boldsymbol{\epsilon}(\textstyle\int_0^t\tilde{\gamma}_n(s)ds)\|^2_{L^2(\Omega_0^s)}+\frac{\mathsf{C}+\lambda_s}{2}\|\nabla\cdot(\textstyle\int_0^t\tilde{\gamma}_n(s)ds)\|^2_{L^2(\Omega_0^s)}-CTM^4\|\nabla(\textstyle\int_0^t\tilde{\gamma}_n(s)ds)\|^2_{L^2(\Omega_0^s)} \\
&\geq \mu_s C_k\|\textstyle\int_0^t\tilde{\gamma}_n(s)ds\|^2_{H^1(\Omega_0^s)}+\frac{\mathsf{C}+\lambda_s}{2}\|\nabla\cdot(\textstyle\int_0^t\tilde{\gamma}_n(s)ds)\|^2_{L^2(\Omega_0^s)}-CT^\kappa M\|\textstyle\int_0^t\tilde{\gamma}_n(s)ds\|^2_{H^1(\Omega_0^s)}.
\end{aligned} \tag{3.75}
$$

On the other hand, using (3.37) and (3.39) in addition to Young's inequality [BF13, Proposition II.2.16] and Lemma 3.2.1 yield

$$
\begin{aligned}
&\left|-\frac{1}{2}\int_{\Omega_0^s}\partial_s\breve{b}_{i\alpha j\beta}\partial_\beta(\textstyle\int_0^s\tilde{\gamma}_n(\tau)d\tau)_j\ \partial_\alpha(\textstyle\int_0^s\tilde{\gamma}_n(\tau)d\tau)_i\ d\tilde{\boldsymbol{x}}\ ds\right| \\
&\leq \frac{1}{4}\|\breve{b}_{i\alpha j\beta}\|_{L^\infty(L^\infty(\Omega_0^s))}\int_0^t \|\nabla\textstyle\int_0^s\tilde{\gamma}_n(\tau)d\tau\|^2_{L^2(\Omega_0^s)}\ ds \\
&\leq C\|\breve{b}_{i\alpha j\beta}\|_{L^\infty(H^2(\Omega_0^s))}\int_0^t \|\nabla\textstyle\int_0^s\tilde{\gamma}_n(\tau)d\tau\|^2_{L^2(\Omega_0^s)}\ ds \\
&\leq CT(M+M^2+M^3+M^4)\|\textstyle\int_0^\cdot\tilde{\gamma}_n(s)ds\|^2_{L^\infty(H^1(\Omega_0^s))} \\
&\leq CT^\kappa M\|\textstyle\int_0^\cdot\tilde{\gamma}_n(s)ds\|^2_{L^\infty(H^1(\Omega_0^s))}.
\end{aligned} \tag{3.76}
$$

Similarly, for $i, \alpha, j, \beta = 1,2,3$,

$$\begin{aligned}
&\left|\frac{1}{2}\int_0^t\int_{\Omega_0^s}\partial_\alpha\breve{b}_{i\alpha j\beta}\partial_\beta(\textstyle\int_0^s\tilde{\gamma}_n(\tau)d\tau)_j\ \partial_s(\int_0^s\tilde{\gamma}_n(\tau)d\tau)_i\ d\tilde{\boldsymbol{x}}\ ds\right| \\
&\quad\le \frac{1}{2}||\partial_\alpha\breve{b}_{i\alpha j\beta}||_{L^\infty(L^\infty(\Omega_0^s))}\int_0^t\int_{\Omega_0^s}\left|\partial_\beta(\textstyle\int_0^s\tilde{\gamma}_n(\tau)d\tau)_j\ \partial_s(\int_0^s\tilde{\gamma}_n(\tau)d\tau)_i\ d\tilde{\boldsymbol{x}}\ ds\right| \\
&\quad\le C||\partial_\alpha\breve{b}_{i\alpha j\beta}||_{L^\infty(H^2(\Omega_0^s))}\int_0^t||\boldsymbol{\nabla}\textstyle\int_0^s\tilde{\boldsymbol{\gamma}}_n(\tau)d\tau||_{L^2(\Omega_0^s)}||\tilde{\boldsymbol{\gamma}}_n(s)||_{L^2(\Omega_0^s)}\ ds \\
&\quad\le C||\breve{b}_{i\alpha j\beta}||_{L^\infty(H^3(\Omega_0^s))}\int_0^t\left(||\boldsymbol{\nabla}\textstyle\int_0^s\tilde{\boldsymbol{\gamma}}_n(\tau)d\tau||^2_{L^2(\Omega_0^s)}+||\tilde{\boldsymbol{\gamma}}_n(s)||^2_{L^2(\Omega_0^s)}\right)\ ds \\
&\quad\le CT(M+M^2+M^3+M^4)\left[||\textstyle\int_0^\bullet\tilde{\boldsymbol{\gamma}}_n(s)ds||^2_{L^\infty(H^1(\Omega_0^s))}+||\boldsymbol{\gamma}_n||^2_{L^\infty(L^2(\Omega_0^s))}\right] \\
&\quad\le CT^\kappa M\left[||\textstyle\int_0^\bullet\tilde{\boldsymbol{\gamma}}_n(s)ds||^2_{L^\infty(H^1(\Omega_0^s))}+||\tilde{\boldsymbol{\gamma}}_n||^2_{L^\infty(L^2(\Omega_0^s))}\right].
\end{aligned} \tag{3.77}$$

Whence,

$$\begin{aligned}
&\left|-\frac{1}{2}\sum_{i,\alpha,j,\beta=1}^{3}\int_0^t\int_{\Omega_0^s}\partial_s\breve{b}_{i\alpha j\beta}\partial_\beta(\textstyle\int_0^s\tilde{\gamma}_n(\tau)d\tau)_j\ \partial_\alpha(\int_0^s\tilde{\gamma}_n(\tau)d\tau)_i\ d\tilde{\boldsymbol{x}}\ ds\right. \\
&\left.+\frac{1}{2}\sum_{i,\alpha,j,\beta=1}^{3}\int_0^t\int_{\Omega_0^s}\partial_\alpha\breve{b}_{i\alpha j\beta}\partial_\beta(\textstyle\int_0^s\tilde{\gamma}_n(\tau)d\tau)_j\ \partial_s(\int_0^s\tilde{\gamma}_n(\tau)d\tau)_i\ d\tilde{\boldsymbol{x}}\ ds\right| \\
&\le CT^\kappa M\left[||\textstyle\int_0^\bullet\tilde{\boldsymbol{\gamma}}_n(s)ds||^2_{L^\infty(H^1(\Omega_0^s))}+||\tilde{\boldsymbol{\gamma}}_n||^2_{L^\infty(L^2(\Omega_0^s))}\right].
\end{aligned} \tag{3.78}$$

Finally, using Young's inequality we have

$$\begin{aligned}
&\left|\int_0^t\int_{\Gamma_c(0)}\boldsymbol{g}\cdot\boldsymbol{\gamma}_n\ d\tilde{\Gamma}\ ds\right| = \left|\int_{\Gamma_c(0)}\boldsymbol{g}(t)\cdot(\textstyle\int_0^t\tilde{\boldsymbol{\gamma}}_n(s)ds)\ d\tilde{\Gamma}-\int_0^t\int_{\Gamma_c(0)}\partial_s\boldsymbol{g}\cdot(\int_0^s\tilde{\boldsymbol{\gamma}}_n(\tau)d\tau)\ ds\ d\tilde{\Gamma}\right| \\
&\le\left|\int_{\Gamma_c(0)}\boldsymbol{g}(t)\cdot(\textstyle\int_0^t\tilde{\boldsymbol{\gamma}}_n(s)ds)\ d\tilde{\Gamma}\right|+\left|\int_0^t\int_{\Gamma_c(0)}\partial_s\boldsymbol{g}\cdot(\int_0^s\tilde{\boldsymbol{\gamma}}_n(\tau)d\tau)\ ds\ d\tilde{\Gamma}\right| \\
&\le||\boldsymbol{g}||_{L^\infty(L^2(\Gamma_c(0)))}||\textstyle\int_0^\bullet\tilde{\boldsymbol{\gamma}}_n(s)ds||_{L^\infty(L^2(\Gamma_c(0)))}+\int_0^t||\partial_s\boldsymbol{g}(s)||_{L^2(\Gamma_c(0))}||\int_0^s\tilde{\boldsymbol{\gamma}}_n(\tau)d\tau||_{L^2(\Gamma_c(0))}\ ds \\
&\le C_\delta||\boldsymbol{g}||^2_{L^\infty(L^2(\Gamma_c(0)))}+\delta||\textstyle\int_0^\bullet\tilde{\boldsymbol{\gamma}}_n(s)ds||^2_{L^\infty(L^2(\Gamma_c(0)))}+\delta T||\int_0^\bullet\tilde{\boldsymbol{\gamma}}_n(s)ds||^2_{L^\infty(L^2(\Gamma_c(0)))}+C_\delta||\partial_s\boldsymbol{g}||^2_{L^2(L^2(\Gamma_c(0)))}.
\end{aligned}$$

But, using the trace inequality [BF13, Theorem III.2.19.], there exists a constant $C_\Omega > 0$ that depends on the domain Ω_0^s, such that

$$||\textstyle\int_0^t\tilde{\boldsymbol{\gamma}}_n(s)ds||^2_{L^2(\Gamma_c(0))}\le C_\Omega||\int_0^t\tilde{\boldsymbol{\gamma}}_n(s)ds||^2_{H^1(\Omega_0^s)}\qquad\forall\ t\in[0,T].$$

On the other hand, as $\boldsymbol{g}(.,0)=0$ we have

$$\boldsymbol{g}(.,t)=\int_0^t\partial_s\boldsymbol{g}(.,s)ds\qquad\forall\ t\in[0,T],$$

then using Hölder's inequality [BF13, Proposition II.2.18]

$$\begin{aligned}
|g(.,t)| &\leq \int_0^t \Big|\partial_s \boldsymbol{g}(.,s)\Big| ds \\
&\leq \left(\int_0^t \Big|\partial_s \boldsymbol{g}(.,s)\Big|^2 ds\right)^{\frac{1}{2}} \left(\int_0^t ds\right)^{\frac{1}{2}} \\
&\leq \sqrt{t}||\partial_s \boldsymbol{g}(.)||_{L^2([0,t])} \\
&\leq \sqrt{t}||\boldsymbol{g}(.)||_{H^1([0,t])}.
\end{aligned}$$

Taking supremum of t in $[0, T]$ and squaring both sides yield

$$||\boldsymbol{g}(.)||^2_{L^\infty([0,T])} \leq T||\boldsymbol{g}(.)||^2_{H^1([0,T])} \quad \text{on } \Gamma_c(0).$$

Consequently we get

$$\left| \int_0^t \int_{\Gamma_c(0)} \boldsymbol{g} \cdot \tilde{\boldsymbol{\gamma}}_n \, d\tilde{\Gamma} \, ds \right| \leq C\delta T||\textstyle\int_0^\bullet \tilde{\boldsymbol{\gamma}}_n(s)ds||^2_{L^\infty(H^1(\Omega_0^s))} + C_\delta ||\boldsymbol{g}||^2_{H^1(L^2(\Gamma_c(0)))}. \tag{3.79}$$

In order to deal with $\displaystyle\int_{\Omega_0} |\tilde{\boldsymbol{\gamma}}_n(0)|^2 d\tilde{\boldsymbol{x}}$, we need the following lemma [DGHL03, Lemma 2.2].

Lemma 3.3.2 *Let π_n denote the weighted $L^2(\Omega_0)$ projection from $L^2(\Omega_0)$ into $\widetilde{\mathcal{W}}_n$. That is*

$$\begin{aligned}
\pi_n : L^2(\Omega_0) &\to \widetilde{\mathcal{W}}_n \\
\tilde{\boldsymbol{\eta}} &\mapsto [[\pi_n \tilde{\boldsymbol{\eta}}, \boldsymbol{z}]] = [[\tilde{\boldsymbol{\eta}}, \boldsymbol{z}]] \qquad \forall\, \boldsymbol{z} \in \widetilde{\mathcal{W}}_n.
\end{aligned}$$

Direct consequences of the definition are the following

1- $||\pi_n \tilde{\boldsymbol{\eta}}||_{L^2(\Omega_0)} \leq ||\tilde{\boldsymbol{\eta}}||_{L^2(\Omega_0)} \qquad \forall\, \tilde{\boldsymbol{\eta}} \in L^2(\Omega_0),$

2- $||\pi_n \tilde{\boldsymbol{\eta}}||_{H^1(\Omega_0)} \leq ||\tilde{\boldsymbol{\eta}}||_{H^1(\Omega_0)} \qquad \forall\, \tilde{\boldsymbol{\eta}} \in \widetilde{\mathcal{W}}.$

Using the first inequality, we have

$$||\tilde{\boldsymbol{\gamma}}_n(0)||^2_{L^2(\Omega(0))} = ||\pi_n \tilde{\boldsymbol{\gamma}}_0||^2_{L^2(\Omega_0)} \leq ||\tilde{\boldsymbol{\gamma}}_0||^2_{L^2(\Omega_0)} = ||\boldsymbol{v}_0||^2_{L^2(\Omega_0^f)} + ||\boldsymbol{\xi}_1||^2_{L^2(\Omega_0^s)}. \tag{3.80}$$

Combining (3.71)-(3.79) and using (3.80) we obtain

$$\begin{aligned}
&\Big(\mu C_k - \mu C T^\kappa M\Big)||\tilde{\boldsymbol{\gamma}}_n||^2_{L^2(H^1(\Omega_0^f))} + \frac{\rho_f}{2}(1 - CT^\kappa M)||\tilde{\boldsymbol{\gamma}}_n||^2_{L^\infty(L^2(\Omega_0^f))} \\
&+ \left(\frac{\rho_s}{2}(1 - CT^\kappa M) - CT^\kappa M\right)||\tilde{\boldsymbol{\gamma}}_n||^2_{L^\infty(L^2(\Omega_0^s))} \\
&+ \Big(\mu_s C_k - CT^\kappa M - C\delta T\Big)||\textstyle\int_0^\bullet \tilde{\boldsymbol{\gamma}}_n(s)ds||^2_{L^\infty(H^1(\Omega_0^s))} \\
&\leq C\left[\frac{\rho_f}{2}||\boldsymbol{v}_0||^2_{L^2(\Omega_0^f)} + \frac{\rho_s}{2}||\boldsymbol{\xi}_1||^2_{L^2(\Omega_0^s)}\right] + C_\delta||\boldsymbol{g}||^2_{H^1(L^2(\Gamma_c(0)))}.
\end{aligned} \tag{3.81}$$

Remark that, the constants μ_s, λ_s and μ are given as large values by the constitutive laws of the structure and the fluid. Moreover, δ is a negligible positive real number, hence norms that are factored by the term δ are being absorbed by larger terms. Finally, we take T small with respect to M and the initial values, that is, the factor $CT^{\kappa}M$ is negligible. These assumptions lead to the following estimate

$$\begin{aligned}&||\tilde{\boldsymbol{\gamma}}_n||^2_{L^2(H^1(\Omega_0^f))}+||\tilde{\boldsymbol{\gamma}}_n||^2_{L^\infty(L^2(\Omega_0))}+||\textstyle\int_0^\cdot\tilde{\boldsymbol{\gamma}}_n(s)ds||^2_{L^\infty(H^1(\Omega_0^s))}\\ &\leq C\Big[\frac{\rho_f}{2}||\boldsymbol{v}_0||^2_{L^2}+\frac{\rho_s}{2}||\boldsymbol{\xi}_1||^2_{L^2}+||\boldsymbol{g}||^2_{H^1(L^2(\Gamma_c(0)))}\Big].\end{aligned} \tag{3.82}$$

Step 2: Estimates on $\partial_t\tilde{\boldsymbol{\gamma}}_n$

The next step is to derive some estimates on $\partial_t\tilde{\boldsymbol{\gamma}}_n$. Consider a function $\tilde{\boldsymbol{\eta}}$ in $\widetilde{\mathcal{W}}$ such that $||\tilde{\boldsymbol{\eta}}||_{L^2(H^1(\Omega_0))}\leq 1$. The function $\tilde{\boldsymbol{\eta}}$ can be written as

$$\tilde{\boldsymbol{\eta}} = \pi_n\tilde{\boldsymbol{\eta}} + (\tilde{\boldsymbol{\eta}} - \pi_n\tilde{\boldsymbol{\eta}}).$$

where π_n is the projection from $L^2(\Omega_0)$ into $\widetilde{\mathcal{W}}_n$ defined in Lemma 3.3.2. Notice that, as we have $\partial_t\tilde{\boldsymbol{\gamma}}_n \in \widetilde{\mathcal{W}}_n$ then

$$[[\partial_t\tilde{\boldsymbol{\gamma}}_n(t), \tilde{\boldsymbol{\eta}}]] = [[\partial_t\tilde{\boldsymbol{\gamma}}_n(t), \pi_n\tilde{\boldsymbol{\eta}}]] + [[\partial_t\tilde{\boldsymbol{\gamma}}_n(t), \tilde{\boldsymbol{\eta}} - \pi_n\tilde{\boldsymbol{\eta}}]] = [[\partial_t\tilde{\boldsymbol{\gamma}}_n(t), \pi_n\tilde{\boldsymbol{\eta}}]].$$

Set $\tilde{\boldsymbol{\eta}}_n = \pi_n\tilde{\boldsymbol{\eta}}$ in (3.64). By integrating over $(0,t)$ we obtain

$$\begin{cases}\rho_f\displaystyle\int_0^t\int_{\Omega_0^f}\det(\boldsymbol{\nabla}\breve{\boldsymbol{\mathcal{A}}})\partial_s\tilde{\boldsymbol{\gamma}}_n\cdot\pi_n\tilde{\boldsymbol{\eta}}\;d\tilde{\boldsymbol{x}}\;ds+\rho_s\int_0^t\int_{\Omega_0^s}\det(\boldsymbol{\nabla}\breve{\boldsymbol{\varphi}})\partial_s\tilde{\boldsymbol{\gamma}}_n\cdot\pi_n\tilde{\boldsymbol{\eta}}\;d\tilde{\boldsymbol{x}}\;ds\\ +\displaystyle\int_0^t\int_{\Omega_0^f}\breve{\boldsymbol{\sigma}}_f^0(\tilde{\boldsymbol{\gamma}}_n):\boldsymbol{\nabla}\pi_n\tilde{\boldsymbol{\eta}}\;d\tilde{\boldsymbol{x}}\;ds\\ +\displaystyle\sum_{i,\alpha,j,\beta=1}^3\int_0^t\int_{\Omega_0^s}\breve{b}_{i\alpha j\beta}\partial_\beta(\textstyle\int_0^s\tilde{\gamma}_n(\tau)d\tau)_j\;\partial_\alpha(\pi_n\tilde{\eta})_i\;d\tilde{\boldsymbol{x}}\;ds\\ +\displaystyle\sum_{i,\alpha,j,\beta=1}^3\int_0^t\int_{\Omega_0^s}\partial_\alpha\breve{b}_{i\alpha j\beta}\partial_\beta(\textstyle\int_0^s\tilde{\gamma}_n(\tau)d\tau)_j(\pi_n\tilde{\eta})_i\;d\tilde{\boldsymbol{x}}\;ds=\displaystyle\int_0^t\int_{\Gamma_c(0)}\boldsymbol{g}\cdot\pi_n\tilde{\boldsymbol{\eta}}\;d\tilde{\Gamma}\;ds.\end{cases} \tag{3.83}$$

This is equivalent to say,

$$(1-CT^{\kappa}M)\int_0^t [[\partial_s\tilde{\boldsymbol{\gamma}}_n(s),\pi_n\tilde{\boldsymbol{\eta}}(s)]]\ ds =$$

$$-\int_0^t\int_{\Omega_0^f}\breve{\boldsymbol{\sigma}}_f^0(\tilde{\gamma}_n):\boldsymbol{\nabla}\pi_n\tilde{\boldsymbol{\eta}}\ d\tilde{\boldsymbol{x}}\ ds-\sum_{i,\alpha,j,\beta=1}^{3}\int_0^t\int_{\Omega_0^s}\breve{b}_{i\alpha j\beta}\partial_\beta(\textstyle\int_0^s\tilde{\gamma}_n(\tau)d\tau)_j\ \partial_\alpha(\pi_n\tilde{\eta})_i\ d\tilde{\boldsymbol{x}}\ ds$$

$$-\sum_{i,\alpha,j,\beta=1}^{3}\int_0^t\int_{\Omega_0^s}\partial_\alpha\breve{b}_{i\alpha j\beta}\partial_\beta(\textstyle\int_0^s\tilde{\gamma}_n(\tau)d\tau)_j(\pi_n\tilde{\eta})_i\ d\tilde{\boldsymbol{x}}\ ds+\int_0^t\int_{\Gamma_c(0)}\boldsymbol{g}\cdot\pi_n\tilde{\boldsymbol{\eta}}\ d\tilde{\Gamma}\ ds.$$

Bounding the terms of the right hand side of the above equality yields

$$\begin{aligned}
&(1-CT^{\kappa}M)\int_0^t [[\partial_s\tilde{\boldsymbol{\gamma}}_n(s),\pi_n\tilde{\boldsymbol{\eta}}(s)]]\ ds\\
&\leq\int_0^t||\breve{\boldsymbol{\sigma}}_f^0(\tilde{\boldsymbol{\gamma}}_n)||_{L^2(\Omega_0^f)}||\boldsymbol{\nabla}\pi_n\tilde{\boldsymbol{\eta}}||_{L^2(\Omega_0^f)}\ ds\\
&\quad+\sum_{i,\alpha,j,\beta=1}^{3}\int_0^t||\breve{b}_{i\alpha j\beta}||_{L^\infty(\Omega_0^s)}||\partial_\beta(\textstyle\int_0^s\tilde{\gamma}_n(\tau)d\tau)_j||_{L^2(\Omega_0^s)}||\partial_\alpha(\pi_n\tilde{\eta})_i||_{L^2(\Omega_0^s)}\ ds\\
&\quad+\sum_{i,\alpha,j,\beta=1}^{3}\int_0^t||\partial_\alpha\breve{b}_{i\alpha j\beta}||_{L^\infty(\Omega_0^s)}||\partial_\beta(\textstyle\int_0^s\tilde{\gamma}_n(\tau)d\tau)_j||_{L^2(\Omega_0^s)}||(\pi_n\tilde{\eta})_i||_{L^2(\Omega_0^s)}\ ds\\
&\quad+||\boldsymbol{g}||_{H^1(L^2(\Gamma_c(0)))}||\pi_n\tilde{\boldsymbol{\eta}}||_{L^2(H^1(\Omega_0^s))}.
\end{aligned}\tag{3.84}$$

First, using Hölder's inequality and the embedding of H^3 in L^∞ we have

$$\begin{aligned}
&\int_0^t||\breve{\boldsymbol{\sigma}}_f^0(\tilde{\boldsymbol{\gamma}}_n)||_{L^2(\Omega_0^f)}||\boldsymbol{\nabla}\pi_n\tilde{\boldsymbol{\eta}}||_{L^2(\Omega_0^f)}\ ds\\
&\leq 2\int_0^t||\boldsymbol{\nabla}\tilde{\boldsymbol{\gamma}}_n(\boldsymbol{\nabla}\breve{\boldsymbol{\mathcal{A}}})^{-1}||_{L^2(\Omega_0^f)}||\mathrm{cof}(\boldsymbol{\nabla}\breve{\boldsymbol{\mathcal{A}}})||_{L^\infty(\Omega_0^f)}||\pi_n\tilde{\boldsymbol{\eta}}||_{H^1(\Omega_0^f)}\ ds\\
&\leq 2\int_0^t||\boldsymbol{\nabla}\tilde{\boldsymbol{\gamma}}_n||_{L^2(\Omega_0^f)}||(\boldsymbol{\nabla}\breve{\boldsymbol{\mathcal{A}}})^{-1}||_{L^\infty(\Omega_0^f)}||\mathrm{cof}(\boldsymbol{\nabla}\breve{\boldsymbol{\mathcal{A}}})||_{L^\infty(\Omega_0^f)}||\pi_n\tilde{\boldsymbol{\eta}}||_{H^1(\Omega_0^f)}\ ds\\
&\leq 2||(\boldsymbol{\nabla}\breve{\boldsymbol{\mathcal{A}}})^{-1}||_{L^\infty(L^\infty(\Omega_0^f))}||\mathrm{cof}(\boldsymbol{\nabla}\breve{\boldsymbol{\mathcal{A}}})||_{L^\infty(H^3(\Omega_0^f))}\int_0^t||\tilde{\boldsymbol{\gamma}}_n||_{H^1(\Omega_0^f)}||\pi_n\tilde{\boldsymbol{\eta}}||_{H^1(\Omega_0^f)}\ ds\\
&\leq C||\tilde{\boldsymbol{\gamma}}_n||_{L^2(H^1(\Omega_0^f))}||\pi_n\tilde{\boldsymbol{\eta}}||_{L^2(H^1(\Omega_0^f))}.
\end{aligned}\tag{3.85}$$

Further,

$$\begin{aligned}
&\sum_{i,\alpha,j,\beta=1}^{3}\int_0^t ||\breve{b}_{i\alpha j\beta}||_{L^\infty(\Omega_0^s)}||\partial_\beta(\textstyle\int_0^s\tilde{\gamma}_n(\tau)d\tau)_j||_{L^2(\Omega_0^s)}||\partial_\alpha(\pi_n\tilde{\eta})_i||_{L^2(\Omega_0^s)}\ ds\\
&\leq \sum_{i,\alpha,j,\beta=1}^{3}\int_0^t ||\breve{b}_{i\alpha j\beta}||_{L^\infty(\Omega_0^s)}||\boldsymbol{\nabla}\textstyle\int_0^s\tilde{\boldsymbol{\gamma}}_n(\tau)d\tau||_{L^2(\Omega_0^s)}||\boldsymbol{\nabla}\pi_n\tilde{\boldsymbol{\eta}}||_{L^2(\Omega_0^s)}\ ds\\
&\leq T^{1/2}\sum_{i,\alpha,j,\beta=1}^{3}||\breve{b}_{i\alpha j\beta}||_{L^\infty(L^\infty(\Omega_0^s))}||\textstyle\int_0^\bullet\tilde{\boldsymbol{\gamma}}_n(s)ds||_{L^\infty(H^1(\Omega_0^s))}||\pi_n\tilde{\boldsymbol{\eta}}||_{L^2(H^1(\Omega_0^s))}\\
&\leq CT^\kappa M||\textstyle\int_0^\bullet\tilde{\boldsymbol{\gamma}}_n(s)ds||_{L^\infty(H^1(\Omega_0^s))}||\pi_n\tilde{\boldsymbol{\eta}}||_{L^2(H^1(\Omega_0^s))}.
\end{aligned}\tag{3.86}$$

In addition, using the embedding of H^2 in L^∞ we have

$$\begin{aligned}
&\sum_{i,\alpha,j,\beta=1}^{3}\int_0^t ||\partial_\alpha\breve{b}_{i\alpha j\beta}||_{L^\infty(\Omega_0^s)}||\partial_\beta(\textstyle\int_0^s\tilde{\gamma}_n(\tau)d\tau)_j||_{L^2(\Omega_0^s)}||(\pi_n\tilde{\eta})_i||_{L^2(\Omega_0^s)}\ ds\\
&\leq \sum_{i,\alpha,j,\beta=1}^{3}\int_0^t ||\partial_\alpha\breve{b}_{i\alpha j\beta}||_{H^2(\Omega_0^s)}||\boldsymbol{\nabla}\textstyle\int_0^s\tilde{\boldsymbol{\gamma}}_n(\tau)d\tau||_{L^2(\Omega_0^s)}||\boldsymbol{\nabla}\pi_n\tilde{\boldsymbol{\eta}}||_{L^2(\Omega_0^s)}\ ds\\
&\leq \sum_{i,\alpha,j,\beta=1}^{3}||\breve{b}_{i\alpha j\beta}||_{L^\infty(H^3(\Omega_0^s))}\int_0^t ||\textstyle\int_0^s\tilde{\boldsymbol{\gamma}}_n(\tau)d\tau||_{H^1(\Omega_0^s)}||\pi_n\tilde{\boldsymbol{\eta}}||_{H^1(\Omega_0^s)}\ ds\\
&\leq CT^\kappa M||\textstyle\int_0^\bullet\tilde{\boldsymbol{\gamma}}_n(s)ds||_{L^\infty(H^1(\Omega_0^s))}||\pi_n\tilde{\boldsymbol{\eta}}||_{L^2(H^1(\Omega_0^s))}.
\end{aligned}\tag{3.87}$$

Combining (3.85)-(3.87) yields,

$$(3.84)\leq\Big[C||\tilde{\boldsymbol{\gamma}}_n||_{L^2(H^1(\Omega_0^f))}+CT^\kappa M||\textstyle\int_0^\bullet\tilde{\boldsymbol{\gamma}}_n(s)ds||_{L^\infty(H^1(\Omega_0^s))}+||\boldsymbol{g}||_{H^1(L^2(\Gamma_c(0)))}\Big]||\pi_n\tilde{\boldsymbol{\eta}}||_{L^2(H^1(\Omega_0))}.\tag{3.88}$$

Then, using the previous estimate (3.82) gives

$$\int_0^t[[\partial_s\tilde{\boldsymbol{\gamma}}_n(s),\pi_n\tilde{\boldsymbol{\eta}}(s)]]\ ds\leq C\Big[\frac{\rho_f}{2}||\boldsymbol{v}_0||_{L^2(\Omega_0^f)}+\frac{\rho_s}{2}||\boldsymbol{\xi}_1||_{L^2(\Omega_0^s)}+C||\boldsymbol{g}||_{H^1(L^2(\Gamma_c(0)))}\Big]||\pi_n\tilde{\boldsymbol{\eta}}||_{L^2(H^1(\Omega_0))}.$$

Using the fact that $||\pi_n\tilde{\boldsymbol{\eta}}||_{L^2(H^1)}\leq||\tilde{\boldsymbol{\eta}}||_{L^2(H^1(\Omega_0))}\leq 1$ we get

$$||\partial_t\tilde{\boldsymbol{\gamma}}_n||^2_{L^2(L^2)}\leq C\Big[\frac{\rho_f}{2}||\boldsymbol{v}_0||^2_{L^2(\Omega_0^f)}+\frac{\rho_s}{2}||\boldsymbol{\xi}_1||^2_{L^2(\Omega_0^s)}+||\boldsymbol{g}||^2_{H^1(L^2(\Gamma_c(0)))}\Big].\tag{3.89}$$

Theorem 3.3.1 (Aubin-Lions-Simon) *Let $B_0\subset B_1\subset B_2$ be three Banach spaces. We assume that the embedding of B_1 in B_2 is continuous and that the embedding of B_0 in B_1 is*

compact. Let p, r such that $1 \leq p, r \leq +\infty$.
For $T > 0$ we define

$$\mathcal{W}_{p,r} = \left\{ u \in L^p(]0,T[, B_0), \frac{du}{dt} \in L^r(]0,T[, B_2) \right\}.$$

i- If $p < +\infty$, then the embedding of $\mathcal{W}_{p,r}$ in $L^p(]0,T[; B_1)$ is compact.

ii- If $p = +\infty$ and $r > 1$, then the embedding of $\mathcal{W}_{p,r}$ in $\mathcal{C}^0([0,T]; B_1)$ is compact.

Proof. For the proof, check [BF13, Theorem II.5.16] ■

From the estimates (3.82) and (3.89) we may extract a subsequence of $\{\tilde{\boldsymbol{\gamma}}_n\}_n$ which we also denote by $\{\tilde{\boldsymbol{\gamma}}_n\}_n$ such that

$$\tilde{\boldsymbol{\gamma}}_n \overset{*}{\rightharpoonup} \tilde{\boldsymbol{\gamma}} \text{ in } L^\infty(0,T; L^2(\Omega_0)), \qquad \tilde{\boldsymbol{\gamma}}_n \rightharpoonup \tilde{\boldsymbol{\gamma}} \text{ in } L^2(0,T; L^2(\Omega_0)),$$

$$\partial_t \tilde{\boldsymbol{\gamma}}_n \rightharpoonup \partial_t \tilde{\boldsymbol{\gamma}} \text{ in } L^2(0,T; L^2(\Omega_0)),$$

$$\tilde{\boldsymbol{\gamma}}_n|_{\Omega_0^f} \overset{*}{\rightharpoonup} \tilde{\boldsymbol{\gamma}}|_{\Omega_0^f} \text{ in } L^\infty(0,T; H^1(\Omega_0^f)), \qquad \tilde{\boldsymbol{\gamma}}_n|_{\Omega_0^f} \rightharpoonup \tilde{\boldsymbol{\gamma}}|_{\Omega_0^f} \text{ in } L^2(0,T; H^1(\Omega_0^f)),$$

and

$$\int_0^t \tilde{\boldsymbol{\gamma}}_n(s)\Big|_{\Omega_0^s} ds \overset{*}{\rightharpoonup} \int_0^t \tilde{\boldsymbol{\gamma}}(s)\Big|_{\Omega_0^s} ds \text{ in } L^\infty(0,T; H^1(\Omega_0^s)).$$

By Theorem 3.3.1 we get

$$\tilde{\boldsymbol{\gamma}}_n \to \tilde{\boldsymbol{\gamma}} \in \mathcal{C}^0\big([0,T]; L^2(\Omega_0)\big).$$

Existence of the Weak Solution

By passing to the limit as $n \to \infty$ in (3.82) and (3.89) gives us the estimates on $\tilde{\boldsymbol{\gamma}}$. To show that $\tilde{\boldsymbol{\gamma}}$ satisfies (3.62) we proceed as follows. We fix an integer N and choose a function $\tilde{\boldsymbol{\eta}} \in \mathcal{C}^1([0,T], \widetilde{\mathcal{W}})$ of the form

$$\tilde{\boldsymbol{\eta}} = \sum_{l=1}^{N} d_l(t) \boldsymbol{\psi}_l(\tilde{\boldsymbol{x}}). \tag{3.90}$$

For $n > N$, we integrate (3.64) with respect to t to get

$$\begin{cases} \rho_f \displaystyle\int_0^T \int_{\Omega_0^f} \det(\boldsymbol{\nabla} \breve{\boldsymbol{\mathcal{A}}})\ \partial_t \tilde{\boldsymbol{\gamma}}_n \cdot \tilde{\boldsymbol{\eta}}\ d\tilde{\boldsymbol{x}}\ dt + \int_0^T \int_{\Omega_0^f} \breve{\boldsymbol{\sigma}}_f^0(\tilde{\boldsymbol{\gamma}}_n) : \boldsymbol{\nabla} \tilde{\boldsymbol{\eta}}\ d\tilde{\boldsymbol{x}}\ dt \\ + \rho_s \displaystyle\int_0^T \int_{\Omega_0^s} \det(\boldsymbol{\nabla} \breve{\boldsymbol{\varphi}}) \partial_t \tilde{\boldsymbol{\gamma}}_n \cdot \tilde{\boldsymbol{\eta}}\ d\tilde{\boldsymbol{x}}\ dt + \sum_{i,\alpha,j,\beta=1}^{3} \int_0^T \int_{\Omega_0^s} \breve{b}_{i\alpha j\beta} \partial_\beta (\textstyle\int_0^t \gamma_n(s) ds)_j\ \partial_\alpha \tilde{\eta}_i\ d\tilde{\boldsymbol{x}}\ dt \\ + \displaystyle\sum_{i,\alpha,j,\beta=1}^{3} \int_0^T \int_{\Omega_0^s} \partial_\alpha \breve{b}_{i\alpha j\beta} \partial_\beta (\textstyle\int_0^t \tilde{\gamma}_n(s) ds)_j\ \tilde{\eta}_i\ d\tilde{\boldsymbol{x}}\ dt = \displaystyle\int_0^T \int_{\Gamma_c(0)} \boldsymbol{g} \cdot \tilde{\boldsymbol{\eta}}\ d\tilde{\Gamma}\ dt. \end{cases} \tag{3.91}$$

By passing to the limit as n goes to infinity we get

$$\begin{cases} \rho_f \displaystyle\int_0^T \int_{\Omega_0^f} \det(\nabla \breve{\mathcal{A}}) \partial_t \tilde{\gamma} \cdot \tilde{\boldsymbol{\eta}} \, d\tilde{\boldsymbol{x}} \, dt + \int_0^T \int_{\Omega_0^f} \breve{\boldsymbol{\sigma}}_f^0(\tilde{\gamma}) : \nabla \tilde{\boldsymbol{\eta}} \, d\tilde{\boldsymbol{x}} \, dt \\ + \rho_s \displaystyle\int_0^T \int_{\Omega_0^s} \det(\nabla \breve{\boldsymbol{\varphi}}) \partial_t \tilde{\gamma} \cdot \tilde{\boldsymbol{\eta}} \, d\tilde{\boldsymbol{x}} \, dt + \sum_{i,\alpha,j,\beta=1}^{3} \int_0^T \int_{\Omega_0^s} \breve{b}_{i\alpha j\beta} \partial_\beta (\textstyle\int_0^t \tilde{\gamma}(s) ds)_j \; \partial_\alpha \tilde{\eta}_i \, d\tilde{\boldsymbol{x}} \, dt \\ + \displaystyle\sum_{i,\alpha,j,\beta=1}^{3} \int_0^T \int_{\Omega_0^s} \partial_\alpha \breve{b}_{i\alpha j\beta} \partial_\beta (\textstyle\int_0^t \tilde{\gamma}(s) ds)_j \; \tilde{\eta}_i \, d\tilde{\boldsymbol{x}} \, dt = \displaystyle\int_0^T \int_{\Gamma_c(0)} \boldsymbol{g} \cdot \tilde{\boldsymbol{\eta}} \, d\tilde{\Gamma} \, dt, \end{cases} \tag{3.92}$$

holds true for all $\tilde{\boldsymbol{\eta}} \in L^2([0,T], \widetilde{\mathcal{W}})$ due to the fact that the space spanned by the functions of the form (3.90) is dense in $L^2([0,T], \widetilde{\mathcal{W}})$. Hence, (3.92) implies (3.62).

To show that the initial conditions are satisfied we will consider $\tilde{\boldsymbol{\eta}} \in \mathcal{C}^1([0,t], \widetilde{\mathcal{W}})$ in (3.92) and integrate by parts to get

$$\begin{cases} \rho_f \displaystyle\int_0^T \int_{\Omega_0^f} \tilde{\gamma} \cdot \partial_t (\tilde{\boldsymbol{\eta}} \det(\nabla \breve{\mathcal{A}})) \, d\tilde{\boldsymbol{x}} \, dt - \int_0^T \int_{\Omega_0^f} \breve{\boldsymbol{\sigma}}_f^0(\tilde{\gamma}) : \nabla \tilde{\boldsymbol{\eta}} \, d\tilde{\boldsymbol{x}} \, dt \\ + \rho_s \displaystyle\int_0^T \int_{\Omega_0^s} \tilde{\gamma} \cdot \partial_t (\tilde{\boldsymbol{\eta}} \det(\nabla \breve{\boldsymbol{\varphi}})) \, d\tilde{\boldsymbol{x}} \, dt - \sum_{i,\alpha,j,\beta=1}^{3} \int_0^T \int_{\Omega_0^s} \breve{b}_{i\alpha j\beta} \partial_\beta (\textstyle\int_0^t \tilde{\gamma}(s) ds)_j \; \partial_\alpha \tilde{\eta}_i \, d\tilde{\boldsymbol{x}} \, dt \\ - \displaystyle\sum_{i,\alpha,j,\beta=1}^{3} \int_0^T \int_{\Omega_0^s} \partial_\alpha \breve{b}_{i\alpha j\beta} \partial_\beta (\textstyle\int_0^t \tilde{\gamma}(s) ds)_j \; \tilde{\eta}_i \, d\tilde{\boldsymbol{x}} \, dt \\ = - \displaystyle\int_0^T \int_{\Gamma_c(0)} \boldsymbol{g} \cdot \tilde{\boldsymbol{\eta}} \, d\tilde{\Gamma} \, dt - \rho_f \int_{\Omega_0^f} \tilde{\boldsymbol{v}}(0) \cdot \tilde{\boldsymbol{\eta}}(0) \, d\tilde{\boldsymbol{x}} - \rho_s \int_{\Omega_0^s} \partial_t \tilde{\boldsymbol{\xi}}(0) \cdot \tilde{\boldsymbol{\eta}}(0) \, d\tilde{\boldsymbol{x}}. \end{cases} \tag{3.93}$$

On the other hand, integrating by parts in time Equation (3.91) and passing to the limit we get

$$\begin{cases} \rho_f \displaystyle\int_0^T \int_{\Omega_0^f} \tilde{\gamma} \cdot \partial_t (\tilde{\boldsymbol{\eta}} \det(\nabla \breve{\mathcal{A}})) d\tilde{\boldsymbol{x}} \, dt - \int_0^T \int_{\Omega_0^f} \breve{\boldsymbol{\sigma}}_f^0(\tilde{\gamma}) : \nabla \tilde{\boldsymbol{\eta}} \, d\tilde{\boldsymbol{x}} \, dt \\ + \rho_s \displaystyle\int_0^T \int_{\Omega_0^s} \tilde{\gamma} \cdot \partial_t (\tilde{\boldsymbol{\eta}} \det(\nabla \breve{\boldsymbol{\varphi}})) \, d\tilde{\boldsymbol{x}} \, dt - \sum_{i,\alpha,j,\beta=1}^{3} \int_0^T \int_{\Omega_0^s} \breve{b}_{i\alpha j\beta} \partial_\beta (\textstyle\int_0^t \tilde{\gamma}(s) ds)_j \; \partial_\alpha \eta \, d\tilde{\boldsymbol{x}} \, dt \\ - \displaystyle\sum_{i,\alpha,j,\beta=1}^{3} \int_0^T \int_{\Omega_0^s} \partial_\alpha \breve{b}_{i\alpha j\beta} \partial_\beta (\textstyle\int_0^t \tilde{\gamma}(s) ds)_j \; \tilde{\eta}_i \, d\tilde{\boldsymbol{x}} \, dt \\ = - \displaystyle\int_0^T \int_{\Gamma_c(0)} \boldsymbol{g} \cdot \tilde{\boldsymbol{\eta}} \, d\tilde{\Gamma} \, dt - \rho_f \int_{\Omega_0^f} \boldsymbol{v}_0 \cdot \tilde{\boldsymbol{\eta}}(0) \, d\tilde{\boldsymbol{x}} - \rho_s \int_{\Omega_0^s} \boldsymbol{\xi}_1 \cdot \tilde{\boldsymbol{\eta}}(0) \, d\tilde{\boldsymbol{x}}. \end{cases} \tag{3.94}$$

Comparing (3.93) and (3.94) yields

$$[[\tilde{\boldsymbol{\gamma}}_0, \tilde{\boldsymbol{\eta}}(0)]] = [[\tilde{\gamma}(0), \tilde{\boldsymbol{\eta}}(0)]].$$

Since $\tilde{\boldsymbol{\eta}}(0) \in \widetilde{\mathcal{W}}$ is arbitrary, then the initial conditions are verified.
Finally, by passing to the limit in (3.66), we obtain $(3.62)_3$. This yields the existence of the weak solution $\tilde{\boldsymbol{\gamma}}$ of System (3.57).

Uniqueness of the Weak Solution

To prove the uniqueness of the weak solution we assume that $\tilde{\boldsymbol{\gamma}}_1$ and $\tilde{\boldsymbol{\gamma}}_2$ are two solutions of (3.62) associated to $(\breve{\boldsymbol{v}}, \breve{\boldsymbol{\xi}})$. Setting $\tilde{\boldsymbol{\varsigma}} = \tilde{\boldsymbol{\gamma}}_1 - \tilde{\boldsymbol{\gamma}}_2$. Then for all $\tilde{\boldsymbol{\eta}} \in \mathcal{C}^0(0,T;\widetilde{\mathcal{W}})$, the solution $\tilde{\boldsymbol{\varsigma}}$ satisfies the following variational formulation

$$\begin{cases} \rho_f \displaystyle\int_{\Omega_0^f} \det(\boldsymbol{\nabla}\breve{\boldsymbol{\mathcal{A}}})\partial_t\tilde{\boldsymbol{\varsigma}} \cdot \tilde{\boldsymbol{\eta}} \; d\tilde{\boldsymbol{x}} + \int_{\Omega_0^f} \tilde{\boldsymbol{\sigma}}(\tilde{\boldsymbol{\varsigma}}) : \boldsymbol{\nabla}\tilde{\boldsymbol{\eta}} \; d\tilde{\boldsymbol{x}} + \rho_s \int_{\Omega_0^s} \det(\boldsymbol{\nabla}\breve{\boldsymbol{\varphi}})\partial_t\tilde{\boldsymbol{\varsigma}} \cdot \tilde{\boldsymbol{\eta}} \; d\tilde{\boldsymbol{x}} \\ + \displaystyle\sum_{i,\alpha,j,\beta=1}^{3} \int_{\Omega_0^s} \breve{b}_{i\alpha j\beta}\partial_\beta(\textstyle\int_0^t \tilde{\varsigma}(s)ds)_j \; \partial_\alpha\tilde{\eta}_i \; d\tilde{\boldsymbol{x}} \\ + \displaystyle\sum_{i,\alpha,j,\beta=1}^{3} \int_{\Omega_0^s} \partial_\alpha\breve{b}_{i\alpha j\beta}\partial_\beta(\textstyle\int_0^t \tilde{\varsigma}(s)ds)_j \; \tilde{\eta}_i \; d\tilde{\boldsymbol{x}} = 0. \end{cases} \tag{3.95}$$

Taking $\tilde{\boldsymbol{\eta}} = \tilde{\boldsymbol{\varsigma}}$ and integrating over $(0,t)$ we get

$$\begin{cases} \dfrac{\rho_f}{2} \displaystyle\int_{\Omega_0^f} \det(\boldsymbol{\nabla}\breve{\boldsymbol{\mathcal{A}}})|\tilde{\boldsymbol{\varsigma}}(t)|^2 \; d\tilde{\boldsymbol{x}} + \int_0^t \int_{\Omega_0^f} \tilde{\boldsymbol{\sigma}}(\tilde{\boldsymbol{\varsigma}}) : \boldsymbol{\nabla}\tilde{\boldsymbol{\varsigma}} \; d\tilde{\boldsymbol{x}} \; ds + \dfrac{\rho_s}{2} \int_{\Omega_0^s} \det(\boldsymbol{\nabla}\breve{\boldsymbol{\varphi}})|\tilde{\boldsymbol{\varsigma}}(t)|^2 \; d\tilde{\boldsymbol{x}} \\ -\dfrac{\rho_f}{2} \displaystyle\int_0^t \int_{\Omega_0^f} |\tilde{\boldsymbol{\varsigma}}|^2 \partial_s\det(\boldsymbol{\nabla}\breve{\boldsymbol{\mathcal{A}}}) \; d\tilde{\boldsymbol{x}} \; ds - \dfrac{\rho_s}{2} \int_0^t \int_{\Omega_0^s} |\tilde{\boldsymbol{\varsigma}}|^2 \partial_s\det(\boldsymbol{\nabla}\breve{\boldsymbol{\varphi}}) \; d\tilde{\boldsymbol{x}} \; ds \\ +\dfrac{1}{2} \displaystyle\sum_{i,\alpha,j,\beta=1}^{3} \int_{\Omega_0^s} \breve{b}_{i\alpha j\beta}(t)\partial_\beta(\textstyle\int_0^t \tilde{\varsigma}(s)ds)_j \; \partial_\alpha\tilde{\varsigma}_i(t) \; d\tilde{\boldsymbol{x}} \\ -\dfrac{1}{2} \displaystyle\sum_{i,\alpha,j,\beta=1}^{3} \int_0^t \int_{\Omega_0^s} \partial_s\breve{b}_{i\alpha j\beta}\partial_\beta(\textstyle\int_0^s \tilde{\varsigma}(\tau)d\tau)_j \; \partial_\alpha\tilde{\varsigma}_i \; d\tilde{\boldsymbol{x}} \; ds \\ + \displaystyle\sum_{i,\alpha,j,\beta=1}^{3} \int_0^t \int_{\Omega_0^s} \partial_\alpha\breve{b}_{i\alpha j\beta}\partial_\beta(\textstyle\int_0^s \tilde{\varsigma}(\tau)d\tau)_j \; \partial_s\tilde{\varsigma}_i \; d\tilde{\boldsymbol{x}} \; ds = 0. \end{cases} \tag{3.96}$$

Using (3.72)-(3.78) we get

$$||\tilde{\boldsymbol{\varsigma}}||^2_{L^2(H^1(\Omega_0^f))} + ||\tilde{\boldsymbol{\varsigma}}||^2_{L^\infty(L^2(\Omega_0))} + ||\textstyle\int_0^\bullet \tilde{\boldsymbol{\varsigma}}(s)ds||^2_{L^\infty(L^2(\Omega_0^s))} + ||\int_0^\bullet \tilde{\boldsymbol{\varsigma}}(s)ds||^2_{L^\infty(H^1(\Omega_0^s))} \leq 0, \tag{3.97}$$

which yields that $\tilde{\boldsymbol{\gamma}}_1 = \tilde{\boldsymbol{\gamma}}_2$. Therefore, $\tilde{\boldsymbol{\gamma}}$ is a unique solution of (3.62). In addition, we have

$$\tilde{\gamma}|_{\Omega_0^f} \in L^\infty(L^2(\Omega_0^f)) \cap L^2(H^1(\Omega_0^f)), \quad \tilde{\gamma}|_{\Omega_0^s} \in L^\infty(L^2(\Omega_0^s)) \quad \text{and} \quad \int_0^t \tilde{\gamma}(s)|_{\Omega_0^s} ds \in L^\infty(H^1(\Omega_0^s)). \tag{3.98}$$

Consequently, setting $\tilde{\boldsymbol{v}} = \tilde{\boldsymbol{\gamma}}|_{\Omega_0^f}$ and $\tilde{\boldsymbol{\xi}} = \boldsymbol{\xi}_0 + \displaystyle\int_0^t \tilde{\boldsymbol{\gamma}}(s)|_{\Omega_0^s} \; ds$, we obtain the existence and uniqueness of the weak solution $(\tilde{\boldsymbol{v}}, \tilde{\boldsymbol{\xi}}) \in F_1^T \times S_1^T$ for the System (3.57).

3.4 Existence of Solution for the Linearized System

The linear problem is given by the following system

$$\begin{cases} \rho_f \det(\boldsymbol{\nabla}\breve{\boldsymbol{\mathcal{A}}})\partial_t \tilde{\boldsymbol{v}} - \boldsymbol{\nabla}\cdot\breve{\boldsymbol{\sigma}}_f^0(\tilde{\boldsymbol{v}},\tilde{p}_f) = 0 & \text{in } \Omega_0^f\times(0,T), \\ \nabla\cdot(\det(\boldsymbol{\nabla}\breve{\boldsymbol{\mathcal{A}}})(\boldsymbol{\nabla}\breve{\boldsymbol{\mathcal{A}}})^{-1}\tilde{\boldsymbol{v}}) = 0 & \text{in } \Omega_0^f\times(0,T), \\ \tilde{\boldsymbol{v}} = \boldsymbol{v}_{\text{in}}\circ\breve{\boldsymbol{\mathcal{A}}} & \text{on } \Gamma_{\text{in}}(0)\times(0,T), \\ \breve{\boldsymbol{\sigma}}_f^0(\tilde{\boldsymbol{v}},\tilde{p}_f)\ \tilde{\boldsymbol{n}} = 0 & \text{on } \Gamma_{\text{out}}(0)\times(0,T), \\ \rho_s\det(\boldsymbol{\nabla}\breve{\boldsymbol{\varphi}})\partial_t^2\tilde{\xi}_i - \displaystyle\sum_{\alpha,j,\beta=1}^{3}\breve{b}_{i\alpha j\beta}\partial^2_{\alpha\beta}\tilde{\xi}_j = 0 \quad i=1,2,3, & \text{in } \Omega_0^s\times(0,T), \\ \tilde{\boldsymbol{\xi}} = \boldsymbol{0} & \text{on } \Gamma_2(0)\times(0,T), \\ \tilde{\boldsymbol{v}} = \partial_t\tilde{\boldsymbol{\xi}} & \text{on } \Gamma_c(0)\times(0,T), \\ \left[\breve{\boldsymbol{\sigma}}_f^0(\tilde{\boldsymbol{v}},\tilde{p}_f)\tilde{\boldsymbol{n}}\right]_i = \displaystyle\sum_{\alpha,j,\beta=1}^{3}\left(\int_0^t \breve{b}_{i\alpha j\beta}\partial^2_{s\beta}\tilde{\xi}_j ds\right)\tilde{n}_\alpha \quad i=1,2,3, & \text{on } \Gamma_c(0)\times(0,T), \\ \tilde{\boldsymbol{v}}(.,0) = \boldsymbol{v}_0 \quad \text{and} \quad \tilde{p}_f(.,0) = p_{f0} & \text{in } \Omega_0^f, \\ \tilde{\boldsymbol{\xi}}(.,0) = \boldsymbol{0} \quad \text{and} \quad \partial_t\tilde{\boldsymbol{\xi}}(.,0) = \boldsymbol{\xi}_1 & \text{in } \Omega_0^s, \end{cases} \tag{3.99}$$

which is nothing but the auxiliary problem (3.57) when considering

$$g_i = -\sum_{\alpha,j,\beta=1}^{3}\left(\int_0^t \partial_s\breve{b}_{i\alpha j\beta}\partial_\beta\tilde{\xi}_j\ ds\right)\tilde{n}_\alpha, \quad i=1,2,3.$$

Proposition 3.4.1 *Let $(\breve{\boldsymbol{v}},\breve{\boldsymbol{\xi}}) \in A_M^T$, $\boldsymbol{v}_0 \in H^1(\Omega_0^f)$, and $\boldsymbol{\xi}_1 \in H^1(\Omega_0^s)$ satisfying (3.4) and $(3.30)_1$. For T small with respect to M and the initial conditions, there exists a unique weak solution $(\tilde{\boldsymbol{v}},\tilde{\boldsymbol{\xi}}) \in F_2^T \times S_2^T$ of (3.99). Moreover we get an a piori estimate on the solution that is given by*

$$||\tilde{\boldsymbol{v}}||^2_{F_2^T} + ||\tilde{\boldsymbol{\xi}}||^2_{S_2^T} \leq C||\boldsymbol{v}_0||^2_{H^1} + C||\boldsymbol{\xi}_1||^2_{H^1}. \tag{3.100}$$

Notice that, increasing the regularity of the initial data by considering $\boldsymbol{v}_0 \in H^1(\Omega_0^f)$ and $\boldsymbol{\xi}_1 \in H^1(\Omega_0^s)$ will lead to a more regular solution [Eva98, Bre10]. Using the regularity results we will achieve a solution $(\tilde{\boldsymbol{v}},\tilde{\boldsymbol{\xi}}) \in F_2^T \times S_2^T$. Now we prove Proposition 3.4.1. The proof is based on the fixed point theorem. Indeed, the first step is to find estimates on $\partial_t\tilde{\boldsymbol{\gamma}}$ in $F_2^T \times S_2^T$ then we prove the existence and uniqueness of a weak solution of (3.99).
First, we consider System (3.57) with the function

$$g_i = \hat{h}_i = -\sum_{\alpha,j,\beta=1}^{3}\left(\int_0^t \partial_s\breve{b}_{i\alpha j\beta}\partial_\beta\hat{\xi}_j\ ds\right)\tilde{n}_\alpha, \quad i=1,2,3.$$

Observe that $\hat{\boldsymbol{h}} \in H_l^1(0,T;L^2(\Gamma_c(0))$. In fact, using (3.37) with the trace inequality gives

$$\begin{aligned}
||\partial_t \hat{\boldsymbol{h}}||_{L_l^2(L^2(\Gamma_c(0)))} &\leq ||\partial_t \breve{b}_{i\alpha j\beta}\partial_\beta \hat{\xi}_j||_{L^2(L^2(\Gamma_c(0)))} \\
&\leq ||\partial_t \breve{b}_{i\alpha j\beta}||_{L^\infty(L^\infty)}||\partial_\beta \hat{\xi}_j||_{L^2(L^2(\Gamma_c(0)))} \\
&\leq CTM^4||\boldsymbol{\nabla}\hat{\boldsymbol{\xi}}||_{L^\infty(H^1(\Omega_0^s))} \\
&\leq CT^\kappa M||\hat{\boldsymbol{\xi}}||_{L^\infty(H^2(\Omega_0^s))} \leq CT^\kappa M||\hat{\boldsymbol{\xi}}||_{S_2^T},
\end{aligned}$$

and since $\hat{\boldsymbol{h}}(0) = 0$, we use the fact that

$$||\hat{\boldsymbol{h}}||_{L^2(L^2(\Gamma_c(0)))} \leq C||\partial_t \hat{\boldsymbol{h}}||_{L^2(L^2(\Gamma_c(0)))},$$

to get that the function $\hat{\boldsymbol{h}} \in H_l^1(0,T;L^2(\Gamma_c(0)))$ such that

$$||\hat{\boldsymbol{h}}||_{H_l^1(0,T;L^2(\Gamma_c(0)))} \leq CT^\kappa M||\hat{\boldsymbol{\xi}}||_{S_2^T}. \tag{3.101}$$

Therefore, as $\hat{\boldsymbol{\xi}}$ is fixed, by Lemma 3.3.1 we get the existence and uniqueness of $(\tilde{\boldsymbol{v}},\tilde{\boldsymbol{\xi}}) \in F_1^T \times S_1^T$ satisfying

$$||\tilde{\boldsymbol{v}}||^2_{F_1^T} + ||\tilde{\boldsymbol{\xi}}||^2_{S_1^T} \leq C\left[\frac{\rho_f}{2}||\boldsymbol{v}_0||^2_{L^2} + \frac{\rho_s}{2}||\boldsymbol{\xi}_1||^2_{L^2} + T^\kappa M||\hat{\boldsymbol{\xi}}||_{S_2^T}\right]. \tag{3.102}$$

To prove that the solution $(\tilde{\boldsymbol{v}},\tilde{\boldsymbol{\xi}})$ is in the space $F_2^T \times S_2^T$ we use the fixed point theorem. To this end we introduce the map Ψ_0 from S_2^T to S_2^T defined as

$$\Psi_0 : \hat{\boldsymbol{\xi}} \longmapsto \tilde{\boldsymbol{\xi}}.$$

As we mentioned previously, we ensure the existence of a weak solution $(\tilde{\boldsymbol{v}},\tilde{\boldsymbol{\xi}}) \in F_2^T \times S_2^T$ due to the regularity results based on increasing the regularity of the initial data. In order to prove its uniqueness it is sufficient to prove that Ψ_0 is a contraction on S_2^T. This is achieved by deriving some a priori estimates on $\partial_t \tilde{\boldsymbol{\gamma}}$.

3.4.1 Estimates on $\partial_t \tilde{v}$ and $\partial_t^2 \tilde{\xi}$

We proceed to derive *a priori* estimates on $\partial_t \tilde{\boldsymbol{\gamma}}$. Differentiating the weak formulation (3.62) in time yields

$$\begin{cases}
\rho_f \displaystyle\int_{\Omega_0^f} \partial_t(\det(\boldsymbol{\nabla}\breve{\boldsymbol{\mathcal{A}}})\partial_t \tilde{\gamma}) \cdot \tilde{\boldsymbol{\eta}}\, d\tilde{\boldsymbol{x}} + \int_{\Omega_0^f} \partial_t \breve{\boldsymbol{\sigma}}_f^0(\tilde{\gamma}) : \boldsymbol{\nabla}\tilde{\boldsymbol{\eta}}\, d\tilde{\boldsymbol{x}} \\
+\rho_s \displaystyle\int_{\Omega_0^s} \partial_t\big(\det(\boldsymbol{\nabla}\breve{\boldsymbol{\varphi}})\partial_t \tilde{\boldsymbol{\gamma}}\big) \cdot \tilde{\boldsymbol{\eta}}\, d\tilde{\boldsymbol{x}} + \sum_{i,\alpha,j,\beta=1}^{3} \int_{\Omega_0^s} \partial_t\Big(\breve{b}_{i\alpha j\beta}\partial_\beta\big(\textstyle\int_0^t \tilde{\gamma}(s)ds\big)_j\Big)\, \partial_\alpha \tilde{\eta}_i\, d\tilde{\boldsymbol{x}} \\
+ \displaystyle\sum_{i,\alpha,j,\beta=1}^{3} \int_{\Omega_0^s} \partial_t\Big(\partial_\alpha \breve{b}_{i\alpha j\beta}\partial_\beta\big(\textstyle\int_0^t \tilde{\gamma}(s)ds\big)_j\Big)\, \tilde{\eta}_i\, d\tilde{\boldsymbol{x}} = \displaystyle\int_{\Gamma_c(0)} \partial_t \hat{\boldsymbol{h}} \cdot \tilde{\boldsymbol{\eta}}\, d\tilde{\Gamma}.
\end{cases} \tag{3.103}$$

Take $\tilde{\boldsymbol{\eta}} = \partial_t \tilde{\boldsymbol{\gamma}}$ and integrate over $(0,t)$ to get

$$\begin{cases} \rho_f \displaystyle\int_0^t \int_{\Omega_0^f} \partial_s(\det(\nabla \breve{\boldsymbol{\mathcal{A}}})\partial_s \tilde{\boldsymbol{\gamma}}) \cdot \partial_s \tilde{\boldsymbol{\gamma}} \; d\tilde{\boldsymbol{x}} \; ds + \int_0^t \int_{\Omega_0^f} \partial_s \breve{\boldsymbol{\sigma}}_f^0(\tilde{\boldsymbol{\gamma}}) : \partial_s \nabla \tilde{\boldsymbol{\gamma}} \; d\tilde{\boldsymbol{x}} \; ds \\ +\rho_s \displaystyle\int_0^t \int_{\Omega_0^s} \partial_s \big(\det(\nabla \breve{\boldsymbol{\varphi}})\partial_s \tilde{\boldsymbol{\gamma}}\big) \cdot \partial_s \tilde{\boldsymbol{\gamma}} \; d\tilde{\boldsymbol{x}} \; ds \\ + \displaystyle\sum_{i,\alpha,j,\beta=1}^{3} \int_0^t \int_{\Omega_0^s} \partial_s \Big(\breve{b}_{i\alpha j\beta} \partial_\beta (\textstyle\int_0^s \tilde{\gamma}(\tau) d\tau)_j \Big) \; \partial_\alpha \partial_s^2 (\textstyle\int_0^s \tilde{\gamma}(\tau) d\tau)_i \; d\tilde{\boldsymbol{x}} \; ds \\ + \displaystyle\sum_{i,\alpha,j,\beta=1}^{3} \int_0^t \int_{\Omega_0^s} \partial_s \Big(\partial_\alpha \breve{b}_{i\alpha j\beta} \partial_\beta (\textstyle\int_0^s \tilde{\gamma}(\tau) d\tau)_j \Big) \; \partial_s^2 (\textstyle\int_0^s \tilde{\gamma}(\tau) d\tau)_i \; d\tilde{\boldsymbol{x}} \; ds \\ = \displaystyle\int_0^t \int_{\Gamma_c(0)} \partial_s \hat{\boldsymbol{h}} \cdot \partial_s^2 (\textstyle\int_0^s \tilde{\boldsymbol{\gamma}}(\tau) d\tau) \; d\tilde{\Gamma} \; ds. \end{cases} \tag{3.104}$$

First, we have

$$\begin{aligned} &\int_0^t \int_{\Omega_0^s} \partial_s \big(\det(\nabla \breve{\boldsymbol{\varphi}})\partial_s \tilde{\boldsymbol{\gamma}}\big) \cdot \partial_s \boldsymbol{\gamma} \; d\tilde{\boldsymbol{x}} \; ds \\ &\qquad = \int_0^t \int_{\Omega_0^s} \partial_s \det(\nabla \breve{\boldsymbol{\varphi}}) |\partial_s \tilde{\boldsymbol{\gamma}}|^2 \; d\tilde{\boldsymbol{x}} \; ds + \int_0^t \int_{\Omega_0^s} \det(\nabla \breve{\boldsymbol{\varphi}}) \partial_s^2 \tilde{\boldsymbol{\gamma}} \cdot \partial_s \tilde{\boldsymbol{\gamma}} \; d\tilde{\boldsymbol{x}} \; ds, \end{aligned}$$

but applying integration by parts in time to the second integral of the right hand side yields

$$\begin{aligned} &\int_0^t \int_{\Omega_0^s} \det(\nabla \breve{\boldsymbol{\varphi}}) \partial_s^2 \tilde{\boldsymbol{\gamma}} \cdot \partial_s \tilde{\boldsymbol{\gamma}} \; d\tilde{\boldsymbol{x}} \; ds \\ &\quad = \int_0^t \int_{\Omega_0^s} \det(\nabla \breve{\boldsymbol{\varphi}}) \partial_s \tilde{\boldsymbol{\gamma}} \cdot \partial_s^2 \tilde{\boldsymbol{\gamma}} \; d\tilde{\boldsymbol{x}} \; ds \\ &\quad = \frac{1}{2} \int_0^t \int_{\Omega_0^s} \partial_s \big(\det(\nabla \breve{\boldsymbol{\varphi}}) |\partial_s \tilde{\boldsymbol{\gamma}}|^2\big) \; d\tilde{\boldsymbol{x}} \; ds - \frac{1}{2} \int_0^t \int_{\Omega_0^s} \partial_s \det(\nabla \breve{\boldsymbol{\varphi}}) |\partial_s \tilde{\boldsymbol{\gamma}}|^2 \; d\tilde{\boldsymbol{x}} \; ds \\ &\quad = \frac{1}{2} \int_{\Omega_0^s} \det(\nabla \breve{\boldsymbol{\varphi}})(t) |\partial_t \tilde{\boldsymbol{\gamma}}(t)|^2 \; d\tilde{\boldsymbol{x}} - \frac{1}{2} \int_{\Omega_0^s} |\partial_t \tilde{\boldsymbol{\gamma}}(0)|^2 \; d\tilde{\boldsymbol{x}} - \frac{1}{2} \int_0^t \int_{\Omega_0^s} \partial_s \det(\nabla \breve{\boldsymbol{\varphi}}) |\partial_s \tilde{\boldsymbol{\gamma}}|^2 \; d\tilde{\boldsymbol{x}} \; ds. \end{aligned}$$

Whence,

$$\begin{aligned} &\int_0^t \int_{\Omega_0^s} \partial_s \big(\det(\nabla \breve{\boldsymbol{\varphi}})\partial_s \tilde{\boldsymbol{\gamma}}\big) \cdot \partial_s \boldsymbol{\gamma} \; d\tilde{\boldsymbol{x}} \; ds \\ &\qquad = \frac{1}{2} \int_{\Omega_0^s} \det(\nabla \breve{\boldsymbol{\varphi}})(t) |\partial_t \tilde{\boldsymbol{\gamma}}(t)|^2 \; d\tilde{\boldsymbol{x}} - \frac{1}{2} \int_{\Omega_0^s} |\partial_t \tilde{\boldsymbol{\gamma}}(0)|^2 \; d\tilde{\boldsymbol{x}} + \frac{1}{2} \int_0^t \int_{\Omega_0^s} \partial_s \det(\nabla \breve{\boldsymbol{\varphi}}) |\partial_s \tilde{\boldsymbol{\gamma}}|^2 \; d\tilde{\boldsymbol{x}} \; ds. \end{aligned}$$

Further, we have

$$\begin{aligned}
&\int_0^t \int_{\Omega_0^s} \partial_s\Big(\breve{b}_{i\alpha j\beta}\partial_\beta(\textstyle\int_0^s \tilde{\gamma}(\tau)d\tau)_j\Big)\ \partial_\alpha\partial_s^2(\textstyle\int_0^s \tilde{\gamma}(\tau)d\tau)_i\ d\tilde{\boldsymbol{x}}\ ds \\
&\qquad = \frac{1}{2}\int_0^t \int_{\Omega_0^s} \partial_s\Big(\breve{b}_{i\alpha j\beta}\partial_{s\beta}^2(\textstyle\int_0^s \tilde{\gamma}(\tau)d\tau)_j\partial_{s\alpha}^2(\int_0^s \tilde{\gamma}(\tau)d\tau)_i\Big)\ d\tilde{\boldsymbol{x}}\ ds \\
&\qquad\quad - \frac{1}{2}\int_0^t \int_{\Omega_0^s} \partial_s\breve{b}_{i\alpha j\beta}\partial_{s\beta}^2(\textstyle\int_0^s \tilde{\gamma}(\tau)d\tau)_j\partial_{s\alpha}^2(\int_0^s \tilde{\gamma}(\tau)d\tau)_i\ d\tilde{\boldsymbol{x}}\ ds \\
&\qquad\quad + \int_0^t \int_{\Omega_0^s} \partial_s\breve{b}_{i\alpha j\beta}\partial_\beta(\textstyle\int_0^s \tilde{\gamma}(\tau)d\tau)_j\partial_\alpha\Big(\partial_s^2(\int_0^s \tilde{\gamma}(\tau)d\tau)_i\Big)\ d\tilde{\boldsymbol{x}}\ ds
\end{aligned} \tag{3.105}$$

and

$$\begin{aligned}
&\int_0^t \int_{\Omega_0^s} \partial_s\Big(\partial_\alpha\breve{b}_{i\alpha j\beta}\partial_\beta(\textstyle\int_0^s \tilde{\gamma}(\tau)d\tau)_j\Big)\ \partial_s^2(\textstyle\int_0^s \tilde{\gamma}(\tau)d\tau)_i\ d\tilde{\boldsymbol{x}}\ ds \\
&\qquad = \int_0^t \int_{\Omega_0^s} \partial_s(\partial_\alpha\breve{b}_{i\alpha j\beta})\partial_\beta(\textstyle\int_0^s \tilde{\gamma}(\tau)d\tau)_j\ \partial_s^2(\int_0^s \tilde{\gamma}(\tau)d\tau)_i\ d\tilde{\boldsymbol{x}}\ ds \\
&\qquad\quad + \int_0^t \int_{\Omega_0^s} \partial_\alpha\breve{b}_{i\alpha j\beta}\partial_{s\beta}^2(\textstyle\int_0^s \tilde{\gamma}(\tau)d\tau)_j\ \partial_s^2(\int_0^s \tilde{\gamma}(\tau)d\tau)_i\ d\tilde{\boldsymbol{x}}\ ds \\
&\qquad = \int_0^t \int_{\Omega_0^s} \partial_\alpha(\partial_s\breve{b}_{i\alpha j\beta})\partial_\beta(\textstyle\int_0^s \tilde{\gamma}(\tau)d\tau)_j\ \partial_s^2(\int_0^s \tilde{\gamma}(\tau)d\tau)_i\ d\tilde{\boldsymbol{x}}\ ds \\
&\qquad\quad + \int_0^t \int_{\Omega_0^s} \partial_\alpha\breve{b}_{i\alpha j\beta}\partial_{s\beta}^2(\textstyle\int_0^s \tilde{\gamma}(\tau)d\tau)_j\ \partial_s^2(\int_0^s \tilde{\gamma}(\tau)d\tau)_i\ d\tilde{\boldsymbol{x}}\ ds,
\end{aligned} \tag{3.106}$$

but,

$$\begin{aligned}
&\int_0^t \int_{\Omega_0^s} \partial_s\breve{b}_{i\alpha j\beta}\partial_\beta(\textstyle\int_0^s \tilde{\gamma}(\tau)d\tau)_j\partial_\alpha\Big(\partial_s^2(\int_0^s \tilde{\gamma}(\tau)d\tau)_i\Big)\ d\tilde{\boldsymbol{x}}\ ds \\
&\qquad = -\int_0^t \int_{\Omega_0^s} \partial_\alpha\Big(\partial_s\breve{b}_{i\alpha j\beta}\partial_\beta(\textstyle\int_0^s \tilde{\gamma}(\tau)d\tau)_j\Big)\partial_s^2(\int_0^s \tilde{\gamma}(\tau)d\tau)_i\ d\tilde{\boldsymbol{x}}\ ds \\
&\qquad\quad + \int_0^t \int_{\Gamma_c(0)} \partial_s\breve{b}_{i\alpha j\beta}\partial_\beta(\textstyle\int_0^s \tilde{\gamma}(\tau)d\tau)_j\partial_s^2(\int_0^s \tilde{\gamma}(\tau)d\tau)_i\ n_\alpha\ d\tilde{\Gamma}\ ds \\
&\qquad = -\int_0^t \int_{\Omega_0^s} \partial_\alpha(\partial_s\breve{b}_{i\alpha j\beta})\partial_\beta(\textstyle\int_0^s \tilde{\gamma}(\tau)d\tau)_j\partial_s^2(\int_0^s \tilde{\gamma}(\tau)d\tau)_i\ d\tilde{\boldsymbol{x}}\ ds \\
&\qquad\quad - \int_0^t \int_{\Omega_0^s} \partial_s\breve{b}_{i\alpha j\beta}\partial_{\alpha\beta}^2(\textstyle\int_0^s \tilde{\gamma}(\tau)d\tau)_j\partial_s^2(\int_0^s \tilde{\gamma}(\tau)d\tau)_i\ d\tilde{\boldsymbol{x}}\ ds \\
&\qquad\quad + \int_0^t \int_{\Gamma_c(0)} \partial_s\breve{b}_{i\alpha j\beta}\partial_\beta(\textstyle\int_0^s \tilde{\gamma}(\tau)d\tau)_j\partial_s^2(\int_0^s \tilde{\gamma}(\tau)d\tau)_i\ n_\alpha\ d\tilde{\Gamma}\ ds.
\end{aligned} \tag{3.107}$$

Then, combining Relation (3.105) with (3.106) and using (3.107) yield

$$
\begin{aligned}
&\frac{1}{2}\int_0^t\int_{\Omega_0^s}\partial_s\Big(\breve{b}_{i\alpha j\beta}\partial^2_{s\beta}(\textstyle\int_0^s\tilde{\gamma}(\tau)d\tau)_j\partial^2_{s\alpha}(\int_0^s\tilde{\gamma}(\tau)d\tau)_i\Big)\,d\tilde{\boldsymbol{x}}\,ds\\
&-\frac{1}{2}\int_0^t\int_{\Omega_0^s}\partial_s\breve{b}_{i\alpha j\beta}\partial^2_{s\beta}(\textstyle\int_0^s\tilde{\gamma}(\tau)d\tau)_j\partial^2_{s\alpha}(\int_0^s\tilde{\gamma}(\tau)d\tau)_i\,d\tilde{\boldsymbol{x}}\,ds\\
&+\int_0^t\int_{\Omega_0^s}\partial_\alpha\breve{b}_{i\alpha j\beta}\partial^2_{s\beta}(\textstyle\int_0^s\tilde{\gamma}(\tau)d\tau)_j\;\partial^2_{s}(\int_0^s\tilde{\gamma}(\tau)d\tau)_i\,d\tilde{\boldsymbol{x}}ds\\
&-\int_0^t\int_{\Omega_0^s}\partial_s\breve{b}_{i\alpha j\beta}\partial^2_{\alpha\beta}(\textstyle\int_0^s\tilde{\gamma}(\tau)d\tau)_j\partial^2_{s}(\int_0^s\tilde{\gamma}(\tau)d\tau)_i\,d\tilde{\boldsymbol{x}}\,ds\\
&+\int_0^t\int_{\Gamma_c(0)}\partial_s\breve{b}_{i\alpha j\beta}\partial_{\beta}(\textstyle\int_0^s\tilde{\gamma}(\tau)d\tau)_j\partial^2_{s}(\int_0^s\tilde{\gamma}(\tau)d\tau)_i\;n_\alpha\;d\tilde{\Gamma}\;ds.
\end{aligned}
$$

Therefore (3.104) is rewritten as

$$
\begin{cases}
\dfrac{\rho_f}{2}\displaystyle\int_{\Omega_0^f}\det(\boldsymbol{\nabla}\breve{\boldsymbol{\mathcal{A}}})(t)|\partial_t\tilde{\boldsymbol{\gamma}}(t)|^2\;d\tilde{\boldsymbol{x}}+\int_0^t\int_{\Omega_0^f}\partial_s\breve{\boldsymbol{\sigma}}^0_f(\tilde{\boldsymbol{\gamma}}):\partial_s\boldsymbol{\nabla}\tilde{\boldsymbol{\gamma}}\;d\tilde{\boldsymbol{x}}\;ds\\
+\dfrac{\rho_s}{2}\displaystyle\int_{\Omega_0^s}\det(\boldsymbol{\nabla}\breve{\boldsymbol{\varphi}})(t)|\partial_t\tilde{\boldsymbol{\gamma}}(t)|^2\;d\tilde{\boldsymbol{x}}+\frac{\rho_f}{2}\int_0^t\int_{\Omega_0^f}\partial_s\det(\boldsymbol{\nabla}\breve{\boldsymbol{\mathcal{A}}})|\partial_s\tilde{\boldsymbol{\gamma}}|^2\;d\tilde{\boldsymbol{x}}\;ds\\
+\dfrac{\rho_s}{2}\displaystyle\int_0^t\int_{\Omega_0^s}\partial_s\det(\boldsymbol{\nabla}\breve{\boldsymbol{\varphi}})|\partial_s\tilde{\boldsymbol{\gamma}}|^2\;d\tilde{\boldsymbol{x}}\;ds+\frac{1}{2}\sum_{i,\alpha,j,\beta=1}^{3}\int_{\Omega_0^s}\Big[\breve{b}_{i\alpha j\beta}\partial_\beta\tilde{\gamma}_j\partial_\alpha\tilde{\gamma}_i\Big](t)\;d\tilde{\boldsymbol{x}}\\
-\dfrac{1}{2}\displaystyle\sum_{i,\alpha,j,\beta=1}^{3}\int_0^t\int_{\Omega_0^s}\partial_s\breve{b}_{i\alpha j\beta}\partial^2_{s\beta}(\textstyle\int_0^s\tilde{\gamma}(\tau)d\tau)_j\;\partial^2_{s\alpha}(\int_0^s\tilde{\gamma}(\tau)d\tau)_i\;d\tilde{\boldsymbol{x}}\;ds\\
+\displaystyle\sum_{i,\alpha,j,\beta=1}^{3}\int_0^t\int_{\Omega_0^s}\partial_\alpha\breve{b}_{i\alpha j\beta}\partial^2_{s\beta}(\textstyle\int_0^s\tilde{\gamma}(\tau)d\tau)_j\;\partial^2_{s}(\int_0^s\tilde{\gamma}(\tau)d\tau)_i\;d\tilde{\boldsymbol{x}}\;ds\\
-\displaystyle\sum_{i,\alpha,j,\beta=1}^{3}\int_0^t\int_{\Omega_0^s}\partial_s\breve{b}_{i\alpha j\beta}\partial^2_{\alpha\beta}(\textstyle\int_0^s\tilde{\gamma}(\tau)d\tau)_j\;\partial^2_{s}(\int_0^s\tilde{\gamma}(\tau)d\tau)_i\;d\tilde{\boldsymbol{x}}\;ds\\
=\displaystyle\int_0^t\int_{\Gamma_c(0)}\partial_s\hat{\boldsymbol{h}}\cdot\partial^2_s(\textstyle\int_0^s\tilde{\boldsymbol{\gamma}}(\tau)d\tau)\;d\tilde{\Gamma}\;ds+\displaystyle\int_{\Omega_0^s}\Big[\mu_s|\boldsymbol{\epsilon}(\tilde{\boldsymbol{\gamma}}(0))|^2+\frac{\lambda_s}{2}|\nabla\cdot(\tilde{\boldsymbol{\gamma}}(0))|^2\Big](t)\;d\tilde{\boldsymbol{x}}\\
+\displaystyle\sum_{i,\alpha,j,\beta=1}^{3}\int_0^t\int_{\Gamma_c(0)}\partial_s\breve{b}_{i\alpha j\beta}\partial_{\beta}(\textstyle\int_0^s\tilde{\gamma}(\tau)d\tau)_j\partial^2_{s}(\int_0^s\tilde{\gamma}(\tau)d\tau)_i\;n_\alpha\;d\tilde{\Gamma}\;ds\\
+\dfrac{\rho_f}{2}\displaystyle\int_{\Omega_0^f}|\partial_t\tilde{\boldsymbol{\gamma}}(0)|^2\;d\tilde{\boldsymbol{x}}+\frac{\rho_s}{2}\int_{\Omega_0^s}|\partial_t\tilde{\boldsymbol{\gamma}}(0)|^2\;d\tilde{\boldsymbol{x}}.
\end{cases}
\tag{3.108}
$$

As for the stress term in (3.108) we have

$$
\begin{aligned}
&\int_0^t \int_{\Omega_0^f} \partial_s \breve{\boldsymbol{\sigma}}_f^0(\tilde{\gamma}) : \partial_s \boldsymbol{\nabla}\tilde{\gamma}\; d\tilde{\boldsymbol{x}}\; ds \\
&\qquad =\mu \int_0^t \int_{\Omega_0^f} \Big(\partial_s \boldsymbol{\nabla}\tilde{\gamma}(\boldsymbol{\nabla}\breve{\boldsymbol{\mathcal{A}}})^{-1} + (\boldsymbol{\nabla}\breve{\boldsymbol{\mathcal{A}}})^{-t}\partial_s(\boldsymbol{\nabla}\tilde{\gamma})^t\Big)\mathrm{cof}(\boldsymbol{\nabla}\breve{\boldsymbol{\mathcal{A}}}) : \partial_s \boldsymbol{\nabla}\tilde{\gamma}\; d\tilde{\boldsymbol{x}}\; ds \\
&\qquad\quad + \mu \int_0^t \int_{\Omega_0^f} \Big(\boldsymbol{\nabla}\tilde{\gamma}\partial_s(\boldsymbol{\nabla}\breve{\boldsymbol{\mathcal{A}}})^{-1} + \partial_s(\boldsymbol{\nabla}\breve{\boldsymbol{\mathcal{A}}})^{-t}(\boldsymbol{\nabla}\tilde{\gamma})^t\Big)\mathrm{cof}(\boldsymbol{\nabla}\breve{\boldsymbol{\mathcal{A}}}) : \partial_s \boldsymbol{\nabla}\tilde{\gamma}\; d\tilde{\boldsymbol{x}}\; ds \\
&\qquad\quad + \mu \int_0^t \int_{\Omega_0^f} \Big(\boldsymbol{\nabla}\tilde{\gamma}(\boldsymbol{\nabla}\breve{\boldsymbol{\mathcal{A}}})^{-1} + \boldsymbol{\nabla}\tilde{\gamma}(\boldsymbol{\nabla}\breve{\boldsymbol{\mathcal{A}}})^{-1}\Big)\partial_s\mathrm{cof}(\boldsymbol{\nabla}\breve{\boldsymbol{\mathcal{A}}}) : \partial_s \boldsymbol{\nabla}\tilde{\gamma}\; d\tilde{\boldsymbol{x}}\; ds \\
&\qquad =\frac{\mu}{2} \int_0^t \int_{\Omega_0^f} \det(\boldsymbol{\nabla}\breve{\boldsymbol{\mathcal{A}}})\Big|\partial_s \boldsymbol{\nabla}\tilde{\gamma}(\boldsymbol{\nabla}\breve{\boldsymbol{\mathcal{A}}})^{-1} + (\boldsymbol{\nabla}\breve{\boldsymbol{\mathcal{A}}})^{-t}\partial_s(\boldsymbol{\nabla}\tilde{\gamma})^t\Big|^2\; d\tilde{\boldsymbol{x}}\; ds \\
&\qquad\quad + \mu \int_0^t \int_{\Omega_0^f} \Big(\boldsymbol{\nabla}\tilde{\gamma}\partial_s(\boldsymbol{\nabla}\breve{\boldsymbol{\mathcal{A}}})^{-1} + \partial_s(\boldsymbol{\nabla}\breve{\boldsymbol{\mathcal{A}}})^{-t}(\boldsymbol{\nabla}\tilde{\gamma})^t\Big)\mathrm{cof}(\boldsymbol{\nabla}\breve{\boldsymbol{\mathcal{A}}}) : \partial_s \boldsymbol{\nabla}\tilde{\gamma}\; d\tilde{\boldsymbol{x}}\; ds \\
&\qquad\quad + \mu \int_0^t \int_{\Omega_0^f} \Big(\boldsymbol{\nabla}\tilde{\gamma}(\boldsymbol{\nabla}\breve{\boldsymbol{\mathcal{A}}})^{-1} + (\boldsymbol{\nabla}\breve{\boldsymbol{\mathcal{A}}})^{-t}(\boldsymbol{\nabla}\tilde{\gamma})^t\Big)\partial_s\mathrm{cof}(\boldsymbol{\nabla}\breve{\boldsymbol{\mathcal{A}}}) : \partial_s \boldsymbol{\nabla}\tilde{\gamma}\; d\tilde{\boldsymbol{x}}\; ds \\
&\qquad\quad = A_1 + A_2 + A_3.
\end{aligned} \tag{3.109}
$$

Where we have used the fact that

$$
\begin{aligned}
&\mu\Big(\partial_s \boldsymbol{\nabla}\tilde{\gamma}(\boldsymbol{\nabla}\breve{\boldsymbol{\mathcal{A}}})^{-1} + (\boldsymbol{\nabla}\breve{\boldsymbol{\mathcal{A}}})^{-t}\partial_s(\boldsymbol{\nabla}\tilde{\gamma})^t\Big)\mathrm{cof}(\boldsymbol{\nabla}\breve{\boldsymbol{\mathcal{A}}}) : \partial_s \boldsymbol{\nabla}\tilde{\gamma} \\
&=\mu\; \det(\boldsymbol{\nabla}\breve{\boldsymbol{\mathcal{A}}})\Big(\partial_s \boldsymbol{\nabla}\tilde{\gamma}(\boldsymbol{\nabla}\breve{\boldsymbol{\mathcal{A}}})^{-1} + (\boldsymbol{\nabla}\breve{\boldsymbol{\mathcal{A}}})^{-t}\partial_s(\boldsymbol{\nabla}\tilde{\gamma})^t\Big) : \partial_s \boldsymbol{\nabla}\tilde{\gamma}(\boldsymbol{\nabla}\breve{\boldsymbol{\mathcal{A}}})^{-1} \\
&=\frac{\mu}{2}\det(\boldsymbol{\nabla}\breve{\boldsymbol{\mathcal{A}}})\Big|\partial_s \boldsymbol{\nabla}\tilde{\gamma}(\boldsymbol{\nabla}\breve{\boldsymbol{\mathcal{A}}})^{-1} + (\boldsymbol{\nabla}\breve{\boldsymbol{\mathcal{A}}})^{-t}\partial_s(\boldsymbol{\nabla}\tilde{\gamma})^t\Big|^2
\end{aligned}
$$

and

$$
(\boldsymbol{A} + \boldsymbol{A}^t) : (\boldsymbol{B} + \boldsymbol{B}^t) = 2(\boldsymbol{A} + \boldsymbol{A}^t) : \boldsymbol{B}, \qquad \forall\; \boldsymbol{A}, \boldsymbol{B} \in \mathbb{M}_n(\mathbb{R}), n \in \mathbb{N}^*.
$$

For A_1 we argue as in (3.72) to get

$$
\begin{aligned}
A_1 &\geq \mu \int_0^t \Big[||\boldsymbol{\epsilon}(\partial_s \tilde{\boldsymbol{\gamma}}_n)||^2_{L^2(\Omega_0^f)}(s) - CT^\kappa M||\partial_s \tilde{\boldsymbol{\gamma}}_n||^2_{H^1(\Omega_0^f)}(s)\Big]\; ds \\
&\geq \mu(C_k - CT^\kappa M)||\tilde{\boldsymbol{\gamma}}_n||^2_{H^1(H^1(\Omega_0^s))}.
\end{aligned} \tag{3.110}
$$

For A_2 we use Young's inequality with Hölder's inequality to obtain

$$\begin{aligned}
|A_2| &\leq \int_0^t \Big|\Big|\Big(\nabla\tilde{\gamma}\partial_s(\nabla\breve{\mathcal{A}})^{-1} + \partial_s(\nabla\breve{\mathcal{A}})^{-t}(\nabla\tilde{\gamma})^t\Big)\mathrm{cof}(\nabla\breve{\mathcal{A}})\Big|\Big|_{L^2(\Omega_0^f)} ||\partial_s\nabla\tilde{\gamma}||_{L^2(\Omega_0^f)}\ ds \\
&\leq \int_0^t 2||\nabla\tilde{\gamma}\partial_s(\nabla\breve{\mathcal{A}})^{-1}||_{L^2(\Omega_0^f)}||\mathrm{cof}(\nabla\breve{\mathcal{A}})||_{L^\infty(\Omega_0^f)}||\partial_s\nabla\tilde{\gamma}||_{L^2(\Omega_0^f)}\ ds \\
&\leq \int_0^t 2||\nabla\tilde{\gamma}||_{L^2(\Omega_0^f)}||\partial_s(\nabla\breve{\mathcal{A}})^{-1}||_{L^\infty(\Omega_0^f)}||\mathrm{cof}(\nabla\breve{\mathcal{A}})||_{L^\infty(\Omega_0^f)}||\partial_s\nabla\tilde{\gamma}||_{L^2(\Omega_0^f)}\ ds \\
&\leq C||\mathrm{cof}(\nabla\breve{\mathcal{A}})||_{L^\infty(L^\infty(\Omega_0^f))}||\nabla\tilde{\gamma}||_{L^\infty(L^2(\Omega_0^f))}\int_0^t ||\partial_s(\nabla\breve{\mathcal{A}})^{-1}||_{L^\infty(\Omega_0^f)}||\partial_s\nabla\tilde{\gamma}||_{L^2(\Omega_0^f)}\ ds \\
&\leq C||\mathrm{cof}(\nabla\breve{\mathcal{A}})||_{L^\infty(L^\infty(\Omega_0^f))}||\tilde{\gamma}||_{L^\infty(H^1)}||\partial_s(\nabla\breve{\mathcal{A}})^{-1}||_{L^\infty(L^2(\Omega_0^f))}||\partial_s\nabla\tilde{\gamma}||_{L^1(L^2(\Omega_0^f))}\ ds \\
&\leq CT^{1/2}M||\tilde{\gamma}||_{L^\infty(H^1(\Omega_0^f))}||\tilde{\gamma}||_{H^1(H^1(\Omega_0^f))} \\
&\leq CT^{1/2}M\Big[C_\delta||\tilde{\gamma}||^2_{L^\infty(H^2(\Omega_0^f))}+\delta||\tilde{\gamma}||^2_{H^1(H^1(\Omega_0^f))}\Big].
\end{aligned} \tag{3.111}$$

Similarly, for A_3 we have

$$\begin{aligned}
|A_3| &\leq \int_0^t \Big|\Big|\Big(\nabla\tilde{\gamma}(\nabla\breve{\mathcal{A}})^{-1} + (\nabla\breve{\mathcal{A}})^{-t}(\nabla\tilde{\gamma})^t\Big)\partial_s\mathrm{cof}(\nabla\breve{\mathcal{A}})\Big|\Big|_{L^2(\Omega_0^f)} ||\partial_s\nabla\tilde{\gamma}||_{L^2(\Omega_0^f)}\ ds \\
&\leq 2\int_0^t ||\nabla\tilde{\gamma}(\nabla\breve{\mathcal{A}})^{-1}||_{L^2(\Omega_0^f)}||\partial_s\mathrm{cof}(\nabla\breve{\mathcal{A}})||_{L^\infty(\Omega_0^f)}||\partial_s\nabla\tilde{\gamma}||_{L^2(\Omega_0^f)}\ ds \\
&\leq 2||(\nabla\breve{\mathcal{A}})^{-1}||_{L^\infty(L^\infty(\Omega_0^f))}\int_0^t ||\nabla\tilde{\gamma}||_{L^2(\Omega_0^f)}||\partial_s\mathrm{cof}(\nabla\breve{\mathcal{A}})||_{L^\infty(\Omega_0^f)}||\partial_s\nabla\tilde{\gamma}||_{L^2(\Omega_0^f)}\ ds \\
&\leq ||(\nabla\breve{\mathcal{A}})^{-1}||_{L^\infty(L^\infty(\Omega_0^f))}\int_0^t ||\tilde{\gamma}||_{H^2(\Omega_0^f)}||\partial_s\mathrm{cof}(\nabla\breve{\mathcal{A}})||_{L^\infty(\Omega_0^f)}||\partial_s\tilde{\gamma}||_{H^1(\Omega_0^f)}\ ds \\
&\leq CT^{1/2}||\gamma||_{L^\infty(H^2(\Omega_0^f))}||\partial_s\mathrm{cof}(\nabla\breve{\mathcal{A}})||_{L^\infty(L^\infty(\Omega_0^f))}||\partial_s\tilde{\gamma}||_{L^2(H^1(\Omega_0^f))} \\
&\leq CT^{1/2}M||\tilde{\gamma}||_{L^\infty(H^2)}||\tilde{\gamma}||_{H^1(H^1(\Omega_0^f))} \\
&\leq CT^{1/2}M\Big[C_\delta||\tilde{\gamma}||^2_{L^\infty(H^2(\Omega_0^f))}+\delta||\tilde{\gamma}||^2_{H^1(H^1(\Omega_0^f))}\Big].
\end{aligned} \tag{3.112}$$

Therefore, the summation of Equations (3.111) and (3.112) is bounded above by

$$CT^{1/2}M\Big[C_\delta||\tilde{\gamma}||^2_{L^\infty(H^2)}+\delta||\tilde{\gamma}||^2_{H^1(H^1(\Omega_0^f))}\Big]. \tag{3.113}$$

As for the integrals over Ω_0^s, first we have

$$\begin{aligned}
\frac{\rho_s}{2}\int_{\Omega_0^s}\det(\nabla\breve{\varphi})(t)|\partial_t\tilde{\gamma}(t)|^2\ d\tilde{\boldsymbol{x}} + \frac{\rho_s}{2}\int_0^t\int_{\Omega_0^s}\partial_s\det(\nabla\breve{\varphi})|\partial_s\tilde{\gamma}|^2\ d\tilde{\boldsymbol{x}}\ ds \\
\geq \frac{\rho_s}{2}(1-CT^\kappa M)||\partial_t\tilde{\gamma}||^2_{L^\infty(L^2(\Omega_0^s))}.
\end{aligned} \tag{3.114}$$

On the contrary, using (3.38) and (3.40) with Korn's inequality gives

$$\begin{aligned}
&\frac{1}{2}\sum_{i,\alpha,j,\beta=1}^{3}\int_{\Omega_0^s}\Big[\breve{b}_{i\alpha j\beta}\partial_\beta\gamma_j\partial_\alpha\gamma_i\Big](t)\ d\tilde{\boldsymbol{x}} \\
&\qquad \geq \mu_s\int_{\Omega_0^s}|\boldsymbol{\epsilon}(\tilde{\boldsymbol{\gamma}})|^2(t)\ dX+\frac{\mathsf{C}+\lambda_s}{2}\int_{\Omega_0^s}|\nabla\cdot\tilde{\boldsymbol{\gamma}}|^2(t)\ dX-CT^\kappa M||\tilde{\boldsymbol{\gamma}}||^2_{L^\infty(H^1)} \\
&\qquad \geq \mu_s C_k||\tilde{\boldsymbol{\gamma}}(t)||^2_{H^1}+\frac{\mathsf{C}+\lambda_s}{2}||\nabla\cdot\tilde{\boldsymbol{\gamma}}(t)||^2_{L^2}-CT^\kappa M||\tilde{\boldsymbol{\gamma}}||_{L^\infty(H^1)} \\
&\qquad \geq \mu_s C_k||\tilde{\boldsymbol{\gamma}}||^2_{L^\infty(H^1(\Omega_0^s))}+\frac{\mathsf{C}+\lambda_s}{2}||\nabla\cdot\tilde{\boldsymbol{\gamma}}||^2_{L^\infty(L^2(\Omega_0^s))}-CT^\kappa M||\tilde{\boldsymbol{\gamma}}||^2_{L^\infty(H^1(\Omega_0^s))}.
\end{aligned}\tag{3.115}$$

On the other hand, using (3.37) and (3.39), for $i,\alpha,j,\beta=1,2,3$, we have

$$\begin{aligned}
&\left|\frac{1}{2}\int_0^t\int_{\Omega_0^s}\partial_s\breve{b}_{i\alpha j\beta}\partial^2_{s\beta}(\textstyle\int_0^s\tilde{\gamma}(\tau)d\tau)_j\partial^2_{s\alpha}(\int_0^s\tilde{\gamma}(\tau)d\tau)_i\ d\tilde{\boldsymbol{x}}\ ds\right| \\
&= \left|\frac{1}{2}\int_0^t\int_{\Omega_0^s}\partial_s\breve{b}_{i\alpha j\beta}\partial_\beta\tilde{\gamma}_j\partial_\alpha\tilde{\gamma}_i\ d\tilde{\boldsymbol{x}}\ ds\right| \\
&\leq \int_0^t||\partial_s\breve{b}_{i\alpha j\beta}(s)||_{L^\infty(\Omega_0^s)}||\boldsymbol{\nabla}\tilde{\boldsymbol{\gamma}}(s)||^2_{L^2(\Omega_0^s)}\ ds \\
&\leq \int_0^t||\partial_s\breve{b}_{i\alpha j\beta}(s)||_{H^2(\Omega_0^s)}||\tilde{\boldsymbol{\gamma}}(s)||^2_{H^1(\Omega_0^s)}\ ds \\
&\leq CT||\partial_t\breve{b}_{i\alpha j\beta}||_{L^\infty(H^2(\Omega_0^s))}||\tilde{\boldsymbol{\gamma}}||^2_{L^\infty(H^1(\Omega_0^s))} \\
&\leq CT(M+M^2+M^3+M^4)||\tilde{\boldsymbol{\gamma}}||^2_{L^\infty(H^2(\Omega_0^s))} \\
&\leq CT^\kappa M||\tilde{\boldsymbol{\gamma}}||^2_{L^\infty(H^2(\Omega_0^s))}.
\end{aligned}\tag{3.116}$$

Similarly, for $i,\alpha,j,\beta=1,2,3$, we use (3.37) and (3.39) in addition to Young's inequality to get

$$\begin{aligned}
&\left|\int_0^t\int_{\Omega_0^s}\partial_\alpha\breve{b}_{i\alpha j\beta}\partial^2_{s\beta}(\textstyle\int_0^s\tilde{\gamma}(\tau)d\tau)_j\partial^2_{s}(\int_0^s\tilde{\gamma}(\tau)d\tau)_i\ d\tilde{\boldsymbol{x}}\ ds\right| \\
&\qquad = \left|\int_0^t\int_{\Omega_0^s}\partial_\alpha\breve{b}_{i\alpha j\beta}\partial_\beta\tilde{\gamma}_j\partial_s\tilde{\gamma}_i\ d\tilde{\boldsymbol{x}}\ ds\right| \\
&\qquad \leq \int_0^t||\partial_\alpha\breve{b}_{i\alpha j\beta}(s)||_{L^\infty(\Omega_0^s)}||\boldsymbol{\nabla}\tilde{\boldsymbol{\gamma}}(s)||_{L^2(\Omega_0^s)}||\partial_s\tilde{\boldsymbol{\gamma}}(s)||_{L^2(\Omega_0^s)}\ ds \\
&\qquad \leq ||\partial_\alpha\breve{b}_{i\alpha j\beta}||_{L^\infty(H^2(\Omega_0^s))}\int_0^t\Big[C_\delta||\tilde{\boldsymbol{\gamma}}(s)||^2_{H^1(\Omega_0^s)}+\delta||\partial_s\tilde{\boldsymbol{\gamma}}(s)||^2_{L^2(\Omega_0^s)}\ \Big]ds \\
&\qquad \leq CT(M+M^2+M^3+M^4)\Big[C_\delta||\tilde{\boldsymbol{\gamma}}||^2_{L^\infty(H^1(\Omega_0^s))}+\delta||\partial_t\tilde{\boldsymbol{\gamma}}||^2_{L^\infty(L^2(\Omega_0^s))}\Big] \\
&\qquad \leq CT^\kappa M\Big[C_\delta||\tilde{\boldsymbol{\gamma}}||^2_{L^\infty(H^1(\Omega_0^s))}+\delta||\partial_t\tilde{\boldsymbol{\gamma}}||^2_{L^\infty(L^2(\Omega_0^s))}\Big].
\end{aligned}\tag{3.117}$$

Further, for $i, \alpha, j, \beta = 1, 2, 3,$

$$\begin{aligned}
&\left| -\int_0^t \int_{\Omega_0^s} \partial_s \breve{b}_{i\alpha j\beta} \partial^2_{\alpha\beta} (\textstyle\int_0^s \tilde{\gamma}(\tau) d\tau)_j \partial^2_s (\int_0^s \tilde{\gamma}(\tau) d\tau)_i \ d\tilde{\boldsymbol{x}} \ ds \right| \\
&\qquad = \left| \int_0^t \int_{\Omega_0^s} \partial_s \breve{b}_{i\alpha j\beta} \partial^2_{\alpha\beta} (\textstyle\int_0^s \tilde{\gamma}(\tau) d\tau)_j \partial_s \tilde{\gamma}_i \ d\tilde{\boldsymbol{x}} \ ds \right| \\
&\qquad \leq \int_0^t ||\partial_s \breve{b}_{i\alpha j\beta}(s)||_{L^\infty(\Omega_0^s)} ||\boldsymbol{\nabla}^2 \textstyle\int_0^s \tilde{\boldsymbol{\gamma}}(\tau) d\tau||_{L^2(\Omega_0^s)} ||\partial_s \tilde{\boldsymbol{\gamma}}(s)||_{L^2(\Omega_0^s)} \ ds \\
&\qquad \leq ||\partial_s \breve{b}_{i\alpha j\beta}||_{L^\infty(H^2(\Omega_0^s))} \int_0^t \Big[C_\delta ||\textstyle\int_0^s \tilde{\boldsymbol{\gamma}}(\tau) d\tau||^2_{H^2(\Omega_0^s)} + \delta ||\partial_s \tilde{\boldsymbol{\gamma}}(s)||^2_{L^2(\Omega_0^s(0))} \Big] \ ds \\
&\qquad \leq CT^\kappa M \Big[C_\delta ||\textstyle\int_0^\bullet \tilde{\boldsymbol{\gamma}}(s) ds||^2_{L^\infty(H^2(\Omega_0^s))} + \delta ||\partial_t \tilde{\boldsymbol{\gamma}}||^2_{L^\infty(L^2(\Omega_0^s))} \Big] \ ds.
\end{aligned}$$

Therefore, combining (3.116)-(3.118) and taking summation over $i, \alpha, j, \beta = 1, 2, 3$ give

$$\begin{aligned}
&\Bigg| \sum_{i,\alpha,j,\beta=1}^{3} \Bigg[-\frac{1}{2} \int_0^t \int_{\Omega_0^s} \partial_s \breve{b}_{i\alpha j\beta} \partial^2_{s\beta} (\textstyle\int_0^s \tilde{\gamma}(\tau) d\tau)_j \ \partial^2_{s\alpha} (\int_0^s \tilde{\gamma}(\tau) d\tau)_i \ d\tilde{\boldsymbol{x}} \ ds \\
&\qquad + \int_0^t \int_{\Omega_0^s} \partial_\alpha \breve{b}_{i\alpha j\beta} \partial^2_{s\beta} (\textstyle\int_0^s \tilde{\gamma}(\tau) d\tau)_j \ \partial^2_{s} (\int_0^s \tilde{\gamma}(\tau) d\tau)_i \ d\tilde{\boldsymbol{x}} \ ds \\
&\qquad - \int_0^t \int_{\Omega_0^s} \partial_s \breve{b}_{i\alpha j\beta} \partial^2_{\alpha\beta} (\textstyle\int_0^s \tilde{\gamma}(\tau) d\tau)_j \ \partial^2_{s} (\int_0^s \tilde{\gamma}(\tau) d\tau)_i \ d\tilde{\boldsymbol{x}} \ ds \Bigg] \Bigg| \\
&\quad \leq CT(M + M^2 + M^3 + M^4) \Big[C_\delta ||\textstyle\int_0^\bullet \tilde{\boldsymbol{\gamma}}(s) ds||^2_{L^\infty(H^2(\Omega_0^s))} + \delta ||\partial_t \tilde{\boldsymbol{\gamma}}||^2_{L^\infty(L^2(\Omega_0^s))} + ||\tilde{\boldsymbol{\gamma}}||^2_{L^\infty(H^1(\Omega_0^s))} \Big] \\
&\quad \leq CT^\kappa M \Big[C_\delta ||\textstyle\int_0^\bullet \tilde{\boldsymbol{\gamma}}(s) ds||^2_{L^\infty(H^2(\Omega_0^s))} + \delta ||\partial_t \tilde{\boldsymbol{\gamma}}||^2_{L^\infty(L^2(\Omega_0^s))} + ||\tilde{\boldsymbol{\gamma}}||^2_{L^\infty(H^1(\Omega_0^s))} \Big].
\end{aligned}$$

For the integrals across the boundary we use (3.101),Young's inequality in addition to the trace inequality to obtain

$$\begin{aligned}
\left| \int_0^t \int_{\Gamma_c(0)} \partial_s \hat{\boldsymbol{h}} \cdot \partial_s \tilde{\boldsymbol{\gamma}} \ d\tilde{\Gamma} \ ds \right| &\leq \int_0^t ||\partial_s \hat{\boldsymbol{h}}(s)||_{L^2(\Gamma_c(0))} ||\partial_s \tilde{\boldsymbol{\gamma}}(s)||_{L^2(\Gamma_c(0))} \ ds \\
&\leq CT^\kappa M ||\hat{\boldsymbol{\xi}}||_{S_2^T} ||\tilde{\boldsymbol{\gamma}}||_{H^1(H^1(\Omega_0^f))} \\
&\leq CT^\kappa M \big[C_\delta ||\hat{\boldsymbol{\xi}}||^2_{S_2^T} + \delta ||\tilde{\boldsymbol{\gamma}}||^2_{H^1(H^1(\Omega_0^f))} \big],
\end{aligned} \tag{3.118}$$

and for $i, \alpha, j, \beta = 1, 2, 3$, we have

$$\begin{aligned}
&\left| \int_0^t \int_{\Gamma_c(0)} \partial_s \breve{b}_{i\alpha j\beta} \partial_\beta (\textstyle\int_0^s \tilde{\gamma}(\tau) d\tau)_j \partial_s \tilde{\gamma}_i \; n_\alpha \; d\tilde{\Gamma} \; ds \right| \\
&\leq \int_0^t ||\partial_s \breve{b}_{i\alpha j\beta}||_{L^\infty(\Omega_0^s)} ||\boldsymbol{\nabla} \textstyle\int_0^s \tilde{\boldsymbol{\gamma}}(\tau) d\tau||_{L^2(\Gamma_c(0))} ||\partial_s \tilde{\boldsymbol{\gamma}}(s)||_{L^2(\Gamma_c(0))} ds \\
&\leq C ||\partial_t \breve{b}_{i\alpha j\beta}||_{L^\infty(H^2(\Omega_0^s))} \int_0^t ||\boldsymbol{\nabla} \textstyle\int_0^s \tilde{\boldsymbol{\gamma}}(\tau) d\tau||_{H^1(\Omega_0^s)} ||\partial_s \tilde{\boldsymbol{\gamma}}(s)||_{H^1(\Omega_0^f)} \; ds \\
&\leq C T^{1/2} (M + M^2 + M^3 + M^4) \; ||\textstyle\int_0^\bullet \tilde{\boldsymbol{\gamma}}(s) ds \; ||_{L^\infty(H^2(\Omega_0^s))} ||\tilde{\boldsymbol{\gamma}}||_{H^1(H^1(\Omega_0^f))} \\
&\leq C T^{1/2} (M + M^2 + M^3 + M^4) \Big[C_\delta ||\textstyle\int_0^\bullet \tilde{\boldsymbol{\gamma}}(s) ds||^2_{L^\infty(H^2(\Omega_0^s))} + \delta ||\tilde{\boldsymbol{\gamma}}||^2_{H^1(H^1(\Omega_0^f))} \Big].
\end{aligned} \tag{3.119}$$

Therefore, considering the restriction of $\tilde{\boldsymbol{\gamma}}$ on each sub-domain, and for T small with respect to M and the initial conditions, i.e, the factors $CT^\kappa M$ and $CT^{1/2}M^4$ are negligible, and using (3.102) we get

$$\begin{aligned}
&||\tilde{\boldsymbol{v}}||^2_{W^{1,\infty}(L^2)} + ||\tilde{\boldsymbol{v}}||^2_{H^1(H^1)} + ||\tilde{\boldsymbol{\xi}}||^2_{W^{2,\infty}(L^2)} + ||\tilde{\boldsymbol{\xi}}||^2_{W^{1,\infty}(H^1)} \\
&\leq C ||\boldsymbol{v}_0||^2_{H^1} + C ||\boldsymbol{\xi}_1||^2_{H^1} + C T^\kappa M \big(||\tilde{\boldsymbol{\xi}}||^2_{S_2^T} + ||\hat{\boldsymbol{\xi}}||^2_{S_2^T} \big).
\end{aligned} \tag{3.120}$$

3.4.2 Estimates Using Spatial Regularity

We have proved that the linear system has a strong solution $(\tilde{\boldsymbol{v}}, \tilde{\boldsymbol{\xi}}) \in F_2^T \times S_2^T$. Therefore, for all $t \in (0, T)$, the fluid velocity $\tilde{\boldsymbol{v}}$ satisfies the following equation

$$\boldsymbol{\nabla} \cdot \breve{\boldsymbol{\sigma}}_f^0(\tilde{\boldsymbol{v}}) = \rho_f \det(\boldsymbol{\nabla} \breve{\boldsymbol{\mathcal{A}}}) \partial_t \tilde{\boldsymbol{v}} \qquad \text{in} \quad \Omega_0^f,$$

which can be rewritten as

$$\mu \boldsymbol{\nabla} \cdot \big(\boldsymbol{\nabla} \tilde{\boldsymbol{v}} + (\boldsymbol{\nabla} \tilde{\boldsymbol{v}})^t \big) = \rho_f \det(\boldsymbol{\nabla} \breve{\boldsymbol{\mathcal{A}}}) \partial_t \tilde{\boldsymbol{v}} + F_{\tilde{v}} \qquad \text{in} \quad \Omega_0^f,$$

with

$$F_{\tilde{v}} = -\mu \nabla \cdot \boldsymbol{f}_{\tilde{\boldsymbol{v}}},$$

where

$$\boldsymbol{f}_{\tilde{\boldsymbol{v}}} = \Big(\boldsymbol{\nabla} \tilde{\boldsymbol{v}} \big((\boldsymbol{\nabla} \breve{\boldsymbol{\mathcal{A}}})^{-1} - \mathbf{Id} \big) + \big((\boldsymbol{\nabla} \breve{\boldsymbol{\mathcal{A}}})^{-t} - \mathbf{Id} \big) \boldsymbol{\nabla} \tilde{\boldsymbol{v}} \big)^t \Big) \mathrm{cof}(\boldsymbol{\nabla} \breve{\boldsymbol{\mathcal{A}}}) - \big(\boldsymbol{\nabla} \tilde{\boldsymbol{v}} + (\boldsymbol{\nabla} \tilde{\boldsymbol{v}})^t \big) \big(\mathrm{cof}(\boldsymbol{\nabla} \breve{\boldsymbol{\mathcal{A}}}) - \mathbf{Id} \big).$$

Using Lemma 3.2.2 we have

$$||F_{\tilde{v}}||_{L^\infty(L^2)} \leq ||\boldsymbol{f}_{\tilde{\boldsymbol{v}}}||_{L^\infty(H^1)} \leq 2\mu C T^\kappa M ||\tilde{\boldsymbol{v}}||_{L^\infty(H^2)}.$$

Hence, we obtain

$$\mu ||\tilde{\boldsymbol{v}}||_{L^\infty(H^2)} \leq \rho_f C T^\kappa M ||\partial_t \tilde{\boldsymbol{v}}||_{L^\infty(L^2)} + 2\mu C T^\kappa M ||\tilde{\boldsymbol{v}}||_{L^\infty(H^2)}. \tag{3.121}$$

Besides, the structure displacement $\tilde{\boldsymbol{\xi}}$ satisfies the following equation

$$-\boldsymbol{\nabla}\cdot\Big(2\mu_s\boldsymbol{\epsilon}(\tilde{\boldsymbol{\xi}})+\lambda_s(\nabla\cdot\tilde{\boldsymbol{\xi}})\mathbf{Id}\Big)=-\rho_s\det(\boldsymbol{\nabla}\breve{\boldsymbol{\varphi}})\partial_t^2\tilde{\boldsymbol{\xi}}+\boldsymbol{H}^{\boldsymbol{c}}_{\tilde{\boldsymbol{\xi}}}+\boldsymbol{H}^{\boldsymbol{d}}_{\tilde{\boldsymbol{\xi}}}, \tag{3.122}$$

with

$$H^c_{\tilde{\xi},i}=\sum_{\alpha,j,\beta=1}^{3}\big(\breve{c}^l_{i\alpha j\beta}+\breve{c}^q_{i\alpha j\beta}\big)\partial^2_{\alpha\beta}\tilde{\xi}_j,\quad \text{for } i=1,2,3,$$

and

$$H^d_{\tilde{\xi},i}=\mathsf{C}\sum_{\alpha,j,\beta=1}^{3}\big(\breve{d}^L_{i\alpha j\beta}+\breve{d}^Q_{i\alpha j\beta}+\breve{d}^T_{i\alpha j\beta}+\breve{d}^F_{i\alpha j\beta}\big)\partial^2_{\alpha\beta}\tilde{\xi}_j,\quad \text{for } i=1,2,3.$$

Using elliptic estimates and thanks to (3.37) we get

$$||\tilde{\boldsymbol{\xi}}||_{L^\infty(H^2)}\leq \rho_s CTM||\partial_t^2\tilde{\boldsymbol{\xi}}||_{L^\infty(L^2)}+CT(M+M^2+M^3+M^4)||\tilde{\boldsymbol{\xi}}||_{L^\infty(H^2)}. \tag{3.123}$$

To bound $||\partial_t\tilde{\boldsymbol{v}}||_{L^\infty(L^2(\Omega_0^f))}$ and $||\partial_t^2\tilde{\boldsymbol{\xi}}||_{L^\infty(L^2(\Omega_0^s))}$ we use (3.120). Finally, taking T small with respect to M and the initial conditions in (3.121) and (3.123), then combining them with (3.120), we achieve the following estimate

$$||\tilde{\boldsymbol{v}}||^2_{F_2^T}+||\tilde{\boldsymbol{\xi}}||^2_{S_2^T}\leq CT^\kappa M||\hat{\boldsymbol{\xi}}||^2_{S_2^T}+C||\boldsymbol{v}_0||^2_{H^1}+C||\boldsymbol{\xi}_1||^2_{H^1}. \tag{3.124}$$

3.4.3 Fixed Point Theorem for the Linearized System

Based on the estimate (3.124) on the solution $(\tilde{\boldsymbol{v}},\tilde{\boldsymbol{\xi}})$ of the linear system (3.99), we proceed to prove that the function Ψ_0 is a contraction on S_2^T. Let $\hat{\boldsymbol{\xi}}_1,\hat{\boldsymbol{\xi}}_2\in S_2^T$. For $a=1,2$, we denote by $(\tilde{\boldsymbol{v}}_a,\tilde{\boldsymbol{\xi}}_a)$ the solution of (3.57) with

$$g_i=\hat{h}_i^a=-\sum_{\alpha,j,\beta=1}^{3}\Big(\int_0^t\partial_s\breve{b}_{i\alpha j\beta}\partial_\beta(\hat{\xi}_a)_j\,ds\Big)\tilde{n}_\alpha,\quad i=1,2,3.$$

Since $(\tilde{\boldsymbol{v}}_1,\tilde{\boldsymbol{\xi}}_1)$ and $(\tilde{\boldsymbol{v}}_2,\tilde{\boldsymbol{\xi}}_2)$ satisfy System (3.57), then we can say that $(\tilde{\boldsymbol{v}}_1-\tilde{\boldsymbol{v}}_2,\tilde{\boldsymbol{\xi}}_1-\tilde{\boldsymbol{\xi}}_2)$ satisfies System (3.57) with $g_i=\hat{h}_i^1-\hat{h}_i^2$ and null initial data. Hence, applying (3.124) to $(\tilde{\boldsymbol{v}}_1-\tilde{\boldsymbol{v}}_2,\tilde{\boldsymbol{\xi}}_1-\tilde{\boldsymbol{\xi}}_2)$ and noticing that the right hand side of the estimate contains only a norm on S_2^T given by $||\hat{\boldsymbol{\xi}}_1-\hat{\boldsymbol{\xi}}_2||_{S_2^T}$ added to some constants, consequently we get

$$||\tilde{\boldsymbol{\xi}}_1-\tilde{\boldsymbol{\xi}}_2||_{S_2^T}=||\Psi_0(\hat{\boldsymbol{\xi}}_{\mathbf{1}})-\Psi_0(\hat{\boldsymbol{\xi}}_{\mathbf{2}})||_{S_2^T}\leq CT^\kappa M||\hat{\boldsymbol{\xi}}_{\mathbf{1}}-\hat{\boldsymbol{\xi}}_{\mathbf{2}}||_{S_2^T}. \tag{3.125}$$

Taking T small enough with respect to M, gives that Ψ_0 is a contraction on S_2^T. Therefore, we assure the existence and uniqueness of a fixed point $\tilde{\boldsymbol{\xi}}\in S_2^T$. Consequently, we obtain the existence and uniqueness of a solution $(\tilde{\boldsymbol{v}},\tilde{\boldsymbol{\xi}})\in F_2^T\times S_2^T$ for the system (3.99). Finally, with the assumption of T being small with respect to M and denoting $C||\boldsymbol{v}_0||^2_{H^1}+C||\boldsymbol{\xi}_1||^2_{H^1}$ by $\boldsymbol{C}_0$ we obtain

$$||\tilde{\boldsymbol{v}}||^2_{F_2^T}+||\tilde{\boldsymbol{\xi}}||^2_{S_2^T}\leq \boldsymbol{C}_0. \tag{3.126}$$

3.5 Regularity of Solution of the Linearized System

3.5.1 Regularity of the solution

Proposition 3.5.1 *Let $(\breve{\boldsymbol{v}}, \breve{\boldsymbol{\xi}}) \in A_M^T$, with the assumption that $\boldsymbol{v}_0 \in H^6(\Omega_0^f)$ and $\boldsymbol{\xi}_1 \in H^3(\Omega_0^s)$ and satisfies (3.30). For T small with respect to M and the initial conditions, the solution $(\tilde{\boldsymbol{v}}, \tilde{\boldsymbol{\xi}})$ is in the space $F_4^T \times S_4^T$. Further, it satisfies*

$$||\tilde{\boldsymbol{v}}||_{F_4^T} + ||\tilde{\boldsymbol{\xi}}||_{S_4^T} \leq \boldsymbol{C}_0, \tag{3.127}$$

where $\boldsymbol{C}_0$ denotes a constant in the norms $||\boldsymbol{v}_0||_{H^6(\Omega_0^f)}$ and $||\boldsymbol{\xi}_1||_{H^3(\Omega_0^s)}$.

By Proposition 3.4.1, we have proved the existence and uniqueness of $(\tilde{\boldsymbol{v}}, \tilde{\boldsymbol{\xi}}) \in F_2^T \times S_2^T$. Increasing the regularity of the initial conditions results a more regular solution [Eva98, Bre10]. The regularity of the solution in case of a linear FSI problem where the structure is considered to be quasi-incompressible have been proved in [CS05]. Hence $(\tilde{\boldsymbol{v}}, \tilde{\boldsymbol{\xi}})$ belongs to $F_4^T \times S_4^T$.

Next, we proceed to derive a priori estimates on the solution $(\tilde{\boldsymbol{v}}, \tilde{\boldsymbol{\xi}})$ in $F_4^T \times S_4^T$.

3.5.2 A Priori estimates on $\tilde{\gamma}$ in A_M^T

A Priori Estimates Using Time Regularity

The solution $\tilde{\boldsymbol{\gamma}}$ satisfies the following variational formulation

$$\begin{cases} \rho_f \displaystyle\int_{\Omega_0^f} \det(\boldsymbol{\nabla}\breve{\boldsymbol{\mathcal{A}}})\partial_t\tilde{\boldsymbol{\gamma}} \cdot \tilde{\boldsymbol{\eta}}\ d\tilde{\boldsymbol{x}} + \rho_s \int_{\Omega_0^s} \det(\boldsymbol{\nabla}\breve{\boldsymbol{\varphi}})\partial_t\tilde{\boldsymbol{\gamma}} \cdot \tilde{\boldsymbol{\eta}}\ d\tilde{\boldsymbol{x}} + \int_{\Omega_0^f} \breve{\boldsymbol{\sigma}}_f^0(\tilde{\boldsymbol{\gamma}}) : \boldsymbol{\nabla}\tilde{\boldsymbol{\eta}}\ d\tilde{\boldsymbol{x}} \\ + \displaystyle\sum_{i,\alpha,j,\beta=1}^{3} \int_{\Omega_0^s} \breve{b}_{i\alpha j\beta}\partial_\beta(\textstyle\int_0^t \tilde{\gamma}(s)ds)_j\ \partial_\alpha\tilde{\eta}_i\ d\tilde{\boldsymbol{x}} + \displaystyle\sum_{i,\alpha,j,\beta=1}^{3} \int_{\Omega_0^s} \partial_\alpha\breve{b}_{i\alpha j\beta}\partial_\beta(\textstyle\int_0^t \tilde{\gamma}(s)ds)_j\ \tilde{\eta}_i\ d\tilde{\boldsymbol{x}} \\ = \displaystyle\int_{\Gamma_c(0)} \boldsymbol{g} \cdot \tilde{\boldsymbol{\eta}}\ d\tilde{\Gamma}, \qquad \forall\ \tilde{\boldsymbol{\eta}} \in \widetilde{\mathcal{W}}, \end{cases} \tag{3.128}$$

with

$$g_i = -\sum_{\alpha,j,\beta=1}^{3} \left(\int_0^t \partial_s\breve{b}_{i\alpha j\beta}\partial_\beta\tilde{\xi}_j\ ds \right)\tilde{n}_\alpha, \qquad i = 1, 2, 3.$$

Differentiating three times with respect to time and taking $\tilde{\boldsymbol{\eta}} = \partial_t^3\tilde{\boldsymbol{\gamma}}$ yield

$$\begin{cases} \rho_f \displaystyle\int_{\Omega_0^f} \det(\boldsymbol{\nabla}\breve{\boldsymbol{\mathcal{A}}})\partial_t^4\tilde{\boldsymbol{\gamma}} \cdot \partial_t^3\tilde{\boldsymbol{\gamma}}\ d\tilde{\boldsymbol{x}} + C_1 + \rho_s \int_{\Omega_0^s} \det(\boldsymbol{\nabla}\breve{\boldsymbol{\varphi}})\partial_t^4\tilde{\boldsymbol{\gamma}} \cdot \partial_t^3\tilde{\boldsymbol{\gamma}}\ d\tilde{\boldsymbol{x}} + C_2 \\ +\mu \displaystyle\int_{\Omega_0^f} \partial_t^3\Big(\boldsymbol{\nabla}\tilde{\gamma}(\boldsymbol{\nabla}\breve{\boldsymbol{\mathcal{A}}})^{-1} + (\boldsymbol{\nabla}\breve{\boldsymbol{\mathcal{A}}})^{-t}(\boldsymbol{\nabla}\tilde{\gamma})^t\Big)\mathrm{cof}(\boldsymbol{\nabla}\breve{\boldsymbol{\mathcal{A}}}) : \boldsymbol{\nabla}\partial_t^3\tilde{\boldsymbol{\gamma}}\ d\tilde{\boldsymbol{x}} + C_3 \\ + \displaystyle\sum_{i,\alpha,j,\beta=1}^{3} \int_{\Omega_0^s} \breve{b}_{i\alpha j\beta}\partial_\beta\partial_t^2\tilde{\gamma}_j\ \partial_\alpha\partial_t^3\tilde{\gamma}_i\ d\tilde{\boldsymbol{x}} + C_4 = \int_{\Gamma_c(0)} \partial_t^3\boldsymbol{g} \cdot \partial_t^3\tilde{\boldsymbol{\gamma}}\ d\tilde{\Gamma}, \end{cases} \tag{3.129}$$

where,

$$\begin{aligned}
C_1 =&3\rho_f \int_{\Omega_0^f} \partial_t \det(\boldsymbol{\nabla}\breve{\boldsymbol{\mathcal{A}}})\partial_t^3\tilde{\boldsymbol{\gamma}} \cdot \partial_t^3\tilde{\boldsymbol{\gamma}}\ d\tilde{\boldsymbol{x}} + 3\rho_f \int_{\Omega_0^f} \partial_t^2 \det(\boldsymbol{\nabla}\breve{\boldsymbol{\mathcal{A}}})\partial_t^2\tilde{\boldsymbol{\gamma}} \cdot \partial_t^3\tilde{\boldsymbol{\gamma}}\ d\tilde{\boldsymbol{x}} \\
&+ \rho_f \int_{\Omega_0^f} \partial_t^3 \det(\boldsymbol{\nabla}\breve{\boldsymbol{\mathcal{A}}})\partial_t\tilde{\boldsymbol{\gamma}} \cdot \partial_t^3\tilde{\boldsymbol{\gamma}}\ d\tilde{\boldsymbol{x}},
\end{aligned}$$

$$\begin{aligned}
C_2 =&3\rho_s \int_{\Omega_0^s} \partial_t \det(\boldsymbol{\nabla}\breve{\boldsymbol{\varphi}})\partial_t^3\tilde{\boldsymbol{\gamma}} \cdot \partial_t^3\tilde{\boldsymbol{\gamma}}\ d\tilde{\boldsymbol{x}} + 3\rho_s \int_{\Omega_0^s} \partial_t^2 \det(\boldsymbol{\nabla}\breve{\boldsymbol{\varphi}})\partial_t^2\tilde{\boldsymbol{\gamma}} \cdot \partial_t^3\tilde{\boldsymbol{\gamma}}\ d\tilde{\boldsymbol{x}} \\
&+ \rho_s \int_{\Omega_0^s} \partial_t^3 \det(\boldsymbol{\nabla}\breve{\boldsymbol{\varphi}})\partial_t\tilde{\boldsymbol{\gamma}} \cdot \partial_t^3\tilde{\boldsymbol{\gamma}}\ d\tilde{\boldsymbol{x}},
\end{aligned}$$

$$\begin{aligned}
C_3 =&3\mu \int_{\Omega_0^f} \partial_t^2 \Big(\boldsymbol{\nabla}\tilde{\boldsymbol{\gamma}}(\boldsymbol{\nabla}\breve{\boldsymbol{\mathcal{A}}})^{-1} + (\boldsymbol{\nabla}\breve{\boldsymbol{\mathcal{A}}})^{-t}(\boldsymbol{\nabla}\tilde{\boldsymbol{\gamma}})^t\Big)\partial_t \mathrm{cof}(\boldsymbol{\nabla}\breve{\boldsymbol{\mathcal{A}}}) : \boldsymbol{\nabla}\partial_t^3\tilde{\boldsymbol{\gamma}}\ d\tilde{\boldsymbol{x}} \\
&+ 3\mu \int_{\Omega_0^f} \partial_t \Big(\boldsymbol{\nabla}\tilde{\boldsymbol{\gamma}}(\boldsymbol{\nabla}\breve{\boldsymbol{\mathcal{A}}})^{-1} + (\boldsymbol{\nabla}\breve{\boldsymbol{\mathcal{A}}})^{-t}(\boldsymbol{\nabla}\tilde{\boldsymbol{\gamma}})^t\Big)\partial_t^2 \mathrm{cof}(\boldsymbol{\nabla}\breve{\boldsymbol{\mathcal{A}}}) : \boldsymbol{\nabla}\partial_t^3\tilde{\boldsymbol{\gamma}}\ d\tilde{\boldsymbol{x}} \\
&+ \mu \int_{\Omega_0^f} \Big(\boldsymbol{\nabla}\tilde{\boldsymbol{\gamma}}(\boldsymbol{\nabla}\breve{\boldsymbol{\mathcal{A}}})^{-1} + (\boldsymbol{\nabla}\breve{\boldsymbol{\mathcal{A}}})^{-t}(\boldsymbol{\nabla}\tilde{\boldsymbol{\gamma}})^t\Big)\partial_t^3 \mathrm{cof}(\boldsymbol{\nabla}\breve{\boldsymbol{\mathcal{A}}}) : \boldsymbol{\nabla}\partial_t^3\tilde{\boldsymbol{\gamma}}\ d\tilde{\boldsymbol{x}},
\end{aligned}$$

and

$$\begin{aligned}
C_4 =& \sum_{i,\alpha,j,\beta=1}^{3} \int_{\Omega_0^s} \partial_t^3 \breve{b}_{i\alpha j\beta}\partial_\beta (\textstyle\int_0^t \tilde{\gamma}(s)ds)_j\ \partial_\alpha \partial_t^3 \tilde{\gamma}_i\ d\tilde{\boldsymbol{x}} + 3\displaystyle\sum_{i,\alpha,j,\beta=1}^{3} \int_{\Omega_0^s} \partial_t^2 \breve{b}_{i\alpha j\beta}\partial_\beta\tilde{\gamma}_j\ \partial_\alpha \partial_t^3 \tilde{\gamma}_i\ d\tilde{\boldsymbol{x}} \\
&+ 3\sum_{i,\alpha,j,\beta=1}^{3} \int_{\Omega_0^s} \partial_t \breve{b}_{i\alpha j\beta}\partial_\beta\partial_t\tilde{\gamma}_j\ \partial_\alpha \partial_t^3 \tilde{\gamma}_i\ d\tilde{\boldsymbol{x}} + \sum_{i,\alpha,j,\beta=1}^{3} \int_{\Omega_0^s} \partial_t\Big(\partial_\alpha \breve{b}_{i\alpha j\beta}\partial_\beta (\textstyle\int_0^t \tilde{\gamma}(s)ds)_j\Big)\ \partial_t^3 \tilde{\gamma}_i\ d\tilde{\boldsymbol{x}}.
\end{aligned}$$

First we have,

$$\begin{aligned}
\rho_f \int_0^t \int_{\Omega_0^f} \det(\boldsymbol{\nabla}\breve{\boldsymbol{\mathcal{A}}})\partial_s^4\tilde{\boldsymbol{\gamma}} \cdot \partial_s^3\tilde{\boldsymbol{\gamma}}\ d\tilde{\boldsymbol{x}}\ ds =&\frac{\rho_f}{2}\int_{\Omega_0^f} \det(\boldsymbol{\nabla}\breve{\boldsymbol{\mathcal{A}}})|\partial_t^3\tilde{\boldsymbol{\gamma}}(t)|^2\ d\tilde{\boldsymbol{x}} - \frac{\rho_f}{2}\int_{\Omega_0^f} |\partial_t^3\tilde{\boldsymbol{\gamma}}(0)|^2\ d\tilde{\boldsymbol{x}} \\
&+ \frac{\rho_f}{2}\int_0^t \int_{\Omega_0^f} \partial_s \det(\boldsymbol{\nabla}\breve{\boldsymbol{\mathcal{A}}})|\partial_s^3\tilde{\boldsymbol{\gamma}}|^2\ d\tilde{\boldsymbol{x}}\ ds.
\end{aligned}$$

Thus proceeding as in (3.71) we get

$$\rho_f \int_0^t \int_{\Omega_0^f} \det(\boldsymbol{\nabla}\breve{\boldsymbol{\mathcal{A}}})\partial_s^4\tilde{\boldsymbol{\gamma}} \cdot \partial_s^3\tilde{\boldsymbol{\gamma}}\ d\tilde{\boldsymbol{x}}\ ds \geq \frac{\rho_f}{2}(1 - CT^\kappa M)||\partial_t^3\tilde{\boldsymbol{\gamma}}||^2_{L^\infty(L^2(\Omega_0^f))} - ||\boldsymbol{v}_0||^2_{H^6}. \tag{3.130}$$

For the fluid stress term we proceed as in (3.109) to get

$$\begin{aligned}
&\mu \int_0^t \int_{\Omega_0^f} \partial_s^3 \Big(\boldsymbol{\nabla}\tilde{\boldsymbol{\gamma}}(\boldsymbol{\nabla}\breve{\boldsymbol{\mathcal{A}}})^{-1} + (\boldsymbol{\nabla}\breve{\boldsymbol{\mathcal{A}}})^{-t}(\boldsymbol{\nabla}\tilde{\boldsymbol{\gamma}})^t\Big)\mathrm{cof}(\boldsymbol{\nabla}\breve{\boldsymbol{\mathcal{A}}}) : \boldsymbol{\nabla}\partial_s^3\tilde{\boldsymbol{\gamma}}\ d\tilde{\boldsymbol{x}}\ ds \\
=&\frac{\mu}{2}\int_0^t \int_{\Omega_0^f} \Big|\partial_s^3 \boldsymbol{\nabla}\tilde{\boldsymbol{\gamma}}(\boldsymbol{\nabla}\breve{\boldsymbol{\mathcal{A}}})^{-1} + (\boldsymbol{\nabla}\breve{\boldsymbol{\mathcal{A}}})^{-t}\partial_s^3(\boldsymbol{\nabla}\tilde{\boldsymbol{\gamma}})^t\Big|^2\ d\tilde{\boldsymbol{x}}\ ds \\
&+ \mu \int_0^t \int_{\Omega_0^f} \Big(\boldsymbol{\nabla}\tilde{\boldsymbol{\gamma}}\partial_s^3(\boldsymbol{\nabla}\breve{\boldsymbol{\mathcal{A}}})^{-1} + \partial_s^3(\boldsymbol{\nabla}\breve{\boldsymbol{\mathcal{A}}})^{-t}(\boldsymbol{\nabla}\tilde{\boldsymbol{\gamma}})^t\Big)\mathrm{cof}(\boldsymbol{\nabla}\breve{\boldsymbol{\mathcal{A}}}) : \boldsymbol{\nabla}\partial_s^3\tilde{\boldsymbol{\gamma}}\ d\tilde{\boldsymbol{x}}\ ds.
\end{aligned}$$

Then, using Korn's inequality we can estimate the right hand side by

$$\mu(C_k - CT^\kappa M)||\partial_t^3\tilde{\boldsymbol{\gamma}}||_{L^2(H^1(\Omega_0^f))}. \tag{3.131}$$

On the domain Ω_0^s, similarly as (3.130), we have

$$\rho_s\int_0^t\int_{\Omega_0^s}\det(\boldsymbol{\nabla}\breve{\boldsymbol{\varphi}})\partial_s^4\tilde{\boldsymbol{\gamma}}\cdot\partial_s^3\tilde{\boldsymbol{\gamma}}\;d\tilde{\boldsymbol{x}}\;ds \geq \frac{\rho_s}{2}(1-CT^\kappa M)||\partial_t^3\tilde{\boldsymbol{\gamma}}||^2_{L^\infty(L^2(\Omega_0^s))} - ||\boldsymbol{\xi}_1||^2_{H^3}. \tag{3.132}$$

In addition,

$$\begin{aligned}
&\sum_{i,\alpha,j,\beta=1}^{3}\int_0^t\int_{\Omega_0^s}\breve{b}_{i\alpha j\beta}\partial_\beta\partial_t^2\tilde{\gamma}_j\;\partial_\alpha\partial_t^3\tilde{\gamma}_i\;d\tilde{\boldsymbol{x}}\;ds\\
&\quad=\frac{1}{2}\sum_{i,\alpha,j,\beta=1}^{3}\int_{\Omega_0^s}\left[\breve{b}_{i\alpha j\beta}\partial_\beta\partial_t^2\tilde{\gamma}_j\partial_\alpha\partial_t^2\tilde{\gamma}_i\right](t)\;d\tilde{\boldsymbol{x}} - \frac{1}{2}\sum_{i,\alpha,j,\beta=1}^{3}\int_{\Omega_0^s}\left[\breve{b}_{i\alpha j\beta}\partial_\beta\partial_t^2\tilde{\gamma}_j\partial_\alpha\partial_t^2\tilde{\gamma}_i\right](0)\;d\tilde{\boldsymbol{x}}\\
&\qquad-\frac{1}{2}\sum_{i,\alpha,j,\beta=1}^{3}\int_0^t\int_{\Omega_0^s}\partial_s\breve{b}_{i\alpha j\beta}\partial_\beta\partial_s^2\tilde{\gamma}_j\;\partial_\alpha\partial_s^2\tilde{\gamma}_i\;d\tilde{\boldsymbol{x}}\;ds.
\end{aligned}$$

Whence, using (3.37)-(3.38) with Korn's inequality give

$$\sum_{i,\alpha,j,\beta=1}^{3}\int_0^t\int_{\Omega_0^s}\breve{b}_{i\alpha j\beta}\partial_\beta\partial_s^2\tilde{\gamma}_j\;\partial_\alpha\partial_s^3\tilde{\gamma}_i\;d\tilde{\boldsymbol{x}}\;ds \geq \mu_s C_k||\partial_t^2\tilde{\boldsymbol{\gamma}}||^2_{L^\infty(H^1(\Omega_0^s))} - CT^\kappa M||\textstyle\int_0^\bullet\tilde{\boldsymbol{\gamma}}(s)ds||^2_{S_4^T}. \tag{3.133}$$

Further, on the boundary $\Gamma_c(0)$ we have

$$\begin{aligned}
&\int_0^t\int_{\Gamma_c(0)}\partial_s^3\boldsymbol{g}\cdot\partial_s^3\tilde{\boldsymbol{\gamma}}\;d\tilde{\Gamma}\;ds = \sum_{i,\alpha,j,\beta=1}^{3}\int_0^t\int_{\Gamma_c(0)}\partial_s^3\breve{b}_{i\alpha j\beta}\partial_\beta(\textstyle\int_0^s\tilde{\gamma}(\tau)d\tau)_j\;\tilde{n}_\alpha\;\partial_s^3\tilde{\gamma}_i\;d\tilde{\Gamma}\;ds\\
&+2\sum_{i,\alpha,j,\beta=1}^{3}\int_0^t\int_{\Gamma_c(0)}\partial_s^2\breve{b}_{i\alpha j\beta}\partial_\beta\tilde{\gamma}_j\;\tilde{n}_\alpha\;\partial_s^3\tilde{\gamma}_i\;d\tilde{\Gamma}\;ds + \sum_{i,\alpha,j,\beta=1}^{3}\int_0^t\int_{\Gamma_c(0)}\partial_s\breve{b}_{i\alpha j\beta}\partial_\beta\partial_s\tilde{\gamma}_j\;\tilde{n}_\alpha\;\partial_s^3\tilde{\gamma}_i\;d\tilde{\Gamma}\;ds.
\end{aligned}$$

Proceeding as in (3.118) and (3.119) we get

$$\left|\int_0^t\int_{\Gamma_c(0)}\partial_s^3\boldsymbol{g}\cdot\partial_s^3\tilde{\boldsymbol{\gamma}}\;d\tilde{\Gamma}\;ds\right| \leq CT^\kappa M||\textstyle\int_0^\bullet\tilde{\boldsymbol{\gamma}}(s)ds||_{S_4^T}||\tilde{\boldsymbol{\gamma}}||_{F_4^T}. \tag{3.134}$$

On the other hand, to deal with C_1, C_2, C_3 and C_4 we use the following bounds

$$||\partial_t^k\det(\boldsymbol{\nabla}\breve{\boldsymbol{\mathcal{A}}})||_{L^\infty(L^\infty(\Omega_0^f))} \leq CM^k, \qquad k=1,2,3. \tag{3.135}$$

$$||\partial_t^k\det(\boldsymbol{\nabla}\breve{\boldsymbol{\varphi}})||_{L^\infty(L^\infty(\Omega_0^s))} \leq CM^k, \qquad k=1,2,3. \tag{3.136}$$

$$||\partial_t^k(\boldsymbol{\nabla}\breve{\boldsymbol{\mathcal{A}}})^{-t}||_{L^\infty(L^\infty(\Omega_0^f))} \leq CM^k, \qquad k=1,2,3. \tag{3.137}$$

$$||\partial_t^k\mathrm{cof}(\boldsymbol{\nabla}\breve{\boldsymbol{\mathcal{A}}})||_{L^\infty(L^\infty(\Omega_0^f))} \leq CM^k, \qquad k=1,2,3. \tag{3.138}$$

Then,

$$\int_0^t C_1 \, ds \leq CT^\kappa M ||\tilde{\gamma}||^2_{F_4^T}. \tag{3.139}$$

Similarly

$$\int_0^t C_2 \, ds \leq CT^\kappa M ||\tilde{\gamma}||^2_{F_4^T}. \tag{3.140}$$

On the other hand,

$$\int_0^t C_3 \, ds \leq CT^\kappa M ||\textstyle\int_0^\cdot \tilde{\gamma}(s) ds||^2_{S_4^T} \tag{3.141}$$

and

$$\int_0^t C_4 \, ds \leq CT^\kappa M ||\textstyle\int_0^\cdot \tilde{\gamma}(s) ds||^2_{S_4^T}. \tag{3.142}$$

Combining (3.130)-(3.134) with (3.139)-(3.142) and considering the restriction of $\tilde{\gamma}$ on each sub-domain give

$$\begin{aligned} &||\partial_t^3 \tilde{\boldsymbol{v}}||^2_{L^\infty(L^2(\Omega_0^f))} + ||\partial_t^2 \tilde{\boldsymbol{v}}||^2_{L^2(H^1(\Omega_0^f))} + ||\partial_t^3 \tilde{\boldsymbol{\xi}}||^2_{L^\infty(H^1(\Omega_0^s))} + ||\partial_t^4 \tilde{\boldsymbol{\xi}}||^2_{L^\infty(L^2(\Omega_0^s))} \\ &\leq CT^\kappa M (||\tilde{\boldsymbol{v}}||^2_{F_4^T} + ||\tilde{\boldsymbol{\xi}}||^2_{S_4^T}) + C(||\boldsymbol{\xi}_1||^2_{H^3} + ||\boldsymbol{v}_0||^2_{H^6}). \end{aligned} \tag{3.143}$$

This estimate together with (3.126) lead to the following estimate

$$\begin{aligned} &||\tilde{\boldsymbol{v}}||^2_{W^{3,\infty}(L^2(\Omega_0^f))} + ||\tilde{\boldsymbol{v}}||^2_{W^{2,\infty}(H^1(\Omega_0^f))} + ||\tilde{\boldsymbol{v}}||^2_{H^3(H^1(\Omega_0^s))} + ||\tilde{\boldsymbol{\xi}}||^2_{W^{3,\infty}(H^1(\Omega_0^s))} + ||\tilde{\boldsymbol{\xi}}||^2_{W^{4,\infty}(L^2(\Omega_0^s))} \\ &\leq CT^\kappa M (||\tilde{\boldsymbol{v}}||^2_{F_4^T} + ||\tilde{\boldsymbol{\xi}}||^2_{S_4^T}) + C(||\boldsymbol{\xi}_1||^2_{H^3} + ||\boldsymbol{v}_0||^2_{H^6}). \end{aligned} \tag{3.144}$$

Spatial Regularity

- **Step 1:** Estimates on $\tilde{\boldsymbol{v}}$ in $W^{2,\infty}(H^2(\Omega_0^f))$ and $\tilde{\boldsymbol{\xi}}$ in $W^{2,\infty}(H^2(\Omega_0^s))$.

The fluid velocity $\tilde{\boldsymbol{v}}$ satisfies the elliptic equation

$$\mu \boldsymbol{\nabla} \cdot \big(\boldsymbol{\nabla} \tilde{\boldsymbol{v}} + (\boldsymbol{\nabla} \tilde{\boldsymbol{v}})^t\big) = \rho_f \det(\boldsymbol{\nabla} \breve{\boldsymbol{\mathcal{A}}}) \partial_t \tilde{\boldsymbol{v}} + F_{\tilde{v}} \qquad \text{in} \quad \Omega_0^f, \tag{3.145}$$

with

$$F_{\tilde{v}} = -\mu \nabla \cdot \boldsymbol{f}_{\tilde{\boldsymbol{v}}},$$

where

$$\boldsymbol{f}_{\tilde{\boldsymbol{v}}} = \Big(\boldsymbol{\nabla} \tilde{\boldsymbol{v}} \big((\boldsymbol{\nabla} \breve{\boldsymbol{\mathcal{A}}})^{-1} - \mathbf{Id}\big) + \big((\boldsymbol{\nabla} \breve{\boldsymbol{\mathcal{A}}})^{-t} - \mathbf{Id}\big) \boldsymbol{\nabla} \tilde{\boldsymbol{v}})^t\Big) \mathrm{cof}(\boldsymbol{\nabla} \breve{\boldsymbol{\mathcal{A}}}) - \big(\boldsymbol{\nabla} \tilde{\boldsymbol{v}} + (\boldsymbol{\nabla} \tilde{\boldsymbol{v}})^t\big) \big(\mathrm{cof}(\boldsymbol{\nabla} \breve{\boldsymbol{\mathcal{A}}}) - \mathbf{Id}\big).$$

as defined in Subsection 3.4.2. First we have

$$||\partial_t^2 \big(\det(\boldsymbol{\nabla} \breve{\boldsymbol{\mathcal{A}}}) \partial_t \tilde{\boldsymbol{v}}\big)||_{L^\infty(L^2)} \leq CM^2 ||\tilde{\boldsymbol{v}}||_{W^{3,\infty}(L^2)} \leq C||\boldsymbol{v}_0||_{H^6} + C||\boldsymbol{\xi}_1||_{H^3} + CT^\kappa M (||\tilde{\boldsymbol{v}}||_{F_4^T} + ||\tilde{\boldsymbol{\xi}}||_{S_4^T}).$$

First, let us estimate $F_{\tilde{v}}$ in $W^{2,\infty}(L^2)$. In fact differentiating $f_{\tilde{\boldsymbol{v}}}$ two times in time gives

$$\begin{aligned}&\Big[\big(\partial_t^2\boldsymbol{\nabla}\tilde{\boldsymbol{v}}\big)\big((\boldsymbol{\nabla}\breve{\boldsymbol{\mathcal{A}}})^{-1}-\mathbf{Id}\big)+2(\partial_t\boldsymbol{\nabla}\tilde{\boldsymbol{v}})\big(\partial_t(\boldsymbol{\nabla}\breve{\boldsymbol{\mathcal{A}}})^{-1}\big)+(\boldsymbol{\nabla}\tilde{\boldsymbol{v}})\big(\partial_t^2(\boldsymbol{\nabla}\breve{\boldsymbol{\mathcal{A}}})^{-1}\big)\Big]\mathrm{cof}(\boldsymbol{\nabla}\breve{\boldsymbol{\mathcal{A}}})\\&+\Big(\partial_t\boldsymbol{\nabla}\tilde{\boldsymbol{v}})\big((\boldsymbol{\nabla}\breve{\boldsymbol{\mathcal{A}}})^{-1}-\mathbf{Id}\big)+(\boldsymbol{\nabla}\tilde{\boldsymbol{v}})\big(\partial_t(\boldsymbol{\nabla}\breve{\boldsymbol{\mathcal{A}}})^{-1}\big)\Big]\big(\partial_t\mathrm{cof}(\boldsymbol{\nabla}\breve{\boldsymbol{\mathcal{A}}})\big)\\&+(\boldsymbol{\nabla}\tilde{\boldsymbol{v}})\big((\boldsymbol{\nabla}\breve{\boldsymbol{\mathcal{A}}})^{-1}-\mathbf{Id}\big)\big(\partial_t^2\mathrm{cof}(\boldsymbol{\nabla}\breve{\boldsymbol{\mathcal{A}}})\big).\end{aligned}$$

Using (3.135) with the embedding of H^2 in L^∞ and taking into consideration that

$$||\tilde{\boldsymbol{v}}||_{L^\infty(H^1)}\leq C||\boldsymbol{v}_0||_{H^6}+T||\tilde{\boldsymbol{v}}||_{H^3(H^1)}$$

yield

$$||F_{\tilde{v}}||_{W^{2,\infty}(L^2)}\leq CT^\kappa M||\tilde{\boldsymbol{v}}||_{W^{2,\infty}(H^1)}+C||\boldsymbol{v}_0||_{H^6}. \tag{3.146}$$

Therefore, using (3.144) and the elliptic estimates on $\tilde{\boldsymbol{v}}$ we obtain

$$||\tilde{\boldsymbol{v}}||_{W^{2,\infty}(H^2)}\leq C||\boldsymbol{v}_0||_{H^6}+C||\boldsymbol{\xi}_1||_{H^3}+CT^\kappa M(||\tilde{\boldsymbol{v}}||_{F_4^T}+||\tilde{\boldsymbol{\xi}}||_{S_4^T}). \tag{3.147}$$

On the other hand, the structure displacement $\tilde{\boldsymbol{\xi}}$ satisfies (3.122). Differentiating two times in time yield

$$-\partial_t^2\Big[\boldsymbol{\nabla}\cdot\Big(2\mu_s\boldsymbol{\epsilon}(\tilde{\boldsymbol{\xi}})+\lambda_s(\nabla\cdot\tilde{\boldsymbol{\xi}})\ \mathbf{Id}\Big)\Big]=-\rho_s\partial_t^2\Big(\det(\boldsymbol{\nabla}\breve{\boldsymbol{\varphi}})\partial_t^2\tilde{\boldsymbol{\xi}}\Big)+\partial_t^2\boldsymbol{H}^{\boldsymbol{c}}_{\tilde{\boldsymbol{\xi}}}+\partial_t^2\boldsymbol{H}^{\boldsymbol{d}}_{\tilde{\boldsymbol{\xi}}},$$

with

$$H^c_{\tilde{\xi},i}=\sum_{\alpha,j,\beta=1}^{3}\big(\breve{c}^l_{i\alpha j\beta}+\breve{c}^q_{i\alpha j\beta}\big)\partial^2_{\alpha\beta}\tilde{\xi}_j,\quad\text{for } i=1,2,3,$$

and

$$H^d_{\tilde{\xi},i}=\mathsf{C}\sum_{\alpha,j,\beta=1}^{3}\big(\breve{d}^L_{i\alpha j\beta}+\breve{d}^Q_{i\alpha j\beta}+\breve{d}^T_{i\alpha j\beta}+\breve{d}^F_{i\alpha j\beta}\big)\partial^2_{\alpha\beta}\tilde{\xi}_j,\quad\text{for } i=1,2,3.$$

First, we have

$$||\det(\boldsymbol{\nabla}\breve{\boldsymbol{\varphi}})\partial_t^2\tilde{\boldsymbol{\xi}}||_{W^{2,\infty}(L^2(\Omega_0^s))}\leq C||\tilde{\boldsymbol{\xi}}||_{W^{4,\infty}(L^2)}.$$

Then using (3.144) we get

$$||\det(\boldsymbol{\nabla}\breve{\boldsymbol{\varphi}})\partial_t^2\tilde{\boldsymbol{\xi}}||_{W^{2,\infty}(L^2(\Omega_0^s))}\leq C||\boldsymbol{v}_0||_{H^6}+C||\boldsymbol{\xi}_1||_{H^3}+CT^\kappa M(||\tilde{\boldsymbol{v}}||_{F_4^T}+||\tilde{\boldsymbol{\xi}}||_{S_4^T}). \tag{3.148}$$

Further, for $\partial_t^2\boldsymbol{H}^{\boldsymbol{c}}_{\tilde{\boldsymbol{\xi}}}$ we have

$$\partial_t^2\boldsymbol{H}^{\boldsymbol{c}}_{\tilde{\boldsymbol{\xi}}}(\tilde{\boldsymbol{x}},t)=\partial_t^2\boldsymbol{H}^{\boldsymbol{c}}_{\tilde{\boldsymbol{\xi}}}(\tilde{\boldsymbol{x}},0)+\int_0^t\partial_s^3\boldsymbol{H}^{\boldsymbol{c}}_{\tilde{\boldsymbol{\xi}}}(\tilde{\boldsymbol{x}},s)\ ds\qquad\forall\ \tilde{\boldsymbol{x}}\in\Omega_0^s. \tag{3.149}$$

Simple calculation of $\partial_t^2 \boldsymbol{H}^{\boldsymbol{c}}_{\tilde{\boldsymbol{\xi}}}(\tilde{\boldsymbol{x}}, s)$ then setting $t=0$ and using the fact that $\partial_t \breve{c}^l_{i\alpha j\beta}(\tilde{\boldsymbol{x}}, 0)$ is a function of $\boldsymbol{\xi}_1$ give $||\partial_t^3 \boldsymbol{H}^{\boldsymbol{c}}_{\tilde{\boldsymbol{\xi}}}(\tilde{\boldsymbol{x}}, s)||_{L^\infty(L^2(\Omega_0^s))} \leq C||\boldsymbol{\xi}_1||_{H^3}$. Moreover,

$$\int_0^t \partial_s^3 \boldsymbol{H}^{\boldsymbol{c}}_{\tilde{\boldsymbol{\xi}}}(\tilde{\boldsymbol{x}}, s)\ ds = \sum_{i,\alpha,j,\beta=1}^{3} \Bigg[\int_0^t \partial_s^3 \big(\breve{c}^l_{i\alpha j\beta} + \breve{c}^q_{i\alpha j\beta}\big) \partial^2_{\alpha\beta} \tilde{\xi}_j\ ds + 3\int_0^t \partial_s \big(\breve{c}^l_{i\alpha j\beta} + \breve{c}^q_{i\alpha j\beta}\big) \partial^2_{\alpha\beta} (\partial_s^2 \tilde{\xi}_j)\ ds$$
$$+ 3\int_0^t \partial_s^2 \big(\breve{c}^l_{i\alpha j\beta} + \breve{c}^q_{i\alpha j\beta}\big) \partial^2_{\alpha\beta} (\partial_s \tilde{\xi}_j)\ ds + \int_0^t \big(\breve{c}^l_{i\alpha j\beta} + \breve{c}^q_{i\alpha j\beta}\big) \partial^2_{\alpha\beta} (\partial_s^3 \tilde{\xi}_j)\ ds \Bigg].$$

Hence, integrating over Ω_0^s and using (3.37), we get that the first three terms of the right hand side can be estimated in $L^\infty(L^2(\Omega_0^s))$ by

$$CT^\kappa M||\tilde{\boldsymbol{\xi}}||_{S_4^T}.$$

On the contrary, integrating by parts in time in the last integral of the right hand side gives

$$\big(\breve{c}^l_{i\alpha j\beta} + \breve{c}^q_{i\alpha j\beta}\big) \partial^2_{\alpha\beta} (\partial_s^2 \tilde{\xi}_j)(t) - \big(\breve{c}^l_{i\alpha j\beta} + \breve{c}^q_{i\alpha j\beta}\big) \partial^2_{\alpha\beta} (\partial_s^2 \tilde{\xi}_j)(0) - \int_0^t \partial_s \big(\breve{c}^l_{i\alpha j\beta} + \breve{c}^q_{i\alpha j\beta}\big) \partial^2_{\alpha\beta} (\partial_s^2 \tilde{\xi}_j)\ ds \tag{3.150}$$

As $\breve{\boldsymbol{\xi}}(0) = 0$, then $\displaystyle\sum_{i,\alpha,j,\beta=1}^{3} \Big[\big(\breve{c}^l_{i\alpha j\beta} + \breve{c}^q_{i\alpha j\beta}\big) \partial^2_{\alpha\beta} (\partial_s^2 \tilde{\xi}_j) \Big](0) = 0$. In addition,

$$||\breve{c}^l_{i\alpha j\beta} + \breve{c}_{i\alpha j\beta}||_{L^\infty(L^2)} \leq T||\partial_t \breve{c}^l_{i\alpha j\beta} + \partial_t \breve{c}^q_{i\alpha j\beta}||_{L^\infty(L^2)} \leq CT^\kappa M.$$

Therefore,

$$(3.150) \leq CT^\kappa M||\tilde{\boldsymbol{\xi}}||_{S_4^T}.$$

Consequently,

$$||\partial_t^2 \boldsymbol{H}^{\boldsymbol{c}}_{\tilde{\boldsymbol{\xi}}}||_{L^\infty(L^2(\Omega_0^s))} \leq CT^\kappa M||\tilde{\boldsymbol{\xi}}||_{S_4^T}. \tag{3.151}$$

Similarly, one can show that

$$||\partial_t^2 \boldsymbol{H}^{\boldsymbol{d}}_{\tilde{\boldsymbol{\xi}}}||_{L^\infty(L^2(\Omega_0^s))} \leq CT^\kappa M||\tilde{\boldsymbol{\xi}}||_{S_4^T}. \tag{3.152}$$

As a result, combining (3.148), (3.151) and (3.152) an estimate on $\tilde{\boldsymbol{\xi}}$ in $W^{2,\infty}(L^2(\Omega_0^s))$ is given by

$$||\tilde{\boldsymbol{\xi}}||_{W^{2,\infty}(H^2(\Omega_0^s))} \leq C||\boldsymbol{v}_0||_{H^6} + C||\boldsymbol{\xi}_1||_{H^3} + CT^\kappa M(||\tilde{\boldsymbol{v}}||_{F_4^T} + ||\tilde{\boldsymbol{\xi}}||_{S_4^T}). \tag{3.153}$$

Finally, combining (3.147) and (3.153) we get

$$||\tilde{\boldsymbol{v}}||_{W^{2,\infty}(H^2(\Omega_0^f))} + ||\tilde{\boldsymbol{\xi}}||_{W^{2,\infty}(H^2(\Omega_0^s))} \leq C||\boldsymbol{v}_0||_{H^6} + C||\boldsymbol{\xi}_1||_{H^3} + CT^\kappa M(||\tilde{\boldsymbol{v}}||_{F_4^T} + ||\tilde{\boldsymbol{\xi}}||_{S_4^T}). \tag{3.154}$$

• **Step 2:** Estimates on $\tilde{\boldsymbol{v}}$ in $L^\infty(H^4(\Omega_0^f))$ and $\tilde{\boldsymbol{\xi}}$ in $L^\infty(H^4(\Omega_0^s))$.
Again, the fluid velocity satisfies (3.145). We estimate $F_{\tilde{v}}$ in $L^\infty(H^2(\Omega_0^f))$. First,

$$||F_{\tilde{v}}||_{L^\infty(H^2(\Omega_0^f))} \leq \mu ||\boldsymbol{f}_{\tilde{\boldsymbol{v}}}||_{L^\infty(H^3(\Omega_0^f))}.$$

But

$$\begin{aligned}
||\boldsymbol{f}_{\tilde{\boldsymbol{v}}}||_{L^\infty(H^3)} \leq & 2||\boldsymbol{\nabla}\breve{\boldsymbol{v}}||_{L^\infty(H^3)}||(\boldsymbol{\nabla}\breve{\boldsymbol{\mathcal{A}}})^{-1} - \mathbf{Id}||_{L^\infty(H^3)}||\mathrm{cof}(\boldsymbol{\nabla}\breve{\boldsymbol{\mathcal{A}}})||_{L^\infty(H^3)} \\
& + ||\mathrm{cof}(\boldsymbol{\nabla}\breve{\boldsymbol{\mathcal{A}}}) - \mathbf{Id}||_{L^\infty(H^3)}||\boldsymbol{\nabla}\breve{\boldsymbol{v}}||_{L^\infty(H^3)} \\
\leq & CT^\kappa M ||\boldsymbol{\nabla}\breve{\boldsymbol{v}}||_{L^\infty(H^3)} \\
\leq & CT^\kappa M ||\tilde{\boldsymbol{v}}||_{L^\infty(H^4)}.
\end{aligned}$$

Further, using Estimate (3.154) we have

$$||\det(\boldsymbol{\nabla}\breve{\boldsymbol{\mathcal{A}}})\partial_t\tilde{\boldsymbol{v}}||_{L^\infty(H^2)} \leq CM||\tilde{\boldsymbol{v}}||_{W^{2,\infty}(H^2)} \leq C||\boldsymbol{v}_0||_{H^6} + C||\boldsymbol{\xi}_1||_{H^3} + CT^\kappa M(||\tilde{\boldsymbol{v}}||_{F_4^T} + ||\tilde{\boldsymbol{\xi}}||_{S_4^T}).$$

Hence, the elliptic estimates yield

$$||\tilde{\boldsymbol{v}}||_{L^\infty(H^4)} \leq C||\boldsymbol{v}_0||_{H^6} + C||\boldsymbol{\xi}_1||_{H^3} + CT^\kappa M(||\tilde{\boldsymbol{v}}||_{F_4^T} + ||\tilde{\boldsymbol{\xi}}||_{S_4^T}). \tag{3.155}$$

Besides, the structure displacement $\tilde{\boldsymbol{\xi}}$ satisfies (3.122). Then, by using the fact that $\boldsymbol{\xi}_0 = 0$ with (3.37) we have

$$||\breve{c}^l_{i\alpha j\beta} + \breve{c}_{i\alpha j\beta}||_{L^\infty(H^2(\Omega_0^s))} \leq T||\partial_t \breve{c}^l_{i\alpha j\beta} + \partial_t \breve{c}^q_{i\alpha j\beta}||_{L^\infty(H^2(\Omega_0^s))} \leq CT^\kappa M.$$

Thus, $\boldsymbol{H}^c_{\tilde{\boldsymbol{\xi}}}$ can be estimated by

$$C||\partial_t^2\tilde{\boldsymbol{\xi}}||_{L^\infty(H^2)} + CT^\kappa M||\tilde{\boldsymbol{\xi}}||_{L^\infty(H^4)}. \tag{3.156}$$

By a similar argument, we find that $\boldsymbol{H}^d_{\tilde{\boldsymbol{\xi}}}$ can be estimated by

$$CT^\kappa M||\tilde{\boldsymbol{\xi}}||_{L^\infty(H^4)}.$$

Thanks to the Estimate (3.154) on $\tilde{\boldsymbol{\xi}}$, (3.156) can be estimated by

$$C||\boldsymbol{v}_0||_{H^6} + C||\boldsymbol{\xi}_1||_{H^3} + CT^\kappa M(||\tilde{\boldsymbol{v}}||_{F_4^T} + ||\tilde{\boldsymbol{\xi}}||_{S_4^T}). \tag{3.157}$$

Therefore, using the elliptic estimate we get

$$||\tilde{\boldsymbol{\xi}}||_{L^\infty(H^4)} \leq C||\boldsymbol{v}_0||_{H^6} + C||\boldsymbol{\xi}_1||_{H^3} + CT^\kappa M(||\tilde{\boldsymbol{v}}||_{F_4^T} + ||\tilde{\boldsymbol{\xi}}||_{S_4^T}). \tag{3.158}$$

Combining (3.155) and (3.158) yields

$$||\tilde{\boldsymbol{v}}||_{L^\infty(H^4(\Omega_0^f))} + ||\tilde{\boldsymbol{\xi}}||_{L^\infty(H^4(\Omega_0^s))} \leq C||\boldsymbol{v}_0||_{H^6} + C||\boldsymbol{\xi}_1||_{H^3} + CT^\kappa M(||\tilde{\boldsymbol{v}}||_{F_4^T} + ||\tilde{\boldsymbol{\xi}}||_{S_4^T}). \tag{3.159}$$

Finally, Estimates (3.144), (3.154) and (3.159) give

$$||\tilde{\boldsymbol{v}}||_{F_4^T} + ||\tilde{\boldsymbol{\xi}}||_{S_4^T} \leq C||\boldsymbol{v}_0||_{H^6} + C||\boldsymbol{\xi}_1||_{H^3} + CT^\kappa M(||\tilde{\boldsymbol{v}}||_{F_4^T} + ||\tilde{\boldsymbol{\xi}}||_{S_4^T}). \tag{3.160}$$

Assuming that T small with respect to M and the initial values yields

$$||\tilde{\boldsymbol{v}}||_{F_4^T} + ||\tilde{\boldsymbol{\xi}}||_{S_4^T} \leq C||\boldsymbol{v}_0||_{H^6} + C||\boldsymbol{\xi}_1||_{H^3} = \boldsymbol{C}_0. \tag{3.161}$$

3.6 Existence of Solution of the Non-Linear Coupled Problem

From Proposition 3.4.1, there exists $\hat{\boldsymbol{C}}_0 > 0$ and $\hat{\kappa} > 0$ such that for all $M > 0$ and $(\breve{\boldsymbol{v}}, \breve{\boldsymbol{\xi}}) \in A^T_M$, there exists $T_1 > 0$ so that the solution of (3.99) satisfies

$$||\tilde{\boldsymbol{v}}||^2_{F^T_4} + ||\tilde{\boldsymbol{\xi}}||^2_{S^T_4} \leq \hat{\boldsymbol{C}}_0, \tag{3.162}$$

for all $T \leq T_1$.
Taking $\hat{M} = \hat{\boldsymbol{C}}_0$ we get

$$||\tilde{\boldsymbol{v}}||^2_{F^T_4} + ||\tilde{\boldsymbol{\xi}}||^2_{S^T_4} \leq \hat{M}. \tag{3.163}$$

We seek to prove the existence of a solution of the non-linear coupled problem (3.5a)-(3.5j). To establish this result we use the fixed point theorem. For this sake, for any $T \leq \hat{T}$, we setting $E = F^T_2 \times S^T_2$ and $W = A^T_{\hat{M}}$. The set W is a closed subset of E. We define the function $\Psi : (\breve{\boldsymbol{v}}, \breve{\boldsymbol{\xi}}) \longrightarrow (\tilde{\boldsymbol{v}}, \tilde{\boldsymbol{\xi}})$ that maps $(\breve{\boldsymbol{v}}, \breve{\boldsymbol{\xi}}) \in W$ into $(\tilde{\boldsymbol{v}}, \tilde{\boldsymbol{\xi}}) \in W$ which is the solution of the linear system (3.99). An element $(a, b) \in \Psi(W)$ is written as $(a, b) = \Psi(\breve{\boldsymbol{v}}, \breve{\boldsymbol{\xi}})$ where $(\breve{\boldsymbol{v}}, \breve{\boldsymbol{\xi}})$ belongs to W. But the definition of Ψ gives that $\Psi(\breve{\boldsymbol{v}}, \breve{\boldsymbol{\xi}}) = (\tilde{\boldsymbol{v}}, \tilde{\boldsymbol{\xi}})$ which is the unique solution of the linear problem (3.99) in W, consequently $(a, b) = (\tilde{\boldsymbol{v}}, \tilde{\boldsymbol{\xi}}) \in W$. Therefore, $\Psi(W) \subset W$.

Consider two pairs $(\breve{\boldsymbol{v}}_1, \breve{\boldsymbol{\xi}}_1)$ and $(\breve{\boldsymbol{v}}_2, \breve{\boldsymbol{\xi}}_2) \in W$ and two solutions $(\tilde{\boldsymbol{v}}_1, \tilde{\boldsymbol{\xi}}_1), (\tilde{\boldsymbol{v}}_2, \tilde{\boldsymbol{\xi}}_2)$ of the linear system (3.99) associated to $(\breve{\boldsymbol{v}}_1, \breve{\boldsymbol{\xi}}_1)$ and $(\breve{\boldsymbol{v}}_2, \breve{\boldsymbol{\xi}}_2)$, respectively. Therefore $\tilde{\boldsymbol{v}}_1, \tilde{\boldsymbol{v}}_2, \tilde{\boldsymbol{\xi}}_1$ and $\tilde{\boldsymbol{\xi}}_2$ satisfy the variational formulations (3.60) and (3.103) with

$$g_i = -\sum_{\alpha,j,\beta=1}^{3} \left(\int_0^t \partial_s \breve{b}_{i\alpha j\beta} \partial_\beta \tilde{\xi}_j \; ds \right) \tilde{n}_\alpha, \quad i = 1, 2, 3.$$

Set $\tilde{\boldsymbol{\zeta}} = \tilde{\boldsymbol{\gamma}}_1 - \tilde{\boldsymbol{\gamma}}_2$, then $\tilde{\boldsymbol{\zeta}}(0) = 0$. The main work in this section is to find estimates on $\tilde{\boldsymbol{\zeta}}$ and $\partial_t \tilde{\boldsymbol{\zeta}}$. These estimates will enable us to apply the fixed point theorem for a suitable choice of T to be precised later.

3.6.1 Estimates on $\tilde{\zeta}$

Consider $\tilde{\boldsymbol{\zeta}} = \tilde{\boldsymbol{\gamma}}_1 - \tilde{\boldsymbol{\gamma}}_2$ in (3.62) then $\tilde{\boldsymbol{\zeta}}$ satisfies the following variational formulation

$$\begin{cases} \rho_f \displaystyle\int_{\Omega_0^f} \det(\boldsymbol{\nabla}\breve{\boldsymbol{\mathcal{A}}}_1)\partial_t\tilde{\boldsymbol{\zeta}} \cdot \tilde{\boldsymbol{\eta}}\ d\tilde{\boldsymbol{x}} + \int_{\Omega_0^f} \breve{\boldsymbol{\sigma}}_1^0(\tilde{\boldsymbol{\zeta}}) : \boldsymbol{\nabla}\tilde{\boldsymbol{\eta}}\ d\tilde{\boldsymbol{x}} + \rho_f \int_{\Omega_0^f} \partial_t\tilde{\boldsymbol{\gamma}}_2 \cdot \big[\det(\boldsymbol{\nabla}\breve{\boldsymbol{\mathcal{A}}}_1) - \det(\boldsymbol{\nabla}\breve{\boldsymbol{\mathcal{A}}}_2)\big]\tilde{\boldsymbol{\eta}}\ d\tilde{\boldsymbol{x}} \\ +\rho_s \displaystyle\int_{\Omega_0^s} \det(\boldsymbol{\nabla}\breve{\boldsymbol{\varphi}}_1)\partial_t\tilde{\boldsymbol{\zeta}} \cdot \tilde{\boldsymbol{\eta}}\ d\tilde{\boldsymbol{x}} + \rho_s \int_{\Omega_0^s} \partial_t\tilde{\boldsymbol{\gamma}}_2 \cdot \big[\det(\boldsymbol{\nabla}\breve{\boldsymbol{\varphi}}_1) - \det(\boldsymbol{\nabla}\breve{\boldsymbol{\varphi}}_2)\big]\tilde{\boldsymbol{\eta}}\ d\tilde{\boldsymbol{x}} \\ + \displaystyle\sum_{i,\alpha,j,\beta=1}^{3} \int_{\Omega_0^s} b_{i\alpha j\beta}(\boldsymbol{\nabla}\breve{\boldsymbol{\xi}}_1)\partial_\beta(\textstyle\int_0^t \tilde{\zeta}(s)ds)_j\ \partial_\alpha\tilde{\eta}_i\ d\tilde{\boldsymbol{x}} + \displaystyle\sum_{i,\alpha,j,\beta=1}^{3} \int_{\Omega_0^s} \partial_\alpha b_{i\alpha j\beta}(\boldsymbol{\nabla}\breve{\boldsymbol{\xi}}_1)\partial_\beta(\textstyle\int_0^t \tilde{\zeta}(s)ds)_j\ \tilde{\eta}_i\ d\tilde{\boldsymbol{x}} \\ + \displaystyle\sum_{i,\alpha,j,\beta=1}^{3} \int_{\Omega_0^s} \Big(b_{i\alpha j\beta}(\boldsymbol{\nabla}\breve{\boldsymbol{\xi}}_1) - b_{i\alpha j\beta}(\boldsymbol{\nabla}\breve{\boldsymbol{\xi}}_2)\Big)\partial_\beta(\textstyle\int_0^t \tilde{\gamma}_2(s)ds)_j\ \partial_\alpha\tilde{\eta}_i\ d\tilde{\boldsymbol{x}} \\ + \displaystyle\sum_{i,\alpha,j,\beta=1}^{3} \int_{\Omega_0^s} \Big(\partial_\alpha b_{i\alpha j\beta}(\boldsymbol{\nabla}\breve{\boldsymbol{\xi}}_1) - \partial_\alpha b_{i\alpha j\beta}(\boldsymbol{\nabla}\breve{\boldsymbol{\xi}}_2)\Big)\partial_\beta(\textstyle\int_0^t \tilde{\gamma}_2(s)ds)_j\tilde{\eta}_i\ d\tilde{\boldsymbol{x}} + \displaystyle\int_{\Omega_0^f} \boldsymbol{F}_0 : \boldsymbol{\nabla}\tilde{\boldsymbol{\eta}}\ d\tilde{\boldsymbol{x}} \\ = \displaystyle\int_{\Gamma_c(0)} \boldsymbol{G} \cdot \tilde{\boldsymbol{\eta}}\ d\tilde{\Gamma} \qquad\qquad \forall\ \tilde{\boldsymbol{\eta}} \in \widetilde{\mathcal{W}}, \end{cases} \tag{3.164}$$

where

$$\breve{\boldsymbol{\sigma}}_1^0(\tilde{\boldsymbol{\zeta}}) = \mu\big[\boldsymbol{\nabla}\tilde{\boldsymbol{\zeta}}(\boldsymbol{\nabla}\breve{\boldsymbol{\mathcal{A}}}_1)^{-1} + (\boldsymbol{\nabla}\breve{\boldsymbol{\mathcal{A}}}_1)^{-t}(\boldsymbol{\nabla}\tilde{\boldsymbol{\zeta}})^t\big]\mathrm{cof}(\boldsymbol{\nabla}\breve{\boldsymbol{\mathcal{A}}}_1) \tag{3.165}$$

and

$$\begin{aligned} \boldsymbol{F}_0 = \mu\big[&\boldsymbol{\nabla}\tilde{\boldsymbol{\gamma}}_2\big((\boldsymbol{\nabla}\breve{\boldsymbol{\mathcal{A}}}_1)^{-1}\mathrm{cof}(\boldsymbol{\nabla}\breve{\boldsymbol{\mathcal{A}}}_1) - (\boldsymbol{\nabla}\breve{\boldsymbol{\mathcal{A}}}_2)^{-1}\mathrm{cof}(\boldsymbol{\nabla}\breve{\boldsymbol{\mathcal{A}}}_2)\big)\big] \\ &+ \mu\big[(\boldsymbol{\nabla}\breve{\boldsymbol{\mathcal{A}}}_1)^{-t}(\boldsymbol{\nabla}\tilde{\boldsymbol{\gamma}}_2)^t\mathrm{cof}(\boldsymbol{\nabla}\breve{\boldsymbol{\mathcal{A}}}_1) - (\boldsymbol{\nabla}\breve{\boldsymbol{\mathcal{A}}}_2)^{-t}(\boldsymbol{\nabla}\tilde{\boldsymbol{\gamma}}_2)^t\mathrm{cof}(\boldsymbol{\nabla}\breve{\boldsymbol{\mathcal{A}}}_2)\big]. \end{aligned} \tag{3.166}$$

Further, for $i = 1, 2, 3$,

$$\begin{aligned} G_i = &\sum_{\alpha,j,\beta=1}^{3} \left(\int_0^t \partial_s b_{i\alpha j\beta}(\boldsymbol{\nabla}\breve{\boldsymbol{\xi}}_1)\partial_\beta(\textstyle\int_0^s \tilde{\zeta}(\tau)d\tau)_j\ ds\right)\tilde{n}_\alpha \\ &+ \sum_{\alpha,j,\beta=1}^{3} \left(\int_0^t \Big[\partial_s b_{i\alpha j\beta}(\boldsymbol{\nabla}\breve{\boldsymbol{\xi}}_1) - \partial_s b_{i\alpha j\beta}(\boldsymbol{\nabla}\breve{\boldsymbol{\xi}}_2)\Big]\partial_\beta(\textstyle\int_0^s \tilde{\gamma}_2(\tau)d\tau)_j\ ds\right)\tilde{n}_\alpha. \end{aligned} \tag{3.167}$$

Moreover, for simplicity, in what follows we set

$$\boldsymbol{L}_0 = \rho_f\partial_t\tilde{\boldsymbol{\gamma}}_2\big[\det(\boldsymbol{\nabla}\breve{\boldsymbol{\mathcal{A}}}_1) - \det(\boldsymbol{\nabla}\breve{\boldsymbol{\mathcal{A}}}_2)\big] \quad \text{and} \quad \boldsymbol{L}_1 = \rho_s\partial_t\tilde{\boldsymbol{\gamma}}_2\big[\det(\boldsymbol{\nabla}\breve{\boldsymbol{\varphi}}_1) - \det(\boldsymbol{\nabla}\breve{\boldsymbol{\varphi}}_2)\big]. \tag{3.168}$$

Taking $\tilde{\boldsymbol{\eta}} = \tilde{\boldsymbol{\zeta}}$ and using the fact that $\tilde{\boldsymbol{\zeta}}(0) = 0$, then proceeding as in (3.70) yield

$$\begin{cases}
\frac{\rho_f}{2}\int_{\Omega_0^f} \det(\boldsymbol{\nabla}\breve{\boldsymbol{\mathcal{A}}}_1)|\tilde{\zeta}(t)|^2 \, d\tilde{\boldsymbol{x}} - \frac{\rho_f}{2}\int_0^t\int_{\Omega_0^f} \partial_s \det(\boldsymbol{\nabla}\breve{\boldsymbol{\mathcal{A}}}_1)|\tilde{\zeta}|^2 \, d\tilde{\boldsymbol{x}}\, ds + \int_0^t\int_{\Omega_0^f} \breve{\boldsymbol{\sigma}}_1^0(\tilde{\boldsymbol{\zeta}}) : \boldsymbol{\nabla}\tilde{\boldsymbol{\zeta}} \, d\tilde{\boldsymbol{x}}\, ds \\
+\frac{\rho_s}{2}\int_{\Omega_0^s} \det(\boldsymbol{\nabla}\breve{\boldsymbol{\varphi}}_1)|\tilde{\boldsymbol{\zeta}}(t)|^2 \, d\tilde{\boldsymbol{x}} - \frac{\rho_s}{2}\int_0^t\int_{\Omega_0^s} \partial_s \det(\boldsymbol{\nabla}\breve{\boldsymbol{\varphi}}_1)|\tilde{\boldsymbol{\zeta}}|^2 \, d\tilde{\boldsymbol{x}}\, ds + \int_0^t\int_{\Omega_0^f} F_0 : \boldsymbol{\nabla}\tilde{\boldsymbol{\zeta}} \, d\tilde{\boldsymbol{x}}\, ds \\
+\int_0^t\int_{\Omega_0^f} \boldsymbol{L}_0 \cdot \tilde{\boldsymbol{\eta}} \, d\tilde{\boldsymbol{x}}\, ds + \int_0^t\int_{\Omega_0^s} \boldsymbol{L}_1 \cdot \tilde{\boldsymbol{\eta}} \, d\tilde{\boldsymbol{x}}\, ds \\
+\frac{1}{2}\sum_{i,\alpha,j,\beta=1}^{3}\int_{\Omega_0^s} b_{i\alpha j\beta}(\boldsymbol{\nabla}\breve{\boldsymbol{\xi}}_1)\partial_\beta(\int_0^t \tilde{\zeta}(s)ds)_j \; \partial_\alpha(\int_0^t \tilde{\zeta}(s)ds)_i \, d\tilde{\boldsymbol{x}} \\
-\frac{1}{2}\sum_{i,\alpha,j,\beta=1}^{3}\int_0^t\int_{\Omega_0^s} \partial_s b_{i\alpha j\beta}(\boldsymbol{\nabla}\breve{\boldsymbol{\xi}}_1)\partial_\beta(\int_0^s \tilde{\zeta}(\tau)d\tau)_j \; \partial_\alpha(\int_0^s \tilde{\zeta}(\tau)d\tau)_i \, d\tilde{\boldsymbol{x}}\, ds \\
+\sum_{i,\alpha,j,\beta=1}^{3}\int_0^t\int_{\Omega_0^s} \partial_\alpha b_{i\alpha j\beta}(\boldsymbol{\nabla}\breve{\boldsymbol{\xi}}_1)\partial_\beta(\int_0^s \tilde{\zeta}(\tau)d\tau)_j \; \partial_s(\int_0^s \tilde{\zeta}(\tau)d\tau)_i \, d\tilde{\boldsymbol{x}}\, ds \\
+\sum_{i,\alpha,j,\beta=1}^{3}\int_0^t\int_{\Omega_0^s} \Big(b_{i\alpha j\beta}(\boldsymbol{\nabla}\breve{\boldsymbol{\xi}}_1) - b_{i\alpha j\beta}(\boldsymbol{\nabla}\breve{\boldsymbol{\xi}}_2)\Big)\partial_\beta(\int_0^s \gamma_2(\tau)d\tau)_j \; \partial^2_{s\alpha}(\int_0^s \tilde{\zeta}(\tau)d\tau)_i \, d\tilde{\boldsymbol{x}}\, ds \\
+\sum_{i,\alpha,j,\beta=1}^{3}\int_0^t\int_{\Omega_0^s} \Big(\partial_\alpha b_{i\alpha j\beta}(\boldsymbol{\nabla}\breve{\boldsymbol{\xi}}_1) - \partial_\alpha b_{i\alpha j\beta}(\boldsymbol{\nabla}\breve{\boldsymbol{\xi}}_2)\Big)\partial_\beta(\int_0^s \tilde{\gamma}_2(\tau)d\tau)_j \partial_s(\int_0^s \tilde{\zeta}(\tau)d\tau)_i \, d\tilde{\boldsymbol{x}}\, ds \\
= \int_0^t\int_{\Gamma_c(0)} \boldsymbol{G}\cdot\partial_s(\int_0^s \tilde{\boldsymbol{\zeta}}(\tau)d\tau) \, d\tilde{\Gamma}\, ds.
\end{cases} \tag{3.169}$$

We proceed to estimate the terms of (3.169) in the spirit of [BG17] by using the fact that

$$\begin{aligned}
||\mathrm{cof}(\boldsymbol{\nabla}\breve{\boldsymbol{\mathcal{A}}}_1) - \mathrm{cof}(\boldsymbol{\nabla}\breve{\boldsymbol{\mathcal{A}}}_2)||_{L^\infty(H^1)} &\leq C||\breve{\boldsymbol{v}}_1 - \breve{\boldsymbol{v}}_2||_{F_2^T}, \\
||(\boldsymbol{\nabla}\breve{\boldsymbol{\mathcal{A}}}_1)^{-1} - (\boldsymbol{\nabla}\breve{\boldsymbol{\mathcal{A}}}_2)^{-1}||_{L^\infty(H^1)} &\leq C||\breve{\boldsymbol{v}}_1 - \breve{\boldsymbol{v}}_2||_{F_2^T}, \\
||\det(\boldsymbol{\nabla}\breve{\boldsymbol{\mathcal{A}}}_1) - \det(\boldsymbol{\nabla}\breve{\boldsymbol{\mathcal{A}}}_2)||_{L^\infty(H^1)} &\leq C||\breve{\boldsymbol{v}}_1 - \breve{\boldsymbol{v}}_2||_{F_2^T} \\
&\text{and} \\
||\det(\boldsymbol{\nabla}\breve{\boldsymbol{\varphi}}_1) - \det(\boldsymbol{\nabla}\breve{\boldsymbol{\varphi}}_2)||_{L^\infty(H^1)} &\leq C||\breve{\boldsymbol{\xi}}_1 - \breve{\boldsymbol{\xi}}_2||_{S_2^T}
\end{aligned} \tag{3.170}$$

which can be established in the similar manner used in Lemma 3.2.2.
First, using Lemma 3.2.3 we have

$$\frac{\rho_s}{2}\int_{\Omega_0^s}\det(\boldsymbol{\nabla}\breve{\boldsymbol{\varphi}}_1)|\tilde{\boldsymbol{\zeta}}(t)|^2\, d\tilde{\boldsymbol{x}} - \frac{\rho_s}{2}\int_0^t\int_{\Omega_0^s}\partial_t\det(\boldsymbol{\nabla}\breve{\boldsymbol{\varphi}}_1)|\tilde{\boldsymbol{\zeta}}|^2\, d\tilde{\boldsymbol{x}}\, ds$$
$$\geq \rho_s(1-CT^{\kappa}M)||\tilde{\boldsymbol{\zeta}}||^2_{L^\infty(L^2(\Omega_0^s))}.$$

Using (3.37) and (3.39), for all $i,\alpha,j,\beta\in\{1,2,3\}$ we have

$$\begin{gathered}||b_{i\alpha j\beta}(\boldsymbol{\nabla}\breve{\boldsymbol{\xi}}_1)-b_{i\alpha j\beta}(\boldsymbol{\nabla}\breve{\boldsymbol{\xi}}_2)||_{L^\infty(H^1)}\leq C||\breve{\boldsymbol{\xi}}_1-\breve{\boldsymbol{\xi}}_2||_{L^\infty(H^2)},\\ ||\partial_\alpha b_{i\alpha j\beta}(\boldsymbol{\nabla}\breve{\boldsymbol{\xi}}_1)-\partial_\alpha b_{i\alpha j\beta}(\boldsymbol{\nabla}\breve{\boldsymbol{\xi}}_2)||_{L^\infty(L^2)}\leq C||\breve{\boldsymbol{\xi}}_1-\breve{\boldsymbol{\xi}}_2||_{L^\infty(H^2)}\\ \text{and}\\ ||\partial_t b_{i\alpha j\beta}(\boldsymbol{\nabla}\breve{\boldsymbol{\xi}}_1)-\partial_t b_{i\alpha j\beta}(\boldsymbol{\nabla}\breve{\boldsymbol{\xi}}_2)||_{L^\infty(L^2)}\leq C||\breve{\boldsymbol{\xi}}_1-\breve{\boldsymbol{\xi}}_2||_{W^{1,\infty}(H^1)}.\end{gathered}\tag{3.171}$$

Then an estimate on $\boldsymbol{G}$ is given by

$$||\boldsymbol{G}||_{H^1(L^2(\Gamma_c(0)))}\leq CT^{\kappa}M\Big(||\breve{\boldsymbol{\xi}}_1-\breve{\boldsymbol{\xi}}_2||_{S_2^T}+||\tilde{\boldsymbol{\zeta}}||_{L^\infty(H^1(\Omega_0^s))}\Big).\tag{3.172}$$

Hence, proceeding similarly as in (3.79) we get

$$\begin{aligned}\int_0^t\int_{\Gamma_c(0)}\boldsymbol{G}\cdot\partial_s(\textstyle\int_0^s\tilde{\boldsymbol{\zeta}}(\tau)d\tau)\, d\tilde{\Gamma}\, ds &\leq C||\boldsymbol{G}||^2_{H^1(L^2(\Gamma_c(0)))}+\delta T||\textstyle\int_0^{\bullet}\tilde{\boldsymbol{\zeta}}(s)\, ds||^2_{L^\infty(H^1(\Omega_0^s))}\\ &\leq CT^{\kappa}M||\breve{\boldsymbol{\xi}}_1-\breve{\boldsymbol{\xi}}_2||^2_{S_2^T}+\delta CT^{\kappa}M||\tilde{\boldsymbol{\zeta}}||^2_{S_2^T}.\end{aligned}\tag{3.173}$$

Taking into consideration (3.171) and the embedding $H^1\subset L^6$ [Bre10, Theorem 9.9] we obtain

$$\begin{aligned}&\Bigg|-\sum_{i,\alpha,j,\beta=1}^{3}\int_0^t\int_{\Omega_0^s}\Big(b_{i\alpha j\beta}(\boldsymbol{\nabla}\breve{\boldsymbol{\xi}}_1)-b_{i\alpha j\beta}(\boldsymbol{\nabla}\breve{\boldsymbol{\xi}}_2)\Big)\partial_\beta(\textstyle\int_0^s\tilde{\gamma}_2(\tau)d\tau)_j\ \partial^2_{s\alpha}(\int_0^s\tilde{\zeta}(\tau)d\tau)_i\ d\tilde{\boldsymbol{x}}\ ds\\ &-\sum_{i,\alpha,j,\beta=1}^{3}\int_0^t\int_{\Omega_0^s}\Big(\partial_\alpha b_{i\alpha j\beta}(\boldsymbol{\nabla}\breve{\boldsymbol{\xi}}_1)-\partial_\alpha b_{i\alpha j\beta}(\boldsymbol{\nabla}\breve{\boldsymbol{\xi}}_2)\Big)\partial_\beta(\textstyle\int_0^s\tilde{\gamma}_2(\tau)d\tau)_j\partial_s(\int_0^s\tilde{\zeta}(\tau)d\tau)_i\ d\tilde{\boldsymbol{x}}\ ds\Bigg|\\ &\leq\sum_{i,\alpha,j,\beta=1}^{3}T||b_{i\alpha j\beta}(\boldsymbol{\nabla}\breve{\boldsymbol{\xi}}_1)-b_{i\alpha j\beta}(\boldsymbol{\nabla}\breve{\boldsymbol{\xi}}_2)||_{L^\infty(L^6)}||\boldsymbol{\nabla}\textstyle\int_0^{\bullet}\tilde{\boldsymbol{\gamma}}_2(s)ds||_{L^\infty(L^3)}||\boldsymbol{\nabla}\int_0^{\bullet}\tilde{\boldsymbol{\zeta}}(s)ds||_{L^\infty(L^2)}\\ &+\sum_{i,\alpha,j,\beta=1}^{3}T||\partial_\alpha b_{i\alpha j\beta}(\boldsymbol{\nabla}\breve{\boldsymbol{\xi}}_1)-\partial_\alpha b_{i\alpha j\beta}(\boldsymbol{\nabla}\breve{\boldsymbol{\xi}}_2)||_{L^\infty(L^2)}||\boldsymbol{\nabla}\textstyle\int_0^{\bullet}\tilde{\boldsymbol{\gamma}}_2(s)ds||_{L^\infty(L^3)}||\tilde{\boldsymbol{\zeta}}||_{L^\infty(L^6)}\\ &\leq CTM||\breve{\boldsymbol{\xi}}_1-\breve{\boldsymbol{\xi}}_2||^2_{L^\infty(H^2(\Omega_0^s))}+CTM||\tilde{\boldsymbol{\zeta}}||^2_{L^\infty(H^1(\Omega_0^s))}.\end{aligned}$$

On the contrary, using (3.38) and (3.40) we have

$$\begin{aligned}&\frac{1}{2}\sum_{i,\alpha,j,\beta=1}^{3}\int_{\Omega_0^s} b_{i\alpha j\beta}(\nabla\breve{\boldsymbol{\xi}}_1)(t)\partial_\beta(\textstyle\int_0^t\tilde{\zeta}(s)ds)_j\partial_\alpha(\int_0^t\tilde{\zeta}(s)ds)_i d\tilde{\boldsymbol{x}}\\ &\geq \mu_s||\textstyle\int_0^{\boldsymbol{\cdot}}\tilde{\boldsymbol{\zeta}}(s)ds||^2_{L^\infty(H^1(\Omega_0^s))}+\dfrac{\lambda_s+\mathsf{C}}{2}||\nabla\cdot\int_0^{\boldsymbol{\cdot}}\tilde{\boldsymbol{\zeta}}(s)\ ds||^2_{L^\infty(L^2(\Omega_0^s))}-CT^\kappa M||\int_0^{\boldsymbol{\cdot}}\tilde{\boldsymbol{\zeta}}(s)\ ds||^2_{L^\infty(H^1(\Omega_0^s))}.\end{aligned} \tag{3.174}$$

Whereas, for the integrals on the fluid domain Ω_0^f we have

$$\begin{aligned}\frac{\rho_f}{2}\int_{\Omega_0^f}\det(\nabla\breve{\boldsymbol{\mathcal{A}}}_1)|\tilde{\boldsymbol{\zeta}}(t)|^2\ d\tilde{\boldsymbol{x}}+\frac{\rho_f}{2}\int_0^t\int_{\Omega_0^f}\partial_t\det(\nabla\breve{\boldsymbol{\mathcal{A}}}_1)|\tilde{\boldsymbol{\zeta}}|^2\ d\tilde{\boldsymbol{x}}\ ds\\ \geq\frac{\rho_f}{2}(1-CT^\kappa M)||\tilde{\boldsymbol{\zeta}}||^2_{L^\infty(L^2(\Omega_0^f))}.\end{aligned}$$

On the other hand, for $\boldsymbol{F}_0$ we have

$$||\boldsymbol{F}_0||^2_{L^2(L^2(\Omega_0^f))}\leq CT||\breve{\boldsymbol{v}}_1-\breve{\boldsymbol{v}}_2||^2_{F_2^T}. \tag{3.175}$$

Then, using Young's inequality we bound the integral $\int_0^t\int_{\Omega_0^f}\boldsymbol{F}_0:\nabla\tilde{\boldsymbol{\zeta}}\ d\tilde{\boldsymbol{x}}\ ds$ as

$$\begin{aligned}\left|\int_0^t\int_{\Omega_0^f}\boldsymbol{F}_0:\nabla\tilde{\boldsymbol{\zeta}}\ d\tilde{\boldsymbol{x}}\ ds\right|&\leq\int_0^t\int_{\Omega_0^f}|\boldsymbol{F}_0||\nabla\tilde{\boldsymbol{\zeta}}|\ d\tilde{\boldsymbol{x}}\ ds\\ &\leq C_\delta||\boldsymbol{F}_0||^2_{L^2(L^2(\Omega_0^f))}+\delta||\tilde{\boldsymbol{\zeta}}||^2_{L^2(H^1(\Omega_0^f))}\\ &\leq C_\delta CT||\breve{\boldsymbol{v}}_1-\breve{\boldsymbol{v}}_2||^2_{F_2^T}+\delta|\tilde{\boldsymbol{\zeta}}||^2_{L^2(H^1(\Omega_0^f))}.\end{aligned} \tag{3.176}$$

In order to deal with the integral in $\boldsymbol{L}_0$ we use (3.170) and Young's inequality to get

$$\begin{aligned}&\left|\int_0^t\int_{\Omega_0^f}\partial_t\gamma_2\big[\det(\nabla\breve{\boldsymbol{\mathcal{A}}}_1)-\det(\nabla\breve{\boldsymbol{\mathcal{A}}}_2)\big]\tilde{\boldsymbol{\zeta}}\ d\tilde{\boldsymbol{x}}\ ds\right|\\ &\leq T||\partial_t\tilde{\boldsymbol{\gamma}}_2||_{L^\infty(L^3(\Omega_0^f))}||\det(\nabla\breve{\boldsymbol{\mathcal{A}}}_1)-\det(\nabla\breve{\boldsymbol{\mathcal{A}}}_2)||_{L^\infty(L^6(\Omega_0^f))}||\tilde{\boldsymbol{\zeta}}||_{L^\infty(L^2(\Omega_0^f))}\\ &\leq T||\tilde{\boldsymbol{\gamma}}_2||_{L^\infty(H^1(\Omega_0^f))}||\det(\nabla\breve{\boldsymbol{\mathcal{A}}}_1)-\det(\nabla\breve{\boldsymbol{\mathcal{A}}}_2)||_{L^\infty(H^1(\Omega_0^f))}||\tilde{\boldsymbol{\zeta}}||_{L^\infty(L^2(\Omega_0^f))}\\ &\leq CTM||\breve{\boldsymbol{v}}_1-\breve{\boldsymbol{v}}_2||_{F_2^T}||\tilde{\boldsymbol{\zeta}}||_{L^\infty(L^2(\Omega_0^f))}\\ &\leq CT^\kappa M\Big[C_\delta||\breve{\boldsymbol{v}}_1-\breve{\boldsymbol{v}}_2||^2_{F_2^T}+\delta||\tilde{\boldsymbol{\zeta}}||^2_{L^\infty(L^2(\Omega_0^f))}\Big].\end{aligned} \tag{3.177}$$

Similarly, for the integral in $\boldsymbol{L}_1$ we have

$$\begin{aligned}&\left|\int_0^t\int_{\Omega_0^s}\partial_t\gamma_2\big[\det(\nabla\breve{\boldsymbol{\varphi}}_1)-\det(\nabla\breve{\boldsymbol{\varphi}}_2)\big]\tilde{\boldsymbol{\zeta}}\ d\tilde{\boldsymbol{x}}\ ds\right|\\ &\qquad\leq CT^\kappa M\Big[C_\delta||\breve{\boldsymbol{\xi}}_1-\breve{\boldsymbol{\xi}}_2||^2_{S_2^T}+\delta||\tilde{\boldsymbol{\zeta}}||^2_{W^{1,\infty}(L^2(\Omega_0^s))}\Big].\end{aligned} \tag{3.178}$$

Finally, proceeding in a similar manner as Subsection 3.3.3 with the use of (3.175)-(3.178) and taking into consideration that T is small with respect to M we get

$$||\tilde{\boldsymbol{\zeta}}||^2_{F_1^T}+||\int_0^{\cdot}\tilde{\boldsymbol{\zeta}}(s)ds||^2_{S_1^T}\leq CT^{\kappa}M\Big[||\breve{\boldsymbol{\xi}}_1-\breve{\boldsymbol{\xi}}_2||^2_{S_2^T}+||\breve{\boldsymbol{v}}_1-\breve{\boldsymbol{v}}_2||^2_{F_2^T}\Big]. \tag{3.179}$$

3.6.2 Estimates on $\partial_t\tilde{\zeta}$

The weak solution $\tilde{\boldsymbol{\zeta}}$ satisfies (3.164). Differentiating (3.164) in times gives the following variational formulation

$$\begin{cases}\rho_f\displaystyle\int_{\Omega_0^f}\det(\boldsymbol{\nabla}\breve{\boldsymbol{\mathcal{A}}}_1)\partial_t^2\tilde{\boldsymbol{\zeta}}\cdot\tilde{\boldsymbol{\eta}}\;d\tilde{\boldsymbol{x}}+\rho_f\int_{\Omega_0^s}\partial_t\det(\boldsymbol{\nabla}\breve{\boldsymbol{\mathcal{A}}}_1)\partial_t\tilde{\boldsymbol{\zeta}}\cdot\tilde{\boldsymbol{\eta}}\;d\tilde{\boldsymbol{x}}+\int_{\Omega_0^f}\partial_t\breve{\boldsymbol{\sigma}}_1^0(\tilde{\boldsymbol{\zeta}}):\boldsymbol{\nabla}\tilde{\boldsymbol{\eta}}\;d\tilde{\boldsymbol{x}}\\[2ex]
+\rho_s\displaystyle\int_{\Omega_0^s}\det(\boldsymbol{\nabla}\breve{\boldsymbol{\varphi}}_1)\partial_t^2\tilde{\boldsymbol{\zeta}}\cdot\tilde{\boldsymbol{\eta}}\;d\tilde{\boldsymbol{x}}+\rho_s\int_{\Omega_0^s}\partial_t\det(\boldsymbol{\nabla}\breve{\boldsymbol{\varphi}}_1)\partial_t\tilde{\boldsymbol{\zeta}}\cdot\tilde{\boldsymbol{\eta}}\;d\tilde{\boldsymbol{x}}\\[2ex]
-\displaystyle\sum_{i,\alpha,j,\beta=1}^{3}\int_{\Omega_0^s}\partial_t b_{i\alpha j\beta}(\boldsymbol{\nabla}\breve{\boldsymbol{\xi}}_1)\partial^2_{\alpha\beta}(\textstyle\int_0^t\tilde{\zeta}(s)ds)_j\;\tilde{\eta}_i\;d\tilde{\boldsymbol{x}}\\[2ex]
+\displaystyle\sum_{i,\alpha,j,\beta=1}^{3}\int_{\Omega_0^s}\partial_\alpha b_{i\alpha j\beta}(\boldsymbol{\nabla}\breve{\boldsymbol{\xi}}_1)\partial^2_{t\beta}(\textstyle\int_0^t\tilde{\zeta}(s)ds)_j\;\tilde{\eta}_i\;d\tilde{\boldsymbol{x}}\\[2ex]
+\displaystyle\sum_{i,\alpha,j,\beta=1}^{3}\int_{\Omega_0^s}b_{i\alpha j\beta}(\boldsymbol{\nabla}\breve{\boldsymbol{\xi}}_1)\partial^2_{t\beta}(\textstyle\int_0^t\tilde{\zeta}(s)ds)_j\;\partial_\alpha\tilde{\eta}_i\;d\tilde{\boldsymbol{x}}+\displaystyle\int_{\Omega_0^f}\partial_t\boldsymbol{F}_0:\boldsymbol{\nabla}\tilde{\boldsymbol{\eta}}\;d\tilde{\boldsymbol{x}}\\[2ex]
+\displaystyle\int_{\Omega_0^f}\partial_t\boldsymbol{L}_0\cdot\tilde{\boldsymbol{\eta}}\;d\tilde{\boldsymbol{x}}+\int_{\Omega_0^s}\partial_t\boldsymbol{L}_1\cdot\tilde{\boldsymbol{\eta}}\;d\tilde{\boldsymbol{x}}\\[2ex]
-\displaystyle\sum_{i,\alpha,j,\beta=1}^{3}\int_{\Omega_0^s}\Big(\partial_t b_{i\alpha j\beta}(\boldsymbol{\nabla}\breve{\boldsymbol{\xi}}_1)-\partial_t b_{i\alpha j\beta}(\boldsymbol{\nabla}\breve{\boldsymbol{\xi}}_2)\Big)\partial^2_{\alpha\beta}(\textstyle\int_0^t\tilde{\gamma}_2(s)ds)_j\;\tilde{\eta}_i\;d\tilde{\boldsymbol{x}}\\[2ex]
+\displaystyle\sum_{i,\alpha,j,\beta=1}^{3}\int_{\Omega_0^s}\Big(\partial_\alpha b_{i\alpha j\beta}(\boldsymbol{\nabla}\breve{\boldsymbol{\xi}}_1)-\partial_\alpha b_{i\alpha j\beta}(\boldsymbol{\nabla}\breve{\boldsymbol{\xi}}_2)\Big)\partial^2_{t\beta}(\textstyle\int_0^t\tilde{\gamma}_2(s)ds)_j\;\tilde{\eta}_i\;d\tilde{\boldsymbol{x}}\\[2ex]
+\displaystyle\sum_{i,\alpha,j,\beta=1}^{3}\int_{\Omega_0^s}\Big(b_{i\alpha j\beta}(\boldsymbol{\nabla}\breve{\boldsymbol{\xi}}_1)-b_{i\alpha j\beta}(\boldsymbol{\nabla}\breve{\boldsymbol{\xi}}_2)\Big)\partial^2_{t\beta}(\textstyle\int_0^t\tilde{\gamma}_2(s)ds)_j\;\partial_\alpha\tilde{\eta}_i\;d\tilde{\boldsymbol{x}}=0\qquad\forall\;\tilde{\boldsymbol{\eta}}\in\widetilde{\mathcal{W}},\end{cases} \tag{3.180}$$

where $\breve{\boldsymbol{\sigma}}_1^0(\tilde{\boldsymbol{\zeta}})$, $\boldsymbol{F}_0$, $\boldsymbol{L}_0$ and $\boldsymbol{L}_1$ are defined in (3.165) and (3.166)-(3.168), respectively.

Take $\tilde{\boldsymbol{\eta}} = \partial_t \tilde{\boldsymbol{\zeta}}$ in (3.180) to get

$$
\begin{cases}
\dfrac{\rho_f}{2}\dfrac{d}{dt}\displaystyle\int_{\Omega_0^f} \det(\boldsymbol{\nabla}\breve{\boldsymbol{\mathcal{A}}}_1)|\partial_t\tilde{\boldsymbol{\zeta}}(t)|^2\ d\tilde{\boldsymbol{x}} + \dfrac{\rho_f}{2}\displaystyle\int_{\Omega_0^f} \partial_t \det(\boldsymbol{\nabla}\breve{\boldsymbol{\mathcal{A}}}_1)|\partial_t\tilde{\boldsymbol{\zeta}}|^2\ d\tilde{\boldsymbol{x}} \\
+\dfrac{\rho_s}{2}\dfrac{d}{dt}\displaystyle\int_{\Omega_0^s} \det(\boldsymbol{\nabla}\breve{\boldsymbol{\varphi}}_1)|\partial_t\tilde{\boldsymbol{\zeta}}(t)|^2\ d\tilde{\boldsymbol{x}} + \dfrac{\rho_s}{2}\displaystyle\int_{\Omega_0^f} \partial_t \det(\boldsymbol{\nabla}\breve{\boldsymbol{\varphi}}_1)|\partial_t\tilde{\boldsymbol{\zeta}}|^2\ d\tilde{\boldsymbol{x}} \\
+\displaystyle\int_{\Omega_0^f} \partial_t \breve{\boldsymbol{\sigma}}_1^0(\tilde{\boldsymbol{\zeta}}) : \partial_t \boldsymbol{\nabla}\tilde{\boldsymbol{\zeta}}\ d\tilde{\boldsymbol{x}} \\
+\dfrac{1}{2}\dfrac{d}{dt}\displaystyle\sum_{i,\alpha,j,\beta=1}^{3}\int_{\Omega_0^s} b_{i\alpha j\beta}(\boldsymbol{\nabla}\breve{\boldsymbol{\xi}}_1)\partial^2_{t\beta}(\textstyle\int_0^t \tilde{\zeta}(s)ds)_j\ \partial^2_{t\beta}(\int_0^t \tilde{\zeta}(s)ds)_i\ d\tilde{\boldsymbol{x}} \\
-\dfrac{1}{2}\displaystyle\sum_{i,\alpha,j,\beta=1}^{3}\int_{\Omega_0^s} \partial_t b_{i\alpha j\beta}(\boldsymbol{\nabla}\breve{\boldsymbol{\xi}}_1)\partial^2_{t\beta}(\textstyle\int_0^t \tilde{\zeta}(s)ds)_j\ \partial^2_{t\beta}(\int_0^t \tilde{\zeta}(s)ds)_i\ d\tilde{\boldsymbol{x}} \\
+\displaystyle\sum_{i,\alpha,j,\beta=1}^{3}\int_{\Omega_0^s} \partial_\alpha b_{i\alpha j\beta}(\boldsymbol{\nabla}\breve{\boldsymbol{\xi}}_1)\partial^2_{t\beta}(\textstyle\int_0^t \tilde{\zeta}(s)ds)_j\ \partial^2_{t}(\int_0^t \tilde{\zeta}(s)ds)_i\ d\tilde{\boldsymbol{x}} \\
-\displaystyle\sum_{i,\alpha,j,\beta=1}^{3}\int_{\Omega_0^s} \partial_t b_{i\alpha j\beta}(\boldsymbol{\nabla}\breve{\boldsymbol{\xi}}_1)\partial_{\alpha\beta}(\textstyle\int_0^t \tilde{\zeta}(s)ds)_j\ \partial^2_{t}(\int_0^t \tilde{\zeta}(s)ds)_i\ d\tilde{\boldsymbol{x}} \\
+\displaystyle\int_{\Omega_0^f} \partial_t \boldsymbol{L}_0 \cdot \partial_t\tilde{\boldsymbol{\zeta}}\ d\tilde{\boldsymbol{x}} + \int_{\Omega_0^s} \partial_t \boldsymbol{L}_1 \cdot \partial_t^2(\textstyle\int_0^t \tilde{\boldsymbol{\zeta}}(s)ds)\ d\tilde{\boldsymbol{x}} \\
+\displaystyle\int_{\Omega_0^f} \partial_t \boldsymbol{F}_0 : \partial_t \boldsymbol{\nabla}\tilde{\boldsymbol{\zeta}}\ d\tilde{\boldsymbol{x}} \\
-\displaystyle\sum_{i,\alpha,j,\beta=1}^{3}\int_{\Omega_0^s} \Big(\partial_t b_{i\alpha j\beta}(\boldsymbol{\nabla}\breve{\boldsymbol{\xi}}_1) - \partial_t b_{i\alpha j\beta}(\boldsymbol{\nabla}\breve{\boldsymbol{\xi}}_2)\Big)\partial_{\alpha\beta}(\textstyle\int_0^t \tilde{\gamma}_2(s)ds)_j\ \partial^2_{t}(\int_0^t \tilde{\zeta}(s)ds)_i\ d\tilde{\boldsymbol{x}} \\
-\displaystyle\sum_{i,\alpha,j,\beta=1}^{3}\int_{\Omega_0^s} \Big(b_{i\alpha j\beta}(\boldsymbol{\nabla}\breve{\boldsymbol{\xi}}_1) - b_{i\alpha j\beta}(\boldsymbol{\nabla}\breve{\boldsymbol{\xi}}_2)\Big)\ \partial_t\partial^2_{\alpha\beta}(\textstyle\int_0^t \tilde{\gamma}_2(s)ds)_j\ \partial^2_{t}(\int_0^t \tilde{\zeta}(s)ds)_i\ d\tilde{\boldsymbol{x}} \\
= -\displaystyle\sum_{i,\alpha,j,\beta=1}^{3}\int_{\Gamma_c(0)} \Big(b_{i\alpha j\beta}(\boldsymbol{\nabla}\breve{\boldsymbol{\xi}}_1) - b_{i\alpha j\beta}(\boldsymbol{\nabla}\breve{\boldsymbol{\xi}}_2)\Big)\partial^2_{t\beta}(\textstyle\int_0^t \tilde{\gamma}_2(s)ds)_j\ \tilde{n}_\alpha\ \partial^2_{t}(\int_0^t \tilde{\zeta}(s)ds)_i\ d\tilde{\Gamma},
\end{cases}
\tag{3.181}
$$

where we have used

$$\begin{aligned}
&\sum_{i,\alpha,j,\beta=1}^{3}\int_{\Omega_0^s} b_{i\alpha j\beta}(\nabla\breve{\boldsymbol{\xi}}_1)\partial^2_{t\beta}(\textstyle\int_0^t\tilde{\zeta}(s)ds)_j\ \partial_\alpha\partial^2_t(\textstyle\int_0^t\tilde{\zeta}(s)ds)_i\ d\tilde{\boldsymbol{x}}\\
&\qquad=\sum_{i,\alpha,j,\beta=1}^{3}\int_{\Omega_0^s} b_{i\alpha j\beta}(\nabla\breve{\boldsymbol{\xi}}_1)\partial^2_{t\beta}(\textstyle\int_0^t\tilde{\zeta}(s)ds)_j\ \partial_t\partial^2_{t\alpha}(\textstyle\int_0^t\tilde{\zeta}(s)ds)_i\ d\tilde{\boldsymbol{x}}\\
&\qquad=\sum_{i,\alpha,j,\beta=1}^{3}\int_{\Omega_0^s}\frac{1}{2}\Bigg[\partial_t\bigg(b_{i\alpha j\beta}(\nabla\breve{\boldsymbol{\xi}}_1)\partial^2_{t\beta}(\textstyle\int_0^t\tilde{\zeta}(s)ds)_j\ \partial^2_{t\alpha}(\textstyle\int_0^t\tilde{\zeta}(s)ds)_i\bigg)\\
&\qquad\quad-\partial_t b_{i\alpha j\beta}(\nabla\breve{\boldsymbol{\xi}}_1)\partial^2_{t\beta}(\textstyle\int_0^t\tilde{\zeta}(s)ds)_j\ \partial^2_{t\alpha}(\textstyle\int_0^t\tilde{\zeta}(s)ds)_i\Bigg]\ d\tilde{\boldsymbol{x}}
\end{aligned}$$

and

$$\begin{aligned}
&\sum_{i,\alpha,j,\beta=1}^{3}\int_{\Omega_0^s}\Big(b_{i\alpha j\beta}(\nabla\breve{\boldsymbol{\xi}}_1)-b_{i\alpha j\beta}(\nabla\breve{\boldsymbol{\xi}}_2)\Big)\partial^2_{t\beta}(\textstyle\int_0^t\tilde{\zeta}(s)ds)_j\partial_\alpha\partial^2_t(\textstyle\int_0^t\tilde{\zeta}(s)ds)_i\ d\tilde{\boldsymbol{x}}\\
&\quad=-\int_{\Omega_0^s}\sum_{i,\alpha,j\beta=1}^{3}\partial_\alpha\Bigg[\bigg(b_{i\alpha j\beta}(\nabla\breve{\boldsymbol{\xi}}_1)-b_{i\alpha j\beta}(\nabla\breve{\boldsymbol{\xi}}_2)\bigg)\partial^2_{t\beta}(\textstyle\int_0^t\tilde{\gamma}_2(s)ds)_j\Bigg]\ \partial^2_t(\textstyle\int_0^t\tilde{\zeta}(s)ds)_i\ d\tilde{\boldsymbol{x}}\\
&\qquad-\sum_{i,\alpha,j,\beta=1}^{3}\int_{\Gamma_c(0)}\Big(b_{i\alpha j\beta}(\nabla\breve{\boldsymbol{\xi}}_1)-b_{i\alpha j\beta}(\nabla\breve{\boldsymbol{\xi}}_2)\Big)\partial^2_{t\beta}(\textstyle\int_0^t\tilde{\gamma}_2(s)ds)_j\ \tilde{n}_\alpha\ \partial^2_t(\textstyle\int_0^t\tilde{\zeta}(s)ds)_i\ d\tilde{\Gamma}\\
&\quad=-\sum_{i,\alpha,j,\beta=1}^{3}\int_{\Omega_0^s}\partial_\alpha\bigg(b_{i\alpha j\beta}(\nabla\breve{\boldsymbol{\xi}}_1)-\breve{b}_{i\alpha j\beta}(\nabla\breve{\boldsymbol{\xi}}_2)\bigg)\partial^2_{t\beta}(\textstyle\int_0^t\tilde{\gamma}_2(s)ds)_j\ \partial^2_t(\textstyle\int_0^t\tilde{\zeta}(s)ds)_i\ d\tilde{\boldsymbol{x}}\\
&\qquad-\sum_{i,\alpha,j,\beta=1}^{3}\int_{\Omega_0^s}\bigg(b_{i\alpha j\beta}(\nabla\breve{\boldsymbol{\xi}}_1)-\breve{b}_{i\alpha j\beta}(\nabla\breve{\boldsymbol{\xi}}_2)\bigg)\ \partial_\alpha\Big(\partial^2_{t\beta}(\textstyle\int_0^t\tilde{\gamma}_2(s)ds)_j\Big)\ \partial^2_t(\textstyle\int_0^t\tilde{\zeta}(s)ds)_i\ d\tilde{\boldsymbol{x}}\\
&\qquad-\sum_{i,\alpha,j,\beta=1}^{3}\int_{\Gamma_c(0)}\Big(b_{i\alpha j\beta}(\nabla\breve{\boldsymbol{\xi}}_1)-b_{i\alpha j\beta}(\nabla\breve{\boldsymbol{\xi}}_2)\Big)\partial^2_{t\beta}(\textstyle\int_0^t\tilde{\gamma}_2(s)ds)_j\ \tilde{n}_\alpha\ \partial^2_t(\textstyle\int_0^t\tilde{\zeta}(s)ds)_i\ d\tilde{\Gamma}.
\end{aligned}$$

Therefore we can write (3.181) as

$$\begin{cases} \frac{\rho_f}{2}\frac{d}{dt}\int_{\Omega_0^f}\det(\boldsymbol{\nabla}\breve{\boldsymbol{\mathcal{A}}}_1)|\partial_t\tilde{\boldsymbol{\zeta}}(t)|^2\ d\tilde{\boldsymbol{x}} + \frac{\rho_f}{2}\int_{\Omega_0^f}\partial_t\det(\boldsymbol{\nabla}\breve{\boldsymbol{\mathcal{A}}}_1)|\partial_t\tilde{\boldsymbol{\zeta}}|^2\ d\tilde{\boldsymbol{x}} \\ +\frac{\rho_s}{2}\frac{d}{dt}\int_{\Omega_0^s}\det(\boldsymbol{\nabla}\breve{\boldsymbol{\varphi}}_1)|\partial_t\tilde{\boldsymbol{\zeta}}(t)|^2\ d\tilde{\boldsymbol{x}} + \frac{\rho_s}{2}\frac{d}{dt}\int_{\Omega_0^s}|\partial_t\tilde{\boldsymbol{\zeta}}(t)|^2\ d\tilde{\boldsymbol{x}} + \int_{\Omega_0^f}\partial_t\breve{\boldsymbol{\sigma}}_1^0(\tilde{\boldsymbol{\zeta}}) : \partial_t\boldsymbol{\nabla}\tilde{\boldsymbol{\zeta}}\ d\tilde{\boldsymbol{x}} \\ +\frac{1}{2}\frac{d}{dt}\sum_{i,\alpha,j,\beta=1}^{3}\int_{\Omega_0^s} b_{i\alpha j\beta}(\boldsymbol{\nabla}\breve{\boldsymbol{\xi}}_1)\partial^2_{t\beta}(\int_0^t\tilde{\zeta}(s)ds)_j\ \partial^2_{t\alpha}(\int_0^t\tilde{\zeta}(s)ds)_i\ d\tilde{\boldsymbol{x}} \\ -\frac{1}{2}\sum_{i,\alpha,j,\beta=1}^{3}\int_{\Omega_0^s}\partial_t b_{i\alpha j\beta}(\boldsymbol{\nabla}\breve{\boldsymbol{\xi}}_1)\partial^2_{t\beta}(\int_0^t\tilde{\zeta}(s)ds)_j\ \partial^2_{t\alpha}(\int_0^t\tilde{\zeta}(s)ds)_i\ d\tilde{\boldsymbol{x}} \\ +\sum_{i,\alpha,j,\beta=1}^{3}\int_{\Omega_0^s}\partial_\alpha b_{i\alpha j\beta}(\boldsymbol{\nabla}\breve{\boldsymbol{\xi}}_1)\partial^2_{t\beta}(\int_0^t\tilde{\zeta}(s)ds)_j\ \partial^2_{t}(\int_0^t\tilde{\zeta}(s)ds)_i\ d\tilde{\boldsymbol{x}} \\ -\sum_{i,\alpha,j,\beta=1}^{3}\int_{\Omega_0^s}\partial_t b_{i\alpha j\beta}(\boldsymbol{\nabla}\breve{\boldsymbol{\xi}}_1)\partial^2_{\alpha\beta}(\int_0^t\tilde{\zeta}(s)ds)_j\ \partial^2_{t}(\int_0^t\tilde{\zeta}(s)ds)_i\ d\tilde{\boldsymbol{x}} \\ = -\int_{\Omega_0^f}\partial_t\boldsymbol{F}_0 : \partial_t\boldsymbol{\nabla}\tilde{\boldsymbol{\zeta}}\ d\tilde{\boldsymbol{x}} + \int_{\Omega_0^s}\partial_t\boldsymbol{H}_0\cdot\partial_t^2(\int_0^t\tilde{\boldsymbol{\zeta}}(s)ds)\ d\tilde{\boldsymbol{x}} \\ -\int_{\Omega_0^f}\partial_t\boldsymbol{L}_0\cdot\partial_t\tilde{\boldsymbol{\zeta}}\ d\tilde{\boldsymbol{x}} - \int_{\Omega_0^s}\partial_t\boldsymbol{L}_1\cdot\partial_t^2(\int_0^t\tilde{\boldsymbol{\zeta}}(s)ds)\ d\tilde{\boldsymbol{x}} \\ -\sum_{i,\alpha,j,\beta=1}^{3}\int_{\Gamma_c(0)}\Big(b_{i\alpha j\beta}(\boldsymbol{\nabla}\breve{\boldsymbol{\xi}}_1) - b_{i\alpha j\beta}(\boldsymbol{\nabla}\breve{\boldsymbol{\xi}}_2)\Big)\partial^2_{t\beta}(\int_0^t\tilde{\gamma}_2(s)ds)_j\ \tilde{n}_\alpha\ \partial_t^2(\int_0^t\tilde{\zeta}(s)ds)_i\ d\tilde{\Gamma}, \end{cases} \tag{3.182}$$

where

$$H_{0,i} = \sum_{\alpha,j,\beta=1}^{3}\Big(b_{i\alpha j\beta}(\boldsymbol{\nabla}\breve{\boldsymbol{\xi}}_1) - b_{i\alpha j\beta}(\boldsymbol{\nabla}\breve{\boldsymbol{\xi}}_2)\Big)\partial^2_{\alpha\beta}(\int_0^t\tilde{\gamma}_2(s)ds)_j \qquad \text{for } i = 1,2,3. \tag{3.183}$$

Step 1

Now we proceed to derive some estimates on

$$\tilde{\boldsymbol{\zeta}}|_{\Omega_0^f} \in H^1(H^1)\cap W^{1,\infty}(L^2), \tilde{\boldsymbol{\zeta}}|_{\Omega_0^s} \in W^{1,\infty}(L^2)\cap L^\infty(H^1) \quad \text{and} \quad \int_0^t \tilde{\boldsymbol{\zeta}}(s)|_{\Omega_0^s} ds \in L^\infty(H^1).$$

First, we have

$$\begin{aligned} \int_{\Omega_0^f}\det(\boldsymbol{\nabla}\breve{\boldsymbol{\mathcal{A}}}_1)|\partial_t\tilde{\boldsymbol{\zeta}}(t)|^2\ d\tilde{\boldsymbol{x}} + \int_0^t\int_{\Omega_0^f}\partial_t\det(\boldsymbol{\nabla}\breve{\boldsymbol{\mathcal{A}}}_1)|\partial_t\tilde{\boldsymbol{\zeta}}|^2\ d\tilde{\boldsymbol{x}}\ ds& \\ \geq (1 - CT^\kappa M)||\tilde{\boldsymbol{\zeta}}||^2_{W^{1,\infty}(L^2(\Omega_0^f))} - CTM||\tilde{\boldsymbol{\zeta}}||^2_{F_2^T}& \\ \geq (1 - CT^\kappa M)||\tilde{\boldsymbol{\zeta}}||^2_{W^{1,\infty}(L^2(\Omega_0^f))} - CT^\kappa M||\tilde{\boldsymbol{\zeta}}||^2_{F_2^T}.& \end{aligned} \tag{3.184}$$

Whereas, for the fluid stress term, proceeding as in (3.110) and (3.113) we get

$$\int_0^t \int_{\Omega_0^f} \partial_s \breve{\boldsymbol{\sigma}}_1^0(\tilde{\boldsymbol{\zeta}}) : \partial_s \boldsymbol{\nabla} \tilde{\boldsymbol{\zeta}} \; d\tilde{\boldsymbol{x}} \; ds \geq \mu C_k ||\partial_t \tilde{\boldsymbol{\zeta}}||^2_{L^2(H^1(\Omega_0^f))} - \mu C T^\kappa M ||\partial_t \tilde{\boldsymbol{\zeta}}||^2_{L^2(H^1(\Omega_0^f))}. \tag{3.185}$$

For $\int_{\Omega_0^f} \partial_t \boldsymbol{F}_0 : \partial_t \boldsymbol{\nabla} \tilde{\boldsymbol{\zeta}} \; d\tilde{\boldsymbol{x}}$, we argue as in (3.176) to obtain

$$\begin{aligned} \left| \int_{\Omega_0^f} \partial_t \boldsymbol{F}_0 : \partial_t \boldsymbol{\nabla} \tilde{\boldsymbol{\zeta}} \; d\tilde{\boldsymbol{x}} \right| &\leq \int_{\Omega_0^f} |\partial_t \boldsymbol{F}_0| |\partial_t \boldsymbol{\nabla} \tilde{\boldsymbol{\zeta}}| \; d\tilde{\boldsymbol{x}} \\ &\leq \int_{\Omega_0^f} C_\delta |\partial_t \boldsymbol{F}_0|^2 \; d\tilde{\boldsymbol{x}} + \int_{\Omega_0^f} \delta |\partial_t \boldsymbol{\nabla} \tilde{\boldsymbol{\zeta}}|^2 \; d\tilde{\boldsymbol{x}} \\ &\leq C_\delta ||\breve{\boldsymbol{v}}_1 - \breve{\boldsymbol{v}}_2||^2_{F_2^T} + \int_{\Omega_0^f} \delta |\partial_t \boldsymbol{\nabla} \tilde{\boldsymbol{\zeta}}|^2 \; d\tilde{\boldsymbol{x}}. \end{aligned} \tag{3.186}$$

Similarly, we have

$$\left| \int_{\Omega_0^f} \partial_t \boldsymbol{L}_0 \cdot \partial_t \tilde{\boldsymbol{\zeta}} \; d\tilde{\boldsymbol{x}} \right| \leq C_\delta ||\breve{\boldsymbol{v}}_1 - \breve{\boldsymbol{v}}_2||^2_{F_2^T} + \delta ||\partial_t \tilde{\boldsymbol{\zeta}}(t)||^2_{L^2(\Omega_0^f)}. \tag{3.187}$$

Combining (3.185)-(3.187) and integrating over $(0,t)$ we get

$$\rho_f ||\tilde{\boldsymbol{\zeta}}||^2_{W^{1,\infty}(L^2)} + \mu ||\tilde{\boldsymbol{\zeta}}||^2_{H^1(H^1)} - C T^\kappa M ||\partial_t \tilde{\boldsymbol{\zeta}}||^2_{L^2(H^1)} \leq C T ||\breve{\boldsymbol{v}}_1 - \breve{\boldsymbol{v}}_2||^2_{F_2^T} + \delta ||\partial_t \boldsymbol{\nabla} \tilde{\boldsymbol{\zeta}}||^2_{L^2(L^2(\Omega_0^f))}. \tag{3.188}$$

As for the integrals on the domain Ω_0^s, first we have

$$\begin{aligned} \int_{\Omega_0^s} \det(\boldsymbol{\nabla} \breve{\boldsymbol{\varphi}}_1) |\partial_t \tilde{\boldsymbol{\zeta}}(t)|^2 \; d\tilde{\boldsymbol{x}} + \int_0^t \int_{\Omega_0^s} \partial_t \det(\boldsymbol{\nabla} \breve{\boldsymbol{\varphi}}_1) |\partial_t \tilde{\boldsymbol{\zeta}}|^2 \; d\tilde{\boldsymbol{x}} \; ds & \\ \geq (1 - C T^\kappa M) ||\tilde{\boldsymbol{\zeta}}||^2_{W^{1,\infty}(L^2(\Omega_0^s))} - C T^\kappa M ||\tilde{\boldsymbol{\zeta}}||^2_{L^\infty(H^1(\Omega_0^s))}. & \end{aligned} \tag{3.189}$$

Further, using (3.38) then taking supremum over $(0,T)$ yield

$$\begin{aligned} \frac{1}{2} \sum_{i,\alpha,j,\beta=1}^{3} \int_{\Omega_0^s} \Big[b_{i\alpha j\beta}(\boldsymbol{\nabla} \breve{\boldsymbol{\xi}}_1) \partial_\beta \tilde{\zeta}_j \; \partial_\alpha \tilde{\zeta}_i \Big](t) \; d\tilde{\boldsymbol{x}} & \\ \geq \mu_s ||\tilde{\boldsymbol{\zeta}}||^2_{L^\infty(H^1(\Omega_0^s))} + \frac{\lambda_s + \mathsf{C}}{2} ||\nabla \cdot \tilde{\boldsymbol{\zeta}}||^2_{L^\infty(L^2(\Omega_0^s))} - C T^\kappa M ||\tilde{\boldsymbol{\zeta}}||^2_{S_2^T}. & \end{aligned} \tag{3.190}$$

On the other hand, using (3.37) we have

$$\begin{aligned} \Bigg| -\frac{1}{2} \sum_{i,\alpha,j,\beta=1}^{3} \int_{\Omega_0^s} \partial_t b_{i\alpha j\beta}(\boldsymbol{\nabla} \breve{\boldsymbol{\xi}}_1) \partial_\beta \tilde{\zeta}_j \; \partial_\alpha \tilde{\zeta}_i \; d\tilde{\boldsymbol{x}} + \sum_{i,\alpha,j,\beta=1}^{3} \int_{\Omega_0^s} \partial_\alpha b_{i\alpha j\beta}(\boldsymbol{\nabla} \breve{\boldsymbol{\xi}}_1) \partial_\beta \tilde{\zeta}_j \; \partial_t \tilde{\zeta}_i \; d\tilde{\boldsymbol{x}} & \\ - \sum_{i,\alpha,j,\beta=1}^{3} \int_{\Omega_0^s} \partial_t b_{i\alpha j\beta}(\boldsymbol{\nabla} \breve{\boldsymbol{\xi}}_1) \partial_{\alpha\beta} (\textstyle\int_0^t \tilde{\zeta}(s) ds)_j \; \partial_t \tilde{\zeta}_i \; d\tilde{\boldsymbol{x}} \Bigg| \leq C T^\kappa M ||\tilde{\boldsymbol{\zeta}}||^2_{S_2^T}. & \end{aligned} \tag{3.191}$$

In order to estimate $\int_{\Omega_0^s} \partial_t \boldsymbol{H}_0 \cdot \partial_t^2 (\int_0^t \tilde{\boldsymbol{\zeta}}(s)ds)\ d\tilde{\boldsymbol{x}}$ we use the following two inequalities

$$||b_{i\alpha j\beta}(\boldsymbol{\nabla}\breve{\boldsymbol{\xi}}_1) - b_{i\alpha j\beta}(\boldsymbol{\nabla}\breve{\boldsymbol{\xi}}_2)||_{L^\infty(H^1)} \leq C||\breve{\boldsymbol{\xi}}_1 - \breve{\boldsymbol{\xi}}_2||_{L^\infty(H^2(\Omega_0^s))} \tag{3.192}$$

and

$$||\partial_t b_{i\alpha j\beta}(\boldsymbol{\nabla}\breve{\boldsymbol{\xi}}_1) - \partial_t b_{i\alpha j\beta}(\boldsymbol{\nabla}\breve{\boldsymbol{\xi}}_2)||_{L^\infty(L^2)} \leq C||\breve{\boldsymbol{\xi}}_1 - \breve{\boldsymbol{\xi}}_2||_{W^{1,\infty}(H^1(\Omega_0^s))}. \tag{3.193}$$

These inequalities together with Young's inequality give

$$\int_{\Omega_0^s} \partial_t \boldsymbol{H}_0 \cdot \partial_t^2 (\textstyle\int_0^t \tilde{\boldsymbol{\zeta}}(s)ds)\ d\tilde{\boldsymbol{x}} \leq C_\delta C\big(||\breve{\boldsymbol{\xi}}_1 - \breve{\boldsymbol{\xi}}_2||^2_{W^{1,\infty}(H^1)} + ||\breve{\boldsymbol{\xi}}_1 - \breve{\boldsymbol{\xi}}_2||^2_{L^\infty(H^2)}\big) + \delta||\partial_t \tilde{\boldsymbol{\zeta}}||^2_{L^\infty(L^2(\Omega_0^s))}. \tag{3.194}$$

Further,

$$\left|\int_{\Omega_0^s} \partial_t \boldsymbol{L}_1 \cdot \partial_t^2 (\textstyle\int_0^t \tilde{\boldsymbol{\zeta}}(s)ds)\ d\tilde{\boldsymbol{x}}\right| \leq C_\delta ||\breve{\boldsymbol{\xi}}_1 - \breve{\boldsymbol{\xi}}_2||^2_{S_2^T} + \delta||\partial_t \tilde{\boldsymbol{\zeta}}(t)||^2_{L^2(\Omega_0^s)}. \tag{3.195}$$

Finally, thanks to the trace inequality and (3.171), for $i, \alpha, j, \beta \in \{1, 2, 3\}$ we have

$$\begin{aligned}
&\left|\left|\int_{\Gamma_c(0)} \Big(b_{i\alpha j\beta}(\boldsymbol{\nabla}\breve{\boldsymbol{\xi}}_1) - b_{i\alpha j\beta}(\boldsymbol{\nabla}\breve{\boldsymbol{\xi}}_2)\Big) \partial^2_{t\beta}(\textstyle\int_0^t \tilde{\gamma}_2(s)ds)_j\ \tilde{n}_\alpha\ \partial_t^2(\int_0^t \tilde{\zeta}(s)ds)_i\ d\tilde{\Gamma}\right|\right|_{L^1(\Gamma_c(0))} \\
&\leq ||b_{i\alpha j\beta}(\boldsymbol{\nabla}\breve{\boldsymbol{\xi}}_1)(t) - b_{i\alpha j\beta}(\boldsymbol{\nabla}\breve{\boldsymbol{\xi}}_2)(t)||_{L^2(\Gamma_c(0))} ||\boldsymbol{\nabla}\tilde{\boldsymbol{\gamma}}_2(t)||_{L^\infty(\Gamma_c(0))} ||\partial_t^2 \textstyle\int_0^t \tilde{\boldsymbol{\zeta}}(s)ds||_{L^2(\Gamma_c(0))} \\
&\leq ||b_{i\alpha j\beta}(\boldsymbol{\nabla}\breve{\boldsymbol{\xi}}_1)(t) - b_{i\alpha j\beta}(\boldsymbol{\nabla}\breve{\boldsymbol{\xi}}_2)(t)||_{H^1(\Gamma_c(0))} ||\boldsymbol{\nabla}\tilde{\boldsymbol{\gamma}}_2(t)||_{H^2(\Omega_0^s)} ||\partial_t \tilde{\boldsymbol{\zeta}}(t)||_{H^1(\Omega_0^f)}.
\end{aligned} \tag{3.196}$$

Hence, after combining (3.189)-(3.191) and (3.194)-(3.196) then integrating over $(0, t)$ we obtain

$$\frac{\rho_s}{2}||\tilde{\boldsymbol{\zeta}}||_{L^\infty(L^2(\Omega_0^s))} + \mu_s||\tilde{\boldsymbol{\zeta}}||_{L^2(H^1(\Omega_0^s))} \leq CT\big[M^4||\tilde{\boldsymbol{\zeta}}||_{S_2^T} + ||\breve{\boldsymbol{\xi}}_1 - \breve{\boldsymbol{\xi}}_2||^2_{W^{1,\infty}(H^1)} + ||\breve{\boldsymbol{\xi}}_1 - \breve{\boldsymbol{\xi}}_2||^2_{L^\infty(H^2)}\big]. \tag{3.197}$$

Step 2

Our next step is to estimate $\tilde{\boldsymbol{\zeta}}|_{\Omega_0^f} \in L^\infty(H^2(\Omega_0^f))$ and $\int_0^t \tilde{\boldsymbol{\zeta}}(s)|_{\Omega_0^s} ds \in L^\infty(H^2(\Omega_0^s))$. The fluid velocity $\tilde{\boldsymbol{\zeta}}|_{\Omega_0^f}$ satisfies the following elliptic equation

$$-\boldsymbol{\nabla}\cdot\big((\boldsymbol{\nabla}\tilde{\boldsymbol{\zeta}}|_{\Omega_0^f}) + (\boldsymbol{\nabla}\tilde{\boldsymbol{\zeta}}|_{\Omega_0^f})^t\big) = \nabla\cdot\boldsymbol{F}_0 + \boldsymbol{\nabla}\cdot\boldsymbol{F}_1 + \boldsymbol{\nabla}\cdot\boldsymbol{L}_0 - \det(\boldsymbol{\nabla}\breve{\boldsymbol{\mathcal{A}}})\partial_t \tilde{\boldsymbol{\zeta}}|_{\Omega_0^f} \quad \text{in } \Omega_0^f \tag{3.198}$$

where $\boldsymbol{F}_0$ is defined in (3.166) and

$$\boldsymbol{F}_1 = \boldsymbol{\nabla}\tilde{\boldsymbol{\zeta}}\Big(\mathbf{Id} - (\boldsymbol{\nabla}\breve{\boldsymbol{\mathcal{A}}}_1)^{-1}\mathrm{cof}(\boldsymbol{\nabla}\breve{\boldsymbol{\mathcal{A}}}_1)\Big) + \Big((\boldsymbol{\nabla}\tilde{\boldsymbol{\zeta}})^t - (\boldsymbol{\nabla}\breve{\boldsymbol{\mathcal{A}}}_1)^{-1}(\boldsymbol{\nabla}\tilde{\boldsymbol{\zeta}})^t\mathrm{cof}(\boldsymbol{\nabla}\breve{\boldsymbol{\mathcal{A}}}_1)\Big). \tag{3.199}$$

We have

$$||\boldsymbol{\nabla}\cdot\boldsymbol{F}_0||_{L^\infty(L^2(\Omega_0^f))}\leq||\boldsymbol{F}_0||_{L^\infty(H^1(\Omega_0^f))}\leq CT||\breve{\boldsymbol{v}}_1-\breve{\boldsymbol{v}}_2||_{F_2^T} \tag{3.200}$$

and

$$||\boldsymbol{\nabla}\cdot\boldsymbol{L}_0||_{L^\infty(L^2(\Omega_0^f))}\leq||\boldsymbol{L}_0||_{L^\infty(H^1(\Omega_0^f))}\leq CT||\breve{\boldsymbol{v}}_1-\breve{\boldsymbol{v}}_2||_{F_2^T}.$$

For $\boldsymbol{F}_1$ we have

$$\begin{aligned}||\boldsymbol{\nabla}\cdot\boldsymbol{F}_1||_{L^\infty(L^2(\Omega_0^f))}\leq&\underbrace{||\nabla\cdot\left[\boldsymbol{\nabla}\tilde{\boldsymbol{\zeta}}\big(\mathbf{Id}-(\boldsymbol{\nabla}\breve{\boldsymbol{\mathcal{A}}}_1)^{-1}\mathrm{cof}(\boldsymbol{\nabla}\breve{\boldsymbol{\mathcal{A}}}_1)\big)\right]||_{L^\infty(L^2(\Omega_0^f))}}_{B_1}\\&+\underbrace{||\nabla\cdot\overbrace{\left[(\boldsymbol{\nabla}\tilde{\boldsymbol{\zeta}})^t-(\boldsymbol{\nabla}\breve{\boldsymbol{\mathcal{A}}}_1)^{-1}(\boldsymbol{\nabla}\tilde{\boldsymbol{\zeta}})^t\mathrm{cof}(\boldsymbol{\nabla}\breve{\boldsymbol{\mathcal{A}}}_1)\right]}^{\boldsymbol{B}_3}||}_{B_2}.\end{aligned}\tag{3.201}$$

For the term B_1 we use the embedding of $H^3\subset L^\infty$ and Lemma 3.2.2 to get

$$\begin{aligned}B_1\leq&\left|\left|\nabla\cdot\left[\boldsymbol{\nabla}\tilde{\boldsymbol{\zeta}}\Big(\mathbf{Id}-(\boldsymbol{\nabla}\breve{\boldsymbol{\mathcal{A}}}_1)^{-1}+(\boldsymbol{\nabla}\breve{\boldsymbol{\mathcal{A}}})^{-1}\big(\mathbf{Id}-\mathrm{cof}(\boldsymbol{\nabla}\breve{\boldsymbol{\mathcal{A}}}_1)\big)\Big)\right]\right|\right|_{L^\infty(L^2)}\\\leq&||\boldsymbol{\nabla}^2\tilde{\boldsymbol{\zeta}}||_{L^\infty(L^2)}\left|\left|\mathbf{Id}-(\boldsymbol{\nabla}\breve{\boldsymbol{\mathcal{A}}}_1)^{-1}+(\boldsymbol{\nabla}\breve{\boldsymbol{\mathcal{A}}})^{-1}\big(\mathbf{Id}-\mathrm{cof}(\boldsymbol{\nabla}\breve{\boldsymbol{\mathcal{A}}}_1)\big)\right|\right|_{L^\infty(H^3)}\\&+||\boldsymbol{\nabla}\tilde{\boldsymbol{\zeta}}||_{L^\infty(L^2)}\left|\left|\mathbf{Id}-(\boldsymbol{\nabla}\breve{\boldsymbol{\mathcal{A}}}_1)^{-1}+(\boldsymbol{\nabla}\breve{\boldsymbol{\mathcal{A}}})^{-1}\big(\mathbf{Id}-\mathrm{cof}(\boldsymbol{\nabla}\breve{\boldsymbol{\mathcal{A}}}_1)\big)\right|\right|_{L^\infty(H^3)}\\\leq&2||\tilde{\boldsymbol{\zeta}}||_{L^\infty(H^2)}\Big[||\boldsymbol{\nabla}\breve{\boldsymbol{\mathcal{A}}}_1-\mathbf{Id}||_{L^\infty(H^3)}+||(\boldsymbol{\nabla}\breve{\boldsymbol{\mathcal{A}}}_1)^{-1}||_{L^\infty(H^3)}||\mathrm{cof}(\boldsymbol{\nabla}\breve{\boldsymbol{\mathcal{A}}}_1)-\mathbf{Id}||_{L^\infty(H^3)}\Big]\\\leq&CT^\kappa M||\tilde{\boldsymbol{\zeta}}||_{L^\infty(H^2)}.\end{aligned}\tag{3.202}$$

On the other hand,

$$\begin{aligned}\boldsymbol{B}_3=&(\boldsymbol{\nabla}\tilde{\boldsymbol{\zeta}})^t-(\mathbf{Id}-\mathbf{Id}+(\boldsymbol{\nabla}\breve{\boldsymbol{\mathcal{A}}}_1)^{-1})(\boldsymbol{\nabla}\tilde{\boldsymbol{\zeta}})^t\mathrm{cof}(\boldsymbol{\nabla}\breve{\boldsymbol{\mathcal{A}}}_1)\\=&(\boldsymbol{\nabla}\tilde{\boldsymbol{\zeta}})^t-((\boldsymbol{\nabla}\breve{\boldsymbol{\mathcal{A}}}_1)^{-1}-\mathbf{Id})(\boldsymbol{\nabla}\tilde{\boldsymbol{\zeta}})^t\mathrm{cof}(\boldsymbol{\nabla}\breve{\boldsymbol{\mathcal{A}}}_1)-(\boldsymbol{\nabla}\tilde{\boldsymbol{\zeta}})^t\mathrm{cof}(\boldsymbol{\nabla}\breve{\boldsymbol{\mathcal{A}}}_1)\\=&(\boldsymbol{\nabla}\tilde{\boldsymbol{\zeta}})^t(\mathbf{Id}-\mathrm{cof}(\boldsymbol{\nabla}\breve{\boldsymbol{\mathcal{A}}}_1))-((\boldsymbol{\nabla}\breve{\boldsymbol{\mathcal{A}}}_1)^{-1}-\mathbf{Id})(\boldsymbol{\nabla}\tilde{\boldsymbol{\zeta}})^t\mathrm{cof}(\boldsymbol{\nabla}\breve{\boldsymbol{\mathcal{A}}}_1).\end{aligned}$$

Thus,

$$\begin{aligned}||B_2||_{L^\infty(L^2)}\leq&||\boldsymbol{\nabla}^2\tilde{\boldsymbol{\zeta}}||_{L^\infty(L^2)}||\mathrm{cof}(\boldsymbol{\nabla}\breve{\boldsymbol{\mathcal{A}}}_1)-\mathbf{Id}||_{L^\infty(H^3)}+||\boldsymbol{\nabla}\tilde{\boldsymbol{\zeta}}||_{L^\infty(L^2)}||\mathrm{cof}(\boldsymbol{\nabla}\breve{\boldsymbol{\mathcal{A}}}_1)-\mathbf{Id}||_{L^\infty(H^3)}\\&+2||(\boldsymbol{\nabla}\breve{\boldsymbol{\mathcal{A}}}_1)^{-1}-\mathbf{Id}||_{L^\infty(H^3)}||\boldsymbol{\nabla}\tilde{\boldsymbol{\zeta}}||_{L^\infty(L^2)}||\mathrm{cof}(\boldsymbol{\nabla}\breve{\boldsymbol{\mathcal{A}}}_1)-\mathbf{Id}||_{L^\infty(H^3)}\\&+||(\boldsymbol{\nabla}\breve{\boldsymbol{\mathcal{A}}}_1)^{-1}-\mathbf{Id}||_{L^\infty(H^3)}||\boldsymbol{\nabla}^2\tilde{\boldsymbol{\zeta}}||_{L^\infty(L^2)}||\mathrm{cof}(\boldsymbol{\nabla}\breve{\boldsymbol{\mathcal{A}}}_1)-\mathbf{Id}||_{L^\infty(H^3)}\\\leq&CT^\kappa M||\tilde{\boldsymbol{\zeta}}||_{L^\infty(H^2)}.\end{aligned}$$

For the calculations done on the divergence of the product of two tensors, check Theorem C.1. Consequently, we obtain

$$||\boldsymbol{\nabla}\cdot\boldsymbol{F}_1||_{L^\infty(L^2)}\leq CT^\kappa M||\tilde{\boldsymbol{\zeta}}||_{L^\infty(H^2)}. \tag{3.203}$$

Therefore, $\tilde{\boldsymbol{\zeta}}|_{\Omega_0^f} \in L^\infty(H^2(\Omega_0^f))$ and

$$\mu||\tilde{\boldsymbol{\zeta}}||_{L^\infty(H^2(\Omega_0^f))} \leq C||\partial_t\tilde{\boldsymbol{\zeta}}||_{L^\infty(L^2(\Omega_0^f))} + CT||\breve{\boldsymbol{v}}_1 - \breve{\boldsymbol{v}}_2||_{F_2^T}. \tag{3.204}$$

Besides, the displacement $\int_0^t \tilde{\boldsymbol{\zeta}}(s)|_{\Omega_0^s} ds$, satisfies the following equation

$$-\mu_s \boldsymbol{\nabla} \cdot (\boldsymbol{\nabla} \int_0^t \zeta(s)|_{\Omega_0^s} ds + (\boldsymbol{\nabla} \int_0^t \tilde{\boldsymbol{\zeta}}(s)|_{\Omega_0^s} ds)^t) = \boldsymbol{H}_0 + \boldsymbol{H}_1 + \boldsymbol{H}_2 - \boldsymbol{\nabla} \cdot \boldsymbol{L}_1, \tag{3.205}$$

where $\boldsymbol{H}_0$ is defined by (3.183). As for $\boldsymbol{H}_1$, it is given by

$$H_{1,i} = -\sum_{\alpha,j,\beta=1}^{3} \left[b^l_{i\alpha j\beta}(\boldsymbol{\nabla}\breve{\boldsymbol{\xi}}_1) + b^q_{i\alpha j\beta}(\boldsymbol{\nabla}\breve{\boldsymbol{\xi}}_1)\right] \partial^2_{\alpha\beta}(\int_0^t \tilde{\zeta}(s)|_{\Omega_0^s} ds)_j \qquad \text{for} \quad i = 1,2,3, \tag{3.206}$$

and the expression of $\boldsymbol{H}_2$ is

$$\boldsymbol{H}_2 = -\det(\boldsymbol{\nabla}\breve{\boldsymbol{\varphi}}_1)\partial_t\tilde{\boldsymbol{\zeta}}.$$

Using (3.192) and (3.193) we have

$$\begin{aligned} ||\boldsymbol{H}_0||_{L^\infty(L^2(\Omega_0^s))} &\leq \sum_{i,\alpha,j,\beta=1}^{3} ||b_{i\alpha j\beta}(\boldsymbol{\nabla}\breve{\boldsymbol{\xi}}_1) - b_{i\alpha j\beta}(\boldsymbol{\nabla}\breve{\boldsymbol{\xi}}_2)||_{L^\infty(L^2(\Omega_0^s))} \; ||\int_0^\bullet \tilde{\gamma}_2(s)|_{\Omega_0^s} ds||_{L^\infty(H^2(\Omega_0^s))} \\ &\leq CT^\kappa M||\breve{\boldsymbol{\xi}}_1 - \breve{\boldsymbol{\xi}}_2||_{L^\infty(H^1(\Omega_0^s))}. \end{aligned}$$

For $\boldsymbol{H}_1$ we use (3.37) to obtain

$$\begin{aligned} ||\boldsymbol{H}_1||_{L^\infty(L^2(\Omega_0^s))} &\leq \sum_{i,\alpha,j,\beta=1}^{3} ||b^l_{i\alpha j\beta}(\boldsymbol{\nabla}\breve{\boldsymbol{\xi}}_1) + b^q_{i\alpha j\beta}(\boldsymbol{\nabla}\breve{\boldsymbol{\xi}}_1)||_{L^\infty(L^2)} \; ||\tilde{\boldsymbol{\zeta}}||_{L^\infty(H^2(\Omega_0^s))} \\ &\leq \sum_{i,\alpha,j,\beta=1}^{3} T||\partial_t b^l_{i\alpha j\beta}(\boldsymbol{\nabla}\breve{\boldsymbol{\xi}}_1) + \partial_t b^q_{i\alpha j\beta}(\boldsymbol{\nabla}\breve{\boldsymbol{\xi}}_1)||_{L^\infty(L^2)} \; ||(\int_0^\bullet \tilde{\boldsymbol{\zeta}}(s)|_{\Omega_0^s} ds)||_{L^\infty(H^2(\Omega_0^s))} \\ &\leq CT(M + M^2)||\int_0^\bullet \tilde{\boldsymbol{\zeta}}(s)|_{\Omega_0^s} ds||_{L^\infty(H^2(\Omega_0^s))}. \end{aligned} \tag{3.207}$$

In addition, we have

$$||\boldsymbol{H}_2||_{L^\infty(L^2(\Omega_0^s))} \leq CT||\det(\boldsymbol{\nabla}\breve{\boldsymbol{\varphi}}_1)\partial_t\tilde{\boldsymbol{\zeta}}||_{L^\infty(L^2(\Omega_0^s))} \leq CTM||\int_0^\bullet \tilde{\boldsymbol{\zeta}}(s)ds||_{W^{2,\infty}(L^2(\Omega_0^s))}.$$

Finally, for $\boldsymbol{L}_1$ it holds

$$||\boldsymbol{\nabla} \cdot \boldsymbol{L}_1||_{L^\infty(L^2(\Omega_0^s))} \leq ||\boldsymbol{L}_1||_{L^\infty(H^1(\Omega_0^s))} \leq CT||\breve{\boldsymbol{\xi}}_1 - \breve{\boldsymbol{\xi}}_2||_{S_2^T}.$$

Whence, $\int_0^t \tilde{\boldsymbol{\zeta}}(s)|_{\Omega_0^s} ds \in L^\infty(H^2(\Omega_0^s))$ and a priori estimate is given as

$$\mu_s||\int_0^\bullet \tilde{\boldsymbol{\zeta}}(s)|_{\Omega_0^s} ds||_{L^\infty(H^2(\Omega_0^s))} \leq CT||\breve{\boldsymbol{\xi}}_1 - \breve{\boldsymbol{\xi}}_2||_{S_2^T}. \tag{3.208}$$

Therefore, combining estimates (3.188), (3.197), (3.204) and (3.208) we arrive to

$$||\tilde{\boldsymbol{\zeta}}|_{\Omega_0^f}||_{F_2^T}+||\int_0^{\cdot}\tilde{\boldsymbol{\zeta}}(s)|_{\Omega_0^s}ds||_{S_2^T}\leq CT^{\kappa}M(||\check{\boldsymbol{v}}_1-\check{\boldsymbol{v}}_2||_{F_2^T}+||\check{\boldsymbol{\xi}}_1-\check{\boldsymbol{\xi}}_2||_{S_2^T}). \tag{3.209}$$

Taking T small with respect to M gives that Ψ is a contraction on A_M^T. This yields the existence of a unique solution $(\tilde{\boldsymbol{v}}, \tilde{\boldsymbol{\xi}})$ in A_M^T of the non-linear coupled system (3.5a)-(3.5j). Using [Ric17, Lemma 2.56], we get the existence and uniqueness of $(\boldsymbol{v}, \boldsymbol{\xi})$ in a subset of $\mathcal{F}_4^T \times \mathcal{S}_4^T$, where, $\mathcal{F}_4^T$ is equivalent to F_4^T and $\mathcal{S}_4^T$ is equivalent to S_4^T, and the functions of $\mathcal{F}_4^T$ and $\mathcal{S}_4^T$ are defined over $\Omega(t)$.

3.7 Existence and Uniqueness of the Fluid Pressure

3.7.1 Existence and Uniqueness of an L^2-Pressure

After we have proved the existence and uniqueness of the fluid velocity $\boldsymbol{v}$ and the structure displacement $\boldsymbol{\xi}$, we need to prove the existence of the fluid pressure p_f so that the proof of the existence of the weak solution for the coupled system (3.5a)-(3.5j) is complete. The proof of existence of the L^2 function p_f is based on Lemma [GR86, p.58, Lemma 4.1] [Bre74] that reduces the proof to showing that the following inf-sup condition holds for the functional spaces $\{\mathcal{W}, L^2(\Omega_f(t))\}$:

$$\inf_{q\in L^2(\Omega_f(t))}\sup_{\boldsymbol{z}\in\mathcal{W}}\frac{b(\boldsymbol{z},q)}{||\boldsymbol{z}||_{H^1(\Omega(t))}||q||_{L^2(\Omega_f(t))}}\geq C_1>0, \tag{3.210}$$

with

$$b(\boldsymbol{z},q)=-\int_{\Omega_f(t)} q\ \mathrm{div}\boldsymbol{z}\ d\boldsymbol{x} \qquad \text{and} \quad \boldsymbol{z}\in\mathcal{W},\ q\in L^2(\Omega_f(t)). \tag{3.211}$$

Theorem 3.7.1 *The inf-sup condition (3.210) holds for the functional spaces* $\{\mathcal{W}, L^2(\Omega_f(t))\}$.

Proof. We will proceed in a similar manner as [BDR98, Lemma 3.1]. To show that the condition holds, it suffices to show that

$$\forall\ q\in L^2(\Omega_f(t)), \exists\ \boldsymbol{z}\in\mathcal{W} \text{ such that, } \mathrm{div}\boldsymbol{z}|_{\Omega_f(t)}=q \text{ in } \Omega_f(t) \text{ and } ||\boldsymbol{z}||_{H^1(\Omega(t))}\leq C_1||q||_{L^2(\Omega_f(t))}. \tag{3.212}$$

Let $\overline{q}\in L^2(\Omega(t))$ be the extension of q obtained by defining

$$\overline{q}=-\frac{1}{|\Omega_s(t)|}\int_{\Omega_f(t)} q\ d\boldsymbol{x}, \quad \text{in } \Omega_s(t). \tag{3.213}$$

Note that $\int_{\Omega(t)}\overline{q}\ d\boldsymbol{x}=\int_{\Omega_f(t)}\overline{q}\ d\boldsymbol{x}+\int_{\Omega_s(t)}\overline{q}\ d\boldsymbol{x}=0$, this gives $\overline{q}\in L_0^2(\Omega(t))$. Hence, by the virtue of [BF13, Theorem IV.3.1], there exists a unique $\boldsymbol{z}\in H_0^1(\Omega(t))$ such that

$$\mathrm{div}\boldsymbol{z}=\overline{q} \quad \text{on} \quad \Omega(t) \quad \text{and} \quad ||\boldsymbol{z}||_{H^1(\Omega(t))}\leq C||\overline{q}||_{L_0^2(\Omega(t))}\leq C_1||q||_{L^2(\Omega_f(t))}. \tag{3.214}$$

Since $H_0^1(\Omega(t)) \subset \mathcal{W}$, then $\boldsymbol{z} \in \mathcal{W}$. Moreover, by restricting $\text{div}\boldsymbol{z} = \overline{q}$ to $\Omega_f(t)$ we get that $\text{div}\boldsymbol{z}|_{\Omega_f(t)} = q$. Therefore (3.212) is proved, consequently the inf-sup Condition (3.210) is verified. ■

By the end of this proof, we get the existence of a pressure $p_f \in L^\infty\big(L^2(\Omega_f(t))\big)$ which is unique due to [BF13, Theorem IV.2.4].

3.7.2 Regularity of the Fluid Pressure

The fluid pressure p_f is related to the fluid velocity $\boldsymbol{v}$ by the Navier-Stokes equations. Indeed, at $t = 0$ we have

$$\rho_f \text{det}(\boldsymbol{\nabla}\boldsymbol{\mathcal{A}})\partial_t \tilde{\boldsymbol{v}} - \boldsymbol{\nabla} \cdot \tilde{\boldsymbol{\sigma}}_f^0(\tilde{\boldsymbol{v}}, \tilde{p}_f) = 0 \qquad \text{in } \Omega_f(0) \times (0, T),$$

As a result, the regularity of $\tilde{p}_f$ is linked to the regularity of $\tilde{\boldsymbol{v}}$ which is proved straight forward using Nečas inequality [BF13, Theorem IV.1.1]. Therefore, as $\tilde{\boldsymbol{v}} \in F_4^T$ then $\tilde{p}_f \in \mathcal{P}_3^T$. Again using [Ric17, Lemma 2.56], we get the existence and uniqueness of a fluid pressure p_f in the set $\mathcal{Q}_3^T$ which is equivalent to $\mathcal{P}_3^T$ where the functions of $\mathcal{Q}_3^T$ are defined over $\Omega_f(t)$.

To this end, we have proved the existence and uniqueness locally in time of a solution $(\boldsymbol{v}, \boldsymbol{\xi}, p_f)$ of the non-linear coupling problem of an incompressible fluid with a quasi-incompressible structure.

Chapter 4

Discretization and Numerical Simulations

Contents

Introduction

Cardiovascular diseases, due to stenosis or aneurysms, are causes with the highest percentage leading to death worldwide. Therefore, the study of human blood flow, in particular in stenosed arteries or those characterized by the existence of aneurysms, has gained great importance and attention, as an auxiliary given tool, that will treat these diseases and decrease or prevent them by suggesting solutions and cures. A deep view of what is happening in the arteries would help us in realizing the processes taking place in the arteries. Consequently, cures can be found to these diseases. Due to the importance of this issue, it gains a lot of concern and interest among mathematicians who; from their point of view; seek to reduce the percentage of death resulting from cardiovascular diseases. Consequently, arose the modeling of the arterial blood flow and simulating results. Many computational techniques and models have been developed to describe the blood flow and study the response of the arteries walls under certain conditions. Recently, the lumen-wall modeling has been adopted using fluid-structure interaction (FSI) model through which the blood and the arterial wall can be represented by their appropriate dynamics and models based on their behavior. An overview of FSI in biomedical applications was considered in [BGN14]. Introduction of a computational model with FSI in order to investigate the wall shear stresses, blood flow field and recirculation zones in stenosed arteries has been studied in [BKS09] where the blood is considered to be an incompressible Newtonian fluid. A most commonly method used when dealing with FSI systems is the Arbitrary Lagrangian-Eulerain (ALE) method which was first proposed in 1982 in the work [DGH82]. This method is effective when combining the fluid formulation in the Eulerian description and the structure formulation in the Lagrangian description.

For most FSI problems, analytic investigation of the solutions of the interaction model between fluid and structure is impossible to realize. Nevertheless, approximate solutions can be obtained by employing numerical simulations. In this context, numerical procedures can be categorized into two approaches. Monolithic solvers [HWD04] consists of formulating the fluid and structure dynamics in the same mathematical framework to achieve one system corresponding to the entire problem. Even though, this approach is unified, parallelizable and strongly coupled as the coupling conditions are implicit in the solution procedure, it is hard to be treated numerically. In fact an *ad hoc* software development is needed. In contrast, the partitioned approach allows the usage of the respective mesh discretization, numerical algorithms and traditional solvers for both the fluid and the structure problems. Coupling conditions are used explicitly to link the solutions of the fluid and the structure problems. If a difficulty arises, it would be due to the implementation of the interaction using convergence methods.

Another classification of the FSI solutions is based on the treatment of meshes. Conforming mesh methods- mostly detected in the numerical works that adopt the partitioned approach- treat the interface as a part of the solution by considering the coupling conditions to be physical ones. This requires meshes to match on the interface. As a result, due to the deformation of the structure at each step a re-meshing or mesh-updating is required. On the contrary, non-conforming mesh methods regard the interface and the corresponding conditions as constraints so that non-conforming meshes can be dealt with. Consequently, the fluid and structure equations can be treated separately with their respective grids without requiring a re-meshing procedure.

This chapter is devoted to develop a mathematical model for the study of blood flow through a stenosed artery. For this aim the interaction between the blood and the stenosed artery is modeled as a FSI model. This is done by introducing a fluid model presenting the blood flow into the lumen of the artery and a structure model describing the artery wall, where we link both models by some coupling conditions which ensure the balance of the energy of the coupled system. The blood is modeled as a homogeneous non-Newtonian incompressible fluid whose dynamics is given by the incompressible Navier-Stokes equations. Whereas for the arterial wall, the quasi-static incompressible elasticity equations govern the elastic behavior of the wall. The medium is a non-linear hyperelastic material characterized by the existence of a function W called the strain-energy density function which relates the first Piola-Kirchhoff stress tensor $\boldsymbol{P}$ to the deformation gradient $\boldsymbol{F}_s$.

These two models are coupled together to form the FSI model which we have already introduced in Chapter 2, and will give us an appearance of the incidents occurring in a stenosed artery. Discretization of the system is needed, in which we configure the best computational approach. To this end our problem is treated using the partitioned approach with a conforming mesh method. Both sub-problems are discretized in space by employing the FEM. The fluid sub-problem is semi-discretized in time. On the other hand, the structure sub-problem is solved using Newton-Raphson method. Upon solving the system, numerical simulations are done with the use of the finite element software FreeFem++ [Hec05] by considering reliable physiological data. We are interested in recognizing the recirculation zones. Moreover, we observe the wall shear stress and analyze its effect on the blood flow. The aim of this chapter is to form a deep view of what is happening in the artery, by studying the behavior of the speed, the viscosity, the shear stress in the lumen as well as the effect of the deformation of the artery wall on the blood flow. These factors will help us in realizing the formation of a clot, consequently will help us to set up our assumptions for a rupture model.

The chapter is composed as follows:

The first section deals with the FSI system. The variational formulation associated to it is derived using appropriate functional spaces. Space and time discretization are applied on both the Navier-Stokes equations and the elastodynamic equations. More precisely, the Navier-Stokes equations are semi-discretized in time, whereas, the elastodynamic equations are solved using the Newton-Rhaphson method by linearizing them with respect to the deformation $\boldsymbol{\varphi}_s$ of the structure domain and the hydrostatic pressure $\tilde{p}_{hs}$. Further, the algorithm needed in the simulations is presented.

The numerical results obtained after performing simulations using FreeFem++ software with the partitioned approach are then presented in Section 4.2. The maximum shear stress and maximum speed of blood are observed. Moreover, the recirculation zones are recognized. Further, a comparison between the case of a Newtonian and a non-Newtonian blood is drawn by analyzing quantities such as shear stresses, velocities and recirculation zones in both cases. In addition, case of a bifurcated artery is considered and the same factors are observed.

The chapter ends up by a conclusion summarizing the results obtained in this chapter.

In Chapter 2 we have introduced the FSI problem that models the blood-wall setting. In this chapter, the FSI model, its weak and discretized formulations are derived in a three dimensional case. However, numerical simulations are performed in a two dimensional space. Our work starts by recalling the FSI system then deriving its associated variational formulation.

4.1 Fluid-Structure Interaction

The total domain $\Omega(t)$ representing the artery in the actual configuration at time $t > 0$ is decomposed into two sub-domains $\Omega_f(t)$ and $\Omega_s(t)$ representing the lumen of the artery and the arterial wall, respectively as defined in Chapter 2.

The motion of the structure of density $\tilde{\rho}_s$ is described by its displacement field $\tilde{\boldsymbol{\xi}}_s : \tilde{\Omega}_s \times \mathbb{R}^+ \longrightarrow \mathbb{R}^3$ that satisfies the quasi-static elastodynamic equations. The evolution of the structure domain is given by the deformation map $\boldsymbol{\varphi}_s : \tilde{\Omega}_s \times \mathbb{R}^+ \longrightarrow \mathbb{R}^3$ defined in terms of the displacement $\tilde{\boldsymbol{\xi}}_s$ as $\boldsymbol{\varphi}_s(\tilde{\boldsymbol{x}}, t) = \tilde{\boldsymbol{x}} + \tilde{\boldsymbol{\xi}}_s(\tilde{\boldsymbol{x}}, t)$. Its deformation gradient $\boldsymbol{F}_s : \tilde{\Omega}_s(t) \longrightarrow \mathbb{R}^{3\times 3}$ which is a second order tensor is given by $\boldsymbol{F}_s = \boldsymbol{\nabla}_{\tilde{\boldsymbol{x}}} \boldsymbol{\varphi}_s$. Its associated Jacobian is $J_s(\tilde{\boldsymbol{x}}, t) = \det(\boldsymbol{F}_s(\tilde{\boldsymbol{x}}, t))$.

On the other hand, the dynamics of the blood flow is described by the incompressible Navier-Stokes equations on the sub-domain $\Omega_f(t)$. We denote by

$$\boldsymbol{v} : \Omega_f \times \mathbb{R}^+ \longrightarrow \mathbb{R}^3$$

and

$$p_f : \Omega_f \times \mathbb{R}^+ \longrightarrow \mathbb{R}$$

the velocity of the homogeneous blood and its pressure, respectively. The constant ρ_f stands for the blood density.
The sub-domain $\Omega_f(t)$ of moving boundaries evolves from the reference configuration $\tilde{\Omega}_f$ according to the ALE map $\boldsymbol{\mathcal{A}}$ given by

$$\begin{aligned} \boldsymbol{\mathcal{A}}(.,t) : \tilde{\Omega}_f &\longrightarrow \Omega_f(t) \\ \tilde{\boldsymbol{x}} &\longrightarrow \mathcal{A}(\tilde{\boldsymbol{x}}, t) = \boldsymbol{x} \quad \text{for } t \in \mathbb{R}^+, \end{aligned} \tag{4.1}$$

that is, $\Omega_f(t) = \boldsymbol{\mathcal{A}}(\tilde{\Omega}_f, t)$.
It is expressed in terms of an extension of the displacement $\tilde{\boldsymbol{\xi}}_s$ of the interface $\tilde{\Gamma}_c$, that is to say

$$\boldsymbol{\mathcal{A}}(\tilde{\boldsymbol{x}}, t) = \tilde{\boldsymbol{x}} + \mathcal{E}xt(\boldsymbol{\xi}_s(\tilde{\boldsymbol{x}}, t)|_{\tilde{\Gamma}_c}). \tag{4.2}$$

The operator $\mathcal{E}xt$ stands for an extension of the displacement of the boundary $\tilde{\Gamma}_c$. Possible extensions can be found in [Ric17, Section 5.3, pp. 247], [Cha13, Chapter 2] (harmonic, biharmonic, wislow, etc.). In particular we consider the harmonic extension as we will see in Subsection 4.1.2.
The associated deformation gradient of $\boldsymbol{\mathcal{A}}$ is $\boldsymbol{F}_f : \tilde{\Omega}_f(t) \longrightarrow \mathbb{R}^{3\times 3}$ defined by $\boldsymbol{F}_f = \boldsymbol{\nabla}_{\tilde{\boldsymbol{x}}} \boldsymbol{\mathcal{A}}$ where the symbol $\boldsymbol{\nabla}_{\tilde{\boldsymbol{x}}}$ indicates the gradient with respect to the variable $\tilde{\boldsymbol{x}} = (\tilde{x}_1, \tilde{x}_2, \tilde{x}_3)$. Its Jacobian is $J_f(\tilde{\boldsymbol{x}}, t) = \det(\boldsymbol{F}_f(\tilde{\boldsymbol{x}}, t))$.

Here, and throughout the context $\tilde{\boldsymbol{\xi}}_f$ denotes the displacement of the domain $\tilde{\Omega}_f$ which we set to be $\mathcal{E}xt(\boldsymbol{\xi}_s|_{\tilde{\Gamma}_c})$. Formulating the Navier-Stokes equations in the ALE frame results a new variable $\boldsymbol{w}$ describing the velocity of the domain $\Omega_f(t)$. It is related to the displacement $\tilde{\boldsymbol{\xi}}_f$ by $\boldsymbol{w} = \partial_t \tilde{\boldsymbol{\xi}}_f \circ \boldsymbol{\mathcal{A}}^{-1}$. It is worth to point out that $\boldsymbol{w} \neq \boldsymbol{v}$. One must distinguish between $\boldsymbol{v}$ the physical velocity of the particles and $\boldsymbol{w}$ the velocity of the fluid domain $\Omega_f(t)$.

In what follows, we refer to the elements in the reference configuration by "$\tilde{}$". In fact the velocity and the pressure of the blood are given on the reference configuration $\tilde{\Omega}_f$ by

$$\tilde{\boldsymbol{v}}(\tilde{\boldsymbol{x}}, t) = \boldsymbol{v}\big(\boldsymbol{\mathcal{A}}(\tilde{\boldsymbol{x}}, t), t\big) \quad \text{and} \quad \tilde{p}_f(\tilde{\boldsymbol{x}}, t) = p_f\big(\boldsymbol{\mathcal{A}}(\tilde{\boldsymbol{x}}, t), t\big) \qquad \forall\ (\tilde{\boldsymbol{x}}, t) \in \tilde{\Omega}_f \times \mathbb{R}^+. \tag{4.3}$$

The Cauchy stress tensor $\boldsymbol{\sigma}_f(\boldsymbol{v}, p_f)$ is expressed in terms of the deformation tensor $\boldsymbol{D}(\boldsymbol{v}) = \dfrac{\boldsymbol{\nabla}\boldsymbol{v} + (\boldsymbol{\nabla}\boldsymbol{v})^t}{2}$ as

$$\boldsymbol{\sigma}_f(\boldsymbol{v}, p_f) = 2\mu \boldsymbol{D}(\boldsymbol{v}) - p_f\ \mathbf{Id}. \tag{4.4}$$

Its counter part in the reference configuration $\tilde{\Omega}_f$ is $J_f \tilde{\boldsymbol{\sigma}}_f(\tilde{\boldsymbol{v}}, \tilde{p}_f) \boldsymbol{F}_f^{-t}$ where

$$\tilde{\boldsymbol{\sigma}}_f(\tilde{\boldsymbol{v}}, \tilde{p}_f) = \big(\boldsymbol{\nabla}\tilde{\boldsymbol{v}}(\boldsymbol{\nabla}\boldsymbol{\mathcal{A}})^{-1} + (\boldsymbol{\nabla}\boldsymbol{\mathcal{A}})^{-t}(\boldsymbol{\nabla}\tilde{\boldsymbol{v}})^t\big) - \tilde{p}_f\ \mathbf{Id}.$$

Since the arterial wall is a hyperelastic material (see Definition 2.2.1) then there exists a strain-energy density function $W(\boldsymbol{F}_s)$ such that the first Piola-Kirchhoff stress tensor $\boldsymbol{P} = \dfrac{\partial W(\boldsymbol{F}_s)}{\partial \boldsymbol{F}_s}$. Further, due to the incompressible behavior of the material its Piola-Kirchhoff stress tensor is of the form

$$\boldsymbol{P}_{\text{inc}} = \boldsymbol{P} + \tilde{p}_{hs}\text{cof}(\boldsymbol{F}_s).$$

The variable $\tilde{p}_{hs}$, called the hydrostatic pressure, plays the role of the Lagrange multiplier associated to the incompressibility condition $\det(\boldsymbol{F}_s) = 1$.

On the fluid domain $\Omega_f(t)$ a volumetric force $\boldsymbol{f}_f : \Omega_f \times \mathbb{R}^+ \longrightarrow \mathbb{R}^3$ is applied. Moreover, a velocity $\boldsymbol{v}_{\text{in}}$ is enforced on the inlet of the artery $\Gamma_{\text{in}}(t)$. On the contrary, a free-exist condition given by $\boldsymbol{\sigma}_f(\boldsymbol{v}, p_f)\ \boldsymbol{n}_f = 0$ is enforced on the outlet $\Gamma_{\text{out}}(t)$.

On the other hand, a volumetric force $\boldsymbol{f}_s : \tilde{\Omega}_s \times \mathbb{R}^+ \longrightarrow \mathbb{R}^3$ is applied on the structure domain which is assumed to be fixed on the boundary $\tilde{\Gamma}_2$, that is to say, $\tilde{\boldsymbol{\xi}}_s = 0$ on $\tilde{\Gamma}_2$.

On the interface $\Gamma_c(t)$, surface forces $\boldsymbol{g}_f : \Omega_f \times \mathbb{R}^+ \longrightarrow \mathbb{R}^3$ and $\boldsymbol{g}_s : \Omega_s \times \mathbb{R}^+ \longrightarrow \mathbb{R}^3$ are exerted from the fluid domain and the structure domain, respectively.

The fluid-structure interaction model describing the blood-wall interaction is obtained by the coupling between the incompressible Navier-Stokes equations which are formulated in the ALE frame and the quasi-static incompressible elasticity equations formulated in the Lagrangian frame on the reference configuration $\tilde{\Omega}_s$. The FSI system is

Find

$$\begin{aligned}
\tilde{\boldsymbol{v}} &: \tilde{\Omega}_f \times \mathbb{R}^+ \longrightarrow \mathbb{R}^3,\\
\tilde{p}_f &: \tilde{\Omega}_f \times \mathbb{R}^+ \longrightarrow \mathbb{R},\\
\tilde{\boldsymbol{\xi}}_{\boldsymbol{f}} &: \tilde{\Omega}_f \times \mathbb{R}^+ \longrightarrow \mathbb{R}^3,\\
\tilde{\boldsymbol{\xi}}_s &: \tilde{\Omega}_s \times \mathbb{R}^+ \longrightarrow \mathbb{R}^3,\\
\tilde{p}_{hs} &: \tilde{\Omega}_s \times \mathbb{R}^+ \longrightarrow \mathbb{R},
\end{aligned}$$

such that

$$\begin{cases}
\rho_f \partial_t \boldsymbol{v}|_{\boldsymbol{\mathcal{A}}} + \rho_f(\boldsymbol{v} - \boldsymbol{w})^t \boldsymbol{\nabla}_{\boldsymbol{x}} \boldsymbol{v} - \boldsymbol{\nabla}_{\boldsymbol{x}} \cdot \boldsymbol{\sigma}_f(\boldsymbol{v}, p_f) = \rho_f \boldsymbol{f}_f & \text{on} \quad \Omega_f(t) \times (0,T),\\
\boldsymbol{\nabla}_{\boldsymbol{x}} \cdot \boldsymbol{v} = 0 & \text{on} \quad \Omega_f(t) \times (0,T),\\
\boldsymbol{v} = \boldsymbol{v}_{\text{in}} & \text{on} \quad \Gamma_{\text{in}}(t) \times (0,T),\\
\boldsymbol{\sigma}_f(\boldsymbol{v}, p_f)\ \boldsymbol{n}_f = 0 & \text{on} \quad \Gamma_{\text{out}}(t) \times (0,T),\\
\boldsymbol{\sigma}_f(\boldsymbol{v}, p_f)\ \boldsymbol{n}_f = \boldsymbol{g}_f & \text{on} \quad \Gamma_c(t) \times (0,T),\\
-\boldsymbol{\nabla}_{\tilde{\boldsymbol{x}}} \cdot \boldsymbol{P}_{\text{inc}}(\tilde{\boldsymbol{x}}) = J_s \tilde{\rho}_s \tilde{\boldsymbol{f}}_s & \text{on} \quad \tilde{\Omega}_s \times (0,T),\\
J_s = 1 & \text{on} \quad \tilde{\Omega}_s \times (0,T),\\
\tilde{\boldsymbol{\xi}}_s = 0 & \text{on} \quad \tilde{\Gamma}_2 \times (0,T),\\
\boldsymbol{P}_{\text{inc}}(\tilde{\boldsymbol{x}})\ \tilde{\boldsymbol{n}}_s = J_s \tilde{\boldsymbol{g}}_s & \text{on} \quad \tilde{\Gamma}_c \times (0,T),\\
\boldsymbol{v} = \boldsymbol{w} & \text{on} \quad \Gamma_c(t) \times (0,T),\\
\boldsymbol{P}_{\text{inc}}(\tilde{\boldsymbol{x}})\ \tilde{\boldsymbol{n}}_s + J_f \tilde{\boldsymbol{\sigma}}_f(\tilde{\boldsymbol{v}}, \tilde{p}_f) \boldsymbol{F}_f^{-t}\ \tilde{\boldsymbol{n}}_f = 0 & \text{on} \quad \tilde{\Gamma}_c \times (0,T),
\end{cases} \tag{4.5}$$

where $\tilde{\boldsymbol{v}}$ and $\tilde{p}_f$ are given by (4.3) and $\tilde{\boldsymbol{g}}_s = \boldsymbol{g}_s \circ \boldsymbol{\varphi}_s$. Further, $\tilde{\Gamma}_c$ is the transformation of Γ_c to the reference configuration given by $\tilde{\Gamma}_c = \Gamma_c \circ \boldsymbol{\varphi}_s$.

Remark 4.1.1 *From Expression (4.2) we get that the ALE map $\boldsymbol{\mathcal{A}}$ and the structure deformation $\boldsymbol{\varphi}_s$ coincide on the interface $\tilde{\Gamma}_c$, that is to say,*

$$\boldsymbol{\varphi}_s \equiv \boldsymbol{\mathcal{A}} \qquad \text{on } \tilde{\Gamma}_c.$$

Remark 4.1.2 *Due to the incompressibility condition the ij-th component of $\boldsymbol{\sigma}_f(\boldsymbol{v}, p_f)$ is*

$$\sigma_{ij} = -p_f \delta_{ij} + \mu\left(\frac{\partial v_i}{\partial x_j} + \frac{\partial v_j}{\partial x_i}\right), \qquad i, j = 1, 2, 3,$$

where δ_{ij} is the Kronecker delta. The shear stress components are σ_{12}, σ_{13} and σ_{23}, whereas σ_{11}, σ_{22} and σ_{33} are the normal stress components.

In a two dimensional space the maximum shear stress- an important parameter in studying the forces exerted on a fluid- is given by the expression [YHSC04]

$$\sigma_{max} = \sqrt{\left(\frac{\sigma_{11} - \sigma_{22}}{2}\right)^2 + \sigma_{12}^2}. \tag{4.6}$$

4.1.1 Variational Formulation of the FSI System

We seek to formulate Problem (4.5) in its weak formulation. This is achieved by deriving the weak formulation associated to each sub-problem using appropriate test functions that consider the boundary conditions and the coupling conditions as well. First, we deal with the formulation associated to the fluid sub-problem. Let us consider the following two functions in the Eulerian configuration

$$\boldsymbol{\eta}_f : \Omega_f(t) \to \mathbb{R}^3 \quad \text{and} \quad q_f : \Omega_f(t) \to \mathbb{R},$$

such that

$$\boldsymbol{\eta}_f \in V_f = \left\{\boldsymbol{\gamma} \in H^1(\Omega_f(t)), \boldsymbol{\gamma} = 0 \quad \text{on} \quad \Gamma_{\text{in}}(t)\right\} \qquad \text{and} \qquad q_f \in L^2(\Omega_f(t)).$$

In order to derive the variational formulation we multiply Equation $(4.5)_1$ by $\boldsymbol{\eta}_f \in V_f$. Then applying integration by parts and considering the boundary conditions yield

$$\begin{aligned} &\int_{\Omega_f(t)} \rho_f \partial_t \boldsymbol{v}|_{\boldsymbol{\mathcal{A}}} \cdot \boldsymbol{\eta}_f \; d\boldsymbol{x} + \int_{\Omega_f(t)} \rho_f (\boldsymbol{v} - \boldsymbol{w})^t \boldsymbol{\nabla}_{\boldsymbol{x}} \boldsymbol{v} \; \boldsymbol{\eta}_f \; d\boldsymbol{x} + \int_{\Omega_f(t)} \boldsymbol{\sigma}_f(\boldsymbol{v}, p_f) : \boldsymbol{\nabla}_{\boldsymbol{x}} \boldsymbol{\eta}_f \; d\boldsymbol{x} \\ &- \int_{\Gamma_c(t)} \boldsymbol{g}_f \cdot \boldsymbol{\eta}_f \; d\Gamma = \int_{\Omega_f(t)} \rho_f \boldsymbol{f}_f \cdot \boldsymbol{\eta}_f \; d\boldsymbol{x}. \end{aligned} \tag{4.7}$$

Further, multiplying the incompressibilty condition $(4.5)_2$ by a test function $q_f \in L^2(\Omega_f(t))$ we obtain

$$\int_{\Omega_f(t)} q_f \; \nabla_{\boldsymbol{x}} \cdot \boldsymbol{v} \; d\boldsymbol{x} = 0. \tag{4.8}$$

For the first term of (4.7) we use Reynolds' Transport theorem (A.1) with a change of variables to the reference configuration $\tilde{\Omega}_f$ to get

$$\begin{aligned}\int_{\Omega_f(t)} \rho_f \partial_t \boldsymbol{v}|_{\boldsymbol{\mathcal{A}}} \cdot \boldsymbol{\eta}_f \; d\boldsymbol{x} &= \int_{\tilde{\Omega}_f} \rho_f J_f \partial_t \tilde{\boldsymbol{v}} \cdot \tilde{\boldsymbol{\eta}}_f \; d\tilde{\boldsymbol{x}} \\ &= \frac{d}{dt} \int_{\tilde{\Omega}_f} J_f \rho_f \tilde{\boldsymbol{v}} \cdot \tilde{\boldsymbol{\eta}}_f \; d\tilde{\boldsymbol{x}} - \int_{\tilde{\Omega}_f} J_f \rho_f \; \nabla_{\tilde{\boldsymbol{x}}} \cdot \tilde{\boldsymbol{w}} \; \tilde{\boldsymbol{v}} \cdot \tilde{\boldsymbol{\eta}}_f \; d\tilde{\boldsymbol{x}} \\ &= \frac{d}{dt} \int_{\Omega_f(t)} \rho_f \boldsymbol{v} \cdot \boldsymbol{\eta}_f \; d\boldsymbol{x} - \int_{\Omega_f(t)} \rho_f (\nabla_{\boldsymbol{x}} \cdot \boldsymbol{w}) \; \boldsymbol{v} \cdot \boldsymbol{\eta}_f \; d\boldsymbol{x}\end{aligned}$$

For the stress tensor, using (A.4), we have

$$\int_{\Gamma_c(t)} \boldsymbol{\sigma}_f(\boldsymbol{v}, p_f) \boldsymbol{n}_f \cdot \boldsymbol{\eta}_f \; d\Gamma = \int_{\tilde{\Gamma}_c} J_f \tilde{\boldsymbol{\sigma}}_f(\tilde{\boldsymbol{v}}, \tilde{p}_f) \boldsymbol{F}_f^{-t} \tilde{\boldsymbol{n}}_f \cdot \tilde{\boldsymbol{\eta}}_f \; d\tilde{\Gamma} = \int_{\tilde{\Gamma}_c} J_f \tilde{\boldsymbol{g}}_f \cdot \tilde{\boldsymbol{\eta}}_f \; d\tilde{\Gamma}.$$

Substituting these two equations in the formulation (4.7)-(4.8) yields

$$\begin{aligned}&\frac{d}{dt} \int_{\Omega_f(t)} \rho_f \boldsymbol{v} \cdot \boldsymbol{\eta}_f \;\; d\boldsymbol{x} + \int_{\Omega_f(t)} \rho_f (\boldsymbol{v} - \boldsymbol{w})^t \boldsymbol{\nabla}_{\boldsymbol{x}} \boldsymbol{v} \cdot \boldsymbol{\eta}_f \; d\boldsymbol{x} - \int_{\Omega_f(t)} \rho_f \nabla_{\boldsymbol{x}} \cdot \boldsymbol{w} \; \boldsymbol{v} \cdot \boldsymbol{\eta}_f \; d\boldsymbol{x} \\ &+ \int_{\Omega_f(t)} \boldsymbol{\sigma}_f(\boldsymbol{v}, p_f) : \boldsymbol{\nabla}_{\boldsymbol{x}} \boldsymbol{\eta}_f \; d\boldsymbol{x} - \int_{\Gamma_c(t)} \boldsymbol{g}_f \cdot \boldsymbol{\eta}_f \; d\Gamma + \int_{\Omega_f(t)} q_f \; \nabla_{\boldsymbol{x}} \cdot \boldsymbol{v} \; d\boldsymbol{x} = \rho_f \int_{\Omega_f(t)} \boldsymbol{f}_f \cdot \boldsymbol{\eta}_f \; d\boldsymbol{x}.\end{aligned} \tag{4.9}$$

On the other hand, to derive the variational formulation associated to the structure sub-problem, we introduce the following functional space

$$\tilde{V}_s = \left\{ \tilde{\boldsymbol{\eta}}_s \in H^1(\tilde{\Omega}_s), \tilde{\boldsymbol{\eta}}_s = 0 \quad \text{on } \tilde{\Gamma}_2 \right\}.$$

Multiplying Equation $(4.5)_6$ by a test function $\tilde{\boldsymbol{\eta}}_s$ in $\tilde{V}_s$, then integrating by parts yields

$$\int_{\tilde{\Omega}_s} \boldsymbol{P} : \boldsymbol{\nabla}_{\tilde{\boldsymbol{x}}} \tilde{\boldsymbol{\eta}}_s \; d\tilde{\boldsymbol{x}} + \int_{\tilde{\Omega}_s} \tilde{p}_{hs} \mathrm{cof}(\boldsymbol{F_s}) : \boldsymbol{\nabla}_{\tilde{\boldsymbol{x}}} \tilde{\boldsymbol{\eta}}_s \; d\tilde{\boldsymbol{x}} - \int_{\tilde{\Gamma}_c} \boldsymbol{P}_{\text{inc}} \; \tilde{\boldsymbol{n}}_s \cdot \tilde{\boldsymbol{\eta}}_s \; d\tilde{\Gamma} = \int_{\tilde{\Omega}_s} J_s \tilde{\rho}_s \tilde{\boldsymbol{f}}_s \cdot \tilde{\boldsymbol{\eta}}_s \; d\tilde{\boldsymbol{x}}. \tag{4.10}$$

Further, multiplying the incompressibilty condition $(4.5)_7$ by a test function $\tilde{q}_s \in L^2(\tilde{\Omega}_s)$ gives

$$\int_{\tilde{\Omega}_s} \tilde{q}_s (J_s - 1) \; d\tilde{\boldsymbol{x}} = 0. \tag{4.11}$$

As a result, the variational formulation associated to the structure sub-problem is
Find $(\tilde{\boldsymbol{\xi}}_{\boldsymbol{s}}, \tilde{p}_{hs}) \in \tilde{V}_s \times L^2(\tilde{\Omega}_s)$ satisfying

$$\begin{cases} \displaystyle\int_{\tilde{\Omega}_s} \boldsymbol{P} : \boldsymbol{\nabla} \tilde{\boldsymbol{\eta}}_s \; d\tilde{\boldsymbol{x}} + \int_{\tilde{\Omega}_s} \tilde{p}_{hs} \mathrm{cof}(\boldsymbol{F_s}) : \boldsymbol{\nabla} \tilde{\boldsymbol{\eta}}_{\boldsymbol{s}} \; d\tilde{\boldsymbol{x}} \\ \displaystyle - \int_{\tilde{\Gamma}_c} J_s \tilde{\boldsymbol{g}}_{\boldsymbol{s}} \cdot \tilde{\boldsymbol{\eta}}_{\boldsymbol{s}} \; d\tilde{\Gamma} - \int_{\tilde{\Omega}_s} J_s \tilde{\rho}_s \tilde{\boldsymbol{f}}_s \cdot \tilde{\boldsymbol{\eta}}_{\boldsymbol{s}} \; d\tilde{\boldsymbol{x}} = 0 \qquad \forall \; \tilde{\boldsymbol{\eta}}_{\boldsymbol{s}} \in \tilde{V}_s, \\ \displaystyle\int_{\tilde{\Omega}_s} \tilde{q}_s (J_s - 1) d\tilde{\boldsymbol{x}} = 0 \qquad \forall \; \tilde{q}_s \in L^2(\tilde{\Omega}_s). \end{cases} \tag{4.12}$$

To sum up, the variational formulation associated to System (4.5) is
Find

$$\begin{aligned}
&\tilde{\boldsymbol{v}} : \tilde{\Omega}_f \times \mathbb{R}^+ \longrightarrow \mathbb{R}^3,\\
&\tilde{p}_f : \tilde{\Omega}_f \times \mathbb{R}^+ \longrightarrow \mathbb{R},\\
&\tilde{\boldsymbol{\xi}}_{\boldsymbol{f}} : \tilde{\Omega}_f \times \mathbb{R}^+ \longrightarrow \mathbb{R}^3,\\
&\tilde{\boldsymbol{\xi}}_s : \tilde{\Omega}_s \times \mathbb{R}^+ \longrightarrow \mathbb{R}^3,\\
&\tilde{p}_{hs} : \tilde{\Omega}_s \times \mathbb{R}^+ \longrightarrow \mathbb{R},
\end{aligned}$$

such that

$$\begin{array}{lll}
\tilde{\boldsymbol{\xi}}_f = \mathcal{E}xt(\tilde{\boldsymbol{\xi}}_s|_{\tilde{\Gamma}_c}) \text{ and } \tilde{\boldsymbol{w}} = \dfrac{\partial \tilde{\xi}_f}{\partial t} & \text{in} & \tilde{\Omega}_f,\\
\boldsymbol{v} = \boldsymbol{w} & \text{on} & \Gamma_c(t),\\
\tilde{\boldsymbol{\xi}}_s = 0 & \text{on} & \tilde{\Gamma}_2.
\end{array} \tag{4.13}$$

and

$$\begin{cases}
\rho_f \displaystyle\int_{\Omega_f(t)} \frac{\partial \boldsymbol{v}}{\partial t}\Big|_{\boldsymbol{\mathcal{A}}} \cdot \boldsymbol{\eta}_f \;\; d\boldsymbol{x} + \rho_f \int_{\Omega_f(t)} (\boldsymbol{v} - \boldsymbol{w})^t \boldsymbol{\nabla}_{\boldsymbol{x}} \boldsymbol{v} \cdot \boldsymbol{\eta}_f \; d\boldsymbol{x}\\
+ \displaystyle\int_{\Omega_f(t)} \boldsymbol{\sigma}_f(\boldsymbol{v}, p_f) : \boldsymbol{\nabla}_{\boldsymbol{x}} \boldsymbol{\eta}_f \; d\boldsymbol{x} - \int_{\Gamma_c(t)} \boldsymbol{g}_f \cdot \boldsymbol{\eta}_f \; d\Gamma = \rho_f \int_{\Omega_f(t)} \boldsymbol{f}_f \cdot \boldsymbol{\eta}_f \; d\boldsymbol{x},\\
\displaystyle\int_{\Omega_f(t)} q_f \; \nabla_{\boldsymbol{x}} \cdot \boldsymbol{v} \; d\boldsymbol{x} = 0,
\end{cases} \tag{4.14}$$

$$\begin{cases}
\displaystyle\int_{\tilde{\Omega}_s} \boldsymbol{P} : \boldsymbol{\nabla}_{\tilde{\boldsymbol{x}}} \tilde{\boldsymbol{\eta}}_s \; d\tilde{\boldsymbol{x}} + \int_{\tilde{\Omega}_s} \tilde{p}_{hs} \; \mathrm{cof}(\boldsymbol{F}_s) : \boldsymbol{\nabla}_{\tilde{\boldsymbol{x}}} \tilde{\boldsymbol{\eta}}_s \; d\tilde{\boldsymbol{x}}\\
- \displaystyle\int_{\tilde{\Gamma}_c} \tilde{\boldsymbol{g}}_s \cdot \tilde{\boldsymbol{\eta}}_s \; d\tilde{\Gamma} = \rho_s \int_{\tilde{\Omega}_s} J_s \tilde{\boldsymbol{f}}_s \cdot \tilde{\boldsymbol{\eta}}_s \; d\tilde{\boldsymbol{x}},\\
\displaystyle\int_{\tilde{\Omega}_s} \tilde{q}_s \; (J_s - 1) \; d\tilde{\boldsymbol{x}} = 0,
\end{cases} \tag{4.15}$$

for all $(\boldsymbol{\eta}_f, q_f) \in V_f \times L^2(\Omega_f(t))$ and $(\tilde{\boldsymbol{\eta}}_s, \tilde{q}_s) \in \tilde{V}_s \times L^2(\tilde{\Omega}_s)$. The coupling conditions on the interface $\tilde{\Gamma}_c$ are given in the strong form as

$$\begin{cases}
\boldsymbol{v} \circ \boldsymbol{\mathcal{A}} = \partial_t \tilde{\boldsymbol{\xi}},\\
\tilde{\boldsymbol{g}}_s = -\tilde{\boldsymbol{g}}_f.
\end{cases} \tag{4.16}$$

4.1.2 The Discrete Variational Formulation of the FSI Problem

The variational formulation (4.13)-(4.16) of the FSI stands for the incompressible homogeneous Navier-Stokes equations coupled with the quasi-static incompressible elasticity equation. We assume that no external forces are exerted on neither the fluid domain nor the structure domain, i.e, $\boldsymbol{f}_f = 0$ and $\tilde{\boldsymbol{f}}_s = 0$. Consider a time step $\Delta t > 0$ and finite element partitions

$\mathcal{V}_h$ and $\mathcal{W}_h$ for the fluid and the structure sub-domains respectively of maximum diameter denoted by h. Our aim is to approximate the solution $(\boldsymbol{v}, p_f, \tilde{\boldsymbol{\xi}}_s, \boldsymbol{\mathcal{A}}, \tilde{p}_{hs})$ at time $t_n = n\Delta t$, for $n \in \mathbb{N}$, in the finite element spaces. The approximation of the solution at time t_n is denoted by $(\boldsymbol{v}^n, p_f^n, \tilde{\boldsymbol{\xi}}_s^n, \boldsymbol{\mathcal{A}}^n, \tilde{p}_{hs}^n)$. The variational formulations associated to the fluid and the structure sub-problems are respectively given by

$$\begin{aligned} &\rho_f \int_{\Omega_f(t)} \frac{\partial \boldsymbol{v}}{\partial t}\Big|_{\boldsymbol{\mathcal{A}}} \cdot \boldsymbol{\eta}_f \; d\boldsymbol{x} + \rho_f \int_{\Omega_f(t)} (\boldsymbol{v} - \boldsymbol{w})^t \boldsymbol{\nabla}_{\boldsymbol{x}} \boldsymbol{v} \cdot \boldsymbol{\eta}_f \; d\boldsymbol{x} + \int_{\Omega_f(t)} \boldsymbol{\sigma}_f(\boldsymbol{v}, p_f) : \boldsymbol{\nabla}_{\boldsymbol{x}} \boldsymbol{\eta}_f \; d\boldsymbol{x} \\ &- \int_{\Gamma_c(t)} \boldsymbol{g}_f \cdot \boldsymbol{\eta}_f \; d\Gamma + \int_{\Omega_f(t)} q_f \; \nabla_{\boldsymbol{x}} \cdot \boldsymbol{v} \; d\boldsymbol{x} = 0 \end{aligned} \tag{4.17}$$

and

$$\begin{aligned} &\int_{\tilde{\Omega}_s} \boldsymbol{P} : \boldsymbol{\nabla}_{\tilde{\boldsymbol{x}}} \tilde{\boldsymbol{\eta}}_s \; d\tilde{\boldsymbol{x}} + \int_{\tilde{\Omega}_s} \tilde{p}_{hs} \; \mathrm{cof}(\boldsymbol{F}_s) : \boldsymbol{\nabla}_{\tilde{\boldsymbol{x}}} \tilde{\boldsymbol{\eta}}_s \; d\tilde{\boldsymbol{x}} - \int_{\tilde{\Gamma}_c} \tilde{\boldsymbol{g}}_s \cdot \tilde{\boldsymbol{\eta}}_s \; d\tilde{\Gamma} \\ &+ \int_{\tilde{\Omega}_s} \tilde{q}_s \; (J_s - 1) \; d\tilde{\boldsymbol{x}} = 0 \end{aligned} \tag{4.18}$$

with

$$\begin{cases} \boldsymbol{v} = \boldsymbol{w} & \text{on } \Gamma_c(t), \\ \boldsymbol{g}_f = -\boldsymbol{g}_s & \text{on } \Gamma_c(t). \end{cases} \tag{4.19}$$

Semi-Discretization in Time of the Fluid Sub-Problem

In order to guarantee the existence and uniqueness of the solution of the fluid sub-problem when performing the numerical simulations, we use the penalty method. This method consists of replacing the natural weak formulation by a regular one by adding a term multiplied by a sufficiently small parameter $\epsilon \ll 1$. Indeed, writing the modified formulation in a matrix form results a positive definite matrix, which assures the existence and the uniqueness of the solution of the discrete sub-problem. The weak formulation associated to the Navier-Stokes equations obtained upon adding a negligible parameter ϵ is then semi-discretized in time, that is, the convective term is considered at the instant t_n, whereas other terms are considered at time t_{n+1}. The discrete formulation reads

$$\begin{aligned} &\rho_f \frac{1}{\Delta t} \int_{\Omega_f(t_n)} \boldsymbol{v}^{n+1} \cdot \boldsymbol{\eta}_f \; d\boldsymbol{x} + \rho_f \frac{1}{\Delta t} \int_{\Omega_f(t_n)} (\boldsymbol{v}^n \circ \boldsymbol{X}^n) \cdot \; \boldsymbol{\eta}_f \;\; d\boldsymbol{x} + 2 \int_{\Omega_f(t_n)} \mu^n \boldsymbol{D}(\boldsymbol{v}^{n+1}) : \boldsymbol{\nabla}_{\boldsymbol{x}} \boldsymbol{\eta}_f \; d\boldsymbol{x} \\ &- \rho_f \int_{\Omega_f(t_n)} (\boldsymbol{w}^{n+1})^t \boldsymbol{\nabla}_{\boldsymbol{x}} \boldsymbol{v}^{n+1} \cdot \boldsymbol{\eta}_f \; d\boldsymbol{x} - \int_{\Omega_f(t_n)} p_f^{n+1} \; \nabla_{\boldsymbol{x}} \cdot \boldsymbol{\eta}_f \; d\boldsymbol{x} - \int_{\Gamma_c(t_n)} \boldsymbol{g}_f^{n+1} \cdot \boldsymbol{\eta}_f \; d\Gamma \\ &+ \int_{\Omega_f(t_n)} q_f \; \nabla_{\boldsymbol{x}} \cdot \boldsymbol{v}^{n+1} \; d\boldsymbol{x} + \int_{\Omega_f(t_n)} \epsilon \; p_f^{n+1} q_f \; d\boldsymbol{x} = 0. \end{aligned} \tag{4.20}$$

The non-linear convective term $\dfrac{1}{\Delta t}(\boldsymbol{v}^n \circ \boldsymbol{X}^n)$ can be approximated by

$$\frac{1}{\Delta t}\Big[\boldsymbol{v}\big(\boldsymbol{x} - \boldsymbol{v}(\boldsymbol{x}, t_n)\Delta t, t_n\big)\Big] \tag{4.21}$$

which is computed in the FreeFem++ using the *convective* operator as indicated in Remark 4.1.3.
Notice that, since the strain rate tensor $\boldsymbol{D}(\boldsymbol{v})$ is symmetric, then we have $\boldsymbol{D}(\boldsymbol{v}) : \boldsymbol{\nabla}\boldsymbol{\eta}_f = \boldsymbol{D}(\boldsymbol{v}) : \boldsymbol{D}(\boldsymbol{\eta}_f)$ which gives

$$\int_{\Omega_f(t_n)} \mu^n \boldsymbol{D}(\boldsymbol{v}^{n+1}) : \boldsymbol{\nabla}_{\boldsymbol{x}}\boldsymbol{\eta}_f \; d\boldsymbol{x} = \int_{\Omega_f(t_n)} \mu^n \boldsymbol{D}(\boldsymbol{v}^{n+1}) : \boldsymbol{D}(\boldsymbol{\eta}_f) \; d\boldsymbol{x}.$$

Remark 4.1.3 1. *If the fluid is considered to be Newtonian, then its dynamic viscosity μ is constant. Thus, the viscosity term is*

$$\int_{\Omega_f(t_n)} \mu^n \boldsymbol{D}(\boldsymbol{v}^{n+1}) : \boldsymbol{D}(\boldsymbol{\eta}_f) \; d\boldsymbol{x} = \mu \int_{\Omega_f(t_n)} \boldsymbol{D}(\boldsymbol{v}^{n+1}) : \boldsymbol{D}(\boldsymbol{\eta}_f) \; d\boldsymbol{x}.$$

2. *In the two dimensional space, when performing numerical simulations at a time step t_n, the non-linear convective term is eliminated using the approximation of the convection part by the term*

$$\frac{1}{\Delta t}(\boldsymbol{v}^n \circ \boldsymbol{X}^n)(\boldsymbol{x}) \equiv \frac{1}{\Delta t} v\big(\boldsymbol{X}(\boldsymbol{x}, t_n), t_n\big) \qquad \forall\; \boldsymbol{x} \in \Omega_f(t_n),$$

where

- *Δt represents the time step.*
- *$\boldsymbol{X}^n(\boldsymbol{x}) \equiv \boldsymbol{X}(\boldsymbol{x}, t_n)$, is an approximation at $t = n\Delta t$ of the solution of the following ordinary differential (ODE) equation*

$$\begin{cases} \dot{\boldsymbol{X}}(\boldsymbol{x}, t) = \dfrac{d\boldsymbol{X}}{dt}(\boldsymbol{x}, t) = \boldsymbol{v}(\boldsymbol{X}(\boldsymbol{x}, t), t_n), \\ \boldsymbol{X}(\boldsymbol{x}, t_n) = \boldsymbol{x}, \end{cases} \tag{4.22}$$

with $\boldsymbol{v}(\boldsymbol{x}, t_n) = \big(v_1(\boldsymbol{x}, t_n), v_2(\boldsymbol{x}, t_n)\big)$.
Using Taylor's expansion, we get the approximation

$$\boldsymbol{v}^n(\boldsymbol{X}^n(\boldsymbol{x})) \approx convect\big([v_i^n, v_j^n], -\Delta t, \boldsymbol{v}^n\big), \;\; i, j \in \{1, 2\}, \;\; i \neq j. \tag{4.23}$$

For the computational details the reader can refer to [Hec05, Section 9.5, p. 267].

The Weak Formulation of the Structure Sub-Problem

To deal with the structure sub-problem at the time iteration t_{n+1}, we will solve the non-linear problem (4.12) using Newton-Raphson method. The variational formulation associated to the structure sub-problem at the iteration t_{n+1} is

$$\begin{cases} \displaystyle\int_{\tilde{\Omega}_s} \boldsymbol{P}^{n+1} : \boldsymbol{\nabla}\tilde{\boldsymbol{\eta}}_{\boldsymbol{s}} \; d\tilde{\boldsymbol{x}} + \int_{\tilde{\Omega}_s} \tilde{p}_{hs}^{n+1} \mathrm{cof}(\boldsymbol{F}_s^{n+1}) : \boldsymbol{\nabla}\tilde{\boldsymbol{\eta}}_{\boldsymbol{s}} \; d\tilde{\boldsymbol{x}} \\ \displaystyle -\int_{\tilde{\Gamma}_c} J_s^{n+1} \tilde{\boldsymbol{g}}_s^{n+1} \cdot \tilde{\boldsymbol{\eta}}_{\boldsymbol{s}} \; d\tilde{\Gamma} - \int_{\tilde{\Omega}_s} J_s^{n+1} \tilde{\rho}_s \tilde{\boldsymbol{f}}_s \cdot \tilde{\boldsymbol{\eta}}_{\boldsymbol{s}} \; d\tilde{\boldsymbol{x}} = 0 \qquad \forall\; \tilde{\boldsymbol{\eta}}_{\boldsymbol{s}} \in \tilde{V}_s, \\ \displaystyle\int_{\tilde{\Omega}_s} \tilde{q}_s (J_s^{n+1} - 1) \; d\tilde{\boldsymbol{x}} = 0, \qquad \forall\; \tilde{q}_s \in L^2(\tilde{\Omega}_s). \end{cases} \tag{4.24}$$

The method depends on linearizing the structure sub-problem (4.24) with respect to the unknowns $\boldsymbol{\varphi}_s$ and $\tilde{p}_{hs}$. We start initialization by considering a suitable choice of the initial values $(\boldsymbol{\varphi}_{s,0}, \tilde{p}_{hs,0})$. In particular, we link the iterations of the Newton-Raphson method to the time iteration t_n by considering $\boldsymbol{\varphi}_{s,0} = \boldsymbol{\varphi}_s^n$ and $\tilde{p}_{hs,0} = \tilde{p}_{hs}^n$. Then, we solve iteratively the obtained system corresponding to the Newton-Raphson method until its solution converges to a solution of the non-linear System (4.12). For simplicity of notation, we omit the subscript s of the deformation $\boldsymbol{\varphi}_s$, that is, we write $\boldsymbol{\varphi}_s \equiv \boldsymbol{\varphi}$. We proceed to derive the formulation of the structure sub-problem corresponding to the Newton-Raphson method.
Let us define the following space

$$\mathcal{Z} = \{\boldsymbol{\varphi} = (\varphi_1, \varphi_2, \varphi_3) : \tilde{\Omega}_s \longmapsto \mathbb{R}^3, \boldsymbol{\varphi} = \boldsymbol{\varphi}^n \text{ on } \tilde{\Gamma}_c \text{ and } \boldsymbol{\varphi} = 0 \text{ on } \tilde{\Gamma}_2\}.$$

Given $N \in \mathbb{N}$, a tolerance *tol* and

$$(\boldsymbol{\varphi}_0, \tilde{p}_{hs,0}) \in \mathcal{Z} \times L^2(\tilde{\Omega}_s)$$

we construct iteratively the two sequences $(\boldsymbol{\varphi}_k)_{k\geq 1}$ and $(\tilde{p}_{hs,k})_{k\geq 1}$ by solving for $(\delta\boldsymbol{\varphi}_k, \delta\tilde{p}_{hs,k})$ the following system
Set $\boldsymbol{\varphi}_0 = \boldsymbol{\varphi}^n$. Repeat: for $0 \leq k \leq N$, while $||\delta\boldsymbol{\varphi}_k||_2 \geq tol$, find $(\delta\boldsymbol{\varphi}_k, \delta\tilde{p}_{hs,k})$ in $\mathcal{Z} \times L^2(\tilde{\Omega}_s)$ satisfying

$$\begin{cases} \displaystyle\int_{\tilde{\Omega}_s} \frac{\partial \boldsymbol{P}}{\partial \boldsymbol{F}_s}(\boldsymbol{\nabla}_{\tilde{\boldsymbol{x}}}\boldsymbol{\varphi}_k)\boldsymbol{\nabla}_{\tilde{\boldsymbol{x}}}\delta\boldsymbol{\varphi}_k : \boldsymbol{\nabla}_{\tilde{\boldsymbol{x}}}\tilde{\boldsymbol{\eta}}_s \, d\tilde{\boldsymbol{x}} + \int_{\tilde{\Omega}_s} \tilde{p}_{hs,k} \frac{\partial \mathrm{cof}}{\partial \boldsymbol{F}_s}(\boldsymbol{\nabla}_{\tilde{\boldsymbol{x}}}\boldsymbol{\varphi}_k)\boldsymbol{\nabla}_{\tilde{\boldsymbol{x}}}\delta\boldsymbol{\varphi}_k : \boldsymbol{\nabla}_{\tilde{\boldsymbol{x}}}\tilde{\boldsymbol{\eta}}_s \, d\tilde{\boldsymbol{x}} \\ \displaystyle + \int_{\tilde{\Omega}_s} \delta\tilde{p}_{hs,k} \, \mathrm{cof}(\boldsymbol{\nabla}_{\tilde{\boldsymbol{x}}}\boldsymbol{\varphi}_k) : \boldsymbol{\nabla}_{\tilde{\boldsymbol{x}}}\tilde{\boldsymbol{\eta}}_s \, d\tilde{\boldsymbol{x}} - \int_{\tilde{\Gamma}_c} \tilde{\boldsymbol{\sigma}}_{s,k}(\tilde{\boldsymbol{x}}) \frac{\partial \mathrm{cof}}{\partial \boldsymbol{F}_s}(\boldsymbol{\nabla}_{\tilde{\boldsymbol{x}}}\boldsymbol{\varphi}_k) : \boldsymbol{\nabla}_{\tilde{\boldsymbol{x}}}\delta\boldsymbol{\varphi}_k \, \tilde{\boldsymbol{n}}_s \cdot \tilde{\boldsymbol{\eta}}_s \, d\tilde{\Gamma} \\ \displaystyle + \int_{\tilde{\Omega}_s} \boldsymbol{P}(\boldsymbol{\nabla}_{\tilde{\boldsymbol{x}}}\boldsymbol{\varphi}_k) : \boldsymbol{\nabla}_{\tilde{\boldsymbol{x}}}\tilde{\boldsymbol{\eta}}_s \, d\tilde{\boldsymbol{x}} + \int_{\tilde{\Omega}_s} \tilde{p}_{hs,k} \, \mathrm{cof}(\boldsymbol{\nabla}_{\tilde{\boldsymbol{x}}}\boldsymbol{\varphi}_k) : \boldsymbol{\nabla}_{\tilde{\boldsymbol{x}}}\tilde{\boldsymbol{\eta}}_s \, d\tilde{\boldsymbol{x}} - \int_{\tilde{\Gamma}_c} \tilde{\boldsymbol{\sigma}}_{s,k}(\tilde{\boldsymbol{x}}) \, \tilde{\boldsymbol{n}}_s \cdot \tilde{\boldsymbol{\eta}}_s \, d\tilde{\Gamma} = 0 \\ \displaystyle \int_{\tilde{\Omega}_s} \tilde{q}_s \, \mathrm{cof}(\boldsymbol{\nabla}_{\tilde{\boldsymbol{x}}}\boldsymbol{\varphi}_k) : \boldsymbol{\nabla}_{\tilde{\boldsymbol{x}}}\delta\boldsymbol{\varphi}_k \, d\tilde{\boldsymbol{x}} + \int_{\tilde{\Omega}_s} \tilde{q}_s(J_{s,k} - 1) \, d\tilde{\boldsymbol{x}} = 0 \end{cases} \tag{4.25}$$

for all $(\tilde{\boldsymbol{\eta}}_s, \tilde{q}_s) \in \tilde{V}_s \times L^2(\tilde{\Omega}_s)$.
Set $\boldsymbol{\varphi}_{k+1} = \delta\boldsymbol{\varphi}_k + \boldsymbol{\varphi}_k$ and $k = k + 1$.

When the condition $||\delta\boldsymbol{\varphi}_k||_2 < tol$ is fulfilled then convergence of the Newton-Raphson method is achieved. Thus, the solution of the structure sub-problem (4.24) is given by $\boldsymbol{\varphi}^{n+1} = \boldsymbol{\varphi}_k$, for the last value of k for which the Newton-Raphson method converges.

Omitting the subscript k- as it is known from the context- the final variational formulation of the problem (4.25) is given by

$$\begin{cases} \text{Find } (\delta\boldsymbol{\varphi}, \delta\tilde{p}_{hs}) \in \mathcal{Z} \times L^2(\tilde{\Omega}_s), \text{such that } \forall \ (\tilde{\boldsymbol{\eta}}_s, \tilde{q}_s) \in \tilde{V}_s \times L^2(\tilde{\Omega}_s) \text{ we have} \\ a_s(\delta\boldsymbol{\varphi}, \tilde{\boldsymbol{\eta}}_s) + b_s(\tilde{\boldsymbol{\eta}}_s, \delta\tilde{p}_{hs}) = l(\tilde{\boldsymbol{\eta}}_s), \\ b_s(\delta\boldsymbol{\varphi}, \tilde{q}_s) = j(\tilde{q}_s). \end{cases} \tag{4.26}$$

where

$$
\begin{aligned}
a_s(\boldsymbol{\varsigma},\tilde{\boldsymbol{\eta}}_s) = &\int_{\tilde{\Omega}_s} \frac{\partial \boldsymbol{P}}{\partial \boldsymbol{F}_s}(\boldsymbol{\nabla}\boldsymbol{\varphi})\boldsymbol{\nabla}\boldsymbol{\varsigma} : \boldsymbol{\nabla}\tilde{\boldsymbol{\eta}}_s \, d\tilde{\boldsymbol{x}} + \int_{\tilde{\Omega}_s} \tilde{p}_{hs} \frac{\partial \mathrm{cof}}{\partial \boldsymbol{F}_s}(\boldsymbol{\nabla}\boldsymbol{\varphi})\boldsymbol{\nabla}\boldsymbol{\varsigma} : \boldsymbol{\nabla}\tilde{\boldsymbol{\eta}}_s \, d\tilde{\boldsymbol{x}} \\
&- \int_{\tilde{\Gamma}_c} \tilde{\boldsymbol{\sigma}}_s(\tilde{\boldsymbol{x}}) \frac{\partial \mathrm{cof}}{\partial \boldsymbol{F}_s}(\boldsymbol{\nabla}\boldsymbol{\varphi}) : \boldsymbol{\nabla}\boldsymbol{\varsigma} \; \boldsymbol{n}_s \cdot \tilde{\boldsymbol{\eta}}_s \, d\tilde{\Gamma}
\end{aligned}
\tag{4.27}
$$

$$
b_s(\tilde{\boldsymbol{\eta}}_s, \tilde{q}_s) = \int_{\tilde{\Omega}_s} \tilde{q}_s \; \mathrm{cof}(\boldsymbol{\nabla}\boldsymbol{\varphi}) : \boldsymbol{\nabla}\tilde{\boldsymbol{\eta}}_s \, d\tilde{\boldsymbol{x}} \tag{4.28}
$$

$$
l(\tilde{\boldsymbol{\eta}}_s) = -\int_{\tilde{\Omega}_s} \boldsymbol{P}(\boldsymbol{\nabla}\boldsymbol{\varphi}) : \boldsymbol{\nabla}\tilde{\boldsymbol{\eta}}_s \, d\tilde{\boldsymbol{x}} - \int_{\tilde{\Omega}_s} \tilde{p}_{hs} \; \mathrm{cof}(\boldsymbol{\nabla}\boldsymbol{\varphi}) : \boldsymbol{\nabla}\tilde{\boldsymbol{\eta}}_s \, d\tilde{\boldsymbol{x}} + \int_{\tilde{\Gamma}_c} \tilde{\boldsymbol{\sigma}}_s(\tilde{\boldsymbol{x}}) \; \cdot \tilde{\boldsymbol{\eta}}_s \, d\tilde{\Gamma} \tag{4.29}
$$

$$
j(\tilde{q}) = -\int_{\tilde{\Omega}_s} \tilde{q}\big(\det(\boldsymbol{\nabla}\boldsymbol{\varphi}) - 1\big) \, d\tilde{\boldsymbol{x}} \tag{4.30}
$$

with

$$
a_s : \mathcal{Z} \times \mathcal{Z} \longmapsto \mathbb{R} \quad \text{and} \quad b_s : \mathcal{Z} \times L^2(\tilde{\Omega}_s) \longmapsto \mathbb{R}
$$

are bilinear forms. Further,

$$
l \in \mathcal{Z}^* \quad \text{and} \quad j \in (L^2(\tilde{\Omega}_s))^* \equiv L^2(\tilde{\Omega}_s).
$$

To ensure the existence of the solution for the structure sub-problem (4.26) we use the penalty method by modifying System (4.26)through adding the penalized term $\epsilon \int_{\tilde{\Omega}_s} \tilde{p}_{hs}\tilde{q}_s \, d\tilde{\boldsymbol{x}}$ with $\epsilon \ll 1$.
A rewriting of the new system in a matrix form yield a positive definite matrix.
Further, the solution of the system converges to a solution of the original system. Therefore, we seek to solve the following system

$$
\begin{cases}
\text{Find } (\delta\boldsymbol{\varphi}, \delta\tilde{p}_{hs}) \in \mathcal{Z} \times L^2(\tilde{\Omega}_s), \text{ such that } \forall \; (\tilde{\boldsymbol{\eta}}_s, \tilde{q}_s) \in \tilde{V}_s \times L^2(\tilde{\Omega}_s) \text{ , we have} \\
a_s(\delta\boldsymbol{\varphi}, \tilde{\boldsymbol{\eta}}_s) + b_s(\tilde{\boldsymbol{\eta}}_s, \delta\tilde{p}_{hs}) = l(\tilde{\boldsymbol{\eta}}_s), \\
b_s(\delta\boldsymbol{\varphi}, \tilde{q}_s) + \epsilon h_s(p_{hs}, \tilde{q}_s) = j(\tilde{q}_s).
\end{cases}
\tag{4.31}
$$

with $h_s(\tilde{p}_{hs}, \tilde{q}_s) = \displaystyle\int_{\tilde{\Omega}_s} \tilde{p}_{hs}\tilde{q}_s \, d\tilde{\boldsymbol{x}}$.

Space Discretization

Space discretization of the variational formulation is carried out using the finite element method (FEM) [GR86]. We consider the two finite element spaces associated to the fluid weak formulation

$$
V_h^f \subset V_f \text{ and } W_h^f \subset L^2(\Omega_f)
$$

and those associated to the structures weak formulation

$$\tilde{V}_h^s \subset \tilde{V}_s \text{ and } \tilde{W}_h^s \subset L^2(\tilde{\Omega}_s),$$

where V_h^f, W_h^f, $\tilde{V}_h^s$ and $\tilde{W}_h^s$ are finite dimensional subspaces described as follows

$$\begin{aligned}
V_h^f &= \{\boldsymbol{\eta}_h^f : \boldsymbol{\eta}_h^f = \eta_1^f \psi_1 + \ldots + \eta_N^f \psi_N\} &&\subset V_f,\\
W_h^f &= \{q_h^f : q_h^f = q_1^f \phi_1 + \ldots + q_N^f \phi_N\} &&\subset L^2(\Omega_f),\\
\tilde{V}_h^s &= \{\tilde{\boldsymbol{\eta}}_h^s : \tilde{\boldsymbol{\eta}}_h^s = \eta_1^s \vartheta_1 + \ldots + \eta_N^s \vartheta_N\} &&\subset \tilde{V}_s,\\
\tilde{W}_h^s &= \{\tilde{q}_h^s : \tilde{q}_h^s = q_1^s \theta_1 + \ldots + q_N^s \theta_N\} &&\subset L^2(\tilde{\Omega}_s)
\end{aligned}$$

with $\{\psi_i\}_i, \{\phi_i\}_i, \{\vartheta_i\}_i$ and $\{\theta_i\}_i$ are families of linearly independent functions of compact support, which are piecewise polynomials, i.e, of degree one or two depending on the accuracy we seek for the approximate solution. More precisely, the functional spaces associated to the velocity and displacement fields are considered to be P_2, whereas those associated to the pressures (fluid and hydrostatic) are considered to be P_1. In what follows, all terms are discretized in space as mentioned above, so that the approximation of solution in finite element spaces is $(\boldsymbol{v}_h, p_h^f, \tilde{\boldsymbol{\xi}}_h^s, \tilde{p}_h^{hs}, \boldsymbol{\mathcal{A}}_h)$ verifying (4.17)-(4.19), though, for simplicity the subscript h is omitted in the context.

Finally, the discrete variational formulation reads:

Given $(\boldsymbol{v}^n, p_f^n, \tilde{\boldsymbol{\xi}}_s^n, \tilde{p}_{hs}^n, \boldsymbol{\mathcal{A}}^n)$ and a tolerance tol, find $(\boldsymbol{v}^{n+1}, p_f^{n+1}, \tilde{\boldsymbol{\xi}}_s^{n+1}, \tilde{p}_{hs}^{n+1}, \boldsymbol{\mathcal{A}}^{n+1})$ such that

$$\begin{cases}
\boldsymbol{\mathcal{A}}^{n+1} = \tilde{\boldsymbol{x}} + \mathcal{E}xt(\tilde{\boldsymbol{\xi}}_s^{n+1}|_{\tilde{\Gamma}_c}) & \text{in } \tilde{\Omega}_f\\
\tilde{\boldsymbol{w}}^{n+1} = \dfrac{1}{\Delta t}(\tilde{\boldsymbol{\xi}}_f^{n+1} - \tilde{\boldsymbol{\xi}}_f^n) \simeq \partial_t \tilde{\boldsymbol{\xi}}_f^{n+1} & \text{in } \tilde{\Omega}_f,\\
\boldsymbol{w}^{n+1} = \partial_t \boldsymbol{\mathcal{A}}^{n+1} \circ (\boldsymbol{\mathcal{A}}^{n+1})^{-1} & \text{on } \boldsymbol{\mathcal{A}}^{n+1}(\tilde{\Gamma}_c),\\
\tilde{\boldsymbol{\xi}}_s^{n+1} = 0 & \text{on } \tilde{\Gamma}_2,
\end{cases} \tag{4.32}$$

$$\begin{aligned}
&\rho_f \frac{1}{\Delta t} \int_{\Omega_f(t_n)} \boldsymbol{v}^{n+1} \cdot \boldsymbol{\eta}^f \, d\boldsymbol{x} + \rho_f \frac{1}{\Delta t} \int_{\Omega_f(t_n)} (\boldsymbol{v}^n \circ \boldsymbol{X}^n) \cdot \boldsymbol{\eta}^f \, d\boldsymbol{x} - \rho_f \int_{\Omega_f(t_n)} (\boldsymbol{w}^{n+1})^t \boldsymbol{\nabla}_{\boldsymbol{x}} \boldsymbol{v}^{n+1} \cdot \boldsymbol{\eta}^f \, d\boldsymbol{x}\\
&+ 2 \int_{\Omega_f(t_n)} \mu^n \boldsymbol{D}(\boldsymbol{v}^{n+1}) : \boldsymbol{\nabla}_{\boldsymbol{x}} \boldsymbol{\eta}^f \, d\boldsymbol{x} - \int_{\Omega_f(t_n)} p_f^{n+1} \, \nabla_{\boldsymbol{x}} \cdot \boldsymbol{\eta}^f \, d\boldsymbol{x} - \int_{\Gamma_c(t_n)} \boldsymbol{g}_f^{n+1} \cdot \boldsymbol{\eta}^f \, d\Gamma\\
&+ \int_{\Omega_f(t_n)} q^f \, \nabla_{\boldsymbol{x}} \cdot \boldsymbol{v}^{n+1} \, d\boldsymbol{x} + \epsilon \int_{\Omega_f(t_n)} p_f^{n+1} q^f \, d\boldsymbol{x} = 0 \qquad \forall\, (\boldsymbol{\eta}^f, q^f) \in V_h^f \times W_h^f,
\end{aligned} \tag{4.33}$$

where the non-linear convective term $\dfrac{1}{\Delta t}(\boldsymbol{v}^n \circ \boldsymbol{X}^n)$ is approximated by the Expression (4.21).

The coupling conditions on $\tilde{\Gamma}_c$ are

$$\begin{cases}
\tilde{\boldsymbol{\sigma}}_s^{n+1} \, \tilde{\boldsymbol{n}}_s = -\Big(\boldsymbol{\sigma}_f(\boldsymbol{v}^{n+1}, p_f^{n+1}) \, \boldsymbol{n}_f\Big) \circ \boldsymbol{\varphi}^n,\\
\partial_t \tilde{\boldsymbol{\xi}}_s^{n+1} = \boldsymbol{v}^{n+1} \circ \boldsymbol{\varphi}^n.
\end{cases} \tag{4.34}$$

Fix $N \in \mathbb{N}$. The variational formulation associated to the structure sub-problem corresponding to the Newton-Raphson method at the time iteration t_{n+1} reads

Set $\boldsymbol{\varphi}_0 = \boldsymbol{\varphi}^n$ and $\tilde{\boldsymbol{\sigma}}_{s,k} = \tilde{\boldsymbol{\sigma}}_s^{n+1}$. Repeat: for $0 \leq k \leq N$, find $(\delta\boldsymbol{\varphi}_k, \delta\tilde{p}_{hs,k})$ in $\mathcal{Z} \times L^2(\tilde{\Omega}_s)$ satisfying

$$\begin{cases} \displaystyle\int_{\tilde{\Omega}_s} \frac{\partial \boldsymbol{P}}{\partial \boldsymbol{F}_s}(\nabla_{\tilde{\boldsymbol{x}}}\boldsymbol{\varphi}_k)\boldsymbol{\nabla}_{\tilde{\boldsymbol{x}}}\delta\boldsymbol{\varphi}_k : \boldsymbol{\nabla}_{\tilde{\boldsymbol{x}}}\tilde{\boldsymbol{\eta}}^s \, d\tilde{\boldsymbol{x}} + \int_{\tilde{\Omega}_s} \tilde{p}_{hs,k} \frac{\partial \mathrm{cof}}{\partial \boldsymbol{F}_s}(\boldsymbol{\nabla}_{\tilde{\boldsymbol{x}}}\boldsymbol{\varphi}_k)\boldsymbol{\nabla}_{\tilde{\boldsymbol{x}}}\delta\boldsymbol{\varphi}_k : \boldsymbol{\nabla}_{\tilde{\boldsymbol{x}}}\tilde{\boldsymbol{\eta}}^s \, d\tilde{\boldsymbol{x}} \\ \displaystyle+\int_{\tilde{\Omega}_s} \delta\tilde{p}_{hs,k} \, \mathrm{cof}(\boldsymbol{\nabla}_{\tilde{\boldsymbol{x}}}\boldsymbol{\varphi}_k) : \boldsymbol{\nabla}_{\tilde{\boldsymbol{x}}}\tilde{\boldsymbol{\eta}}^s \, d\tilde{\boldsymbol{x}} - \int_{\tilde{\Gamma}_c} \tilde{\boldsymbol{\sigma}}_{s,k}(\tilde{\boldsymbol{x}}) \frac{\partial \mathrm{cof}}{\partial \boldsymbol{F}_s}(\boldsymbol{\nabla}_{\tilde{\boldsymbol{x}}}\boldsymbol{\varphi}_k) : \boldsymbol{\nabla}_{\tilde{\boldsymbol{x}}}\delta\boldsymbol{\varphi}_k \, \tilde{\boldsymbol{n}}_s \cdot \tilde{\boldsymbol{\eta}}^s \, d\tilde{\Gamma} \\ \displaystyle+\int_{\tilde{\Omega}_s} \boldsymbol{P}(\boldsymbol{\nabla}_{\tilde{\boldsymbol{x}}}\boldsymbol{\varphi}_k) : \boldsymbol{\nabla}_{\tilde{\boldsymbol{x}}}\tilde{\boldsymbol{\eta}}^s \, d\tilde{\boldsymbol{x}} + \int_{\tilde{\Omega}_s} \tilde{p}_{hs,k} \, \mathrm{cof}(\boldsymbol{\nabla}_{\tilde{\boldsymbol{x}}}\boldsymbol{\varphi}_k) : \boldsymbol{\nabla}_{\tilde{\boldsymbol{x}}}\tilde{\boldsymbol{\eta}}^s \, d\tilde{\boldsymbol{x}} \\ \displaystyle-\int_{\tilde{\Gamma}_c} \tilde{\boldsymbol{\sigma}}_{s,k}(\tilde{\boldsymbol{x}}) \, \mathrm{cof}(\boldsymbol{\nabla}_{\tilde{\boldsymbol{x}}}\boldsymbol{\varphi}_k)\tilde{\boldsymbol{n}}_s \cdot \tilde{\boldsymbol{\eta}}^s \, d\tilde{\Gamma} + \epsilon \int_{\tilde{\Omega}_s} \tilde{p}_{hs,k} \, \tilde{q}^s \, d\tilde{\boldsymbol{x}} = 0 \qquad \forall \, (\tilde{\boldsymbol{\eta}}^s, \tilde{q}^s) \in \tilde{V}_h^s \times \tilde{W}_h^s, \\ \displaystyle\int_{\tilde{\Omega}_s} \tilde{q}^s \, \mathrm{cof}(\boldsymbol{\nabla}_{\tilde{\boldsymbol{x}}}\boldsymbol{\varphi}_k) : \boldsymbol{\nabla}_{\tilde{\boldsymbol{x}}}\delta\boldsymbol{\varphi}_k \, d\tilde{\boldsymbol{x}} + \int_{\tilde{\Omega}_s} \tilde{q}^s(\det(\boldsymbol{\nabla}_{\tilde{\boldsymbol{x}}}\boldsymbol{\varphi}_k) - 1) \, d\tilde{\boldsymbol{x}} = 0 \qquad \forall \, \tilde{q}^s \in \tilde{W}_h^s. \end{cases} \tag{4.35}$$

as long as the error $||\delta\boldsymbol{\varphi}_k||_2 \geq tol$, set $\boldsymbol{\varphi}_{k+1} = \delta\boldsymbol{\varphi}_k + \boldsymbol{\varphi}_k$ and $k = k+1$. If $||\delta\boldsymbol{\varphi}_k||_2 < tol$, then convergence of the Newton-Raphson method is achieved. Thus, the deformation of the structure domain is given by $\boldsymbol{\varphi}^{n+1} = \boldsymbol{\varphi}_k$, for the last value of k for which the convergence is achieved. Whence at the time iteration t_{n+1} the displacement of the structure domain is $\tilde{\boldsymbol{\xi}}_s^{n+1}(\tilde{\boldsymbol{x}}) = \boldsymbol{\varphi}^{n+1}(\tilde{\boldsymbol{x}}) - \tilde{\boldsymbol{x}}$.

Using an appropriate extension [Ric17, Section 5.3, pp. 247], [Cha13, Chapter 2] the ALE map $\boldsymbol{\mathcal{A}}^{n+1}$ is given by

$$\boldsymbol{\mathcal{A}}^{n+1}(\tilde{\boldsymbol{x}}, t) = \tilde{\boldsymbol{x}} + \mathcal{E}xt(\tilde{\boldsymbol{\xi}}_s^{n+1}(\tilde{\boldsymbol{x}}, t)|_{\tilde{\Gamma}_c}).$$

In particular, we consider the standard harmonic extension. The aim is to construct the ALE map, by finding the displacement $\tilde{\boldsymbol{\xi}}_f^{n+1}$ using the harmonic extension of the displacement $\tilde{\boldsymbol{\xi}}_s$ of the boundary $\tilde{\Gamma}_c$. We seek to find the displacement $\tilde{\boldsymbol{\xi}}_f^{n+1}$ verifying the system

$$\begin{cases} -\boldsymbol{\Delta}\tilde{\boldsymbol{\xi}}_f^{n+1} = 0 & \text{in } \tilde{\Omega}_f, \\ \tilde{\boldsymbol{\xi}}_f^{n+1} = \tilde{\boldsymbol{\xi}}_s^{n+1} & \text{on } \tilde{\Gamma}_c, \\ \tilde{\boldsymbol{\xi}}_f^{n+1} = 0 & \text{on } \tilde{\Gamma}_{\text{in}} \cup \tilde{\Gamma}_{\text{out}}. \end{cases} \tag{4.36}$$

Its associated variational formulation is

$$\text{Find } \tilde{\boldsymbol{\xi}}_f^{n+1} \in \mathcal{H} \cap [P_2(\tilde{\Omega}_f)]^3 \text{ such that}$$
$$\int_{\tilde{\Omega}_f} \boldsymbol{\nabla}\tilde{\boldsymbol{\xi}}_f^{n+1} : \boldsymbol{\nabla}\boldsymbol{\eta} = 0, \quad \forall \, \boldsymbol{\eta} \in \mathcal{H},$$

where

$$\mathcal{H} = \{\boldsymbol{\eta} \in H^1(\tilde{\Omega}_f) : \boldsymbol{\eta} = 0 \quad \text{on} \quad \tilde{\Gamma}_{\text{in}} \cup \tilde{\Gamma}_{\text{out}}\}.$$

Hence, at the time iteration t_{n+1}, the ALE map is given by the following relation

$$\boldsymbol{\mathcal{A}}_t^{n+1}(\tilde{\boldsymbol{x}}) = \tilde{\boldsymbol{x}} + \tilde{\boldsymbol{\xi}}_f^{n+1}(\tilde{\boldsymbol{x}}, t).$$

The fluid domain evolves from the reference configuration as

$$\Omega_f^{n+1} = \boldsymbol{\mathcal{A}}^{n+1}(\tilde{\Omega}_f).$$

Further, the structure domain evolves from the initial configuration according to

$$\Omega_s^{n+1} = \boldsymbol{\varphi}^{n+1}(\tilde{\Omega}_s).$$

In the next section we focus on solving System (4.32)-(4.36) numerically.

4.1.3 The Algorithm

The FSI problem is solved using the finite element software FreeFem++. The algorithm used to solve the FSI problem is presented in the diagram below, see Figure 4.1. Notice that, the main tool in the iterations is the ALE map $\boldsymbol{\mathcal{A}}$. Complexity of the algorithm is dependent on the triangulation of the mesh.

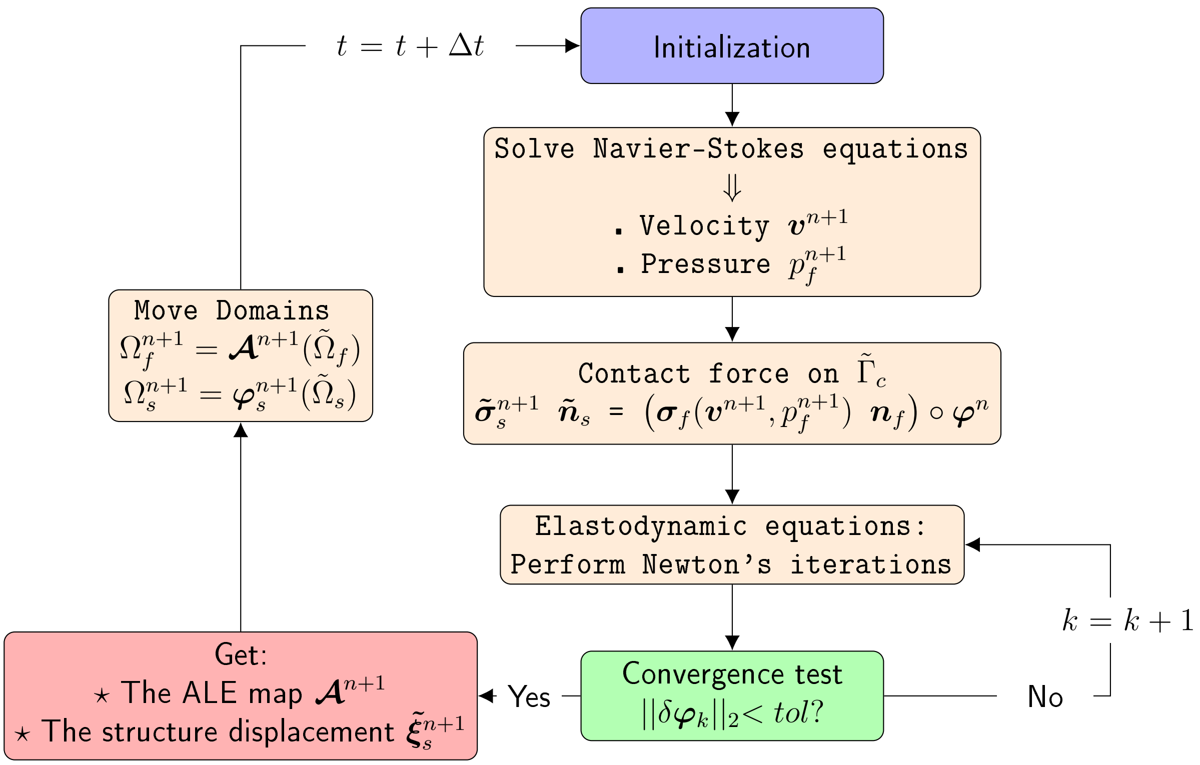

Figure 4.1: Algorithm associated to the FSI problem.

Literally,

1- At the time step t_{n+1}, we solve the Navier-Stokes equations on the domain $\Omega_f(t_n)$ in the ALE frame to find the velocity of the fluid $\boldsymbol{v}^{n+1}$ and its pressure p_f^{n+1}.

2- Using the continuity of stresses (4.34), we are able to get the boundary condition on $\tilde{\Gamma}_c$ expressed in terms of $\boldsymbol{\sigma}_f(\boldsymbol{v}^{n+1}, p_f^{n+1})$.

3- Solve the quasi-static incompressible elasticity equations on the reference configuration $\tilde{\Omega}_s$ using Newton-Raphson method. Check the convergence test of the Newton-Raphson method. When convergence is achieved, the deformation $\boldsymbol{\varphi}_s^{n+1}$ is set to be the solution of the last Newton's iteration k, consequently the deformation $\tilde{\boldsymbol{\xi}}_s^{n+1}$ is obtained. Thus we can proceed to get the ALE map $\boldsymbol{\mathcal{A}}^{n+1}$ using a suitable extension highlighted in [Ric17, Section 5.3, pp. 247], [Cha13, Chapter 2] (harmonic, biharmonic, wislow, etc.).

4- Move the fluid domain using the map $\boldsymbol{\mathcal{A}}^{n+1}$, and the structure domain using its deformation $\boldsymbol{\varphi}_s^{n+1}$ and proceed to the iteration t_{n+2}, then start again from step (1-), and so on.

Remark 4.1.4 *This algorithm is simulated over a defined interval of time.*

4.2 Numerical Results

In this section we present the numerical results concerning the blood flow through stenosed arteries after performing simulations over a defined interval of time. The study is done by solving System (4.32)-(4.36) on the two dimensional domain representing the artery given in Figure 4.2 using the software FreeFem++.

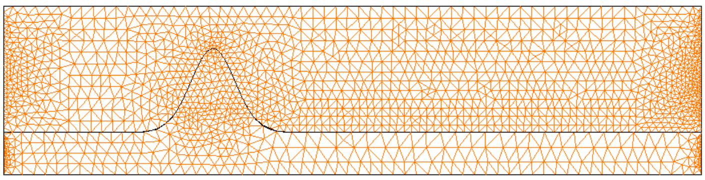

Figure 4.2: The mesh of the artery domain.

Our work is concerned in analyzing variables including the speed, the viscosity and the wall shear stress of blood in a stenosed artery. Further, we intent to locate the recirculation zones in the lumen. In our work we consider the following numerical values

$$\rho_f = 1.056 \text{ g/cm}^3 \text{ and } \Delta t = 10^{-2} \text{ s}.$$

The blood is considered to have a non-Newtonian behavior. Its viscosity is assumed to obey Carreau model [Seq18]; which will be presented in details in the coming chapter

$$\mu(\dot{\gamma}) = \mu_\infty + (\mu_0 - \mu_\infty)\left[1 + (\lambda\dot{\gamma})^2\right]^{\frac{n-1}{2}},$$

where $\dot{\gamma}$ stands for the shear rate defined as

$$\dot{\gamma} = \sqrt{2\ \mathrm{tr}(\boldsymbol{D}(\boldsymbol{v}))^2} = \sqrt{-4I_2}.$$

The parameters present in the Carreau model are

$$\lambda = 3.313\ \mathrm{s}, \quad n = 0.3568, \quad \mu_\infty = 0.00345\ \mathrm{Pa.s} \quad \text{and} \quad \mu_0 = 0.056\ \mathrm{Pa.s}.$$

The blood flow and the pattern of its viscosity in a healthy artery are illustrated on Figure 4.3.

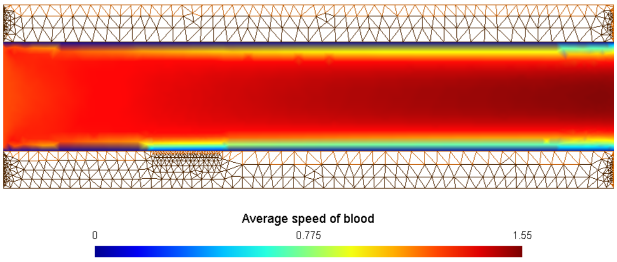

(a) Average speed of blood in a healthy artery.

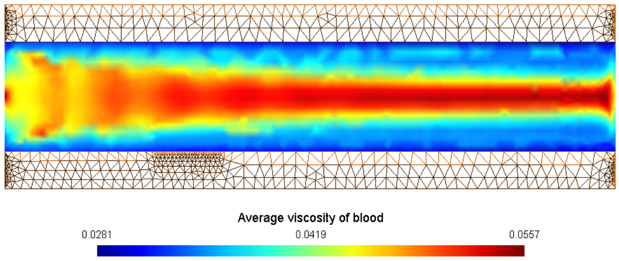

(b) Average viscosity of blood in a healthy artery.

Figure 4.3: Average speed and viscosity in a healthy artery.

In the case of an isotropic material the strain-energy density function W is expressed in terms of the invariants of deformation tensors I_1, I_2 and I_3 [Mal, Ric17]. In particular, we will consider the following constitutive law

$$W(\boldsymbol{F}_s) = C_0 + C_1\big(I_1 - 2\big) + C_2\big(I_2 - 2\big)^2, \tag{4.37}$$

where C_0, C_1 and C_2 are set as follow

$$C_0 = 110\ \mathrm{N.cm}^{-2},\ C_1 = 100\ \mathrm{N.cm}^{-2} \text{ and } C_2 = 110\ \mathrm{N.cm}^{-2}.$$

A velocity $\boldsymbol{v}_{\mathrm{in}}$ is enforced on the inlet of the artery. It is given by

$$\boldsymbol{v}_{\mathrm{in}} = \begin{cases} 5\ \sin^2(\pi t/0.5)\ \mathrm{cm/s} & \text{for } 5\times(2i) \le t \le 5\times(2i+1), \\ 0\ \mathrm{cm/s} & \text{for } 5\times(2i+1) \le t \le 5\times(2i+2), \end{cases} \qquad \text{for } i \in \mathbb{N}.$$

It is a periodic continuous function of period 1 s. It attains its maximum value 5 cm/s at the instants $t = 0.25 + k$ s, $k \in \mathbb{N}$. Its profile during a time interval of 3 seconds is represented by Figure 4.4.

4.2.1 Non-Linear Elastic Modeling of a Pipe-Shaped Stenosed Artery

Blood Flow and Arterial Wall Displacement

The first factor that gains our attention is the behavior of the blood flow in the stenosed arteries. Figure 4.5 shows the speed of blood at different instants. One can observe the speed of the blood, being affected by the existence of the stenosis and the displacement of the arterial wall.

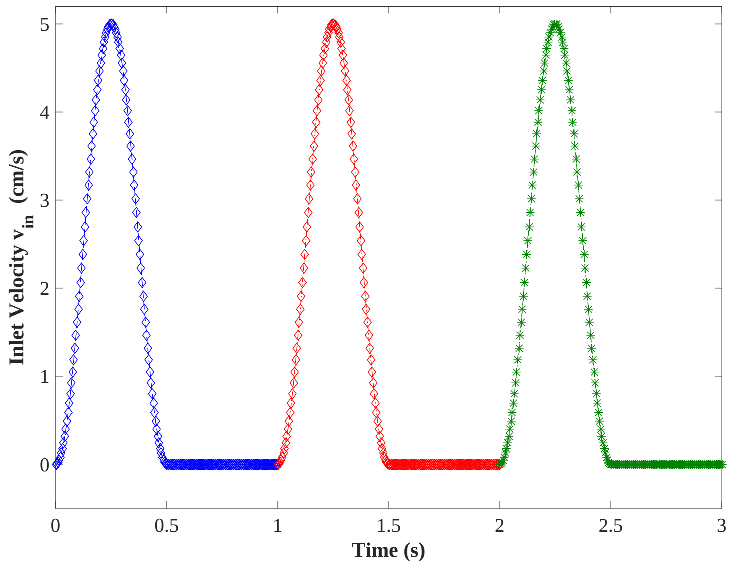

Figure 4.4: The profile of the inlet velocity $\boldsymbol{v}_{\mathrm{in}}$.

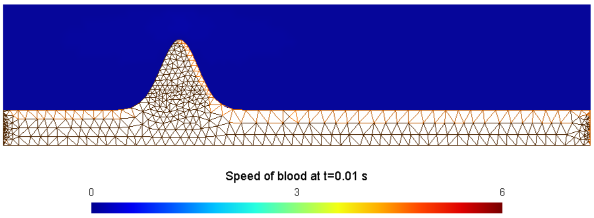

(a) $t = 0.01$ s.

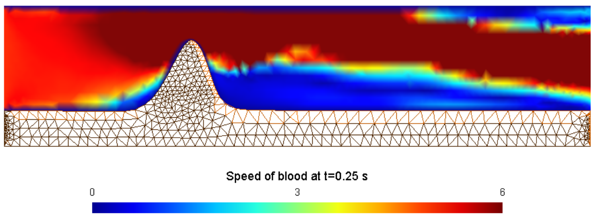

(b) $t = 0.25$ s.

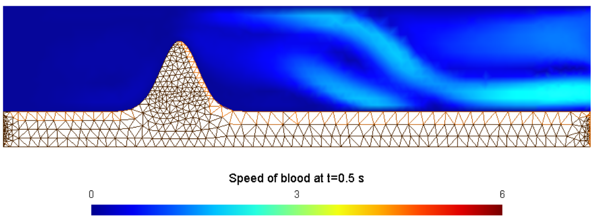

(c) $t = 0.5$ s.

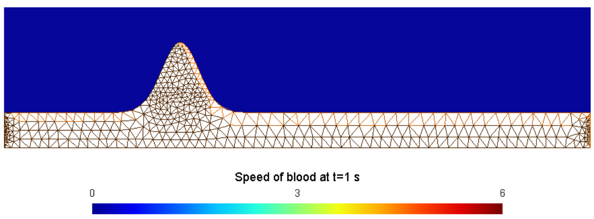

(d) $t = 1$ s.

Figure 4.5: Blood flow in a stenosed artery.

At the first instant of the flow, the blood speed is negligible which can be observed in Figure 4.5a. After that a remarkable change encounters on the blood flow as shown in Figure 4.5b.In fact, it can be observed that the neighborhood of the peak is characterized with a high speed. This is reasonable, indeed, an enforced amount of blood into the artery must pass through it regardless of the diameter of the path or if it is narrowed. Hence, in the narrowed region due to the existence of stenosis, blood speed will become larger. At the instant $t = 0.5$ s, that is when $v_{\mathrm{in}} = 0$ cm/s the blood flow through the artery decreases, consequently, the stenosis returns to its equilibrium position (see Figure 4.5c), however, the flow continues with a negligible speed behavior during the time interval between 0.5 s and 1 s to reach its minimum effect at $t = 1s$ as observed in Figure 4.5d.

Since the displacement of the lumen domain is linked to the displacement of the arterial wall, a view of the displacement of the arterial wall during the same instants will make the observations of Figure 4.5 more obvious. Results during 1 second are given in Figure 4.6.

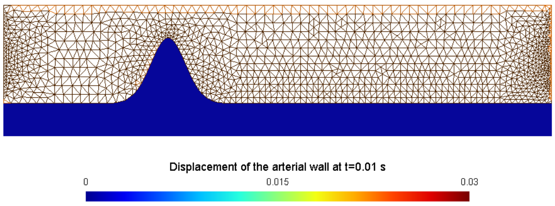

(a) $t = 0.01$ s.

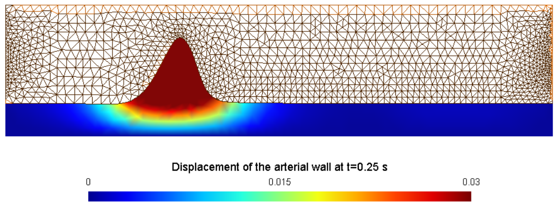

(b) $t = 0.25$ s.

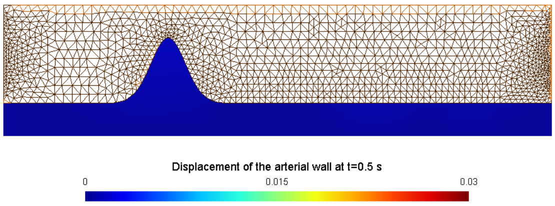

(c) $t = 0.5$ s.

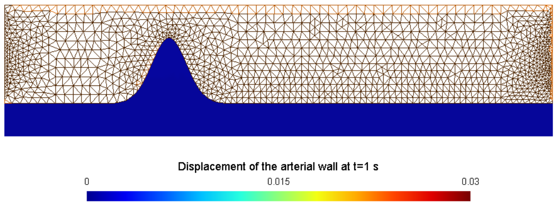

(d) $t = 1$ s.

Figure 4.6: The displacement of the arterial wall.

One can observe that the upper part of the stenosis is the region with the highest displacement. In fact, as we reach the peak of the stenosis, i.e, as the stenosis becomes thinner its stiffness will decrease. Consequently, it will be fragile, sensitive to any external force and easily affected by the wall shear stress.

Shear Stress

It presents the effect exerted by the fluid on itself. Its expression σ_{max} (4.6) in terms of the Cauchy stress tensor $\boldsymbol{\sigma}_f$ reveals its dependence on the strain rate tensor $\boldsymbol{D}(\boldsymbol{v})$ and the blood pressure p_f. This means that regions encountering a change in the velocity are characterized by a higher shear stress. On the contrary, regions where the values of speed are close are of low shear stress. This fact is illustrated on Figure 4.7.

The maximum shear stress is located in the region of stenosis. In fact, the observations show that it is located at the peak of the stenosis. This part of stenosis is the most fragile part, which makes it more affected by the blood flow. As the motion of the blood is considered to be periodic; in general it is pulsatilic; and since the arterial wall undergoes a deformation, then the stenosis will have an oscillating-like motion. Consequently, a variation in the speed of the blood is recognized, which will lead to the existence of a shear stress spotted in the region of the stenosis as in Figure 4.7b.

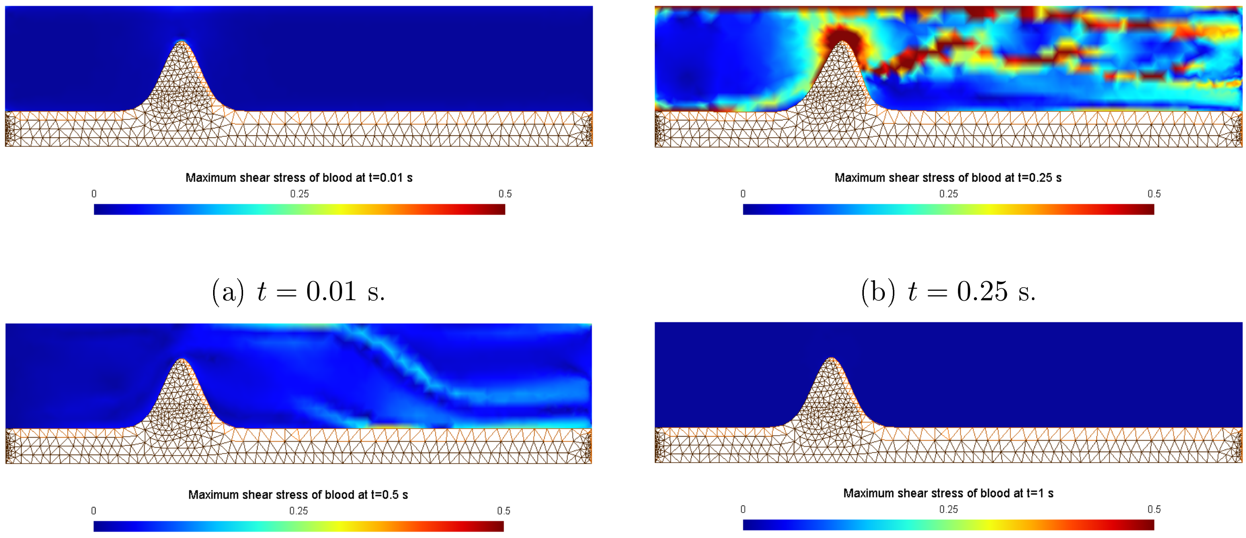

(a) $t = 0.01$ s.

(b) $t = 0.25$ s.

(c) $t = 0.5$ s.

(d) $t = 1$ s.

Figure 4.7: The maximum shear stress.

Recirculation Zones

We are curious about recognizing the recirculation zones. They are the regions formed due to the interruption of the flow as a result of the existence of the stenosis and they represent the regions having a ripple-like manner. A vector representation of the blood velocity is illustrated in Figure 4.8 which will help us in configuring the recirculation zone.

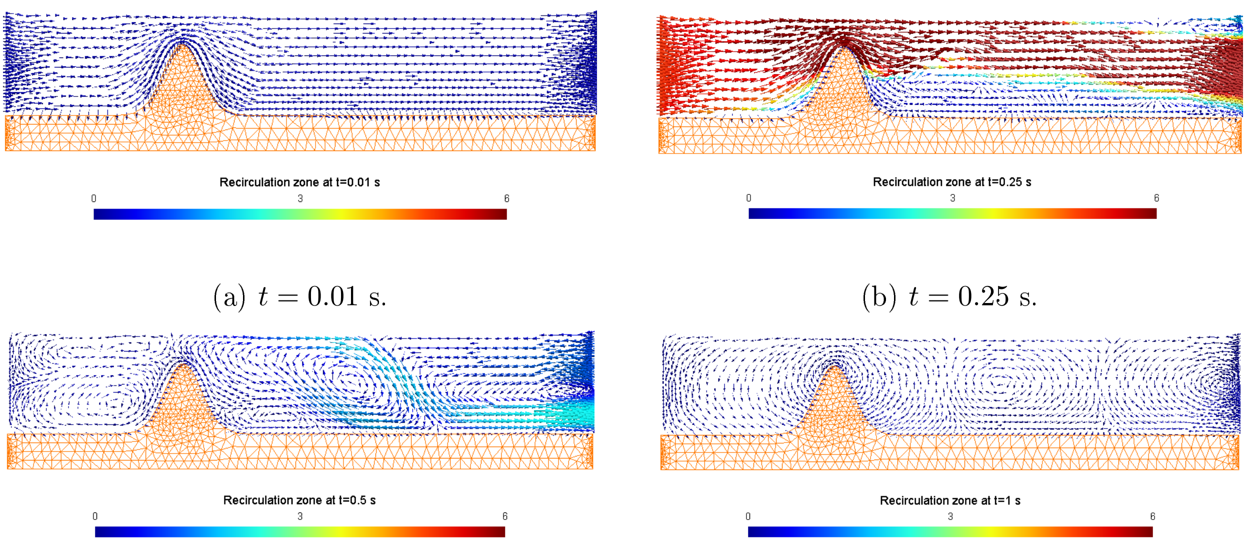

(a) $t = 0.01$ s.

(b) $t = 0.25$ s.

(c) $t = 0.5$ s.

(d) $t = 1$ s.

Figure 4.8: The velocity of blood.

Figure 4.8c shows the recirculation zones at time $t = 0.5$ s. Mainly we can observe a big recirculation zone that is located after the stenosis. The recirculation zone is characterized by a center of negligible speed, which increases as the circular regions becomes wider. Further, a zone of negligible speed is located between the stenosis and the recirculation zone. This zone is the solidification region, which we will be the matter of study in Chapter 5. The effect of the recirculation zone on the solidification zone would constitute an important tool to build up a rupture model.

4.2.2 Non-Linear Elastic Modeling of a Bifurcated Stenosed Artery

Arteries with bifurcations are more important to be studied, due to the higher risk of clot formation in these arteries. We consider a bifurcation with a stenosis rate 50%. The flow of the blood in a bifurcated artery during the first second is given in Figure 4.9.

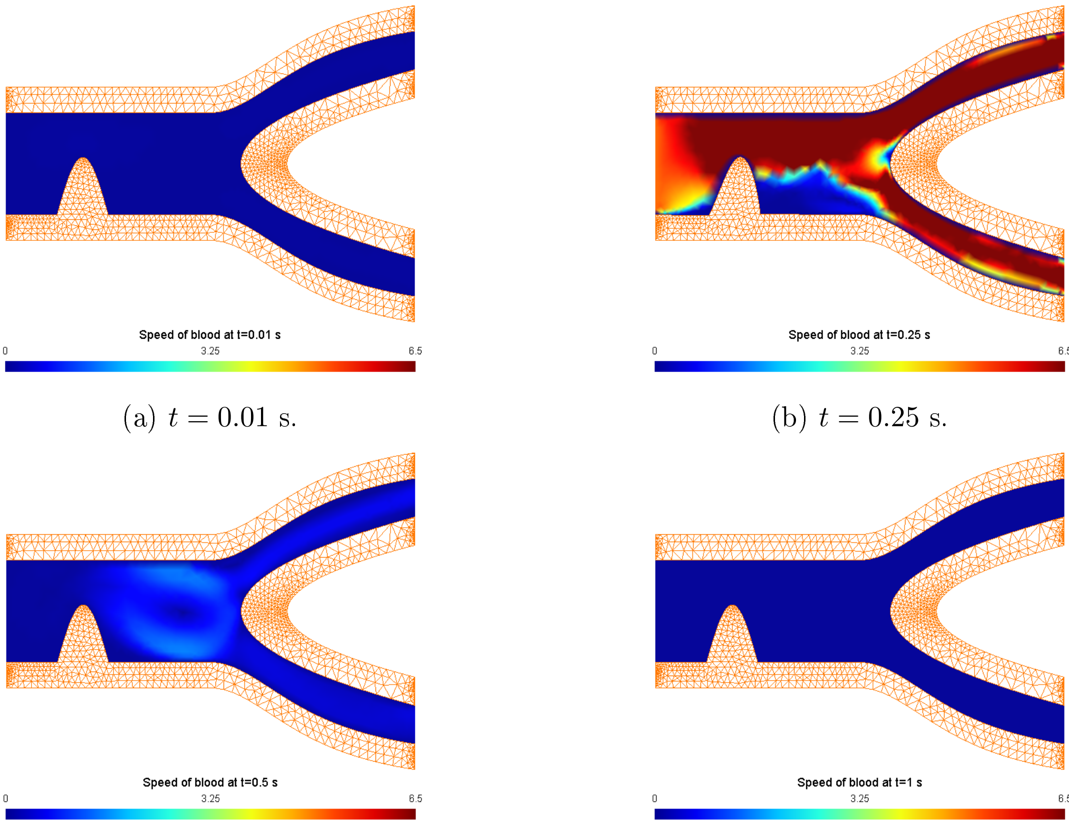

(a) $t = 0.01$ s. (b) $t = 0.25$ s.

(c) $t = 0.5$ s. (d) $t = 1$ s.

Figure 4.9: Blood flow in a bifurcated artery.

Figure 4.9 shows the effect of the blood flow on the plaque. In particular at time $t = 0.25$ s, from Figure 4.9b we observe that the lumen of the artery undergoes a deformation depending on that of the arterial wall. The same holds if more than one stenosis exist. To make it more precise, we observe the displacement of the structure domain at time $t = 0.25$ s, where one and two stenosis exist (see Figure 4.10).

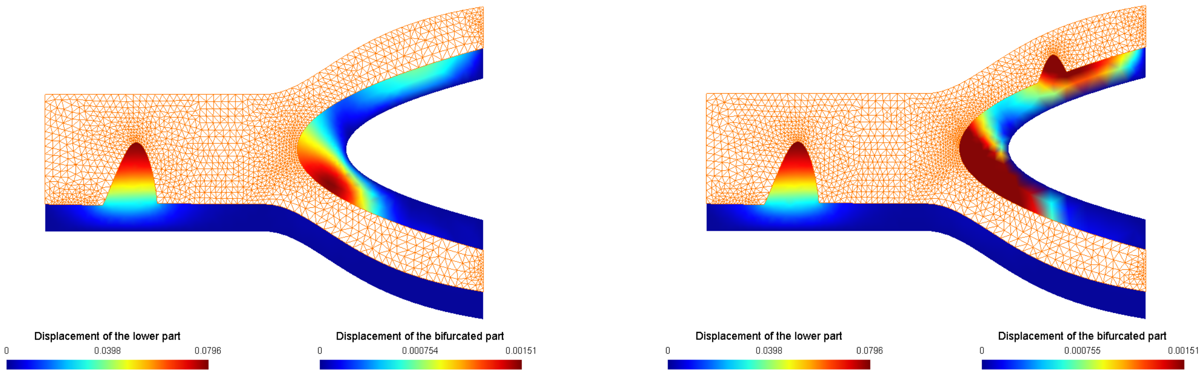

(a) Bifurcation with one stenosis. (b) Bifurcation with two stenosis.

Figure 4.10: Displacement of the arterial wall in bifurcated arteries at $t = 0.25$ s.

From Figure 4.10 we observe that the most deformed part is the plaque, and this deformation is larger at the peak due to the fact that the peak is of low stiffness. In addition, the bifurcated side of the structure is also affected. Indeed, the existence of the plaque will lead to a large flow into both the upper and the lower parts of the bifurcated region. This will results a deformation at this region as we can see in Figure 4.10. In particular, Figure 4.9 shows that due to the existence of a stenosis, the speed of blood (flow) is larger in the upper part of the bifurcation. A simple comparison with Figure 4.10 gives a reasonable conclusion of having a larger displacement of the lower part of bifurcation. Obviously, the large flow into the upper part, will affect the lower part. This effect is recognized by a small deformation in the downward sense. We proceed to locate the recirculation zones. In particular, we analyze the instant when the speed decreases and tends to be negligible, i.e, at the instant $t = 0.5$ s.

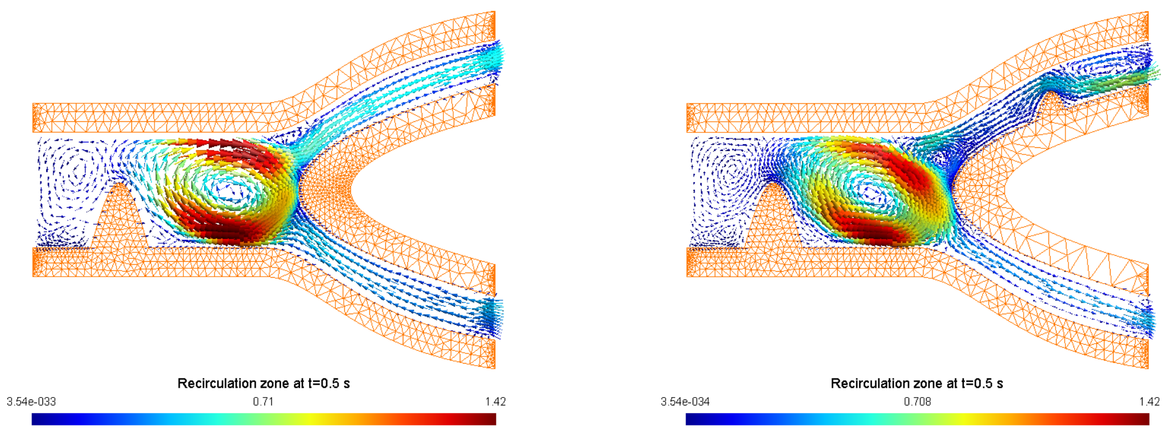

(a) Bifurcation with one stenosis. (b) Bifurcation with two stenosis.

Figure 4.11: Recirculation zone in bifurcated arteries at $t = 0.5$ s.

Similarly as in the case above, we observe from Figure 4.11 that the recirculation zone is located at the right hand side of the stenosis. We observe a negligible speed at its center. This speed increases where the circles constituting the zone are of larger diameter.

Previous figures have shown some remarkable regions where the blood speed varies among them. Similarly for the shear stress and the blood viscosity. More precisely, we focus on three regions. The first region denoted by "A", is located at the peak of the stenosis. Region "B" is located at the adjacent right bottom of the stenosis. And finally, Region "C" is the region including the recirculation zone. The three regions are shown on Figure 4.12.

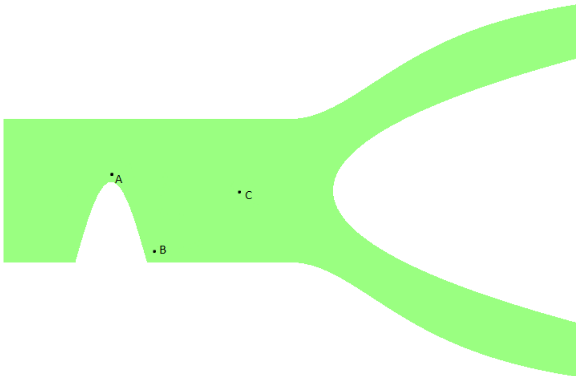

Figure 4.12: Remarkable regions.

The graphs associated to the behavior of the viscosity, the maximum shear stress and the speed of the blood at the positions A, B and C are shown on Figures 4.13, 4.14 and 4.15 respectively.

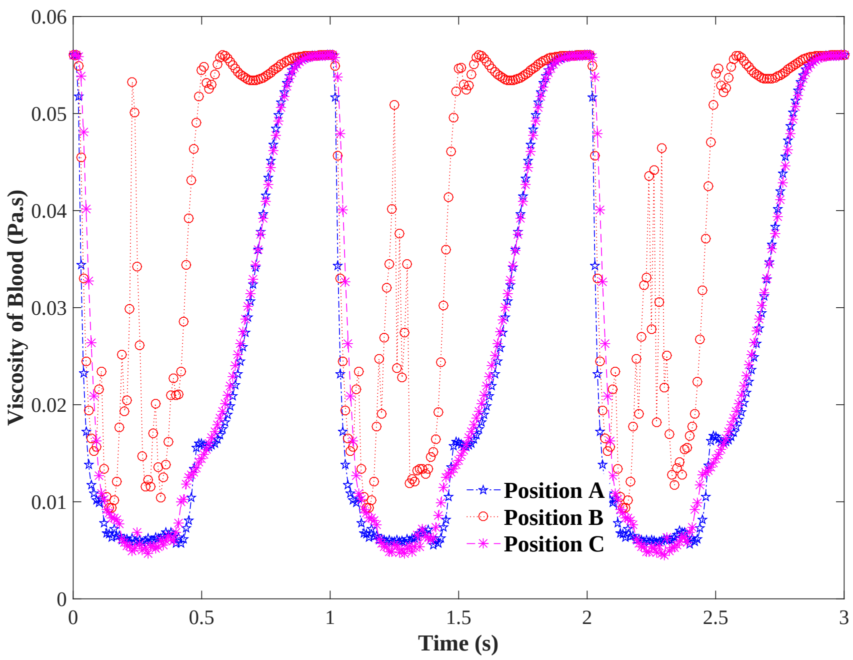

Figure 4.13: Viscosity of blood.

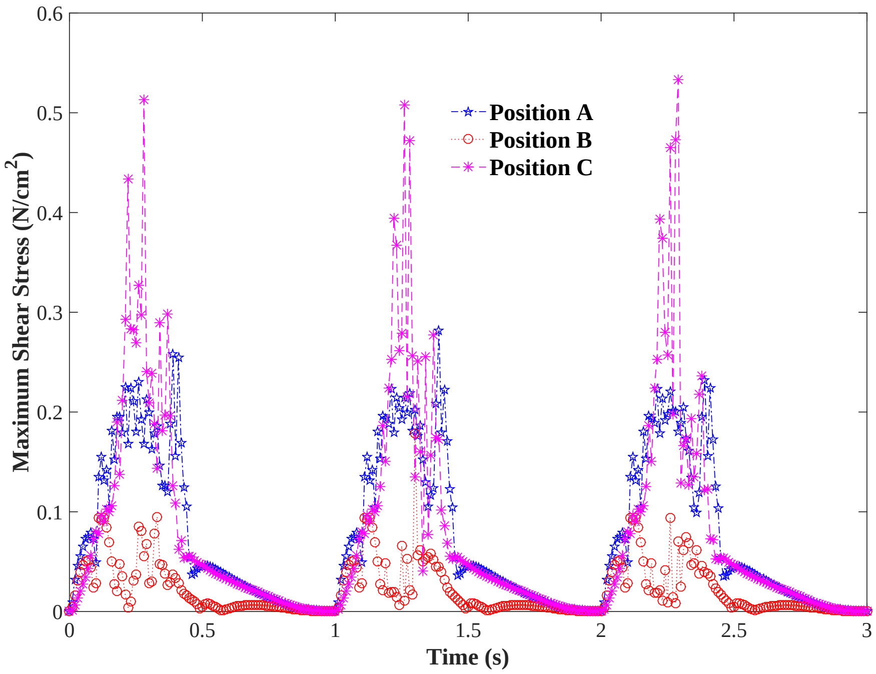

Figure 4.14: Maximum shear stress.

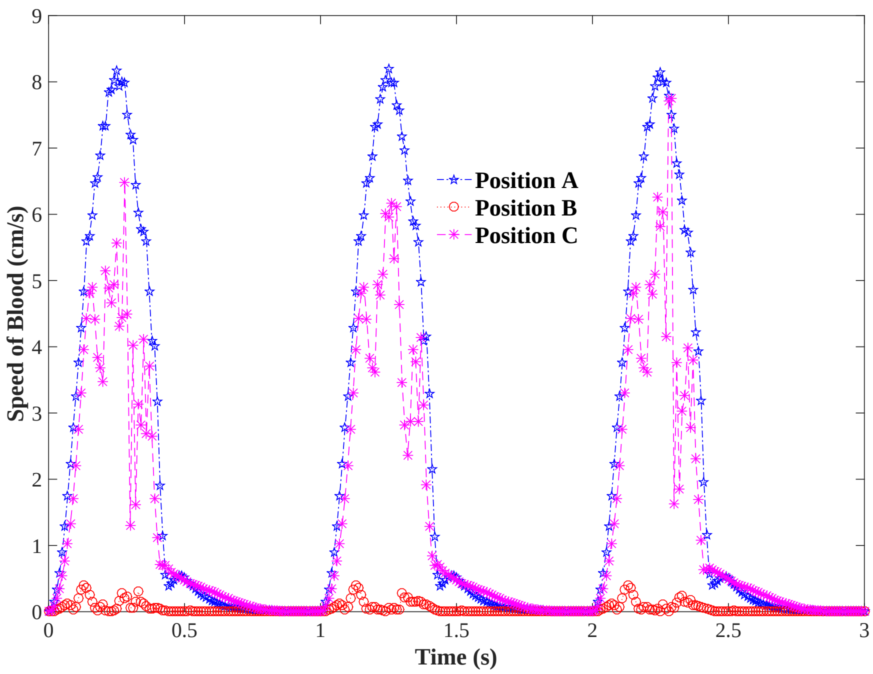

Figure 4.15: Speed of blood.

Figures 4.13, 4.14 and 4.15 show that the position B is characterized by a high viscosity as well as a negligible speed. In fact, the existence of stenosis causes interruption of the flow and prevents it from reaching this region. This which will lead to the formation of a more viscous region at B. Consequently, the shear stress at this position is small. In the next chapter, this region will be identified as a solidification zone. Whereas, the position A is characterized by a high blood speed with a moderate shear stress rate. In fact, due to the narrowing of the artery at the region of stenosis, the blood speed will be high, as we mentioned above. When the blood leaves this narrowed region its speed will decrease. This explains the lower blood speed in Position C. Consequently, the blood viscosity will be negligible. Further, it possesses a high shear stress due to the change encountering on the speed in this region as we can analyze from Figure 4.15. The investigation of these variables at these remarkable positions will help us in locating the solidification zone, where a clot would form, and probably when exposed to high forces exerted by the blood, will be released into the flow, leading to an infarction at some stages of narrow vessels or arterioles.

4.2.3 Newtonian vs. Non-Newtonian Blood

We have studied the case of a non-Newtonian blood. One might be curious about how would variables (speed, viscosity, shear stress) be affected in the case of a Newtonian blood. A Newtonian blood is characterized by a constant dynamic viscosity $\mu = 0.00345$ Pa.s. The space average viscosity μ and the global in time average viscosity $\overline{\mu}$ of blood during 3 seconds for both cases are given on Figure 4.16.

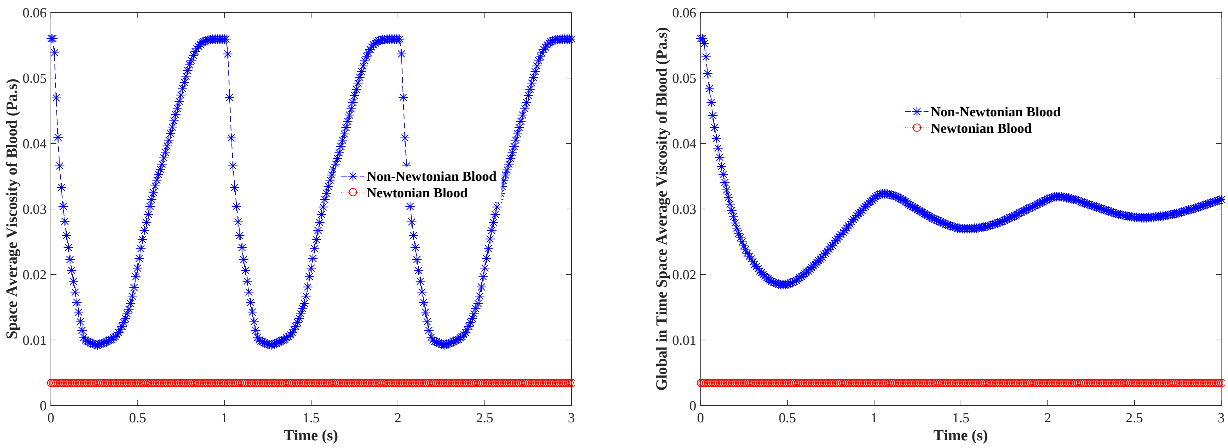

(a) Space average viscosity of blood. (b) Global in time space average viscosity of blood.

Figure 4.16: Space average viscosity (left) and global in time space average viscosity (right) of a Newtonian and a non-Newtonian blood.

At each iteration k the global in time average viscosity $\overline{\mu}_k$ is given by the following relation

$$\overline{\mu}_k(t) = \frac{1}{k+1}\sum_{i=0}^{k}\mu_i(t),$$

where $\mu_i(t)$ represents the space average viscosity of blood at iteration i, $0 \leq i \leq k$. Its expression is given by

$$\mu_i(t) = \frac{1}{|\Omega_f(t)|}\int_{\Omega_f(t)} \mu_i(\boldsymbol{x},t)\, d\boldsymbol{x}, \qquad \forall\, \boldsymbol{x} \in \Omega_f(t).$$

with $|\Omega_f(t)|$ is the area of the blood domain at any instant t.
For $i = 0$, we set $\mu_i = \mu_0 = 0.056$ Pa.s, for a non-Newtonian blood, and $\mu_i = 0.00345$ Pa.s for a Newtonian blood. At the instant $t = 0.5$ s, the blood flow is given in Figure 4.17.

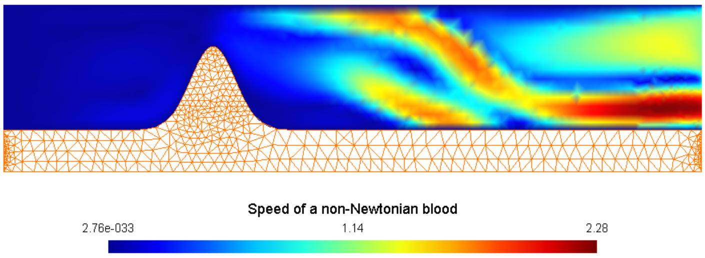

(a) Case of a non-Newtonian blood.

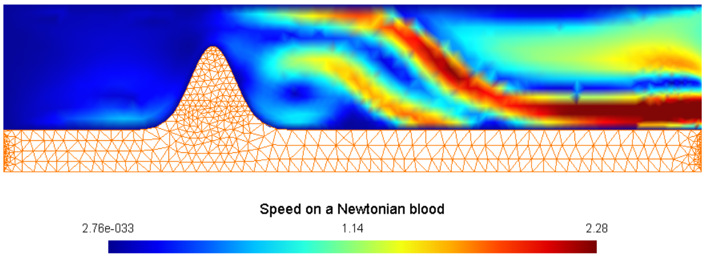

(b) Case of a Newtonian blood.

Figure 4.17: The speed of a Newtonian and non-Newtonian blood at $t = 0.5$ s.

Considering a vector-representation of the flow at $t = 0.5$ s helps us in locating the recirculation zones in both cases of a Newtonian and a non-Newtonian blood. The results are shown on Figure 4.18.

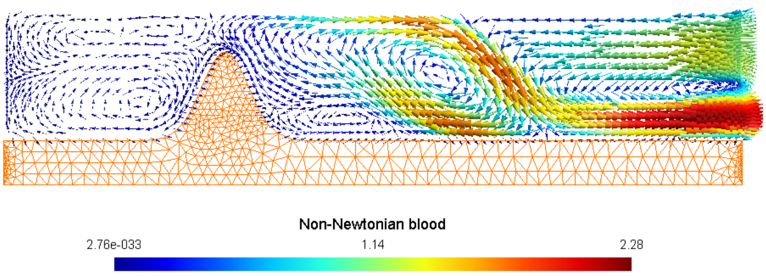

(a) Case of a non-Newtonian blood.

A comparison between Figures 4.17 and 4.18 shows that a non-Newtonian blood is characterized by a speed smaller than in the case of a Newtonian blood. Further, the recirculation zones appear clearer in the case of a Newtonian blood.

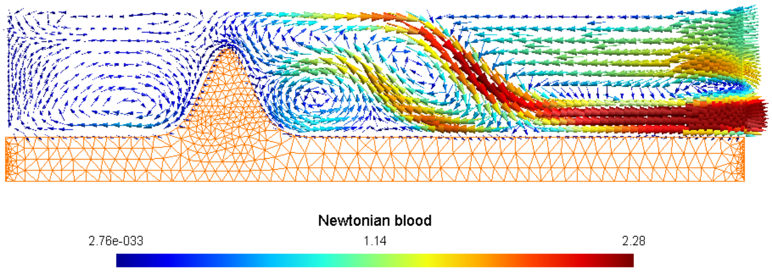

(b) Case of a Newtonian blood.

Figure 4.18: The recirculation zone at $t = 0.5$ s.

Comparison of the global in time average speed and the global in time average maximum shear stress (4.6) of a Newtonian and a non-Newtonian blood after a duration of 3 seconds are given on Figures 4.19 and 4.20 respectively.

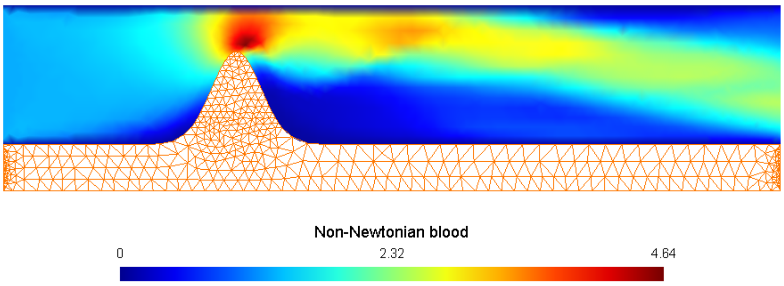

(a) Case of a non-Newtonian blood.

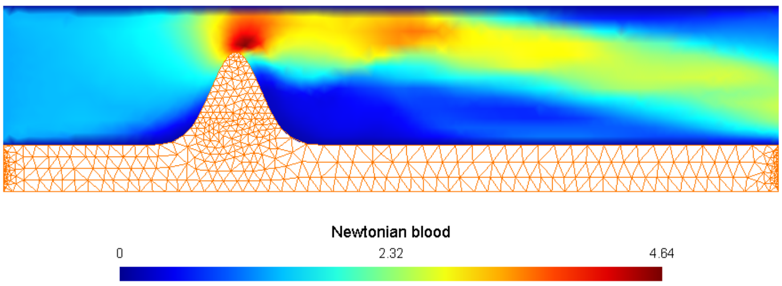

(b) Case of a Newtonian blood.

Figure 4.19: Global in time average speed of a Newtonian and a non-Newtonian blood during 3 seconds.

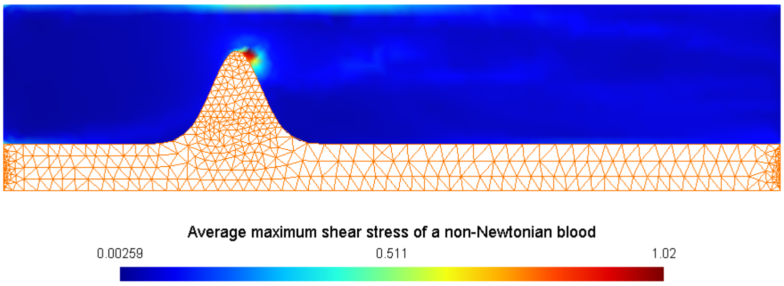

(a) Case of a non-Newtonian blood.

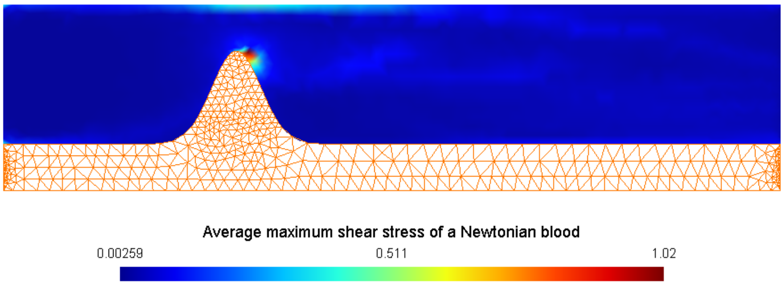

(b) Case of a Newtonian blood.

Figure 4.20: Global in time average maximum shear stress of a Newtonian and a non-Newtonian blood.

These figures show that, in general, a Newtonian blood is characterized by a speed greater than that of non-Newtonian blood. On the contrary, the maximum shear stress of a Newtonian blood is smaller than that of a non-Newtonian blood. These results are reasonable, indeed, Figure 4.16 shows that the average viscosity of a non-Newtonian blood is greater than that of a Newtonian blood. The viscosity, plays the role of a sticking obstacle or possesses a frictional manner which causes the decrease of speed as well as it increases the force between the fluid and itself, consequently leads to an increase in the shear stress. This shear stress constitutes the main component of the forces exerted by blood, which will be highlighted in the next chapter.

4.3 Conclusion

This chapter is devoted for the numerical study of the fluid-structure interaction problem between the blood flow and an existing stenosis in arteries, where the blood is considered to be a homogeneous incompressible fluid whose dynamics is given by the incompressible Navier-Stokes equations, and the arterial wall is a non-linear hyperelastic material described by the quasi-static elasticity equations. The simulations have shown a deep view of what is happening in the stenosed artery and how it would be affected with some variables that we can analyze. They helped us in configuring the existence of mainly three remarkable regions (see Figure 4.12). Indeed, the wall shear stress and speed of blood have been studied and the recirculation zones have been observed. These zones exist after the stenosis. In these zones the blood speed is negligible at the center, and increases as the diameter of the circular region increases. Between these zones and the stenosis, we observe a region which is located at the adjacent right bottom of the stenosis. This region is identified as the solidification zone which is characterized by a negligible blood speed and a high blood viscosity and thus results a more viscous blood. The deformation of the stenosis and the shear stress which constitute the main component of the forces acting on this zone will probably play a role in the detach of the accumulated blood in gel-like state into the flow and would lead to the generation of the infarction.

These results help us in setting up a rupture model, which will be the objective of the next chapter.

Chapter 5

Solidification of Blood and a First Step Towards a Rupture Model

Contents

Introduction

Heart is a muscular organ which pumps blood through the blood vessels that constitute the circulatory system also known as cardiovascular system. This system, in particular the blood vessels, are responsible for transporting supplies needed from and into the target destination "cells". The circulatory system has been studied long time ago since the seventeenth century B.C. until the 1628, when the English physician William Harvey correctly described blood circulation. History and advances in the study of the cardiovascular system can be found in [Seq18, Col15].

Cardiovascular diseases, mainly due to atherosclerosis, enthused mathematicians to study the rheological[1] behavior of blood and its flow from the mathematical viewpoint, in particular, in case of pathologies. Modeling of blood repeatedly progressed, and yet it is. Models are identified and proposed to study the blood flow through the blood vessels, the characteristics of the blood cells and plasma as well as of the heart [Pes02, PM89, TBA11, TBE+11, BKS09].

[1]Haemorheology is the study of the blood flow properties of both the plasma and the cells.

Further, a fluid-structure interaction (FSI) model is considered to investigate the interaction between the blood flow and the arterial wall. Due to difficulties arising from the complexity of the arterial wall formed of several layers each with its own unique mechanics, reduced shell or membrane models have been employed [ČTG+06] under the assumptions of negligibly thin structural components or by considering the ratio between the thickness of the vessel wall and the vessel radius is small. Additional conditions can be induced [FQV09]. Constitutive models are derived to capture the rheological behavior of blood, as a consequence, they constitute an effective tool in the diagnosis of the pathologies and investigating appropriate remedies [Mac94, BHW89]. Moreover, models describing the coagulation of blood have been subject of intensive research [Bou17, GHZ09, Zhu07]. The complex process of coagulation depends on the platelets and insoluble fibrin proteins which are formed by the coagulation cascade process [DR64, Bou17].

Advection-diffusion-reaction models are employed to describe the concentration of the clotting factors and the fibrin polymers while the blood flow dynamics is given by the Navier-Stokes equations. A continuous approach is used to describe the interaction of the blood flow and the clot growth which is given in spatiotemporal representation inside the blood vessel. Both models are simulated on the same domain and solved on the same numerical mesh. Some models have assumed that the fribin polymers do not affect the blood flow dynamics [JC11]. Whereas, others have proposed that the viscosity is a function of the fibrin polymers by employing the generalized Newtonian model for the blood flow [BS08, SB14]. Further, some continuous models have dealt with the clot as a solid [SvdV14] and detected its growth using FSI system. In contrast, other models have considered the fibrin as a porous medium [LF10, GRRM16].

Hybrid models have also been employed. They aim to achieve a realistic representation of the clot formation by combining the blood flow described by continuous and discrete methods with blood cells and clotting factors [FG08, XCL+12, YLHK17, TAB+13, TAB+15].

To our knowledge, the process of a clot rupture which is enthusing scientists and mathematicians is yet under investigation. Indeed, many predictions have arisen concerning the species of the ruptured particle. Most predictions state that the lipids and fats that form the plaque, when being under the effect of some external forces due to the blood flow, will be released into the blood flow.

The aim of this chapter is to propose the first step step towards a rupture model based on the rheological properties of blood, and on the FSI model presented in Chapter 4. We have already analyzed the behavior of blood in a stenosed artery. In fact, we have spotted three major regions where the behavior of blood is of significant pattern. These results will constitute an important tool to set up the rupture model. To achieve the desired aim, we give in Section 5.1 a brief overview of the blood viscosity when assumed to be a non-Newtonian fluid, and highlight the widely used constitutive models that are introduced to describe this property. Then, we introduce our model to detect the solidification zone and give its characteristics based on some numerical simulations that are performed using the FreeFem++ software. Blood in this zone will be considered to be a linear elastic material, hence, by solving the elastodynamic equations we get the deformation of this zone. At last, upon detecting the solidification zone, the first step in a rupture model is set up by investigating the magnitude of the external forces exerted on this zone.

5.1 A Non-Newtonian Property of Blood: The Viscosity

In order to study the properties of blood, we must consider a sample of blood that contains a suspension of particles[2]. A fluid is said to be *Newtonian* if the shear stress is proportional to the strain rate tensor $\boldsymbol{D}(\boldsymbol{v})$ where the viscosity μ is the proportionality constant. However, if the viscosity is a function of the strain rate tensor $\boldsymbol{D}(\boldsymbol{v})$, then this fluid is identified as a *non-Newtonian*. We assume that the blood cells are small compared to the macroscopic length of the blood vessels to be able to approximate the blood by a homogeneous non-Newtonian fluid. Otherwise, some difficulties may arise which prevent us from modeling the blood as a homogeneous fluid. The presence of the blood cells can cause a remarkable change in the rheological properties of blood. In this case models are constructed depending on reliable measurements and experiments.

Viscosity depends on the internal frictional or resistance forces of adjacent layers sliding past one another. One must distinguish between two viscosity-related terms. In case of a non-Newtonian fluid, the *apparent viscosity* or *effective viscosity* usually denoted by μ is the quantity measured by the viscometer for shear rates in the optimal range. Its SI unit is Pa.s. Somehow, it represents an average measure of the resistance to flow. On the other hand, the ratio of the apparent viscosity to the viscosity of the solvent used, i.e, to the viscosity of the plasma, is refereed to as the *relative viscosity* denoted by μ_{rel}.

The blood is characterized by a high viscosity than plasma due to the presence of the suspensions. An increase in the hematocrit[3] (HCT or Ht) leads to an increase of the viscosity of the suspensions which makes the non-Newtonian behavior more significant, more precisely, at very low shear rates. This is due to a biological phenomenon [FSLSS78, KS82] that is undergone by the red blood cells (RBCs) and leads to a decrease in the apparent viscosity. However, if either the fibrinogen or the globulins[4] are absent, then we detect the Newtonian behavior. In addition to the shear rate, the viscosity depends on the temperature. This dependence is similar to that of water for a temperature range 10° and 40°C and shear rates between 1 and 100 s^{-1} [MMCG65].

5.1.1 Constitutive Models of Blood

In order to model the behavior of blood, one should consider its components which affect its rheology. To achieve a well built model, we consider the blood to be a fluid containing a suspension of particles designating the cellular components of blood. Moreover, to achieve the continuum hypothesis and attain a homogeneous non-Newtonian fluid, we must assume that the length and the timescales at each RBC is sufficiently small compared to all the macroscopic length and timescales, thus the introduced models cannot be adopted in modeling blood flow through capillaries.

As we have seen in Chapter 2, the blood flow obeys the conservation principles; conservation of mass, conservation of momentum and conservation of energy. We consider the general

[2]A mixture where the particles do not dissolve and are left to leave freely, but will settle at the end.

[3]Volume percentage of red blood cells. Its normal range varies according to sexes and ages. For adult men the normal range is [42%-54%], whereas in women it is [38%-46%].

[4]Plasma proteins.

constitutive law of the incompressible viscous fluid that defines the Cauchy stress tensor $\boldsymbol{\sigma}_f$ by

$$\boldsymbol{\sigma}_f = \boldsymbol{\tau}_d - p_f\,\mathbf{Id}, \tag{5.1}$$

where $\boldsymbol{\tau}_d$ is the deviatoric stress tensor and p_f is the fluid pressure. For convenience, we recall that the incompressible Navier-Stokes equations are

$$\begin{cases} \rho_f\left(\dfrac{\partial \boldsymbol{v}}{\partial t} + (\boldsymbol{v}\cdot\boldsymbol{\nabla})\boldsymbol{v}\right) - \boldsymbol{\nabla}\cdot\boldsymbol{\tau}_d + \boldsymbol{\nabla} p_f &= \rho_f \boldsymbol{f}_f \quad \text{on } \Omega_f(t)\times(0,T), \\ \nabla\cdot\boldsymbol{v} &= 0 \qquad \text{on } \Omega_f(t)\times(0,T), \end{cases} \tag{5.2}$$

where $\boldsymbol{v}$ is the fluid velocity and ρ_f is its density.

To get a well posed system, an additional equation that relates the state of stress to the kinematic variables such as rate of deformation of fluid elements is required. This equation is known as the constitutive equation. In what follows we introduce various kinds of these models that are widely used.

5.1.2 A Newtonian Model

In general, blood is modeled as a non-Newtonian fluid. However in large vessels it behaves as a Newtonian fluid. The deviatoric stress tensor is then given by

$$\boldsymbol{\tau}_d = 2\mu\boldsymbol{D}(\boldsymbol{v}),$$

where μ is a constant that represents the dynamic viscosity and $\boldsymbol{D}(\boldsymbol{v})$ is the strain rate tensor given in terms of the blood velocity $\boldsymbol{v}$ by $\boldsymbol{D}(\boldsymbol{v}) = \dfrac{1}{2}(\boldsymbol{\nabla}\boldsymbol{v} + (\boldsymbol{\nabla}\boldsymbol{v})^t)$. This model yields the well-known incompressible Newtonian Navier-Stokes equations

$$\begin{cases} \rho_f\left(\dfrac{\partial \boldsymbol{v}}{\partial t} + (\boldsymbol{v}\cdot\boldsymbol{\nabla})\boldsymbol{v}\right) - \mu\boldsymbol{\Delta}\boldsymbol{v} + \boldsymbol{\nabla} p &= \rho_f \boldsymbol{f}_f \quad \text{on } \Omega_f(t)\times(0,T), \\ \nabla\cdot\boldsymbol{v} &= 0 \qquad \text{on } \Omega_f(t)\times(0,T). \end{cases} \tag{5.3}$$

The term $(\boldsymbol{v}\cdot\boldsymbol{\nabla})\boldsymbol{v}$ is the non-linear convective term, whereas the term $\boldsymbol{\Delta}\boldsymbol{v}$ is the diffusion term related to the role of viscosity in the propagating momentum. In large arteries the inertia term characterized by the convective term dominates the viscous term. In some literatures, the blood flow is modeled by rescaling the Navier-Stokes equations. This yields dimensionless quantities and the so-called Reynolds number Re[5] which is the ratio of the momentum forces to the viscous forces. Indeed, if $Re \ll 1$ then laminar flows occur which can be modeled by the Stokes equations. On the contrary, for high Reynolds number we have turbulent flows which can tend to produce flow instabilities. Even though in the case of an atherosclerosis laminar–turbulent transition can occur, turbulent models are not used in cardiovascular modeling and simulations. Our focus is restricted to Equation (5.2) and the appropriate constitutive blood models.

In what follows, as it is known from the context that $\boldsymbol{\tau}_d$ stands for the deviatoric stress tensor then the subindex d is omitted.

[5]It was named by Arnold Sommerfeld in 1908, after Osborne Reynolds (1842–1912), who popularized its use in 1883. It helps predict fluid flow patterns in different situations.

5.1.3 Viscosity Models

If we consider working with arteries of diameters less than 100 μm or possessing low shear rates, then a non-Newtonian behavior is observed. In this case, a more general and complex constitutive model associated to the non-Newtonian behavior must be adopted. Indeed, the constitutive equation is the main tool to develop this model. The general form of (5.1) can be attained by considering $\boldsymbol{\tau} = \boldsymbol{\tau}(\boldsymbol{\nabla v})$; a function of the velocity gradient $\boldsymbol{\nabla v}$. It is written in terms of the principal invariants as

$$\boldsymbol{\tau} = \psi_1(I_2, I_3)\boldsymbol{D}(\boldsymbol{v}) + \psi_2(I_2, I_3)(\boldsymbol{D}(\boldsymbol{v}))^2, \tag{5.4}$$

where I_2 and I_3 are respectively the second and the third principle invariants given by

$$I_2 = \frac{1}{2}\Big[\mathrm{tr}^2\big(\boldsymbol{D}(\boldsymbol{v})\big) - \mathrm{tr}\big(\boldsymbol{D}(\boldsymbol{v})\big)^2\Big] \quad \text{and} \quad I_3 = \det\big(\boldsymbol{D}(\boldsymbol{v})\big).$$

Incompressible fluids of the form (5.4) are called *Reiner-Rivlin fluids*. Notice that, in the case of divergence-free velocity fields (isochoric motions), the first invariant I_1 is null.

If ψ_2 is a non-zero function in simpler shear flows, the behavior of this fluid would not match the experimental results possessed by the real fluids ($\psi_2 = 0$) [AM74]. Further, for real fluids, the third invariant I_3 is identically zero [AM74]. Thus, based on these assumptions we deal with a special class of Reiner-Rivlin fluids called *generalised Newtonian fluids* whose deviatoric stress is of the form

$$\boldsymbol{\tau} = \psi_1(I_2)\boldsymbol{D}(\boldsymbol{v}). \tag{5.5}$$

Since $I_1 = 0$, then the principle invariant $I_2 = -\dfrac{1}{2}\mathrm{tr}\big(\boldsymbol{D}(\boldsymbol{v})\big)^2$ is negative. Hence, it is helpful to introduce the concept of shear rate to be a measure of the rate of deformation. It is denoted by $\dot{\gamma}$ and its expression is

$$\dot{\gamma} = \sqrt{2\ \mathrm{tr}(\boldsymbol{D}(\boldsymbol{v}))^2} = \sqrt{-4I_2}, \tag{5.6}$$

with the SI unit s^{-1}. Therefore the generalized Newtonian model (5.5) can be rewritten as

$$\tau = 2\mu(\dot{\gamma})\boldsymbol{D}(\boldsymbol{v}), \tag{5.7}$$

where $\mu(\dot{\gamma})$ represents a viscosity function that depends on the shear rate $\dot{\gamma}$. Now we present various types of generalized Newtonian models. We start by introducing the simpler model among all other models which is known as the *Power-Law model*.

Power-Law Model

The Power-law model is characterized by the viscosity function

$$\mu(\dot{\gamma}) = k\dot{\gamma}^{n-1}, \tag{5.8}$$

where k is a positive constant representing the consistency of SI unit Pa.s^n and n is a dimensionless positive constant representing the power-law index. A remarkable value for n is 1. If

$n = 1$ then the fluid is of a Newtonian behavior. Whereas if $n < 1$ then we get pseudoplastic fluids characterized by a low apparent viscosity at high shear rates, these fluids are also known by shear thinning fluid. On the contrary, if $n > 1$ then a fluid is said to be dilatant, also known as shear thickening fluids whose apparent viscosity increases at high shear rates. Dilatant fluids are rarely detected. Figure 5.1 shows the variation of the apparent viscosity μ as a function of the shear rate $\dot{\gamma}$ for all the fluids types mentioned above.

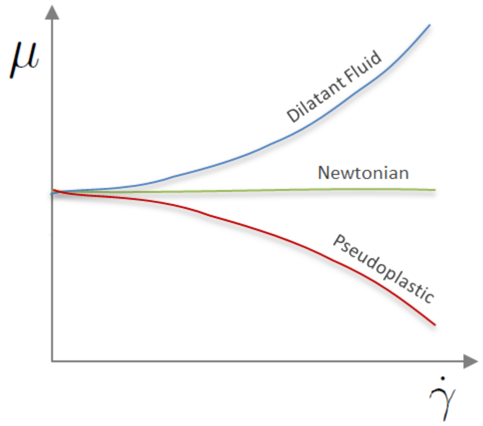

Figure 5.1: The variation of the apparent viscosity as a function of shear rate.

In 1976, the power-law model was extended to a fruitful one in the work [WS76]. It was proposed that as blood is rich in RBCs, which have a great impact on the changes encountering on the viscosity, then a more reliable model would be derived by considering characteristics related to them. Indeed, since the non-Newtonian behavior of blood arises mainly from the interaction of RBCs with each other, then the most known characteristic of them which is the hematocrit will have a significant influence on this behavior. Hence, by using multiple regression procedures it was found that the shear rate and the Ht are the most significant independent variables. Therefore, the viscosity function has been considered to be a function of the shear rate as well as on the Ht. Due to this observation, the constants k and n have been reformulated and set to be

$$k = C_1 \exp(C_2\ Ht), \quad n = 1 - C_3\ Ht, \tag{5.9}$$

where

$$C_1 = 0.0148\ \text{Pa}.s^{n-1}, \quad C_2 = 0.0512, \quad \text{and} \quad C_3 = 0.00499.$$

By employing the best three variable model, it has been shown that the three significant independent variables are mainly the shear stress, the Ht and the TPMA [6](solutions with unit g/dL (gram per deciliter)), in particular the fibrinogen and globulins. As a result, the constant k is then

$$k = C_1 \exp\big(C_2(Ht)\big) \times \exp\big(C_4(\text{TPMA}/Ht^2)\big), \tag{5.10}$$

[6]Proteins that exist in the plasma

with

$$C_1 = 0.00797 \text{ Pa.}s^{n-1}, \quad C_2 = 0.0608, \quad C_3 = 0.00499, \quad \text{and} \quad C_4 = 145.85\ textupdL/g.$$

Notice that, all the variables in the viscosity function (5.10) are independent, that is, any change occurring to one of them does not affect the others. This seems to be impractical. Indeed, the chemical changes, shear rates and interactions in the cardiovascular system are numerous and complex which prohibit us from considering them to be independent. Nevertheless, the assumption of independency seems reasonable when dealing with approximations.

Viscosity functions that are characterized by bounded non-zero limiting values can be written in the general form

$$\mu(\dot{\gamma}) = \mu_\infty + (\mu_0 - \mu_\infty)F(\dot{\gamma}),$$

which can be rewritten in the non-dimensional form as

$$\frac{\mu(\dot{\gamma}) - \mu_\infty}{\mu_0 - \mu_\infty}, \tag{5.11}$$

where μ_0 and μ_∞ corresponds to the asymptotic values of the viscosity at zero and infinity respectively. In other words,

$$\mu_0 = \lim_{\dot{\gamma}\to 0} \mu(\dot{\gamma}) \quad \text{and} \quad \mu_\infty = \lim_{\dot{\gamma}\to\infty} \mu(\dot{\gamma}).$$

Moreover, the function $F(\dot{\gamma})$ depends on the shear rate $\dot{\gamma}$ and it satisfies the following conditions

$$\lim_{\dot{\gamma}\to 0} F(\dot{\gamma}) = 1, \quad \text{and} \quad \lim_{\dot{\gamma}\to\infty} F(\dot{\gamma}) = 0.$$

In practice, the lower limit of $\dot{\gamma}$ to obtain the value of μ_0 is related to some experimental challenges and the rheometer [7]. On the contrary, this is not the case at the upper limit, due to the fact that at higher shear rates the viscosity is approximately constant[8] [FQV09, Section 6.2.3]. Nevertheless, the asymptotic values of viscosity are meaningful from the theoretical viewpoint. Furthermore, considering different forms of the function $F(\dot{\gamma})$ gives various generalized Newtonian models.

Some values for the density of blood ρ and the asymptotic viscosities μ_0 and μ_∞ at the body temperature 37° that are widely used in the literature are [CK91]

$$\rho = 1056 \text{ kg/m}^3, \quad \mu_0 = 0.056 \text{ Pa.s}, \quad \mu_\infty = 0.00345 \text{ Pa.s}.$$

In Table 5.1 we give the most commonly used generalized Newtonian models for the human blood. The values for the material constants given in this table were demonstrated in [CK91] for a collection of human and canine blood of Ht ranging from 33–45%, based on a non-linear least squares analysis.

[7] A laboratory device used to measure the way in which a liquid, suspension or slurry flows in response to applied forces.

[8] The cells will dissolute at high shear rates. We take μ_∞ to be the limit of the shear rate at the high shear plateau value.

The Model	The non Dimensional Form	Material Constants
Powell-Eyring	$\dfrac{\sinh^{-1}(\lambda\dot{\gamma})}{\lambda\dot{\gamma}}$	$\lambda = 5.383$ s
Cross	$\dfrac{1}{1+(\lambda\dot{\gamma})^m}$	$\lambda = 1.007$ s, $m = 1.028$
Modified Cross	$\dfrac{1}{(1+(\lambda\dot{\gamma})^m)^a}$	$\lambda = 3.736$ s, $m = 2.406$, $a = 0.254$.
Carreau	$\left[1+(\lambda\dot{\gamma})^2\right]^{\frac{n-1}{2}}$	$\lambda = 3.313$ s, $n = 0.3568$.
Carreau-Yasuda	$\left[1+(\lambda\dot{\gamma})^a\right]^{\frac{n-1}{a}}$	$\lambda = 1.902$ s, $n = 0.22$, $a = 1.25$.

Table 5.1: Material constants for different generalized Newtonian models [FQV09, Table 6.2].

For these material constants we plot on Figure 5.2 the corresponding graphs of the viscosity function μ.

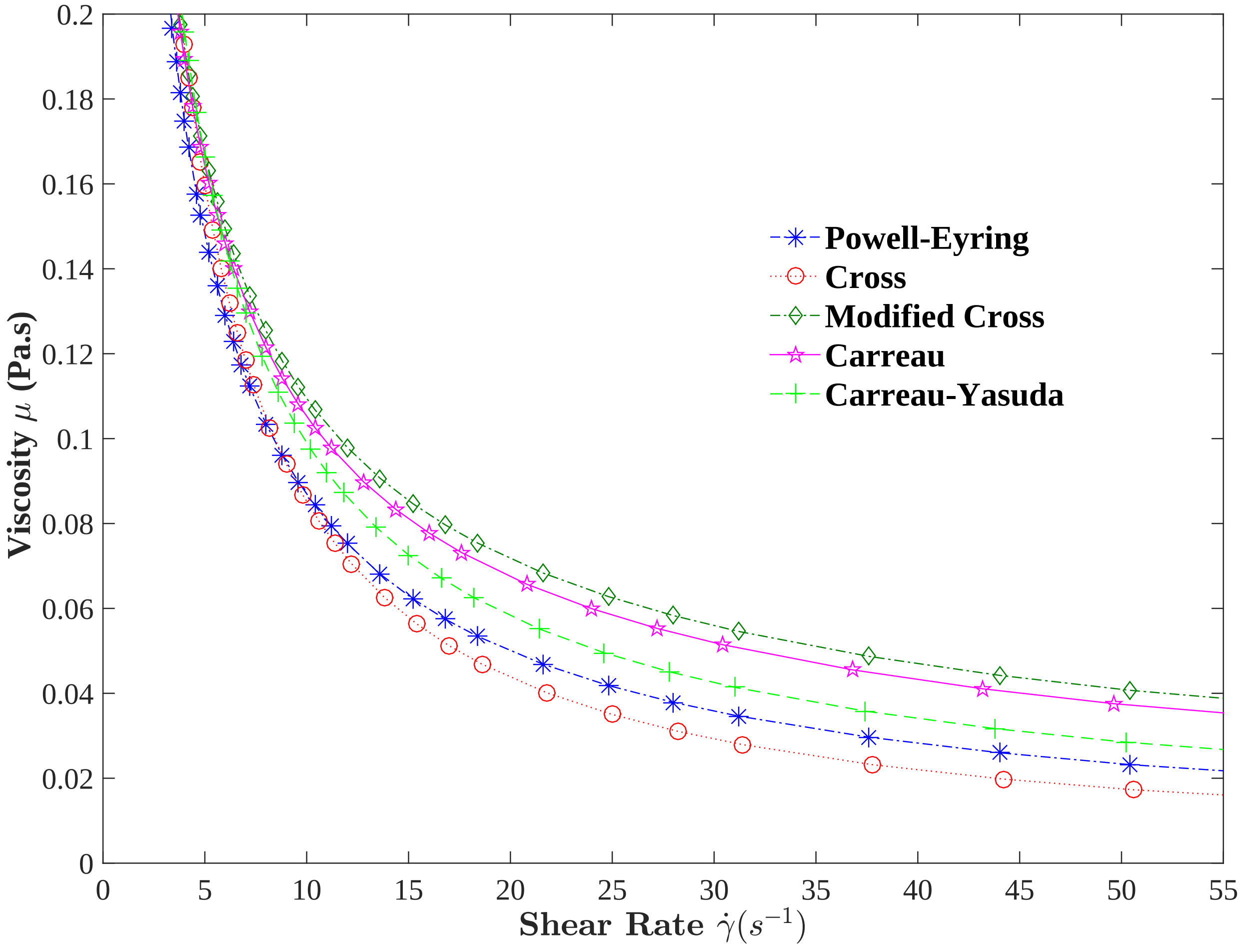

Figure 5.2: The manner of the different generalized Newtonian models.

For a more rich knowledge in the most significant and suitable constitutive models from the phenomenological viewpoint the reader can refer to [RSK] [FQV09, Chapter 6].

5.2 Solidification of Blood and its Rupture

The process of blood coagulation is widely observed in case of a bleeding wound. The termination of bleeding is the platelets mission which are stimulated by the RBCs. Platelets adhere to the vessel wall to form a layer on the site of the injury. This layer is known as a clot, which with time its exterior surface dries to form a solid crust. Blood clots are formed whenever the flowing blood comes in contact with a foreign substance in the skin or in the blood vessels wall. They can be classified into two types: thrombi, which are stationary clots, though they can cause the blockage of a flow; emboli, which detach into the blood flow and can, somewhere in a site faraway from the thrombi, block the flow. This type of clots is dangerous and causes infarctions, more precisely, if the blockage occurs in the brain it results a stroke, if it occurs in the heart a heart attack would result, or in the lungs it would cause pulmonary embolism. In particular, in the situations where plaques formed from fats, lipids, cholesterol or other foreign substances found in the blood are identified, over time, they harden causing the narrowing of the artery. Figure 5.3 shows a plaque (yellow in color) formed in a blood vessel.

Figure 5.3: A stenosed artery.

In 1988, the work [AvdBP+88] demonstrated that in vitro large numbers of RBCs flow in the vessel pushing platelets to the wall; a phenomenon that is known as platelet margination. Hence, the platelets are highly concentrated near the wall. In 2011, a model was formulated in [TBA11, TBE+11] to analyze the response of platelets and their adhesion rates to factors including the Ht, RBC collisions and platelet size. Results showed that platelets would be the major cause of the formation of the thrombosis. A view of what we have, gives a big expectation of a thrombosis formed near the plaque by RBCs, platelets and Fibrinogen (Factor I)[9] which breaks down to fibrin by the enzyme thrombin to form clots. Clots composed of platelets are likely to enlarge based on the fact that platelets produce chemicals that attract other platelets, which will lead them to stick together. A thrombus in the site of injury would take 4-10 minutes to form. This would give an evidence that a clot in the blood vessels of a healthy human as a result of plaque would take a long time to form, or to block the vessel entirely. We believe that

[9]One of the 13 factors responsible for coagulation.

in many cases the stage of an entire block is not reached, rather, some factors in the blood flow will force the clot to be released into the blood, and at some levels the clot will block it. We deal with the solidification of blood as a coagulation process which takes place within the artery.

5.2.1 Detection of the Solidification Zone

The final step in the formation of plaque- which is rupture- does not always occur. We believe that it is linked to the solidified blood and is influenced by some factors that we will discuss later from the numerical viewpoint. For this reason, the first step in building a rupture model is characterized by spotting the region of solidification. That is, we investigate based on the rheology of blood, constitutive models and numerical results achieved in Chapter 4, the region where the blood transits into a gel state. In general, in vivo, blood is liquid in state, then a change in its state from liquid to gel is linked to a change in the viscosity. Indeed, as the viscosity increases, a more solidified material is acquired. Hence, a solidification zone should be identified by a sufficiently large viscosity. Though, we can detect many regions that are characterized by high viscosity values. In fact, in regions where the values of the velocities are almost equal, the viscosity is of high values, this fact is due to the relation between the viscosity μ and the deformation tensor $\boldsymbol{D}(\boldsymbol{v})$. In other words, as the rate of change of the velocity expressed by $\boldsymbol{D}(\boldsymbol{v})$ is negligible then the viscosity tends to reach its highest asymptotic value μ_0 (Figure 5.2). This reveals that the condition of possessing a high viscosity is insufficient to detect the solidification zone. Hence, another condition is essential to achieve a precise location of the solidification zone. It is recognized that gel and jelly-like materials spread and flow slowly. Consequently, the solidification zone must also possess a negligible speed.

Results in Chapter 4 have shown the existence of a recirculation zone that is located after the stenosis due to the blockage of the flow by the stenosis. This zones is characterized by a negligible speed at its center which increases as the circles formed in this zone become larger in diameter. Between the recirculation zone and the stenosis, in particular at the adjacent right bottom of the stenosis, we detect a region where the flow is of negligible speed and of high viscosity. This region is identified as the solidification zone since it possesses the characteristics mentioned above (high blood viscosity and a negligible blood speed).

Notice that, as the formation of atherosclerosis is a long-time process, the formation of the solidification region is as well. Literally, viscosity is a time-dependent function. In fact, the formation of these regions depends on the blood flow at each pulse, that is, the viscosity depends on its history.

Numerically, we consider a threshold value μ_{th} of the blood viscosity such that when the computed viscosity μ exceeds μ_{th} a region $\mathcal{D}_\mu$ of a high viscosity is identified. Similarly, we consider a threshold value v_{th} of the blood speed. If the speed $||\boldsymbol{v}||_2$ is such that it is less than v_{th} then we locate a region $\mathcal{D}_v$ of a negligible speed. The solidification region $\mathcal{R}_\mathfrak{s}$ is the intersection of the two located regions $\mathcal{D}_\mu$ and $\mathcal{D}_v$. More precisely, the region $\mathcal{R}_\mathfrak{s}$ satisfies possessing a high viscosity as well as a negligible speed.

We model the blood using the Carreau model. We recall that the associated viscosity is formulated as follows

$$\mu(\dot\gamma) = \mu_\infty + (\mu_0 - \mu_\infty)\big[1 + (\lambda\dot\gamma)^2\big]^{\frac{n-1}{2}},$$

where

$$\lambda = 3.313 \text{ s}, \quad n = 0.3568, \quad \mu_0 = 0.056 \text{ Pa.s} \quad \text{and} \quad \mu_\infty = 0.00345 \text{ Pa.s}.$$

Further, the term $\dot\gamma$ is the shear rate expressed in terms of the second invariant I_2 as

$$\dot\gamma = \sqrt{2\ \mathrm{tr}(\boldsymbol{D}(\boldsymbol{v}))^2} = \sqrt{-4I_2}.$$

A modification is applied to Carreau model so that the viscosity becomes a time-dependent function expressed in terms of its history. As we are performing iterative simulations, then at each time iteration k, for $k \in \mathbb{N}$, we will express the viscosity μ_k in terms of the local in time average viscosity $\hat\mu_k$ given by

$$\hat\mu_k = \begin{cases} \mu_0 = 0.056 & \text{if } k = 0, \\ 0.035 & \text{for } 1 \le k \le 4, \\ \dfrac{1}{5}\displaystyle\sum_{i=1}^{5} \mu_{k-i} & \text{for } k \ge 5, \end{cases}$$

where μ_{k-i} represents the viscosity of blood at each iteration $k-i$. Then at each time iteration $k \in \mathbb{N}$, we set

$$\mu_{\infty,k} = \mu_\infty + t \times 10^{-3} \times \hat\mu_k^{0.2}$$

and

$$\mu_{0,k} = \mu_0 + t \times 10^{-3} \times \hat\mu_k^{0.2},$$

where $t = k \times \Delta t$ with $\Delta t = 10^{-2}$ s is the time step.
Hence, at the iteration k, the viscosity expression becomes

$$\mu_k = \mu_{\infty,k} + (\mu_{0,k} - \mu_{\infty,k})\big[1 + (\lambda\dot\gamma_k)^2\big]^{\frac{n-1}{2}}, \tag{5.12}$$

with $\dot\gamma_k$ given by (5.6) as $\sqrt{2\mathrm{tr}\big(\boldsymbol{D}(\boldsymbol{v}^{k-1})\big)^2}$. In a two dimensional space, its explicit expression is

$$\sqrt{2\left(\frac{d}{dx}v_1^{k-1}\right)^2 + 2\left(\frac{d}{dy}v_2^{k-1}\right)^2 + \left(\frac{d}{dy}v_1^{k-1} + \frac{d}{dx}v_2^{k-1}\right)^2}.$$

It should be noticed from the context that the superindices $k-1$ and k refer to the time iteration, while the subindices 1 and 2 stand for the vector components of $\boldsymbol{v}$.

To set the threshold values μ_{th} and v_{th}, we plot the most remarkable values on a specified time interval $[t_0, T]$, $t_0 > 0$. The highest remarkable value is set to be the threshold in case of viscosity. At each iteration k, the global in time average viscosity $\overline{\mu}_k$ is given by the following relation

$$\overline{\mu}_k(t) = \frac{1}{k+1}\sum_{i=0}^{k} \mu_i(t),$$

where $\mu_i(t)$ represents the space average viscosity of the blood at iteration i, $0 \leq i \leq k$ whose expression is given by

$$\mu_i(t) = \frac{1}{|\Omega_f(t)|} \int_{\Omega_f(t)} \mu_i(\boldsymbol{x}, t)\, d\boldsymbol{x}, \qquad \forall\, \boldsymbol{x} \in \Omega_f(t),$$

with $|\Omega_f(t)|$ is the area of the blood domain $\Omega_f(t)$ at any instant t and $\mu_i(\boldsymbol{x}, t)$ is the viscosity function at any time iteration i.
We set $\overline{\mu}_0 = \mu_0 = 0.056$ Pa.s. The graphs corresponding to the viscosity and the average viscosity obeying (5.12) during 3 seconds are plotted on Figure 5.4.

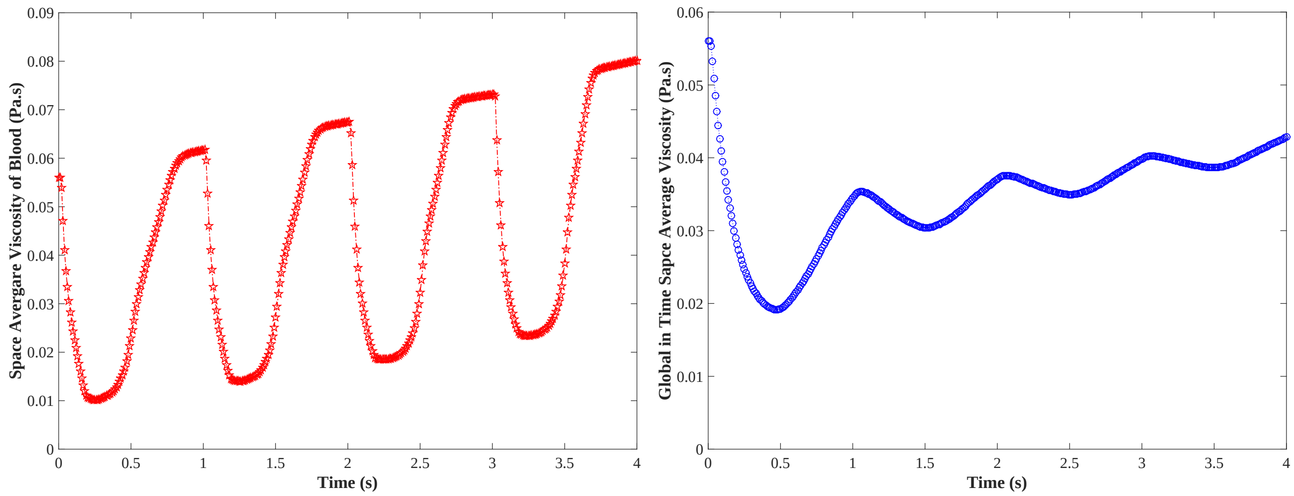

(a) Space average viscosity of blood. (b) Global in time space average viscosity of blood.

Figure 5.4: Space average viscosity (left) and global in time space average viscosity (right) of a non-Newtonian blood.

The pattern of the global in time average viscosity within the lumen of the artery at the instant $t_0 = 3$ s is illustrated on Figure 5.5.

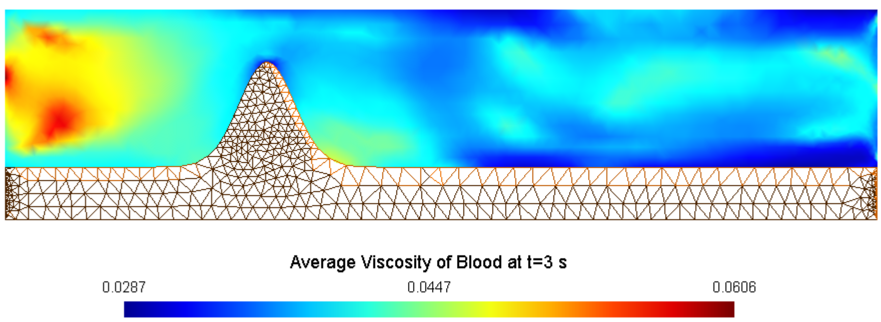

Figure 5.5: Global in time average viscosity of blood at time $t_0 = 3$ s.

From Figure 5.5 we observe mainly two regions possessing a high average viscosity. The first region, located at the inlet of the artery, is a region where the particles constituting it are characterized by values of velocity that are almost equal. Thus, based on the expression of the viscosity in terms of the rate of deformation tensor $\boldsymbol{D}(\boldsymbol{v})$ a high viscosity results. On the other hand, the second region of a high average viscosity, is located near the stenosis. The existence of stenosis prevents the flow from reaching the spot at the edge of the stenosis. Consequently, blood will become more viscous. In particular, the values of the viscosity in these two remarkable regions are greater than 0.04 Pa.s. Rescaling the data we get a precise location of the regions which are characterized by an average viscosity greater than 0.04 Pa.s (see Figure 5.6).

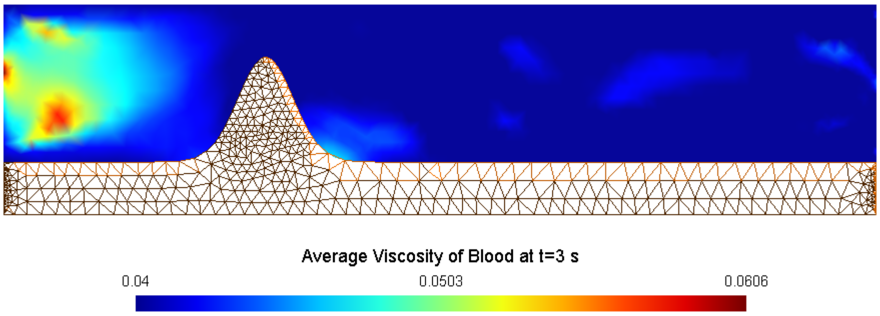

Figure 5.6: Regions of average viscosity greater than 0.04 Pa.s.

As a result, we set the threshold μ_{th} to be 0.04 Pa.s. As we mentioned previously, another condition is desired to obtain a precise location of the solidification zone. More precisely, the zone must be characterized by a negligible speed. The average speed at time $t_0 = 3$ s is illustrated on Figure 5.7.

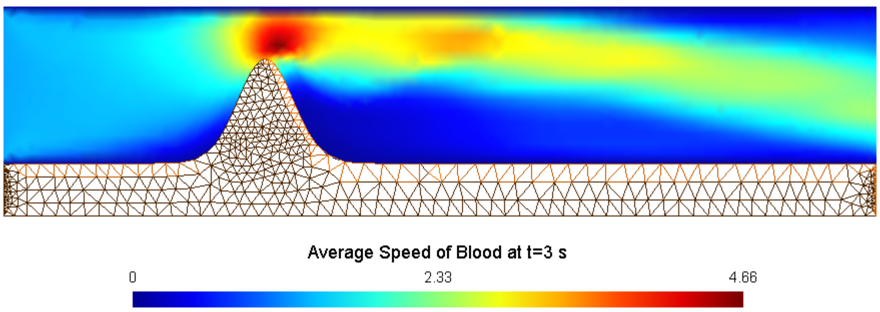

Figure 5.7: Average speed of blood at time $t_0 = 3$ s.

Figure 5.7 shows that the average speed attains its highest value above the peak of the stenosis. In contrast, the lowest value is observed at the edge of the stenosis. A rescaling of the values would help us get a precise data. Indeed, Figure 5.8 reveals that the speed of the blood existing at the edge of the stenosis is of maximum value 0.1 cm/s.

To sum up, at $t_0 = 3$ s, Figures 5.6 and 5.8 showed a region at the edge of the stenosis where the blood is characterized by a high viscosity and a negligible speed. In fact, by setting

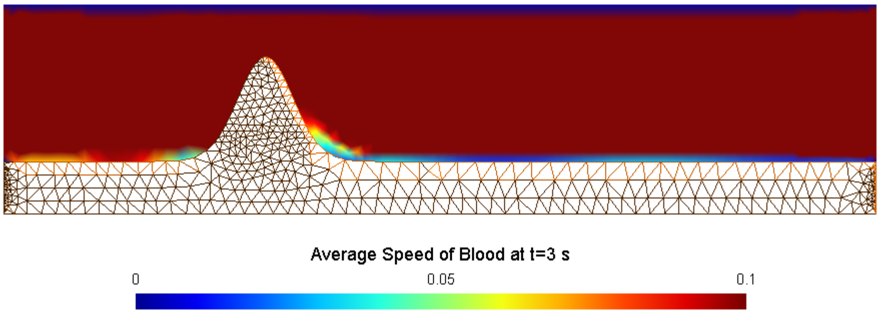

Figure 5.8: Regions of average speed less than 0.1 cm/s.

$\mu_{th} = 0.04$ Pa.s and $v_{th} = 0.1$ s we get an accurate detection of the solidification zone at the edge of the stenosis. The solidification zone is given in Figure 5.9.

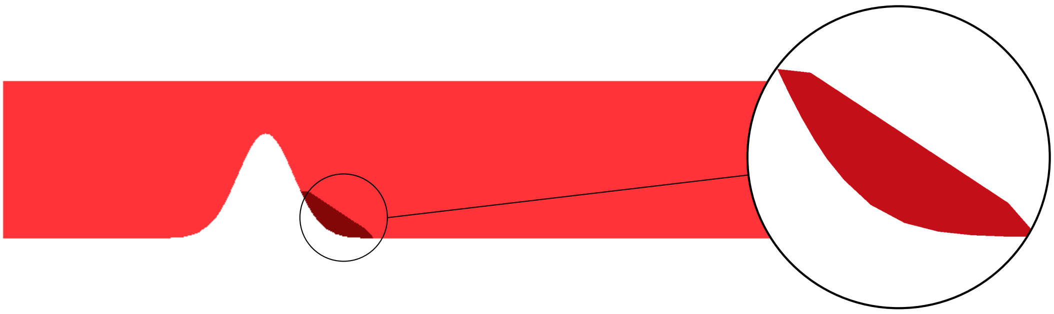

Figure 5.9: The solidification zone $\mathcal{R}_\mathfrak{s}(t)$.

5.2.2 Forces Acting on the Solidification Zone

Having located the region of solidification $\mathcal{R}_\mathfrak{s}(t)$, $t > t_0 > 0$, we proceed to identify the factors that we believe will lead to the rupture of the solidified blood. The solidification region is made up of blood in gel state, which similarly as the plaque, will be under the effect of a force exerted by the pressure of the blood and the shear stress. Moreover, being located at the edge of the stenosis, it will be affected by the stenosis deformation. At any instant $t > 0$, we denote by $\Omega_f(t)$ the domain corresponding to the lumen of the artery and by $\Omega_s(t)$ the domain representing the arterial wall. On $\Omega_f(t)$ we define $\boldsymbol{v}$ the velocity of the blood and p_f to be its pressure. On the other hand, the motion of the arterial wall is defined by its displacement $\boldsymbol{\xi}_s$. The boundary $\partial\mathcal{R}_\mathfrak{s}(t)$ of the solidification zone is decomposed into $\Gamma_1(t)$ and $\Gamma_2(t)$ as shown on Figure 5.10.

Linear Elasticity of the Solidified Blood

We deal with the solidification zone from the perspective of being an elastic material that obeys Hooke's law. Let us designate by $\boldsymbol{u} = (u_1, u_2)$ the displacement of the domain $\mathcal{R}_\mathfrak{s}(t)$. The solidification zone is under the effect of an external surface force. In particular, a surface force

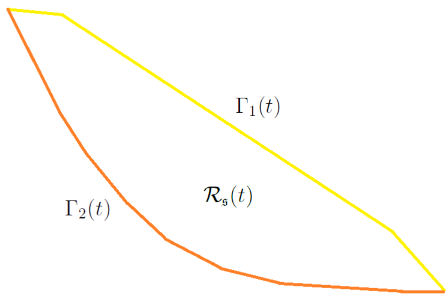

Figure 5.10: The domain of the solidification zone.

$\boldsymbol{f}_\mathfrak{s}$, representing the shear stress is applied from the blood surrounding the solidification zone to the boundary $\Gamma_1(t)$. Thus, the expression of $\boldsymbol{f}_\mathfrak{s}$ is given in terms of the Cauchy stress tensor $\boldsymbol{\sigma}_f(\boldsymbol{v}, p_f)$ by

$$\boldsymbol{f}_\mathfrak{s} = -\boldsymbol{\sigma}_f(\boldsymbol{v}, p_f)\ \boldsymbol{n}_f \qquad \text{on} \quad \Gamma_1(t) \times (t_0, T), \tag{5.13}$$

where $\boldsymbol{n}_f$ is the outward normal to the domain $\Omega_f(t) \setminus \mathcal{R}_\mathfrak{s}(t)$.
On the other hand, since the border $\Gamma_2(t)$ constitutes a part of the common boundary $\Gamma_c(t) = \partial\Omega_f(t) \cap \partial\Omega_s(t)$ then we must ensure the continuity of the deformation on this boundary, that is, we impose the condition

$$\boldsymbol{u} = \boldsymbol{\xi}_s \qquad \text{on} \quad \Gamma_2(t) \times (t_0, T). \tag{5.14}$$

As a result, the elasticity equations describing the displacement of the solidification zone $\mathcal{R}_\mathfrak{s}(t)$ are

$$\begin{cases} -\mathbf{div}\ \boldsymbol{\sigma}_\mathfrak{s}(\boldsymbol{u}) = 0 & \text{in} \quad \mathcal{R}_\mathfrak{s}(t) \times (t_0, T), \\ \boldsymbol{\sigma}_\mathfrak{s}(\boldsymbol{u})\ \boldsymbol{n}_\mathfrak{s} = \boldsymbol{f}_\mathfrak{s} & \text{on} \quad \Gamma_1(t) \times (t_0, T), \\ \boldsymbol{u} = \boldsymbol{\xi}_s & \text{on} \quad \Gamma_2(t) \times (t_0, T), \end{cases} \tag{5.15}$$

where $\boldsymbol{n}_\mathfrak{s}$ is the outward normal to the solidification zone $\mathcal{R}_\mathfrak{s}(t)$. The Cauchy stress tensor $\boldsymbol{\sigma}_\mathfrak{s}(\boldsymbol{u})$ is expressed in terms of the strain tensor $\boldsymbol{\varepsilon}(\boldsymbol{u}) = \dfrac{1}{2}\big(\boldsymbol{\nabla u} + (\boldsymbol{\nabla u})^t\big)$ by Hooke's law

$$\boldsymbol{\sigma}_\mathfrak{s}(\boldsymbol{u}) = 2\mu_\mathfrak{s}\boldsymbol{\varepsilon}(\boldsymbol{u}) + \lambda_\mathfrak{s}\mathrm{tr}(\boldsymbol{\varepsilon}(\boldsymbol{u}))\ \mathbf{Id}, \tag{5.16}$$

with $\mu_\mathfrak{s}$ and $\lambda_\mathfrak{s}$ are the Lamé constants that are given in terms of the Young's modulus E and the Poisson's ratio ν as

$$\lambda_\mathfrak{s} = \frac{\nu E}{(1-2\nu)(1+\nu)} \qquad \text{and} \qquad \mu_\mathfrak{s} = \frac{E}{2(1+\nu)}.$$

For a clot, which is is assumed to be an incompressible material, the Poisson's ratio is $\nu = 0.492$ [WRB+15]. Further, its Young's modulus (Elastic modulus) $E = 14.5$ MPa [CSL+05].

For the sake of convenience, we recall that the Cauchy stress tensor $\boldsymbol{\sigma}_f(\boldsymbol{v}, p_f)$ is give in terms of the deformation tensor $\boldsymbol{D}(\boldsymbol{v}) = \dfrac{\boldsymbol{\nabla v} + (\boldsymbol{\nabla v})^t}{2}$ by

$$\boldsymbol{\sigma}_f(\boldsymbol{v}, p_f) = 2\mu \boldsymbol{D}(\boldsymbol{v}) - p_f \ \mathbf{Id},$$

where $\boldsymbol{v}$ and p_f are the velocity and the pressure of the blood, respectively.

In order to write the variational formulation associated to System (5.15), we rewrite it as a partial differential equation (PDE) with homogeneous Dirichlet boundary condition. For this reason, we consider a function $\mathfrak{h} \in H^1(\mathcal{R}_\mathfrak{s}(t))$ such that $\gamma_0(\mathfrak{h}) = \boldsymbol{\xi}_s$, where

$$\gamma_0 : H^{1/2}(\Gamma_2(t)) \mapsto H^1(\mathcal{R}_\mathfrak{s}(t))$$

is the trace operator.
Take $\boldsymbol{\varsigma} = \boldsymbol{u} - \mathfrak{h}$ which is a function in $H^1(\mathcal{R}_\mathfrak{s}(t))$ that vanishes on $\Gamma_2(t)$. Since $\boldsymbol{\sigma}_\mathfrak{s}(\boldsymbol{u})$ is a function of $\boldsymbol{\varepsilon}(\boldsymbol{u})$ which is linear, then we have

$$\boldsymbol{\sigma}_\mathfrak{s}(\boldsymbol{\varsigma}) = \boldsymbol{\sigma}_\mathfrak{s}(\boldsymbol{u}) - \boldsymbol{\sigma}_\mathfrak{s}(\mathfrak{h}).$$

Therefore, System (5.15) is equivalent to

$$\begin{cases} -\mathbf{div}\ \boldsymbol{\sigma}_\mathfrak{s}(\boldsymbol{\varsigma}) = \mathbf{div}\ \boldsymbol{\sigma}_\mathfrak{s}(\mathfrak{h}) & \text{in} \quad \mathcal{R}_\mathfrak{s}(t) \times (t_0, T), \\ \boldsymbol{\sigma}_\mathfrak{s}(\boldsymbol{\varsigma})\ \boldsymbol{n}_c = \boldsymbol{f}_c - \boldsymbol{\sigma}_\mathfrak{s}(\mathfrak{h})\ \boldsymbol{n}_c & \text{on} \quad \Gamma_1(t) \times (t_0, T), \\ \boldsymbol{\varsigma} = \mathbf{0} & \text{on} \quad \Gamma_2(t) \times (t_0, T), \end{cases} \tag{5.17}$$

The variational formulation associated to System (5.17) is derived by considering a test function

$$\boldsymbol{\eta}_\mathfrak{s} \in \mathcal{W}_\mathfrak{s} = \{\boldsymbol{\eta} \in H^1(\mathcal{R}_\mathfrak{s}(t)),\ \boldsymbol{\eta} = \mathbf{0} \text{ on } \Gamma_2(t)\}$$

to get

$$\int_{\mathcal{R}_\mathfrak{s}(t)} \boldsymbol{\sigma}_\mathfrak{s}(\boldsymbol{\varsigma}) : \boldsymbol{\nabla \eta}_\mathfrak{s}\ d\boldsymbol{x} - \int_{\Gamma_1(t)} \boldsymbol{\sigma}_\mathfrak{s}(\boldsymbol{\varsigma})\ \boldsymbol{n}_\mathfrak{s} \cdot \boldsymbol{\eta}_\mathfrak{s}\ d\Gamma = \int_{\mathcal{R}_\mathfrak{s}(t)} [\mathbf{div}\ \boldsymbol{\sigma}_\mathfrak{s}(\mathfrak{h})] \cdot \boldsymbol{\eta}_\mathfrak{s}\ d\boldsymbol{x}. \tag{5.18}$$

Substituting $\boldsymbol{\sigma}_\mathfrak{s}(\boldsymbol{\varsigma})$ by its expression (5.16) and $\boldsymbol{f}_\mathfrak{s}$ by (5.13) we can rewrite (5.18) as

$$\begin{cases} 2\mu_\mathfrak{s} \displaystyle\int_{\mathcal{R}_\mathfrak{s}(t)} \boldsymbol{\varepsilon}(\boldsymbol{\varsigma}) : \boldsymbol{\varepsilon}(\boldsymbol{\eta}_\mathfrak{s})\ d\boldsymbol{x} + \lambda_\mathfrak{s} \int_{\mathcal{R}_\mathfrak{s}(t)} (\nabla \cdot \boldsymbol{\varsigma})(\nabla \cdot \boldsymbol{\eta}_\mathfrak{s})\ d\boldsymbol{x} - \int_{\Gamma_1(t)} \boldsymbol{\sigma}_f(\boldsymbol{v}, p_f)\ \boldsymbol{n}_\mathfrak{s} \cdot \boldsymbol{\eta}_\mathfrak{s}\ d\Gamma \\ + \displaystyle\int_{\Gamma_1(t)} \boldsymbol{\sigma}_\mathfrak{s}(\mathfrak{h})\ \boldsymbol{n}_\mathfrak{s} \cdot \boldsymbol{\eta}_\mathfrak{s}\ d\Gamma = \int_{\mathcal{R}_\mathfrak{s}(t)} [\mathbf{div}\ \boldsymbol{\sigma}_\mathfrak{s}(\mathfrak{h})] \cdot \boldsymbol{\eta}_\mathfrak{s}\ d\boldsymbol{x} \qquad \forall\ \boldsymbol{\eta}_\mathfrak{s} \in \mathcal{W}_\mathfrak{s}. \end{cases} \tag{5.19}$$

Consider a time step $\Delta t > 0$ and a finite element partition $\mathcal{U}_h$ of the solidification zone $\mathcal{R}_\mathfrak{s}(t)$ of maximum diameter h. Our aim is to approximate the solution $\boldsymbol{\varepsilon}$ at time $t_n = n\Delta t$, for $n \in \mathbb{N}$ in the finite element space. At any time t consider the finite dimensional sub-space

$$U_h = \{\boldsymbol{\eta}_h : \boldsymbol{\eta}_h = \eta_1\psi_1 + \ldots + \eta_N\psi_N\} \subset \mathcal{W}_c,$$

where $\{\psi_i\}_i$ is a family of linearly independent functions with compact support, which are piecewise polynomials. In particular, we consider them to be of degree 2. Thus, at the time iteration t_n, the discretized formulation is

$$\begin{cases} 2\mu_c \displaystyle\int_{\mathcal{R}_\mathfrak{s}(t_n)} \boldsymbol{\varepsilon}(\varsigma_h^n) : \boldsymbol{\varepsilon}(\boldsymbol{\eta}_h)\ d\boldsymbol{x} + \lambda_c \int_{\mathcal{R}_\mathfrak{s}(t_n)} (\nabla\cdot\varsigma_h^n)(\nabla\cdot\boldsymbol{\eta}_h)\ d\boldsymbol{x} - \int_{\Gamma_1(t_n)} \boldsymbol{\sigma}_f(\boldsymbol{v}^n, p_f^n)\ \boldsymbol{n}_c\cdot\boldsymbol{\eta}_h\ d\Gamma \\ + \displaystyle\int_{\Gamma_1(t_n)} \boldsymbol{\sigma}_\mathfrak{s}(\mathfrak{h}_h^n)\ \boldsymbol{n}_c\cdot\boldsymbol{\eta}_h\ d\Gamma = \int_{\mathcal{R}_\mathfrak{s}(t_n)} [\mathbf{div}\ \boldsymbol{\sigma}_\mathfrak{s}(\mathfrak{h}_h^n)]\cdot\boldsymbol{\eta}_h\ d\boldsymbol{x} \qquad \forall\ \boldsymbol{\eta}_h \in U_h. \end{cases} \tag{5.20}$$

Upon solving (5.20) using FreeFem++ software [Hec05] we obtain the displacement of the domain $\mathcal{R}_\mathfrak{s}(t)$, consequently, we get its deformation that is illustrated on Figure 5.11.

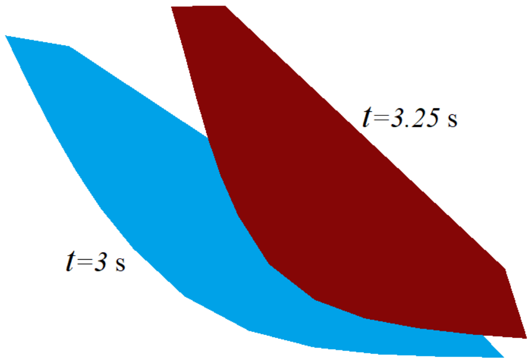

Figure 5.11: The deformation of the solidification zone between $t = 3$ s and $t = 3.25$ s.

The deformation of the stenosis due to the blood external stress, results a deformation of the solidification zone. Indeed, this is due to the continuity of displacements on the stenosis-zone interface $\Gamma_2(t)$ given by the condition (5.14). The graphs corresponding to the space average displacement $\overline{\boldsymbol{u}}_{av}(t)$ of the solidification zone and the boundaries $\Gamma_1(t)$ and $\Gamma_2(t)$ during the time interval between 3 s and 4 s, are illustrated on Figure 5.12. The space average displacement $\overline{\boldsymbol{u}}_{av}(t)$ is defined by

$$\overline{\boldsymbol{u}}_{av}(t) = \frac{1}{|\mathcal{R}_\mathfrak{s}(t)|}\int_{\mathcal{R}_\mathfrak{s}(t)} ||\boldsymbol{u}(\boldsymbol{x},t)||_2\ d\boldsymbol{x},$$

where $||.||_2$ is the Euclidean norm in $\mathbb{R}^2$ and $|\mathcal{R}_\mathfrak{s}(t)|$ is the area of $\mathcal{R}_\mathfrak{s}(t)$ provided that it is strictly positive. In a similar way we define the space average displacements of $\Gamma_1(t)$ and $\Gamma_2(t)$.
From Figure 5.12 we observe that the boundary $\Gamma_1(t)$ possesses the highest displacement. This fact is shown on Figure 5.13 which shows the time average displacement $\overline{\boldsymbol{u}}_k(\boldsymbol{x})$ of the solidification zone on the time interval [3 s-4 s]. The time average displacement at any position $\boldsymbol{x}$ is given by the formula

$$\overline{\boldsymbol{u}}_k(\boldsymbol{x}) = \frac{1}{k+1}\sum_{i=0}^{k} \boldsymbol{u}(\boldsymbol{x}, i),$$

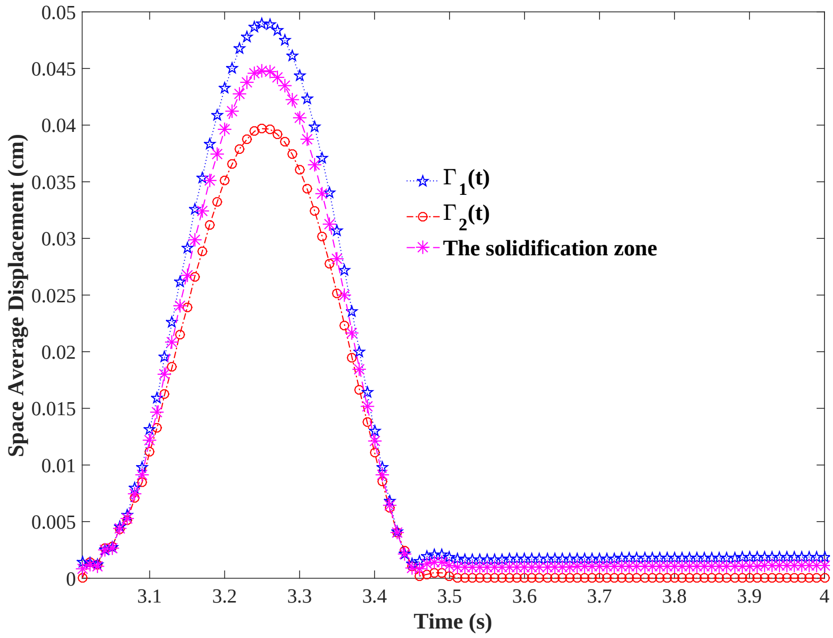

Figure 5.12: The space average displacement of the solidification zone and its boundaries $\Gamma_1(t)$ and $\Gamma_2(t)$.

where $\boldsymbol{u}(\boldsymbol{x}, i)$ is the displacement of the solidification zone at any time iteration $i \in \mathbb{N}$.

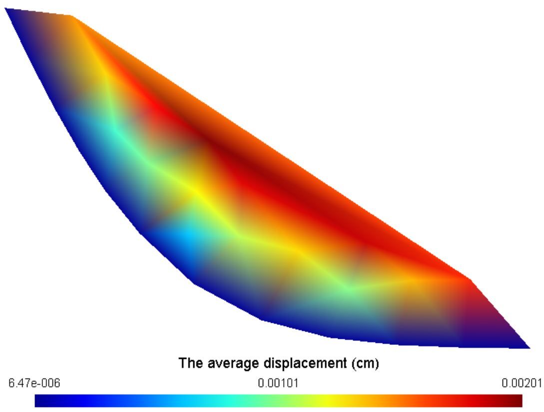

Figure 5.13: The time average displacement of the solidification zone $\mathcal{R}_{\mathfrak{s}}(t)$.

It seems reasonable for $\Gamma_1(t)$ to possess the highest displacement, in fact, the displacement of the boundary $\Gamma_2(t)$ represents the displacement of the stenosis-zone boundary, while the displacement of the boundary $\Gamma_1(t)$ is a result of the deformation of the whole zone. The high displacement of $\Gamma_1(t)$ rises our curiosity to analyze the external stress exerted by blood on this boundary. Its average is given by the expression

$$\frac{1}{|\Gamma_1(t)|}\int_{\Gamma_1(t)} \boldsymbol{\sigma}_f(\boldsymbol{v}, p_f)\ \boldsymbol{n}_c\ d\Gamma,$$

where $|\Gamma_1(t)|$ stands for the length of the border $\Gamma_1(t)$ provided that its length is strictly positive.

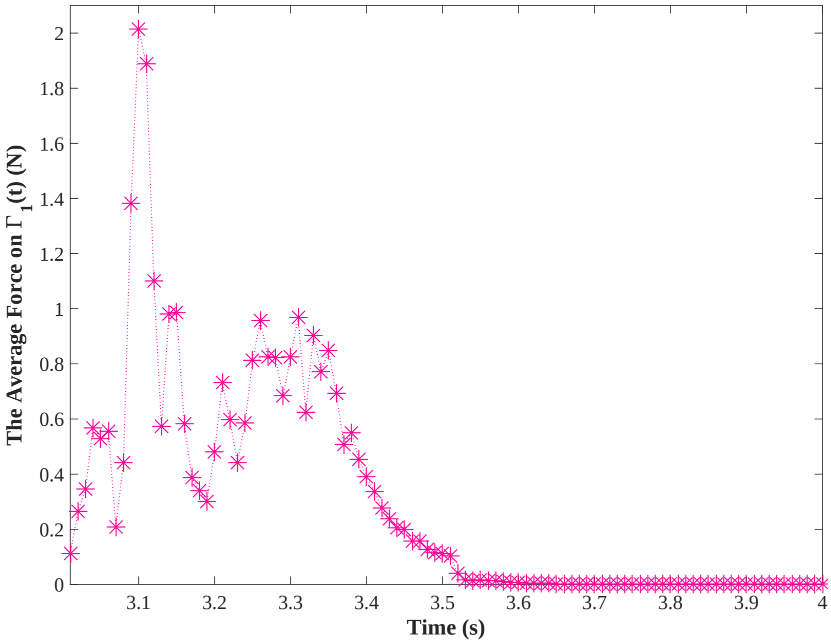

Figure 5.14: The magnitude of the average external force exerted on $\Gamma_1(t)$ at any time t.

Figure 5.14 shows that the magnitude of the average force exerted by the blood flow on the boundary $\Gamma_1(t)$ is large, hence, it results an inward resistance effect on this boundary which is large compared to the average displacement of the boundary $\Gamma_1(t)$ (see Figures 5.12). In other words, the force on the boundary $\Gamma_1(t)$ is opposed by the deformation of the solidification zone resulting from the deformation of the stenosis. Whence, the stress exerted on $\Gamma_1(t)$ will form a resistance factor against the motion of the solidification zone, which will end up with the fragmentation of the crusted solidified blood. To investigate the effect of the stress on the solidification zone, we will analyze the maximum shear stress σ_{max} given by the expression [YHSC04]

$$\sigma_{max} = \sqrt{\left(\frac{\sigma_{11} - \sigma_{22}}{2}\right)^2 + \sigma_{12}^2}. \tag{5.21}$$

Its pattern within the solidification zone is illustrated on Figure 5.15 at $t = 3.5$ s.

Figure 5.15 shows that the upper part of the solidification zone and the blood-zone interface $\Gamma_1(t)$ possess the highest maximum shear stress value. Indeed, as we have mentioned previously, as we come closer to the peak of the stenosis its stiffness decreases, thus its displacement increases and it will deform easily, consequently, the upper part of the solidification zone will be more

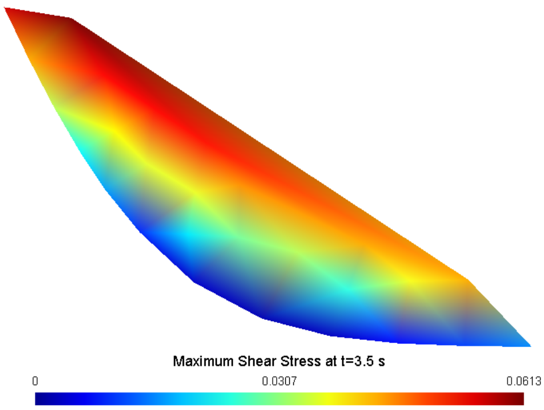

Figure 5.15: The maximum shear stress within the solidification zone at time $t = 3.5$ s .

affected by the motion of the stenosis. Further, the stress exerted by blood on $\Gamma_1(t)$ which is of high magnitude (see Figure 5.14) will lead to a high maximum shear stress. The space average maximum shear stress on the boundary $\Gamma_1(t)$ at any time t is given by the formula

$$\overline{\sigma}_{max}(t) = \frac{1}{|\Gamma_1(t)|} \int_{\Gamma_1(t)} ||\sigma_{max}(\boldsymbol{x}, t)||_2 \; d\boldsymbol{x},$$

where $||.||_2$ is the Euclidean norm in $\mathbb{R}^2$ and $|\Gamma_1(t)|$ is the length of $\Gamma_1(t)$ provided that it is strictly positive. The graph corresponding to the magnitude of the average maximum shear stress $\overline{\sigma}_{max}$ on the boundary $\Gamma_1(t)$ is given in Figure 5.16.

The force exerted by the blood on the solidification zone which opposes its motion will form a frictional force on the solidification zone (digging manner). Further, from Figure 5.16, we observe that at the instant $t = 3.5$ s when the solidification zone returns to its equilibrium position, the boundary $\Gamma_1(t)$ is still under the effect of the maximum shear stress. As a result, the maximum shear stress will scrape the crust leading to the release of some pieces of the solidified blood into the flow, which at some sites will block the flow causing an infarction.

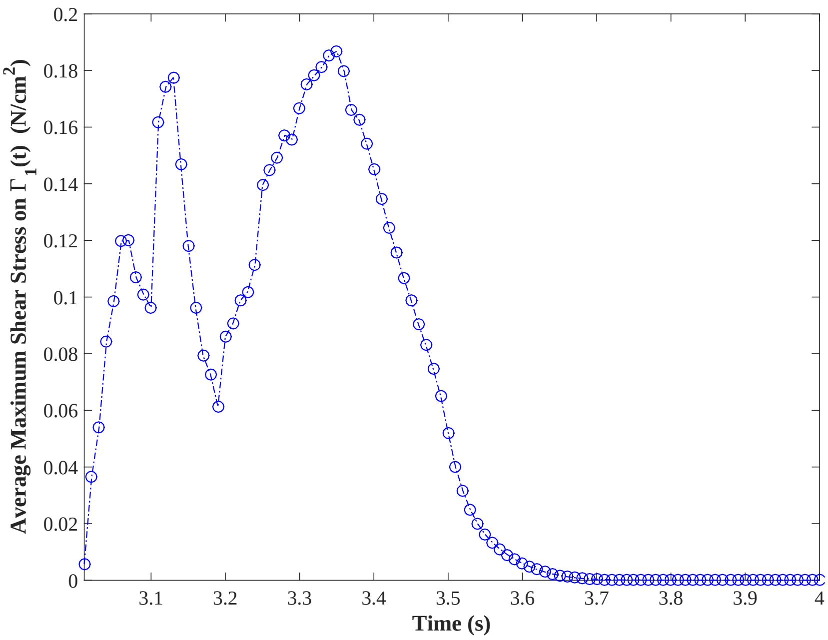

Figure 5.16: The magnitude of the average maximum shear stress on $\Gamma_1(t)$ at any time t.

5.3 Conclusion

In this chapter we have introduced a first step towards a rupture model based on the rheological property of the blood. The blood is considered to be a non-Newtonian fluid with a time-dependent viscosity μ that obeys Carreau model. In fact, the viscosity has been modified so that it is a function of the viscosity at previous iterations using the local in time average viscosity $\hat{\mu}_k$. We believe that what is ruptured is not the plaque, rather, the solidified blood near the stenosis. In fact, the fibrous cap is a stiffened part of the artery wall which is enlarged due to the inflammation beneath it, which rebut the assumption of being released into the flow. Hence, a first step towards a rupture model is to locate the solidification zone as we believe that the jelly-like material in this zone is the ruptured substance.

In general, in vivo, blood is in liquid state, thus, a transit to a jelly-like material is linked to changes encountering on the viscosity. Indeed, acquiring a jelly-like material is associated to an increase in the viscosity. As a result, the viscosity is reformulated so that it is a time-dependent function related to its history represented by the local in time average viscosity $\hat{\mu}_k$. Based on the properties of viscous materials, we can assume that the blood constituting the solidification zone is characterized by a high viscosity and a negligible speed. Using the numerical results obtained in Chapter 4 and investigating the pattern of the average speed and the average viscosity, we consider a viscosity threshold μ_{th} such that when the computed viscosity μ exceeds it, regions $\mathcal{D}_\mu$ of high viscosity are detected. Similarly, if the speed of blood is less than the speed threshold v_{th}, then we locate the regions possessing negligible speed. The solidification zone $\mathcal{R}_\mathfrak{s}$, spotted at the edge of the stenosis, is the intersection of the regions $\mathcal{D}_\mu$ and $\mathcal{D}_v$.

A first step to a rupture model is derived based on the forces acting on the solidification zone $\mathcal{R}_s$. For this sake, blood forming the solidification zone is considered to be a linear elastic material that obeys Hooke's law and that is under the effect of an external stress exerted by the blood and the deformation of the stenosis. Upon solving the elasticity equations numerically results have shown an external force representing the shear stress exerted by the blood on this zone. This force opposes the deformation of the solidification zone. Further, a shear stress is observed on the crust of the solidification zone, namely on the zone-blood interface, which will scrape the crust of this zone. We believe, the opposite effects and the shear stress will lead to the fragmentation of the solidified blood in the solidification zone. As a consequence, detached pieces will be drifted by the flow and at some sites will block the artery causing an infarction.

Appendix A

Conservation Laws and Transformation Formulas

Theorem A.1 (Reynolds' Transport Theorem) *Let $\Omega(t) \in \mathbb{R}^d$ be a material volume. For any differentiable function f defined on $\Omega(t)$ it holds*

$$\frac{d}{dt}\int_{\Omega(t)} f(\boldsymbol{x},t)\; d\boldsymbol{x} = \int_{\Omega(t)} \left(\frac{\partial f}{\partial t} + \nabla\cdot(f\boldsymbol{v})\right)\, d\boldsymbol{x}. \tag{A.1}$$

where $\boldsymbol{v}$ is a vector field in $\mathbb{R}^d$ representing the velocity of any particle that is on the position $\boldsymbol{x}$ on the time t.

Proposition A.1 (Continuity Equation) *Let $\Omega(t) \in \mathbb{R}^d$ be a material volume. For any vector $\boldsymbol{v} \in \mathbb{R}^d$ and a scalar function ρ we have*

$$\frac{\partial \rho}{\partial t} + \nabla\cdot(\rho\boldsymbol{v}) = 0 \qquad \text{in } \Omega(t). \tag{A.2}$$

Definition A.1 (Cauchy Equation of Motion) *The Cauchy equation of motion is based on Newton's second law. It is given as*

$$\rho\frac{\partial \boldsymbol{v}}{\partial t} + \rho(\boldsymbol{v}\nabla\cdot)\boldsymbol{v} = \nabla\nabla\cdot\boldsymbol{\sigma}(\boldsymbol{v},p) + \rho f \qquad \text{in } \Omega(t)\times(0,T). \tag{A.3}$$

Lemma A.1 (Piola Transform [Ric17, Lemma 2.12]) *Let $\boldsymbol{w} : \Omega(t) \to \mathbb{R}^3$ be a differentiable vector field, and $\tilde{\boldsymbol{w}}$ its representation in the reference configuration $\tilde{\Omega}$. The Piola transformation of $\boldsymbol{w}$ is given by*

$$J\boldsymbol{F}^{-1}\tilde{\boldsymbol{w}}. \tag{A.4}$$

Moreover, for the normal component of $\boldsymbol{w}$ we have

$$\int_{\partial\Omega(t)} \boldsymbol{n}\cdot\boldsymbol{w}\; d\Gamma = \int_{\partial\tilde{\Omega}} \tilde{\boldsymbol{n}}\cdot J\boldsymbol{F}^{-1}\tilde{\boldsymbol{w}}\; d\tilde{\Gamma}. \tag{A.5}$$

For the divergence of $\boldsymbol{w}$ it holds

$$\int_{\Omega(t)} \operatorname{div}(\boldsymbol{w})\, d\boldsymbol{x} = \int_{\tilde{\Omega}} \widetilde{\operatorname{div}}(J\boldsymbol{F}^{-1}\tilde{\boldsymbol{w}})\, d\tilde{\boldsymbol{x}}. \tag{A.6}$$

Furthermore, point-wisely we have

$$J\operatorname{div}(\boldsymbol{w}) = \widetilde{\operatorname{div}}(J\boldsymbol{F}^{-1}\tilde{\boldsymbol{w}}). \tag{A.7}$$

Corollary A.1 *Let $\boldsymbol{\sigma} : \Omega(t) \to \mathbb{M}_3(\mathbb{R})$ be a regular tensor field, and $\tilde{\boldsymbol{\sigma}}$ its representation in the reference configuration $\tilde{\Omega}$. The Piola transformation $\boldsymbol{T}$ of $\boldsymbol{\sigma}$ is given by*

$$\boldsymbol{T} = J\tilde{\boldsymbol{\sigma}}\boldsymbol{F}^{-t}. \tag{A.8}$$

Moreover, the divergence of $\boldsymbol{T}$ is

$$\widetilde{\mathbf{div}}\ \boldsymbol{T} = J\mathbf{div}\boldsymbol{\sigma}. \tag{A.9}$$

Appendix B

Useful Inequalities

Theorem B.1 (Grönwall Inequality[1]) *Let $t_0 \geq 0$ and consider the functions u, f and g to be continuous on $[t_0, T)$ with $T \leq \infty$ and $g(t)$ a non-negative function, such that we have*

$$u(t) \leq f(t) + \int_{t_0}^{t} g(s)\ u(s)\ ds, \qquad t \in [t_0, T),$$

then the function u satisfies

$$u(t) \leq f(t) + \int_{t_0}^{t} f(s)g(s) \exp\left(\int_{s}^{t} g(\tau)\ d\tau \right) ds, \qquad t \in [t_0, T). \tag{B.1}$$

If further, $g(t)$ is a non-decreasing function, then

$$u(t) \leq f(t) \exp\left(\int_{t_0}^{t} g(s)\ ds \right), \qquad t \in [t_0, T).$$

Remark B.1 *If the functions $f(t)$ and $g(t)$ are constants say C_1 and C_2, then the function u will satisfy*

$$u(t) \leq \frac{C_1}{C_2} \exp(C_2 t).$$

For the proof of this theorem, some additive versions and related inequalities see [BF13, Section 4.2]

Proposition B.1 (Young's Inequality) *Let $n \geq 2$, and $x_1, \cdots, x_n$ be non-negative real numbers. Moreover, let $p_1, \cdots, p_n$ be positive real numbers satisfying*

$$\frac{1}{p_1} + \cdots + \frac{1}{p_n} = 1. \tag{B.2}$$

Then we have

$$x_1 \cdots x_n \leq \frac{x_1^{p_1}}{p_1} + \cdots + \frac{x_n^{p_n}}{p_n}$$

The following corollary gives a version of Young's inequality which is widely used.

Corollary B.1 *Let $p_1, \cdots, p_n$ be positive real numbers satisfying (B.2). For all real positive numbers $\varepsilon_1, \cdots, \varepsilon_n$, there exists a constant $C = C(\varepsilon_1, \cdots, \varepsilon_{n_1})$, such that for all $x_1, \cdots, x_n$ positive, we have*

$$x_1 \cdots x_n \leq \varepsilon_1 x_1^{p_1} + \cdots + \varepsilon_{n-1} x_{n-1}^{p_{n-1}} + C(\varepsilon_1, \cdots, \varepsilon_{n-1}) x_n^{p_n}.$$

Obviously, we can fix all coefficients except for one that can be found from the fixed coefficients.

The proof of Young's inequality is based on the concavity property of the logarithmic function.

Theorem B.2 (Hölder's Inequality) *Let Ω be an open set of $\mathbb{R}^d$ and $p_1, \cdots, p_n$ be positive real numbers. Let $r \in [1, \infty)$ be such that*

$$\frac{1}{r} = \frac{1}{p_1} + \cdots + \frac{1}{p_n}.$$

For all functions $f_i \in L^{p_i}(\Omega), \quad \forall\ i = 1, \cdots, n$, the product $f_1 \cdots f_n$ belongs to $L^r(\Omega)$ and we have

$$||f_1 \cdots f_n||_{L^r} \leq \prod_{i=1}^{n} ||f_i||_{L^{p_i}}. \tag{B.3}$$

The proof is based on using Young's inequality.

Appendix C

Vectors and Tensors

C.1 Vectors

Definition C.1.1 (Gradient and Divergence of a Vector) *Let $\boldsymbol{v}$ be a vector field in $\Omega \subset \mathbb{R}^d$, that is sufficiently regular. We define the gradient of $\boldsymbol{v}$ denoted by* grad$\boldsymbol{v}$ *or $\boldsymbol{\nabla v}$ by the n-by-n matrix given by*

$$\boldsymbol{\nabla v} = \begin{pmatrix} \dfrac{\partial v_1}{\partial x_1} & \cdots & \cdots & \dfrac{\partial v_1}{\partial x_n} \\ & \ddots & \ddots & \\ \vdots & & & \vdots \\ & \ddots & \ddots & \\ \dfrac{\partial v_n}{\partial x_1} & \cdots & \cdots & \dfrac{\partial v_n}{\partial x_n} \end{pmatrix}.$$

Further, the divergence of $\boldsymbol{v}$ denoted by $\mathrm{div}(\boldsymbol{v})$ *or $\nabla \cdot \boldsymbol{v}$ is defined by*

$$\nabla \cdot \boldsymbol{v} = \sum_{i=0}^{n} \frac{\partial v_i}{\partial x_i}.$$

Definition C.1.2 (Scalar Product of Vectors) *Let $\boldsymbol{u}$ and $\boldsymbol{v}$ be two vector fields in $\mathbb{R}^d$. The scalar product of $\boldsymbol{u}$ and $\boldsymbol{v}$ denoted by $\boldsymbol{u} \cdot \boldsymbol{v}$ is the scalar value defined by*

$$\boldsymbol{u} \cdot \boldsymbol{v} = \sum_{i=1}^{n} u_i v_i. \tag{C.1}$$

C.2 Tensors

Definition C.2.1 (Divergence of a Tensor) *Let $\boldsymbol{A} = (A_{ij})_{1 \leq i,j \leq n}$ be a regular tensor field in $\mathbb{M}_n(\mathbb{R})$. The divergence of $\boldsymbol{A}$ is defined by*

$$\boldsymbol{\nabla} \cdot \boldsymbol{A} = \begin{pmatrix} \displaystyle\sum_{i=0}^{n} \frac{\partial A_{1i}}{\partial x_i} \\ \vdots \\ \displaystyle\sum_{i=0}^{n} \frac{\partial A_{ni}}{\partial x_i} \end{pmatrix}, \tag{C.2}$$

Theorem C.1 *Let $\boldsymbol{A}, \boldsymbol{B}$ be two regular tensors in $\mathbb{M}_n(\mathbb{R})$. We denote by $\boldsymbol{A}_i$, for $i = 1, \ldots, n$, the i-the row of $\boldsymbol{A}$. The i-th element of $\boldsymbol{\nabla} \cdot (\boldsymbol{AB})$ is given by*

$$[\boldsymbol{\nabla} \cdot (\boldsymbol{AB})]_i = \boldsymbol{\nabla} A_i : \boldsymbol{B}^t + A_i \cdot (\boldsymbol{\nabla} \cdot \boldsymbol{B}). \tag{C.3}$$

Proof. The ij-th element of $\boldsymbol{AB}$ is

$$c_{ij} = (AB)_{ij} = \sum_{k=1}^{n} A_{ik} B_{kj}.$$

We have

$$\begin{aligned} [\boldsymbol{\nabla} \cdot (\boldsymbol{AB})]_i &= \sum_{j=1}^{n} \frac{\partial c_{ij}}{\partial x_j} \\ &= \sum_{j=1}^{n} \sum_{k=1}^{n} \frac{\partial A_{ik} B_{kj}}{\partial x_j} \\ &= \sum_{j=1}^{n} \sum_{k=1}^{n} \left(\frac{\partial A_{ik}}{\partial x_j} B_{kj} + A_{ik} \frac{\partial B_{kj}}{\partial x_j} \right) \\ &= \sum_{k=1}^{n} \boldsymbol{\nabla} A_{ik} \cdot \overrightarrow{B}_k + \sum_{k=1}^{n} A_{ik} \sum_{j=1}^{n} \frac{\partial B_{kj}}{\partial x_j} \\ &= \boldsymbol{\nabla} \boldsymbol{A}_i : \boldsymbol{B}^t + \sum_{k=1}^{n} \boldsymbol{A}_i \cdot (\nabla \cdot \boldsymbol{B}_k) \\ &= \boldsymbol{\nabla} \boldsymbol{A}_i : \boldsymbol{B}^t + \boldsymbol{A}_i \cdot (\boldsymbol{\nabla} \cdot \boldsymbol{B}), \end{aligned} \tag{C.4}$$

where $\boldsymbol{\nabla} \boldsymbol{A}_i \in \mathbb{M}_n(\mathbb{R})$ is the Jacobian matrix of the vector $\boldsymbol{A}_i$. ■

Bibliography

[ADK12] K. Aksu, A. Donmez, and G. Keser. Inflammation-induced thrombosis: mechanisms, disease associations and management. *Curr. Pharm. Des.*, 18(11):1478–1493, 2012.

[AM74] G. Astarita and G. Marrucci. *Principles of non-Newtonian Fluid Mechanics*. McGraw Hill, 1974.

[AvdBP+88] P. A. Aarts, S. A. van den Broek, G. W. Prins, G. D. Kuiken, J. J. Sixma, and R. M. Heethaar. Blood platelets are concentrated near the wall and red blood cells, in the center in flowing blood. *Arteriosclerosis*, 8(6):819–824, 1988.

[BD12] M. Bulelzai and J. Dubbeldam. Long time evolution of atherosclerotic plaques. *Journal of Theoretical Biology*, 297:1–10, March 2012.

[BDR98] A. Bermúdez, R. Durán, and Rodolfo Rodríguez. Finite element analysis of compressible and incompressible fluid-solid systems. *Mathematics of Computation of the American Mathematical Society*, 67(221):111–136, January 1998.

[BF13] Franck Boyer and Pierre Fabrie. *Mathematical Tools for the Study of the Incompressible Navier-Stokes Equations and Related Models*, volume 183. Springer New York, 2013.

[BG10] M. Boulakia and S. Guerrero. Regular solutions of a problem coupling a compressible fluid and an elastic structure. *Journal de Mathématiques Pures et Appliquées*, 94(4):341–365, October 2010.

[BG17] M. Boulakia and S. Guerrero. On the interaction problem between a compressible fluid and a Saint-Venant Kirchhoff elastic structure. *Advances in Differential Equations*, 22(1-2), January 2017.

[BGN14] T. Bodnár, G. P. Galdi, and Š. Nečasová, editors. *Fluid-Structure Interaction and Biomedical Applications*. Springer Basel, 2014.

[BHW89] H.A. Barnes, J.F. Hutton, and K. Walters. *An Introduction to Rheology (Rheology Series)*. Elsevier Science, 1989.

[BKS09] B. Buriev, T. Kim, and T. Seo. Fluid-structure interactions of physiological flow in stenosed artery. *Korea Australia Rheology Journal*, 21:39–46, March 2009.

[Bou06] M. Boulakia. Existence of weak solutions for the three-dimensional motion of an elastic structure in an incompressible fluid. *Journal of Mathematical Fluid Mechanics*, 9(2):262–294, September 2006.

[Bou17] Anass Bouchnita. *Mathematical modelling of blood coagulation and thrombus formation under flow in normal and pathological conditions.* Thèses, Université de Lyon, December 2017.

[Bre74] F. Brezzi. On the existence, uniqueness and approximation of saddle-point problems arising from lagrangian multipliers. *ESAIM: Mathematical Modelling and Numerical Analysis - Modélisation Mathématique et Analyse Numérique*, 8(R2):129–151, 1974.

[Bre10] H. Brezis. *Functional Analysis, Sobolev Spaces and Partial Differential Equations.* Springer New York, 2010.

[BS08] T. Bodnár and A. Sequeira. Numerical simulation of the coagulation dynamics of blood. *Computational and Mathematical Methods in Medicine*, 9(2):83–104, 2008.

[BZOC+12] K. Brummel-Ziedins, T. Orfeo, P. Callas, M. Gissel, K. Mann, and E. Bovill. The prothrombotic phenotypes in familial protein c deficiency are differentiated by computational modelling of thrombin generation. *PLoS ONE*, 7(9):e44378, September 2012.

[CEMR09] V. Calvez, A. Ebde, N. Meunier, and A. Raoult. Mathematical modelling of the atherosclerotic plaque formation. *ESAIM: Proceedings*, 28:1–12, 2009.

[Cha13] V. Chabannes. *Vers la simulation numérique des écoulements sanguins.* Thèses, Université de Grenoble, July 2013.

[CHM+10] V. Calvez, J. Houot, N. Meunier, A. Raoult, and G. Rusnakova. Mathematical and numerical modeling of early atherosclerotic lesions. *ESAIM: Proceedings*, 30:1–14, August 2010.

[Cia88] P. G. Ciarlet. *Mathematical Elasticity. Vol I : Three-Dimensional Elasticity.* North-Holland, 1988.

[CK91] Y. I. Cho and K. R. Kensey. Effects of the non-Newtonian viscosity of blood on flows in a diseased arterial vessel. Part 1: Steady flows. *Biorheology*, 28(3-4):241–262, 1991.

[Col15] B. S. Coller. Blood at 70: its roots in the history of hematology and its birth. *Blood*, 126(24):2548–2560, December 2015.

[CS04] D. Coutand and S. Shkoller. Motion of an elastic solid inside an incompressible viscous fluid. *Archive for Rational Mechanics and Analysis*, 176(1):25–102, November 2004.

[CS05] D. Coutand and S. Shkoller. The interaction between quasilinear elastodynamics and the navier-stokes equations. *Archive for Rational Mechanics and Analysis*, 179(3):303–352, June 2005.

[CSL+05] J. P. Collet, H. Shuman, R. E. Ledger, S. Lee, and J. W. Weisel. The elasticity of an individual fibrin fiber in a clot. *Proceedings of the National Academy of Sciences*, 102(26):9133–9137, June 2005.

[ČTG+06] Sunčica Čanić, Josip Tambača, Giovanna Guidoboni, Andro Mikelić, Craig J. Hartley, and Doreen Rosenstrauch. Modeling viscoelastic behavior of arterial walls and their interaction with pulsatile blood flow. *SIAM Journal on Applied Mathematics*, 67(1):164–193, jan 2006.

[DE99] B. Desjardins and M. J. Esteban. On weak solutions for fluid-rigid structure interaction: Compressible and incompressible models. *Communications in Partial Differential Equations*, 25(7-8):263–285, January 1999.

[DGH82] J. Donea, S. Giuliani, and J.P. Halleux. An arbitrary lagrangian-eulerian finite element method for transient dynamic fluid-structure interactions. *Computer Methods in Applied Mechanics and Engineering*, 33(1-3):689–723, September 1982.

[DGHL03] Q. Du, M. Gunzburger, L. Hou, and J. Lee. Analysis of a linear fluid-structure interaction problem. *Discrete and Continuous Dynamical Systems*, 9(3):633–650, February 2003.

[DR64] E. W. Davie and O. D. Ratnoff. Waterfall sequence for intrinsic blood clotting. *Science*, 145(3638):1310–1312, September 1964.

[Eul89] L. Euler. Principia pro motu sanguinis per arterias determinando. In *Leonhard Euler, Opera Omnia*, volume 16, pages 178–196. Birkhäuser Basel, 1989.

[Eva98] L. C. Evans. *Partial Differential Equations.* American Mathematical Society, 1998.

[FG08] Aaron L. Fogelson and Robert D. Guy. Immersed-boundary-type models of intravascular platelet aggregation. *Computer Methods in Applied Mechanics and Engineering*, 197(25-28):2087–2104, April 2008.

[Fic73] G. Fichera. Existence theorems in elasticity. In *Linear Theories of Elasticity and Thermoelasticity*, pages 347–389. Springer Berlin Heidelberg, 1973.

[FO99] F. Flori and P. Orenga. Analysis of a nonlinear fluid–structure interaction problem in velocity–displacement formulation. *Nonlinear Analysis: Theory, Methods & Applications*, 35(5):561–587, March 1999.

[FQV09] L. Formaggia, A. Quarteroni, and A. Veneziani, editors. *Cardiovascular Mathematics:Modeling and Simulation of the Circulatory System.* Springer Milan, 2009.

[FSLSS78] T. M. Fischer, M. Stohr-Lissen, and H. Schmid-Schonbein. The red cell as a fluid droplet: tank tread-like motion of the human erythrocyte membrane in shear flow. *Science*, 202(4370):894–896, November 1978.

[Gaw02] J. A. Gawinecki. Initial-boundary value problem in nonlinear hyperbolic thermoelasticity. some applications in continuum mechanics. *Dissertationes Mathematicae*, 407:1–51, 2002.

[GHZ09] G. Th. Guria, M. Herrero, and K. E. Zlobina. A mathematical model of blood coagulation induced by activation sources. *Discrete and Continuous Dynamical Systems*, 25(1):175–194, June 2009.

[GM00] C. Grandmont and Y. Maday. Existence for an unsteady fluid-structure interaction problem. *ESAIM: Mathematical Modelling and Numerical Analysis*, 34(3):609–636, May 2000.

[GR86] V. Girault and P. Raviart. *Finite Element Methods for Navier-Stokes Equations.* Springer Berlin Heidelberg, 1986.

[Gra98] C. Grandmont. Existence for a two-dimensional, steady state fluid-structure interaction problem. *Comptes Rendus de l'Académie des Sciences - Series I - Mathematics*, 326(5):651–656, March 1998.

[Gra02] C. Grandmont. Existence for a three-dimensional steady state fluid-structure interaction problem. *Journal of Mathematical Fluid Mechanics*, 4(1):76–94, February 2002.

[GRRM16] V. Govindarajan, V. Rakesh, J. Reifman, and A. Mitrophanov. Computational study of thrombus formation and clotting factor effects under venous flow conditions. *Biophysical Journal*, 110(8):1869–1885, April 2016.

[Hec05] F. Hecht. Tutorial freefem++. 2005.

[HGO00] G. A. Holzapfel, T. C. Gasser, and R. W. Ogden. *Journal of Elasticity*, 61(1/3):1–48, 2000.

[HWD04] B. Hübner, E. Walhorn, and D. Dinkler. A monolithic approach to fluid–structure interaction using space–time finite elements. *Computer Methods in Applied Mechanics and Engineering*, 193(23-26):2087–2104, June 2004.

[JC11] S. Jordan and E. Chaikof. Simulated surface-induced thrombin generation in a flow field. *Biophysical Journal*, 101(2):276–286, July 2011.

[KGKV09] N. El Khatib, S. Génieys, B. Kazmierczak, and V. Volpert. Mathematical modelling of atherosclerosis as an inflammatory disease. *Philosophical Transactions of the Royal Society A: Mathematical, Physical and Engineering Sciences*, 367(1908):4877–4886, December 2009.

[KGKV11] N. El Khatib, S. Genieys, B. Kazmierczak, and V. Volpert. Reaction–diffusion model of atherosclerosis development. *Journal of Mathematical Biology*, 65(2):349–374, August 2011.

[KGV07] N. El Khatib, S. Génieys, and V. Volpert. Atherosclerosis initiation modeled as an inflammatory process. *Mathematical Modelling of Natural Phenomena*, 2(2):126–141, 2007.

[KP88] T. Kato and G. Ponce. Commutator estimates and the euler and navier-stokes equations. *Communications on Pure and Applied Mathematics*, 41(7):891–907, October 1988.

[KS82] S. R. Keller and R. Skalak. Motion of a tank-treading ellipsoidal particle in a shear flow. *Journal of Fluid Mechanics*, 120(-1):27–47, July 1982.

[LF10] K. Leiderman and A. L. Fogelson. Grow with the flow: a spatial-temporal model of platelet deposition and blood coagulation under flow. *Mathematical Medicine and Biology*, 28(1):47–84, May 2010.

[LT10] B. Liu and D. Tang. Computer simulations of atherosclerotic plaque growth in coronary arteries. *Mol Cell Biomech*, 7(4):193–202, December 2010.

[Mac94] C. W. Macosko. *Rheology: Principles, Measurements, and Applications*. Wiley-VCH, 1994.

[Mal] S. J. A Malham. *Lecture Notes Introductory Fluid Mechanics*.

[MMCG65] E. Merrill, W. Margetts, G. Cokelet, and E. Gilliland. The casson equation and rheology of the blood near shear zero. In *Proceedings Fourth International Congress on Rheology, Part 4*, pages 135–143. Interscience, New York, 1965.

[MMM+05] C. Mckay, S. Mckee, N. Mottram, T. Mulholl, S. Wilson, S. Kennedy, and R. Wadsworth. Towards a model of atherosclerosis, 2005.

[MNR08] J. Makin, S. Narayanan, and R. Ramamoorthi. Hybrid-system modelling of human blood clotting. 2008.

[Pes72] C. Peskin. *Flow patterns around heart valves*. Ph.d. thesis, Albert Einstein College of Medicine, New York, 1972.

[Pes02] C. S. Peskin. The immersed boundary method. *Acta Numerica*, 11, January 2002.

[PM89] C. S. Peskin and D. M McQueen. A three-dimensional computational method for blood flow in the heart i. immersed elastic fibers in a viscous incompressible fluid. *Journal of Computational Physics*, 81(2):372–405, April 1989.

[Ric17] T. Richter. *Fluid-structure Interactions, Models, Analysis and Finite Elements*. Springer International Publishing, 2017.

[RSK] A. M. Robertson, A. Sequeira, and M. V. Kameneva. Hemorheology. In *Oberwolfach Seminars*, pages 63–120. Birkhäuser Basel.

[SB14] A. Sequeira and T. Bodnár. Blood coagulation simulations using a viscoelastic model. *Mathematical Modelling of Natural Phenomena*, 9(6):34–45, 2014.

[Seq18] A. Sequeira. Hemorheology: Non-newtonian constitutive models for blood flow simulations. In *Lecture Notes in Mathematics*, pages 1–44. Springer International Publishing, 2018.

[SSB11] A. Sequeira, R. Santos, and T. Bodnár. Blood coagulation dynamics: mathematical modeling and stability results. *Mathematical Biosciences and Engineering*, 8(2):425–443, April 2011.

[SV15] A. Sagar and J. Varner. Dynamic modeling of the human coagulation cascade using reduced order effective kinetic models. *Processes*, 3(1):178–203, March 2015.

[SvdV14] F. Storti and F. N. van de Vosse. A continuum model for platelet plug formation, growth and deformation. *International Journal for Numerical Methods in Biomedical Engineering*, 30(12):1541–1557, September 2014.

[TAB+13] A. Tosenberger, F. Ataullakhanov, N. Bessonov, M. Panteleev, A. Tokarev, and V. Volpert. Modelling of thrombus growth in flow with a DPD-PDE method. *Journal of Theoretical Biology*, 337:30–41, November 2013.

[TAB+15] A. Tosenberger, F. Ataullakhanov, N. Bessonov, M. Panteleev, A. Tokarev, and V. Volpert. Modelling of platelet–fibrin clot formation in flow with a DPD–PDE method. *Journal of Mathematical Biology*, 72(3):649–681, May 2015.

[TBA11] A.A. Tokarev, A.A. Butylin, and F.I. Ataullakhanov. Platelet adhesion from shear blood flow is controlled by near-wall rebounding collisions with erythrocytes. *Biophysical Journal*, 100(4):799–808, February 2011.

[TBE+11] A.A. Tokarev, A.A. Butylin, E.A. Ermakova, E.E. Shnol, G.P. Panasenko, and F.I. Ataullakhanov. Finite platelet size could be responsible for platelet margination effect. *Biophysical Journal*, 101(8):1835–1843, October 2011.

[WRB+15] Adam R. Wufsus, Kuldeepsinh Rana, Andrea Brown, John R. Dorgan, Matthew W. Liberatore, and Keith B. Neeves. Elastic behavior and platelet retraction in low- and high-density fibrin gels. *Biophysical Journal*, 108(1):173–183, January 2015.

[WS76] F. J. Walburn and D. J. Schneck. A constitutive equation for whole human blood. *Biorheology*, 13(3):201—-210, Jun 1976.

[XCL+12] Z. Xu, S. Christley, J. Lioi, O. Kim, C. Harvey, W. Sun, E. D. Rosen, and M. Alber. Multiscale model of fibrin accumulation on the blood clot surface and platelet dynamics. In *Methods in Cell Biology*, pages 367–388. Elsevier, 2012.

[YHSC04] X. Yue, F. N. Hwang, R. Shandas, and X. C. Cai. Simulation of branching blood flows on parallel computers. *Biomed Sci Instrum*, 40:325–330, 2004.

[YLHK17] A. Yazdani, H. Li., J. D. Humphrey, and G. E. Karniadakis. A general shear-dependent model for thrombus formation. *PLOS Computational Biology*, 13(1):e1005291, jan 2017.

[Zhu07] D. Zhu. Mathematical modeling of blood coagulation cascade: kinetics of intrinsic and extrinsic pathways in normal and deficient conditions. *Blood Coagulation & Fibrinolysis*, 18(7):637–646, October 2007.